Durham E-Theses

Electronic properties of thin phosphor films

Husain, M. Razi

How to cite:

Husain, M. Razi (1973) *Electronic properties of thin phosphor films*, Durham theses, Durham University. Available at Durham E-Theses Online: http://etheses.dur.ac.uk/8235/

Use policy

The full-text may be used and/or reproduced, and given to third parties in any format or medium, without prior permission or charge, for personal research or study, educational, or not-for-profit purposes provided that:

- a full bibliographic reference is made to the original source
- a link is made to the metadata record in Durham E-Theses
- the full-text is not changed in any way

The full-text must not be sold in any format or medium without the formal permission of the copyright holders.

Please consult the full Durham E-Theses policy for further details.

Academic Support Office, The Palatine Centre, Durham University, Stockton Road, Durham, DH1 3LE
e-mail: e-theses.admin@durham.ac.uk Tel: +44 0191 334 6107
http://etheses.dur.ac.uk

ELECTRONIC PROPERTIES OF THIN PHOSPHOR FILMS

by

M. RAZI HUSAIN M.Sc.

A thesis presented in candidature for the degree of Doctor of Philosophy in the University of Durham

October 1973

DURHAM UNIVERSITY
SCIENCE
4 JUL 1974
SECTION
LIBRARY

ACKNOWLEDGEMENTS

The author wishes to acknowledge his gratitude for the guidance, constructive criticism and help given to him by Dr. M.J. Morant during the course of the work, and in the preparation of this thesis. Permission from Professor Wright to use the laboratory and workshop facilities for research purposes is gratefully acknowledged. It is also a pleasure to thank the highly skilled workshop staff headed by Mr. F. Spence for their co-operation and good will and Mrs. Pennington for her help in the preparation of the diagrams.

My appreciation is extended to the Vice Chancellor, University of Karachi, Pakistan, for granting me study leave with monetary support. Finally I am deeply indebted to my parents for their financial help and for the encouragement during my absence from them.

ABSTRACT

Electronic properties of thin films of zinc silicate phosphor (Zn_2SiO_4:Mn-willemite) prepared by a high temperature reaction between evaporated films of silicon monoxide and zinc fluoride, have been studied using metal electrodes. The samples were made using precise control of cleanliness and processing conditions. Silica substrates gave mechanical defects in sputtered films of platinum used as the base electrode for the thin film samples. This was due to the thermal mismatch between the two materials and it led to erratic conduction results. These defects do not occur using highly polished sapphire substrates with which reproducible characteristics have been obtained. Aluminium top contacts having a diameter of 0.04 cm were used both on the willemite films and on a section of the oxide for a comparison of their current-voltage characteristics. A few other electrode metals were also used.

The high temperature bake in oxygen used for the formation of the willemite also makes the oxide films more resistive and increases their breakdown strength. With platinum top contacts such films show bulk limited Poole-Frenkel type of conduction, but with aluminium, strong polarity dependence is shown. This is explained by the presence of a thin film of aluminium oxide, believed to form under the metal with the particular fabrication techniques used.

The willemite films were very brightly cathodoluminescent at thicknesses down to about 200 Å. Some thicker films also showed very weak but reproducible d.c. electroluminescence. In the conditions used, the willemite forms, leaving a considerable thickness of unreacted oxide

underneath. Conduction features of these films were generally similar to those of the oxide, and they have been explained by a simple band model. Electroluminescence is believed to arise due to the tunnelling of electrons through the aluminium oxide layer. The results of the work may have applications in the development of a further thin film display device.

CONTENTS

Chapter 1 INTRODUCTION 1

Chapter 2 REVIEW OF THE CLASSICAL WORK ON WILLEMITE 6

2.1 Structure 6

2.2 The Luminescence and Electrical Properties of Willemite 8

Chapter 3 CONDUCTION MECHANISMS IN THIN INSULATING FILMS 12

3.1 Introduction 12

3.2 Conduction Mechanisms - Theoretical 12

3.2.1 Band structure 12

3.2.2 Contact effects 14

3.2.3 List of conduction processes 16

3.2.4 Tunnelling in very thin films 16

3.2.5 Fowler-Nordheim tunnelling 17

3.2.6 Schottky emission 18

3.2.7 Poole-Frenkel effect 21

3.2.8 Temperature-field emission 26

3.2.9 Space charge limited current flow 27

3.2.10 Impurity conduction 31

3.2.11 Ionic conductivity 33

3.3 Conduction in Films of Silicon Oxide 34

Chapter 4 SAMPLE PREPARATION TECHNIQUES 44

4.1 Introduction 44

4.2 Sample Geometry 45

4.3 Vacuum System 45

4.3.1 Description 46

4.3.2 Development of vacuum system 47

4.4 Sample Fabrication 48

4.4.1 Mask production 48

4.4.2 Substrate cleaning 49

4.4.3 Deposition of films 50

(a) Sputtered base electrode 50

(b) Evaporated films 51

4.4.4 Willemite conversion reaction 54

4.4.5 Top contacts 56

4.5 Sample Measurement Techniques 56

4.5.1 Visual observations 56

4.5.2 Electrical measurements 57

Chapter 5 RESULTS FOR SAMPLES ON SILICA AND SINTERED ALUMINA SUBSTRATES 59

5.1 Description of Samples 59

5.2 Visual Examination of Samples 60

5.3 Results for the Silicon Oxide Films 62

5.4 Results for the Willemite Films 65

5.5 Stability of Currents 67

5.6 Cathodoluminescence of Samples 69

5.7 Conclusions 70

Chapter 6 RESULTS FOR SAMPLES ON SAPPHIRE SUBSTRATES 72

6.1 Description of Samples 72

6.2 Visual Observations on Samples 75

6.3 Electrical Measurements on Silicon Oxide Films 77

6.4 Results for Willemite on Sample S_1 79

6.5 Results for Willemite on Sample S_2 80

6.6 Results for Willemite on Sample S_3 81

6.7 Results for Willemite on Sample S_6 82

6.8 Stability of Currents 84

6.9 Luminescence of Samples 84

6.10 Conclusions 85

Chapter 7 DISCUSSION OF RESULTS 87

7.1 Problems of Film Quality 87

7.2 Willemite Conversion Reaction 90

7.3 Discussion of Oxide Measurements 92

7.4 Discussion of Willemite Measurements 96

Chapter 8 PHYSICAL INTERPRETATION OF RESULTS 101

8.1 Field Enhancement Phenomenon in Phosphors 101

8.2 Potential Barriers in Thin Insulating films 103

8.3 Conduction Processes in Uniform Thin Films 109

8.4 Detailed Comparison of Uniform Film Measurements with the Poole-Frenkel Theory 115

8.5 Conduction Process in Oxide Films with Pt-Al Electrodes 118

8.6 Conduction Process in Composite Oxide-Willemite Films 120

8.7 Luminescence of Willemite Films 126

Chapter	9	CONCLUSIONS AND SUGGESTIONS FOR FURTHER WORK	130
		9.1 Main Conclusions	130
		9.2 Suggestions for Further Work	133

CHAPTER 1

INTRODUCTION

The present work is part of a programme of research aimed at finding out whether a new type of display device based on silicon could be developed. The device of interest would be a low cost numeric or alphanumeric display for up to about 10 characters as required for a wide range of instruments, calculating machines etc. The proposed new type of device would have integrated addressing circuitry on the silicon chip with direct control of a light emitting phosphor on the top surface, so that there would be no problem of interconnections between two units.

The whole subject of information display devices has been very thoroughly reviewed recently [1]. At present light emitting diode (LED) arrays are dominating the field of solid state displays of this type. Although diodes which can emit radiation in the green, yellow and blue have been fabricated the most common are still the red emitting GaAsP and GaP diodes, the technology of which is now well under control. For the light-emitting elements the manufacturers have successfully made arrays of diodes on one chip, the operating power requirements of which are compatible with silicon integrated circuitry. For control, the addressing and decoding circuitry is also being produced in integrated form. However one problem in making complete displays with these units is the complexity and cost of the interconnections between the light emitting and the circuitry chips. It was realized in this Department that this problem, which is due to the use of two semiconductor materials, would be overcome by using electroluminescent (EL) films of some phosphor

DURHAM UNIVERSITY SCIENCE - 4 JUL 1974 SECTION LIBRARY

deposited on a silicon chip containing the control circuitry and thus ultimately developing a monolithic display device. This approach has not yet been reported from anywhere else although a brief report of a liquid crystal device [2] is similar.

G.S. Edwards started experimental work on this problem in Durham in 1966 [3]. He attempted to grow epitaxial films of ZnS on Si as the phosphor material, because thin films of ZnS have been widely studied [4-6]. He had great problems with the reproducibility etc. and did not produce satisfactory films. Since then films of ZnS on Si have been grown elsewhere [7], but still their luminescent properties are not under control[8]. During the course of his work Edwards considered alternative materials and he discovered a novel method for producing thin films of zinc orthosilicate doped with manganese (corresponding to the mineral 'willemite') on silicon.

Willemite is an excellent cathodoluminescent (CL) material which is widely used as a phosphor in cathode ray tubes. Edwards produced films by evaporating manganese-activated zinc fluoride on to thermally oxidized silicon and then baking the samples in an oxygen atmosphere at about 1100°C for ten minutes. The resulting films were proved to be the phosphor willemite by electron diffraction investigations and they were as brightly cathodoluminescent as the commercial phosphors. He established that the willemite films were highly compatible with silicon and its technology. He also observed weak electroluminescence on some samples under d.c. field conditions. More details of some of this work will be given in Chapter 2, together with a short

review of the previous work on willemite that is relevant.

Edwards' work showed for the first time that brightly luminescent films could be produced on silicon and these remain unique as far as is known. This formed the basis of the programme of more detailed investigations of this material in the Department. It was thought that the weak electroluminescence observed in the metal-insulator-silicon (MIS) structure was due to an insufficient number of electrons getting into the willemite layer. Therefore it was desirable to thoroughly investigate the structure and electronic properties of the willemite films and hence the conduction mechanism in order to understand and develop the right conditions for the injection of electrons from the silicon or an outer metal contact. In the literature there does not seem to be any mention of investigation of this type for willemite films and in any case they would have had to be re-investigated for films produced by this unique method on silicon.

The present work was on a simpler system than the MIS structures being investigated by others in the Department. Willemite films were produced by a similar method to that used with silicon but sandwiched between two metal electrodes, forming a metal-insulator-metal (MIM) structure. It was hoped that this work, apart from solving some of the problems mentioned above, would allow larger currents to be passed through the willemite. More electrons would be available for tunnelling into willemite from a metal than from silicon and also the high resistance due to the depletion layer for one polarity would be eliminated which would increase the chances of brighter electroluminescence. This project therefore supplements the willemite work on silicon which has continued in the Department since 1969 by

G.D. Davies and others (see Chapter 2). Davies also obtained electroluminescence on some samples for both types (p- and n-) of silicon substrate, and his work supports Edwards' conclusions on the importance of ionic movement in willemite. He also focussed attention on the importance of the purity of the materials used and the cleanliness of the processing.

The method of investigation used in the present work was to measure the I-V characteristics of MIM structures where the insulating film was either silicon oxide or a combination of silicon oxide and willemite. The measurements on the oxide were intended for comparison with published results for this material as a check of their purity and the film processing. The method of producing willemite used in this work is also thought to leave an underlying film of silicon oxide. Theoretical aspects of conduction in insulating films (in particular silicon oxide) are described in Chapter 3.

Since the base electrode used in the present work was to be metal rather than silicon, a new source of silicon oxide had to be found for the formation of willemite. In the new process, used here, silicon oxide films were deposited on to the base electrode to replace the thermal oxide used by Edwards. There is no evidence that the resulting willemite films were markedly different from those produced on silicon.

The metal-oxide-metal and metal-oxide-willemite-metal structures investigated here used films of platinum as the base electrode because a high temperature metal was required. The films were deposited on silica substrate by sputtering. The phosphor constituents were then deposited by evaporating silicon monoxide and manganese-activated zinc fluoride on

to the platinum. The samples were next baked at a high temperature to convert the oxide fluoride films into willemite and finally the metallic top contacts were added. Chapter 4 describes the techniques in detail.

The films on the earlier samples were badly cracked and tended to peel off the silica. These problems were partially overcome by improving and controlling all the processing techniques from the cleaning of the substrate onwards. Chapter 5 describes electrical measurements made on these films.

It was eventually recognized that the residual problems of the films cracking were due to the incompatibility of the silica substrates and the deposited layers. When the substrate material was replaced by sapphire the films were of much better quality. Chapter 6 describes the results obtained for a range of films on sapphire substrates.

Light green electroluminescence was observed on some of the silica-substrate samples. It was probably a lot brighter than that reported by Edwards and was observed at field strengths approaching breakdown.

Chapters 7 and 8 present a discussion of the electrical measurements on all samples and of the possible conduction mechanisms. Chapter 9 gives the conclusions of this work and includes suggestions for further investigations.

CHAPTER 2

REVIEW OF THE CLASSICAL WORK ON WILLEMITE

Since willemite is an unconventional material for both thin film and conduction current studies, a brief review of some of the previous work that is relevant to this thesis is given in this chapter.

2.1 Structure

Willemite was originally known as a naturally occurring mineral although it has been produced synthetically for many years. It has been known for a very long time to be a good cathodo- and photo-luminescent phosphor. Chemically it is based on zinc orthosilicate (Zn_2SiO_4) which luminesces pale blue in the pure state. Willemite also contains a small proportion of manganese in the form of Mn^{2+} ions which replace the Zn^{2+} ions because ~~of being~~ they have the same valence and roughly the same size [9] and it then luminesces bright green. The emission spectrum is broad and structureless with a peak at 5253Å, the position of which depends slightly on the manganese concentration [10]. The spectrum does not therefore give any information about the interaction of the Mn^{2+} with the crystal field, or the energy levels of the system involved in the transition. It is, however, known from the photo-excitation spectrum that the green emission is entirely due to the Mn^{2+} ion. Klick and Schulman [11] have reviewed this subject.

Nearly all of the extensive work on willemite reported in the literature refers to synthetic powder samples. There appear to be only a few reports of the preparation of thin films of willemite. Feldman and O'Hara [12] developed

techniques for the evaporation of willemite. They produced films of the phosphor on silica glass by first evaporating the powder and then firing the resulting films at $1100^{o}C$ for half an hour in oxygen. A recent paper by di Giacomo [13] describes two methods for depositing a polycrystalline thin film of willemite on quartz, sapphire and silicon wafers having approximately one micron of oxide on top. The first method used a vapour phase process represented by the following equation in which $MnCl_2$ was used as a dopant.

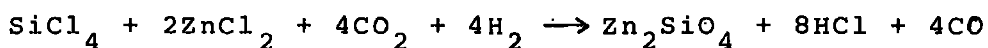

$$SiCl_4 + 2ZnCl_2 + 4CO_2 + 4H_2 \longrightarrow Zn_2SiO_4 + 8HCl + 4CO$$

In the other method the phosphor was evaporated, (during which there were problems due to decomposition) and later fired. It appears, however, that this was not a very successful process. Edwards [3] has reviewed the crystal structure of willemite and Edwards and Rushby [14] have studied the structure of willemite films on silicon which they identified as the normal α-form of zinc orthosilicate (α - Zn_2SiO_4). There also exists another form of this material called β - Zn_2SiO_4 which is considered to be an intermediate state in the formation of the first as it can be converted to the α-form by heating to above $800^{o}C$. Goldberg [15] pointed out that the methods used up to that time for the preparation of phosphor films in general were not as clean and controlled as semiconductor technology demands. The work at Durham is probably about the only work on thin phosphor films (willemite) in which semiconductor level of control has been used.

2.2 The Luminescence and Electrical Properties of Willemite

The luminescent properties of willemite have been extensively studied and it has been intensively developed as an excellent cathodoluminescent material for use in cathode ray tubes [16]. Electroluminescence in willemite has only occasionally been reported since its discovery by Destriau in 1947 [17]. All of the work reported on willemite seems to have been done by pressing the phosphor powder mixed with salts and/or metallic particles, between two conducting plates. Potassium silicate and tin chloride were frequently used. The powdered form of the phosphor helped in attaining locally high fields. Two examples of the work done during and after the 1950's are given here.

Bramley and Rosenthal in 1952 [18] studied the a.c. electroluminescence of different thicknesses of willemite by embedding it in a glass held between two conducting electrodes, and varying the voltage (100-500 V) and frequency (120-16,000 Hz). They reported the emission of radiation from the interface between the electrodes, although it was much less intense as compared to ZnS for approximately the same field. The light emission was considered to be due to field emission of electrons from the electrodes. In some further experiments a.c. electroluminescence was discovered by using an insulating layer at one electrode. Nicoll and Kazan [19] investigated the electroluminescence of cathode ray tube phosphors, including willemite, by coating the outside glass with a transparent conductive layer and applying a voltage between this and the aluminium backing layer of the phosphor inside the tube. The tube was heated to increase

the conductivity and weak light emission was then observed at very high voltages (2000V, 700 mA through 2 cm sq. area) for both polarities.

Neither the conduction mechanism nor any other electrical properties have been described in the literature on willemite and the work seems to have been concentrated almost entirely on the luminescent properties. The electroluminescent investigations also do not provide any real evidence for conduction mechanisms.

Herman and Hofstadter [20] reported a peak in the dark current conductivity of a single crystal of willemite at about 213°K when it was being warmed up and was previously irradiated with UV light. However, since the rate of warming up of the crystal was not controlled they did not make any quantitative measurements of the dependence of dark current on temperature, time and exposure to UV light. Later, Garlick and Gibson [21] investigated the thermoluminescence characteristics of willemite after exciting the phosphor at 90°K with 2537Å radiation and heating at a uniform rate. They found a single thermoluminescent peak at about 280°K and did not find any evidence of retrapping of the released electrons, because they always appeared to recombine either sufficiently close to the activator or at the Mn^{2+} ion itself to excite luminescence. The photoconductivity of willemite has not been investigated in detail but the study of the sintered materials and natural single crystals has shown ohmic d.c. photoconduction up to the highest fields used (2 Kv/cm) [22,23]. The measurements of Hill and Aronin [24] on pure and manganese activated willemite show that the photocurrents are independent of manganese concentration.

The only report of investigations on thin films of willemite is that of Morant and Edwards [25] on silicon substrates and the work presented in this thesis is the first study of thin films of this material between metal electrodes.

In his work on thin films of willemite described in Chapter 1, Edwards [3] investigated the I-V and C-V characteristics of MIS structures. He obtained larger currents for the positive polarity of the metal electrode for which electroluminescence was also observed on some samples. Positive ion movement in the willemite with the subsequent build up of space charge at the silicon surface was thought to give rise to a field intensification at the interface between the silicon and willemite (probably due to a thin layer of oxide). The resulting hot electron current through the willemite was considered to be the cause of the larger currents for this polarity. The process was also thought to produce the right conditions for electroluminescence in some samples although it was feared that the ionic movement might lead to the deterioration of the device with time.

The much more extensive and recent work by Davies and others [26] has cast doubts on the complete validity of Edwards' model for conduction in willemite on silicon. In particular it has shown the large influence of an outer insulating layer between the willemite and the metal top electrode. The processes appear to be extremely complicated and no detailed model has yet been proposed. In a detailed review of the luminescent properties of willemite Morant [27] has pointed out that in the Department's work on the electro-luminescence of willemite, the charge injection conditions

may have been far from optimum and he has expressed optimism about the possibility of bright EL if the required conditions of the charge injection can be obtained. By going through a detailed explanation of the possible excitation mechanisms of the Mn^{2+} ion (3d electrons of the Mn^{2+} in willemite) he has shown that the most likely methods which can be tried are:-

(i) By resonance excitation (exciton transfer) from electron hole recombination occurring within about 100Å of the Mn^{2+}.

(ii) By inelastic collision of a hot conduction electron or an injected electron with the Mn^{2+}.

Since it is difficult to make a good hole injecting contact, (and even if possible the holes would probably have negligible mobility in willemite), process (i) is not as easily conceivable as process (ii). He has therefore concluded by saying that the combination of phosphor and silicon technologies (in willemite on silicon) will have to be used to achieve hot electron injection for the second process of electroluminescence. This is being attempted in the Department by making solid state hot-electron emission structures in the silicon substrate below the willemite.

CHAPTER 3

CONDUCTION MECHANISMS IN THIN INSULATING FILMS

3.1 Introduction

Conduction in thin insulating films covers a wide range of processes which are not very well understood even now. The properties of polycrystalline and amorphous films have been investigated for at least twenty five years [28-30], and the once conflicting views on the subject now differ only in detail [31]. In the present work an attempt has been made to investigate the electronic properties of willemite which, in thin film form, is basically a polycrystalline insulator composed of very small crystallites [14].* Conduction in insulators is an extrinsic property because the wide band gap (∿3 eV) makes very few carriers available in the conduction and valence bands, so that one would hardly expect any conduction. In the first section of this Chapter, the conduction mechanisms which are considered to be important for insulating films of 1000-2000Å (thickness) sandwiched between metal electrodes have been presented as a theoretical basis for the next section in which relevant experimental work (mostly on evaporated films of silicon oxide) has been discussed. The flow of current in such films is not only determined by the charge transfer mechanisms inside the bulk (and broadly speaking due to defects in the bulk) but is also sometimes determined by the shape of the interface barrier formed at the metal-insulator contacts.

3.2 Conduction Mechanisms - Theoretical

3.2.1 Band Structure

Since it is generally accepted that a band picture

*Measurements were also made on amorphous silicon oxide films.

similar to that for crystalline solids can be applied to amorphous insulating films [32-34], a brief account is given of the band picture and of the theory of the contacts on such films before discussing the actual conduction mechanisms.
In an amorphous material the short range order, defined as the arrangement of the nearest neighbours within 10-20Å, remains much the same as in a crystalline solid, but the long range order is no longer maintained. However, it is the short range order which determines the main properties of the band structure [30,35]. Due to the loss of long range order in an amorphous solid, the band edges are not sharply defined. Also several localized levels are formed in the forbidden gap, due to impurities, defects and/or disorder in the material [36-38]. These levels may behave as traps, donors or acceptors during the conduction process [36]. One of the frequent causes of traps in evaporated films is said to be mechanical stresses built in during their growth. In a recent review Jonscher [39] has described the electronic levels in a disordered solid. Figure 3.1 compares a crystalline and an amorphous solid on an energy v.s. density of states diagram. The shapes of the edges shown are only one of several possible. For instance they can also be badly distorted or overlapping etc. [49,50]. However, whatever the shape may be, quantities like the barrier height at the contact with a metal have been found to be the same as for crystalline solids even in extremely thin (∿30Å) films of Al_2O_3 [40]. It is therefore concluded that for theoretical purposes an amorphous or polycrystalline insulator still has a full valence band separated from an empty conduction band by a forbidden gap, although this may be of smaller width than in the crystalline state [41-43]. This must also be true for a polycrystalline insulator.

3.2.2 Contact effects

To observe conduction through an insulating film two metallic contacts are required [39]. In the simplest form of contact, the Fermi levels of the two materials become aligned to satisfy the electrochemical equilibrium requirements, and thus charge transfer takes place depending on the work functions of the material. For an insulator which is free from surface states, one of the following three situations, shown in Fig. (3.2) may arise:-

(a) If the work function of the metal is lower than that of the insulator then electrons transfer from the metal into the conduction band of the insulator leaving a layer of positive charge on the metal side of the interface. Within limits determined by the bias conditions this contact would give rise to an ohmic or SCL I-V relationship for electronic conduction because there will always be an ample supply of electrons at the cathode.

(b) If the work function is the same for both the metal and the insulator then the conduction band of the insulator remains flat and a rectangular barrier forms at the interface after the Fermi levels are aligned. In this situation the characteristic of the junction may be ohmic or otherwise, depending upon the biasing conditions, the second contact, and the conduction process through the bulk. The type of contact is called 'neutral.'

(c) If the work function of the insulator is less than that of the metal, the transfer of electrons takes place from the insulator conduction band into the metal. This depletes the conduction band of the insulator at the interface and forms

(a)

energy

(b)

density of states

Fig. 3·1 Band model of a) crystalline and
b) amorphous solids

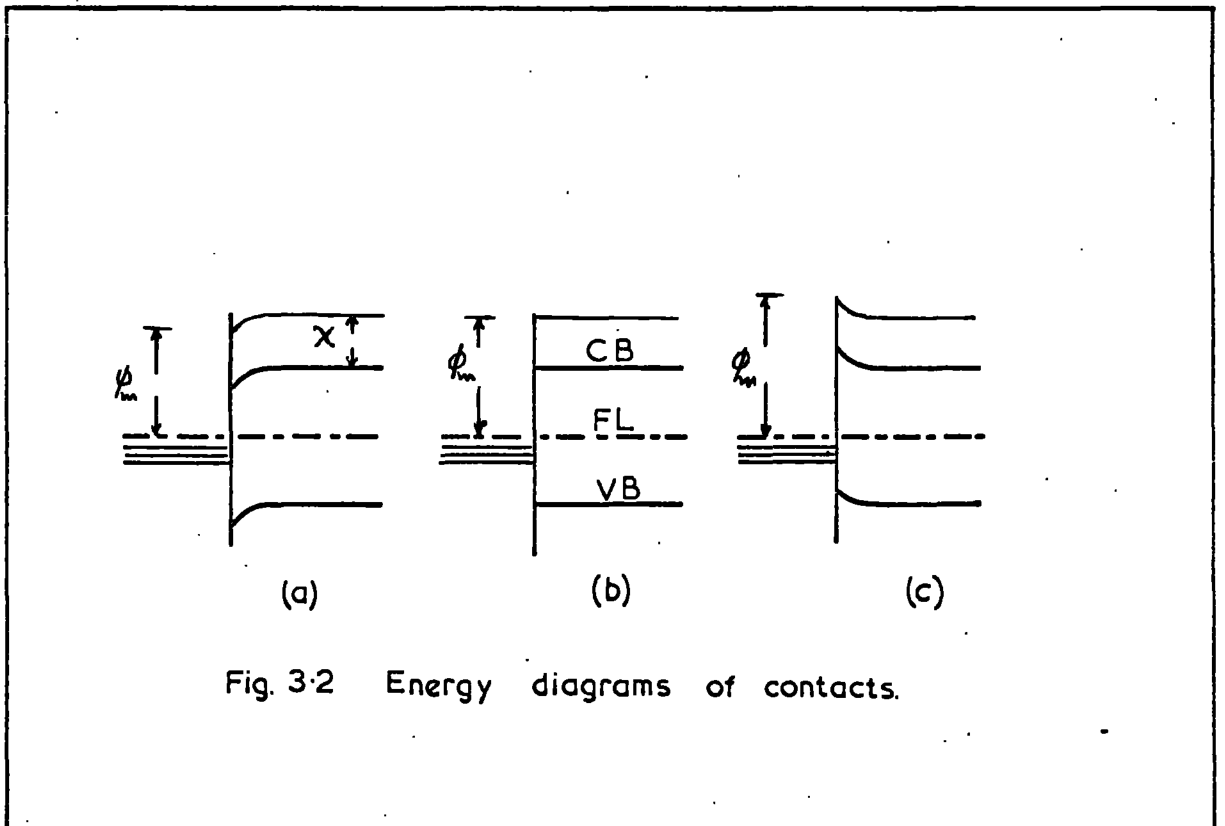

Fig. 3·2 Energy diagrams of contacts.

a thin layer of negative charge on the metal. In the literature this contact is sometimes referred to as blocking contact because the current is limited by the number of electrons which can pass over the barrier at the cathode contact. This type of barrier is more likely for a metal to semiconductor contact (Schottky barrier [48]) and it is not so important for insulators because an intrinsic insulator cannot supply sufficient electrons to the metal. As a result, the depletion region formed is so thin that it can be treated virtually like the neutral contact discussed above. However, as in the case of a vacuum diode, for high field strengths the current with both the neutral and blocking contacts is limited by the supply of the electrons from the cathode and can then be calculated by using the Richardson Schottky equation which has been corrected for solid state use [44,45]. A final limit to the flow of current is set by Joule heating.

In the simplified discussion above, surface states have been neglected. The situation becomes quite complicated if a certain amount of charge is trapped in surface states, because the applied voltage is then partly dropped across the depletion region formed due to the interaction of the charge in the states and the insulator. Furthermore, the types of contact described above represent only the more common situations which can occur at a metal-insulator interface, and practically one contact type may behave as described above only for a particular conduction process. The theory of metallic contacts on high resistivity solids has recently been reviewed by Simmons [46,47].

3.2.3 List of Conduction processes

A theoretical discussion will now be presented of the various conduction mechanisms in amorphous insulating films. These mechanisms can be broadly divided into injection-limited and bulk-limited processes and the following are to be discussed below:-

1. Tunnelling
   a. Tunnelling in very thin films
   b. Fowler-Nordheim tunnelling
2. Schottky emission
3. Poole-Frenkel effect
4. Temperature-field emission
5. Space charge limited conduction
6. Impurity conduction
7. Ionic conduction

The emphasis will be on Schottky emission and Poole-Frenkel effect as these are important in the temperature and field range of interest to the present work.

3.2.4 Tunnelling in very thin films

When two metal electrodes are separated by an insulating film of thickness about 50Å or less and a small voltage is applied current can flow by the quantum mechanical tunnelling of electrons from the cathode to the empty levels in the anode. Neglecting the effects of the image forces, space charge, and traps [51,52], such a structure can be represented by a rectangular barrier as shown in Figure 3.3. (Consideration of these effects modifies the shape of the barrier). The mechanism of tunnelling is that the incident electron wave is partly reflected and partly transmitted through the barrier depending on the barrier shape. Inside the barrier the amplitude of the electron wave decays

exponentially with distance and if the barrier is thin enough for the amplitude not to decay to appreciably zero in the width, the electrons tunnel through. Excellent reviews on the subject are available [45,53]. Since very thin films have not been used in the present work, however, this mechanism will not be discussed further.

3.2.5 Fowler-Nordheim tunnelling

Tunnelling can control the conduction in films thicker than those considered above if the width of a barrier at the cathode interface can be sufficiently thinned down (to less than 50Å) by the application of a high field strength. The interface can then be represented by a triangular barrier through which electrons can tunnel into the conduction band of the insulator as shown in Fig. 3.4. This Fowler-Nordheim [54] tunnelling is important at temperatures around 300°K and below, and the currents can be quite large compared to the high-temperature low-field case to be described later. The I-V relationship for this type of tunnelling, which was initially derived for the metal-vacuum interface, has been corrected for solid state use [55,56]. Using the WKB approximation for the tunnelling probability and applying corrections for the image force and temperature effects, the current density is given by [57].

$$J = \left(q^3\mathcal{E}^2/8\pi h\phi m^*\right)\left[1/t^2(y)\right]\left[\pi c kT/\sin(\pi c kT)\right]\exp\left\{-\left[4(2m^*)^{1/2}\phi^{3/2}/3\hbar q\mathcal{E}\right]v(y)\right\} \quad -(1)$$

where q is the electronic charge, $\mathcal{E}$ is the electric field strength, m is the free electron mass and m^* the effective mass, ϕ is the barrier height, h is Plank's constant $t(y)$ and $v(y)$ are tabulated elliptic integrals.

$$C = 2(2m^*\phi)^{1/2}\, t(\gamma)/\hbar q \mathcal{E}$$
$$\gamma = (1/\phi)(\mathcal{E} q^3/4\pi \epsilon_r \epsilon_o)^{1/2}$$

ϵ_o is the permittivity of free space

ϵ_r is the relative dielectric constant

k is the Boltzmann constant and T the absolute temperature.

3.2.6 Schottky emission

One of the effects which frequently controls the conduction in relatively thin films and which can also act together with some other mechanisms of charge transfer through the bulk in relatively thick films (>300Å), is Schottky emission similar to that at a metal-vacuum interface. This process is the emission of electrons from the cathode into the conduction band of the dielectric over the field-modified metal-insulator contact barrier. The rectangular barrier which is rounded off due to the electrode image force effects [58] is lowered under the application of the applied field as shown in Fig.3.5. Simmons [45] has described the Richardson Schottky effect in detail and corrected the original equation to take into account the transfer ~~to~~ of electrons inside the solid dielectric. The first treatment given below closely follows that of Simmons.

Consider an electron at a small distance x from the surface of the metal where x is greater than the inter-atomic distance. . The potential energy of the field-reduced barrier is

$$\phi(x) = \phi_o - \frac{q^2}{16\pi \epsilon_r \epsilon_o x} - q\mathcal{E}x \qquad \text{—— (2)}$$

where ϕ_o is the total barrier height, the second term is the potential energy of the electron due to the image force and $-q\mathcal{E}x$ is the potential energy due to the field $\mathcal{E}$. ϵ_r is the high frequency dielectric constant. The reduction $\Delta\phi_s$,

of the barrier height is given by

$$\Delta\phi_s = \left(\frac{q^3}{4\pi\epsilon_r\epsilon_0}\right)^{1/2}\mathcal{E}^{1/2} = \beta_s\,\mathcal{E}^{1/2} \qquad \text{—— (3)}$$

The Richardson Schottky equation for the current density

J is then given by

$$J = AT^2 \exp\left(\frac{\beta_s\,\mathcal{E}^{1/2} - \phi_0}{kT}\right) \qquad \text{—— (4)}$$

where k is the Boltzmann constant and

$$A = \frac{4\pi m q k^2}{h^3} \qquad \text{—— (5)}$$

According to Simmons [44 , 45] this equation can be applied directly to materials in which the thickness is less than the mean free path, in which case the electron energy is conserved across the interspace. For thick insulators the current at all points (including the cathode insulator interface) is described by the equation

$$J = qn\mu\mathcal{E} \qquad \text{—— (6)}$$

where n is the density of free carriers and μ the electron mobility in the insulator. The effect of this correction is to change the pre-exponential term in (4) from

$$AT^2 = 4\pi m(kT)^2 q/h^3 \quad \text{to} \quad 2q(2\pi m^* kT)^{3/2}\mu\mathcal{E}/h^3$$

where the replacement of the free electron mass by m^* is due to Crowell [59].

Lamb [60] has derived the Richardson Schottky equation from first principles assuming a particular shape of image-force lowered barrier and his expression includes an average coefficient of reflection, r , for the electrons incident on the barrier, but does not have any term for the motion of the electrons in the solid. His result is

$$J = A(1-r)T^2 \exp\left(\frac{q^{3/2}\mathcal{E}^{1/2}/2\sqrt{4\pi\epsilon_0\epsilon_r} - \phi_0}{kT}\right) \qquad \text{—— (7)}$$

This equation also gives a different value for β_s .

O'Dwyer [61] has calculated the I-V characteristics of dielectric films in the range of 300 to 1200Å thickness, using the Frölich model of the dielectric [62] (shown in Figure 3.6) and has assigned a temperature other than that of the lattice to the conduction electrons under the influence of a high applied field. The effect of the dependence of conductivity on space charge and field strength have also been included. The current and field are related using either the standard Fowler Nordheim equation or using the Schottky equation (equation 4). The cathode value rather than the average of the field is used in computation. The voltage is then calculated as a function of thickness for a given current. His work shows that linear plots of log I versus $\sqrt{V}$ can also be obtained for Fowler Nordheim tunnelling in the presence of space charge.

In arriving at the above expressions, a neutral contact was always assumed. If the barrier is ohmic, then at moderate to high temperatures high field strengths may invoke Schottky emission. However, if the interface has a depletion region then, even if the conduction starts due to Schottky emission at moderate field strengths, the barrier would thin down under the action of high fields and probably sufficient for Fowler Nordheim tunnelling to take over.

Whatever the details of the transfer of electrons after emission the conductivity is always of the form $\log I \propto V^{\frac{1}{2}}$ which is the same as for Poole-Frenkel effect, a bulk limited conduction mechanism discussed in the next section. Many workers have discussed methods of differentiating between the two and these will be described in Section 3.3.

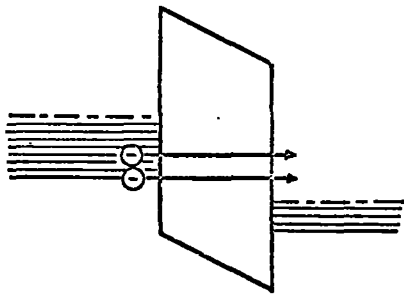

Fig. 3·3 Tunnelling

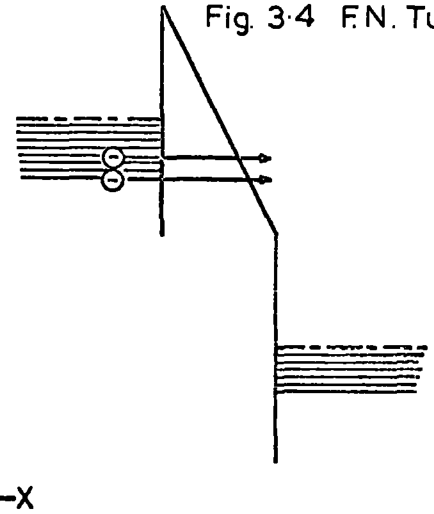

Fig. 3·4 F.N. Tunnelling.

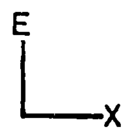

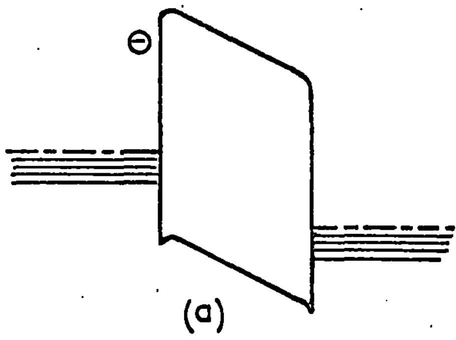

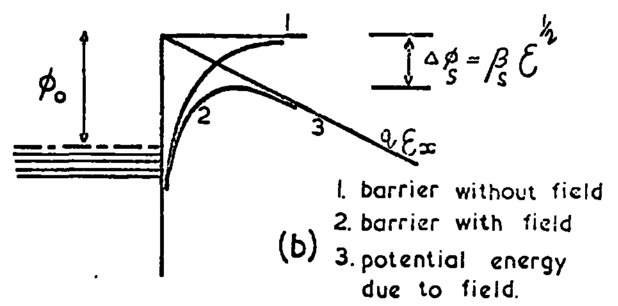

Fig. 3·5 Schottky emission.

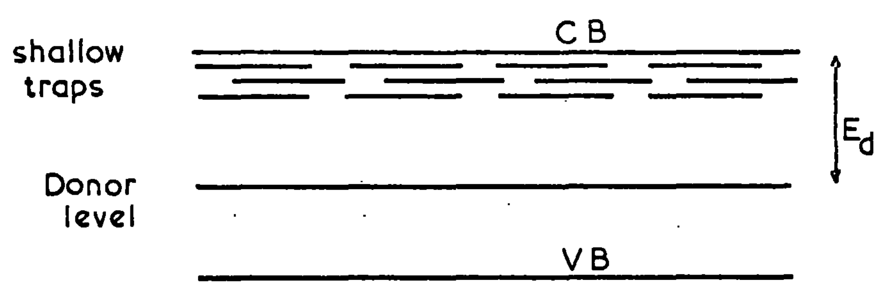

Fig. 3·6. Frölich model as used by O'Dwyer (61)

3.2.7 Poole-Frenkel effect

The Poole-Frenkel effect is based on Frenkel's [63] original concept of the increase of electrical conductivity of an insulator or semiconductor in an electric field due to the lowering of the ionization potential of the atoms. Amorphous insulating films usually show a conductivity of the form $\log I \propto \mathcal{E}^{1/2}$ where $\mathcal{E}$ is the field strength over the moderate to high range [64]. This behaviour has been ascribed to either Schottky or Poole-Frenkel conduction and particularly the latter when no evidence of electrode dependence is found. The Poole-Frenkel model has been developed to include various complicated processes which may take place inside an amorphous insulating solid [65-67]. Different ways in which an electron can be released from the Poole-Frenkel site, its position after relase, the effect of the field on the shape of the barrier and on the effective temperature of the electrons [67,68], and the influence of traps and donor and acceptor levels on the conductivity have all been considered [64,69-71]. Several workers have used the same fundamental model differing only in detail. However, there have also been basic differences and some of these are described here.

Considering first the elementary Poole-Frenkel model, [63], illustrated in Fig.3.7, the potential energy of an electron in the field of a positively charged centre is given by

$$- q^2/4\pi\epsilon_r\epsilon_0 x$$

where x is the distance from the centre and the other symbols have the meanings used previously.

The lowering of the barrier in the presence of the field $\mathcal{E}$ is given by

$$\Delta \phi_{PF} = \left(\frac{q^3}{\pi \epsilon_r \epsilon_0}\right)^{1/2} \mathcal{E}^{1/2} = \beta_{PF} \mathcal{E}^{1/2} \quad \text{——} \quad (8)$$

and the resulting conductivity by

$$\sigma = \sigma_0 \exp\left(\frac{\beta_{PF}\sqrt{\mathcal{E}}}{2kT}\right) \quad \text{——} \quad (9)$$

where

$$\sigma_0 = q \mu N_c \exp\left(-E_g/2kT\right) \quad \text{——} \quad (10)$$

is the low field conductivity. The current density is

$$J = J_0 \exp\left(\frac{\beta_{PF}\sqrt{\mathcal{E}}}{2kT}\right) \text{ where } J_0 = \sigma_0 \mathcal{E} \quad \text{——} \quad (11)$$

Mead [69] after investigating Ta-Ta_2O_5-Au sandwiches of various thicknesses assumed a high density of traps in the bulk and proposed field-enhanced thermal excitation of trapped electrons into the conduction band at high fields and high temperatures (Poole-Frenkel effect). He did not find evidence of hot electrons [72] and considered the mean free path to be very short, approximately 10Å or less. From these considerations the current density in thin film insulators with traps can be shown to be

$$J = J_0 \exp\left(\frac{\beta_{PF}\sqrt{\mathcal{E}}}{kT}\right) \quad \text{——} \quad (12)$$

which has the coefficient of $\sqrt{\mathcal{E}}$ twice that in equation (11).

A plot of log I *versus* $\sqrt{V}$ should give a straight line for both the Schottky and Poole-Frenkel effects although the slope is either β_S or $\beta_{PF} = 2\beta_S$. In order to resolve an anomally in thin films of Ta_2O_5 and SiO, which gave the experimental value of β fitting Schottky emission but otherwise showed bulk limited effects, Simmons [70] proposed the

band model shown in Fig.3.8 after considering six possible combinations. The model contains shallow traps and deep donor levels. The bulk I-V characteristics of the film is given by

$$J = J_0 \exp\left(\frac{\beta_{PF}\sqrt{\mathcal{E}}}{2kT}\right) \qquad (13)$$

where
$$J_0 = q\mu N_c \left(\frac{N_d}{N_t}\right)^{1/2} \mathcal{E} \exp\left(-\frac{E_d + E_t}{2kT}\right) \qquad (14)$$

Since equation (13) has $\frac{\beta_{PF}}{2} = \beta_S$ as the coefficient of $\sqrt{\mathcal{E}}$ it explains the results and has been successfully used by various workers [73]. An interesting feature of equation (13) is that it is of the same form as equation (11) which was derived for a solid without traps.

Yeargan and Taylor [71] have reviewed the Poole-Frenkel effect and have proposed a model with acceptors and donors. In their equation for Poole-Frenkel conduction

$$J = q\mu n_0 \mathcal{E} \exp\left[-(\phi_{PF} - \Delta\phi_{PF})/rkT\right] \qquad (15)$$

where
$$\Delta\phi_{PF} = \left(\frac{q^3 \mathcal{E}}{\pi \epsilon_r \epsilon_0}\right)^{1/2}$$

r varies from 1 to 2 depending on the position of the Fermi level and therefore the conductivity may be either

$$\sigma = \sigma_0 \exp\frac{\Delta\phi_{PF}}{2kT} \quad \text{or} \quad \sigma_0 \exp\frac{\Delta\phi_{PF}}{kT}$$

(where $\sigma_0 = q\mu n$ and μ is the mobility in the insulator) depending on the carrier density, n, which itself depends on the compensation between the relative densities of donor and acceptor sites.

Jonscher [39,67,74,75] has also reviewed different aspects of Poole-Frenkel conduction. He proposed that the maximum barrier lowering takes place between the directions of the emission of electrons and the field, and that the emitted electrons are retrapped in the quasicontinuum of

more-or-less localized levels below the conduction band before being re-emitted.

In a more recent review [67,75] Jonscher has suggested a model in which donor-like levels (neutral when occupied) are superposed on trap like levels ($\sim 10^{21}\,cm^{-3}\,eV^{-1}$ and neutral when occupied) which are randomly distributed in space and in energy as shown in Fig.3.9. Under the action of a high electric field ($>10^{4}$ V/cm), the energy distribution of electrons in traps changes and causes a rise in the effective electron temperature. The expression given for current is

$$J = J_o \; T_c^2 \; exp\left(\frac{q \beta_{PF} \sqrt{\mathcal{E}}}{kT}\right) \qquad (16)$$

On the basis of the fact that the field-dependent component of the activation energy at high field strengths is the same as at low fields, Masayuki Ieda et al [76] have proposed a three-dimensional model similar to that of Hartke [77]. They have allowed for the fact that together with the decrease of barrier height in the direction of the field, there is an increase in the direction opposite to the field. Assuming that the electron is a free carrier with a field independent mobility and that its escape probability from a trap is spherically symmetric, they have derived an equation which gives ohmic conductivity at low field strengths and Poole-Frenkel conduction at high fields, giving the coefficient for $\sqrt{\mathcal{E}}$ the same as for the Schottky effect.

Hill [65,66,78] has analysed the conduction in amorphous solids by assuming a large density of ionized sites within a limited energy range in the forbidden gap. He has assumed an increase of barrier height in the reverse direction of the applied field equal to the decrease in the

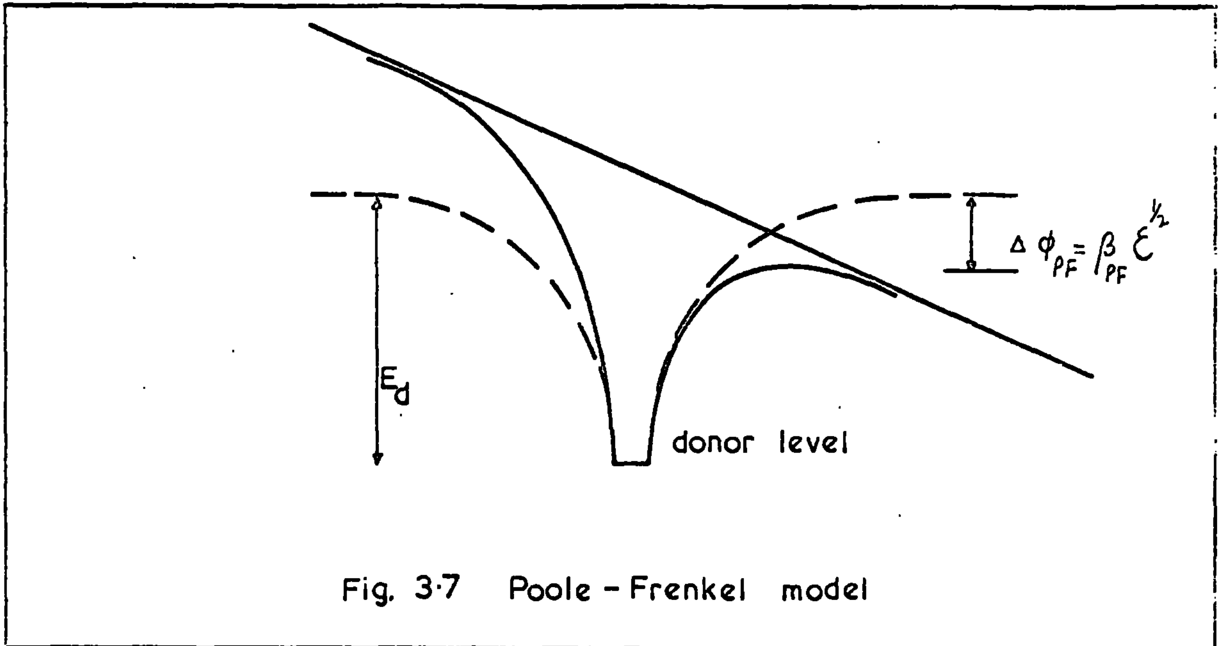

Fig. 3·7 Poole - Frenkel model

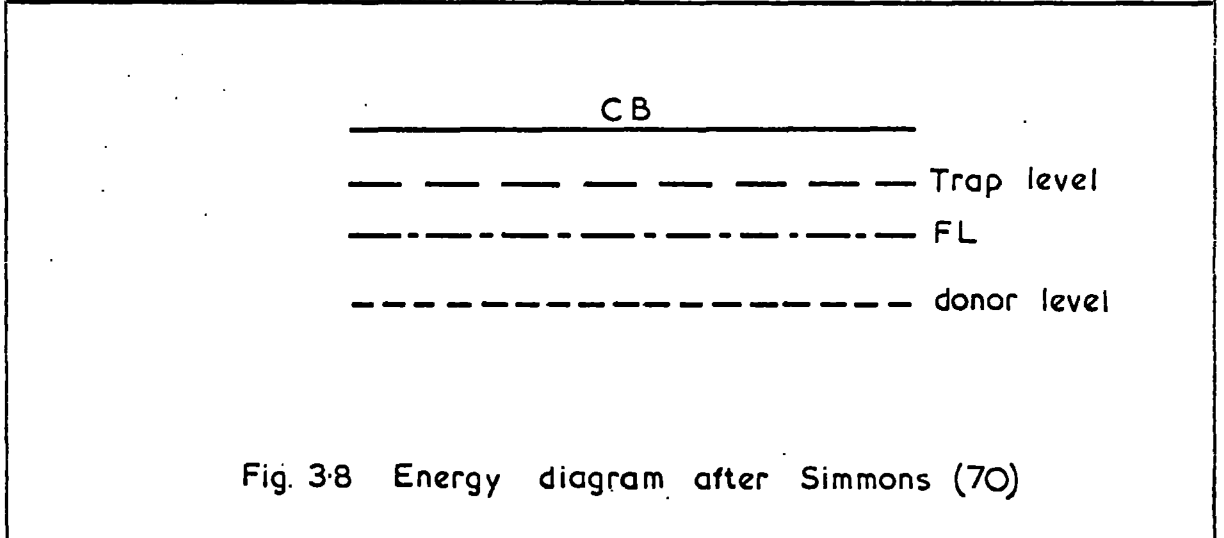

Fig. 3·8 Energy diagram after Simmons (70)

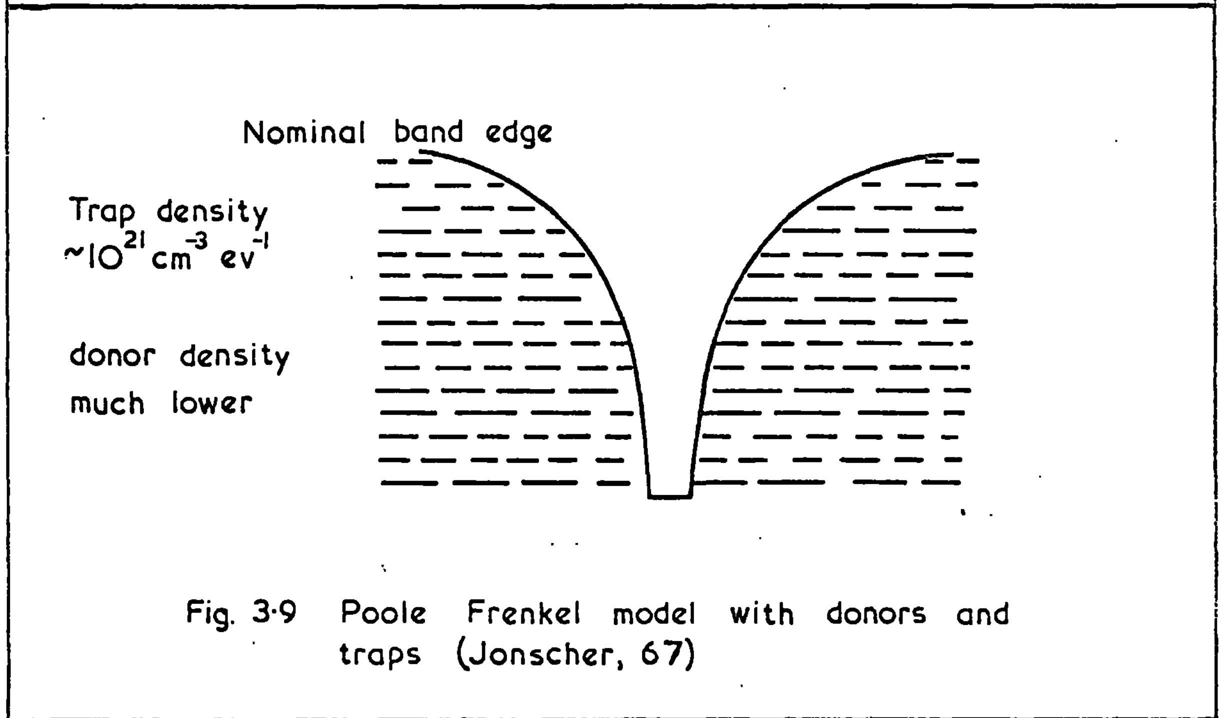

Fig. 3·9 Poole Frenkel model with donors and traps (Jonscher, 67)

forward direction. For low fields, when the emission from single centres is spherically uniform, the current density is given by

$$J = 2qN_i(kT)^3 \beta^{-1}\mu_2 \exp -(E_i/kT)\, \alpha^{-1}(\alpha \cosh\alpha - \sinh\alpha) \qquad (17)$$

$$\alpha = \beta_{PF}\sqrt{\mathcal{E}}/kT$$

where $N_i = \frac{\partial N_a}{\partial E}$, E is the energy of the carrier in the centre and N_a the density of states of the centre, so that N_i is the effective density of centres at an energy level E_i. μ_1 and μ_2 are the mobilities defined by the expressions of the form

$$\frac{\partial V_x}{\partial E} \cdot dE = \mu_1 \mathcal{E} \quad \text{and} \quad \frac{\partial V_x}{\partial E} \cdot \partial E = \mu_2 \sqrt{\mathcal{E}}$$

$\frac{\partial V_x}{\partial E}$ is the velocity of the carriers with energy in the region of the quasi conduction band edge. The density of ionized traps may be large enough to form multiple centres by overlap in the potential wells as shown in Fig.3.10. At low field strengths only emission over the central barrier could be considered while at high fields the barrier surrounding the complete group of centres will have to be considered. For amorphous materials with spherically uniform emission the low-field current is then given by

$$J = 2qN_i s(kT)^2 \nu \exp -\left(E_a/kT\right) \alpha'^{-2}(\alpha' \cosh\alpha' - \sinh\alpha') \qquad (18)$$

where $\alpha' = q\mathcal{E}s/2kT$ and ν is the attempt to escape frequency. For high field strengths Hill has derived an equation for intercentre tunnelling.

After considering the transition region Hill has also shown the evidence for the Poole-Frenkel effect by plotting $J T^{-2} \exp(E_a/kT)$ against $\mathcal{E}/T$ when all the points corresponding to the Poole-Frenkel effect fall on a continuous curve. He has suggested that the value of the dielectric constant to be used for calculating β may be of the form

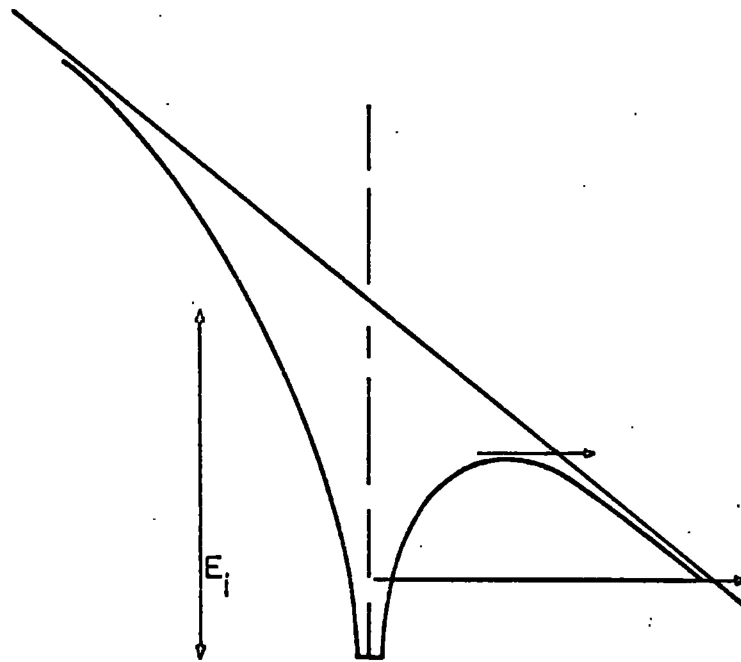

single centre

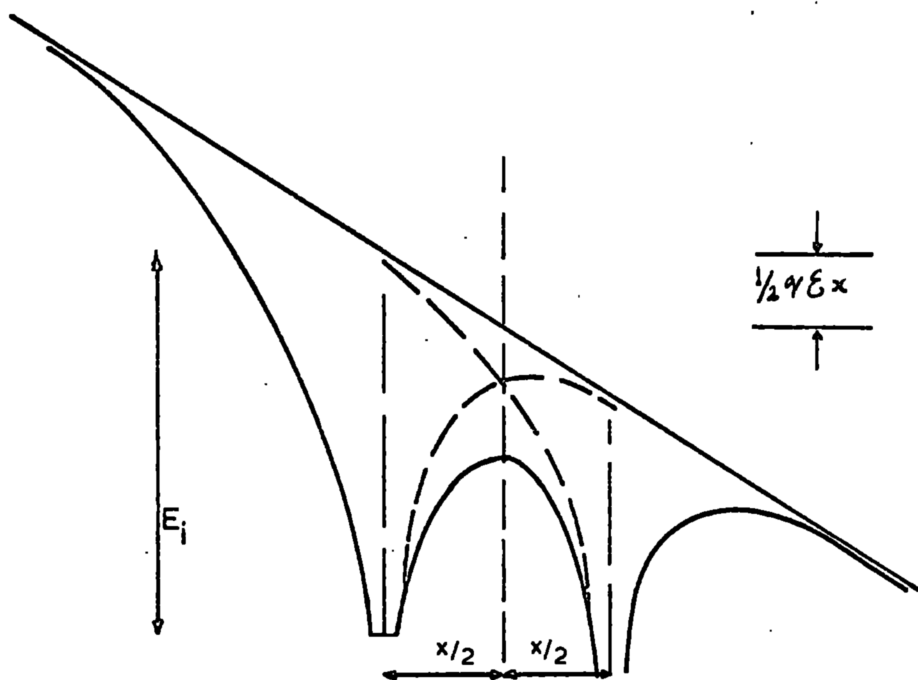

multiple centre

Fig. 3·10 (Figures 1 and 2 from Ref. 66)

$$\epsilon = \frac{1}{\epsilon_1^{-1} - \epsilon_2^{-1}} \quad \text{where } \epsilon_1 \text{ and } \epsilon_2 \text{ are the} \qquad (19)$$

high and low frequency values.

To complete the theoretical discussion of the Poole-Frenkel effect it is necessary to point out the two latest references on the subject. Connell et al [79] have reviewed the subject and proposed some changes based on the emission probability, carrier motion and the variation of barrier height with field. J. Antula [68] has proposed further changes based on the temperature dependence of conductivity and has introduced hot electron effects using the Frölich model of the band structure.

3.2.8 Temperature-field emission

Temperature-field emission takes place in the transition region between the low-temperature high-field (Fowler-Nordheim tunnelling) and the high-temperature low-field (Richardson-Schottky thermionic emission) regions. The term is used for the thermally assisted tunnelling of electrons from the cathode into the conduction band of the dielectric. Murphy and Good [80] proposed a unified theory for all three regions for emission into vacuum, which was extended for emission into solid dielectric by Tantraporn [81]. Hill [65] has reviewed the single carrier transport through thin dielectric films and reproduced the current density equations for the three regions. Mann [82] has considered the region between field strength of 10^6 and 10^7 V/cm and temperature between 100 and 300°K which are between pure thermionic and pure field emission. Christov [83,84] has proposed analytical theories for emission into vacuum covering even higher field and temperature ranges and he

later extended them to emission into solids. He has very recently reviewed the whole subject of electron currents through barriers between metals and revised the theories for the three regions [85].

3.2.9 Space charge limited current flow

When metallic contacts on the insulator are ohmic (i.e. they do not offer any restriction to the supply of carriers from the electrodes) the carrier injection at sufficiently high field strengths produces a considerable space charge which may result in a space charge limited current (SCLC) flow. The present work is concerned only with the electronic currents and therefore the two carrier SCLC (electron injection from the cathode and hole injection from the anode) which is important for some semiconductors, will not be discussed. The SCLC flow is not very commonly found in amorphous insulating films and it has usually been observed in single crystal or nearly single crystal materials [86]. The theory for trap-free single crystal materials was first proposed by Mott and Gurney [87] and later extended to solids with traps by Rose and Lampert [88-92]. In a trap-free material the situation is very similar to that in a vacuum diode where a space charge is built up if the electron emission is high and the applied field is insufficient to remove all the electrons. Assuming that the field at the cathode is reduced to zero by the space charge, the space charge limited current density through an insulator of thickness S with an applied voltage V is given by

$$J = \frac{9}{8} \epsilon_r \epsilon_0 \mu \frac{V^2}{S^3} \quad A/m^2 \qquad \text{———} \quad (20)$$

This expression is very similar to Child's law for the vacuum diode. If the space charge is such that the field lines terminate in front of the cathode, the cathode will be virtually displaced towards the anode by a small amount. With an increase in the applied field, the space charge decreases and once all the field lines terminate on the cathode a further increase in the applied voltage changes the nature of the conduction so that it becomes injection limited. This has been explained by Simmons [42] who has also derived equation (20) from first principles. However, the practical situation in a solid and especially in an amorphous insulator is quite complex because of the presence of defects and traps so that the currents observed are less than predicted by equation (20).

With shallow traps below the conduction band the current density decreases by a factor θ , equal to the ratio of free to trapped charge, i.e.

$$J = \frac{9}{8} \theta \epsilon_r \epsilon_0 \mu \frac{V^2}{s^3} \qquad (21)$$

θ is often approximately 10^{-5} to 10^{-7}. At low fields, before the onset of SCLC, i.e. when the density of thermally generated free carriers, n_0 , is greater than the injected charge, the current is ohmic and given by

$$J = q n_0 \mu \frac{V}{s} \qquad (22)$$

as shown at (a) in Fig.3.11. The transition voltage at which ohmic conduction changes to SCLC of equation (21), (b) in Fig.3.11 is given by

$$V_x = \frac{q n_0 s^2}{\theta \epsilon_r \epsilon_0} \qquad (23)$$

At high fields, due to the increase in the injected charge, the traps become filled and the current rapidly builds up to the trap free value given by equation (20) as shown at

(c) and (d) respectively in Fig.3.11. Lampert [88-91] has considered the subject of SCLC in great detail and has reported SCLC in single crystals of CdS, ZnS, SbS_3, SiC, Ge, GaAs etc. but it is noteworthy that SiO_x has not been mentioned in this context. He has also explained the SCLC in solids with deep traps and with exponential and uniform distributions of traps. Sworakowski [93] has given a detailed theoretical analysis of SCLC for a solid containing shallow traps, deep traps, and traps distributed in the vicinity of the injecting electrode, the collecting electrode and inside the solid.

Murgatroyd [95] has considered the reduction in the effective depth of a single set of shallow traps, comparing Frenkel's model and Hartke's three dimensional model [96] and he pointed out that Frenkel's theory overestimates the effective reduction in trap depth.

Raykerus [94] has investigated SCLC for an insulator with shall monoenergetic traps taking into consideration the decrease in the effective trap depth caused by the electric field and assuming the mobility to be field independent. He used a parametric method for calculating the current at different field strengths using Frenkel's [63] one-dimensional and Hartke's [96] three-dimensional model of traps and found the latter to be more accurate. For low field strengths Child's law (including the effect of traps) is obeyed. For medium and high fields Poole-Frenkel conduction, and for very high fields, when the effective trap depth reduced so much that all the electrons entered the conduction band, trap-free SCLC was obtained.

Other authors [97-99] have investigated SCLC for particular ranges of field and with specialized trap

distributions or for special materials. Shousha and Young [100] investigated the discharge current of Ta_2O_5 capacitors which had previously been held at constant potential. They considered that the SCLC could only constitute an appreciable part of the total discharge current when the applied field was sufficiently low. Brander et al [101] interpreted the conduction in thermally grown SiO_2 films as SCLC modified by shallow traps. For high fields the trap free Mott and Gurney law was suggested.

In a solid with traps an equilibrium is always achieved between the injected charge and the charge which constitutes the current. When the injection level is increased more traps become filled and the quasi-Fermi level (QFL) moves up, representing a different equilibrium. Lamb's calculations [60] of the SCLC for the deep trapping case show an exponential current-voltage relationship. For this he considers an insulator with a uniform distribution of traps. When some of the traps near the Fermi level get filled the QFL moves such that the shift in its position, ΔE , is proportional to the space charge (which is proportional to the applied voltage v)

$$\Delta E = \frac{Q}{q N_t s} \simeq \frac{C V}{q N_t s} \qquad (24)$$

assuming a uniform charge distribution, where Q is the injected charge, N_t the trap density, C the capacitance and s the film thickness.

The free-carrier density is then

$$n = N_c \exp\left[(E_F - E_c)/kT \right] \exp \Delta E/kT \qquad (25)$$

$$= n_0 \exp\left[\Delta E/kT\right] = n_0 \exp\left[CV/(N_t s q kT)\right] = n_0 \exp(t V) \quad \cdots \quad (26)$$

where n_0 is the initial free carrier concentration and

$$t = C/N_t q s kT$$

The density of the trapped charge is given by

$$n_t = \frac{Q}{qs} = \frac{cV}{qs} \qquad (27)$$

and therefore the current density is

$$J = \frac{9}{8}\epsilon_r\epsilon_o\mu\frac{V}{s^2}\left(\frac{n_o q}{c}\right)\exp\left(tV\right) \qquad (28)$$

Sworakowski [93] has considered the effect on SCLC of traps non-uniformly distributed in space. He has obtained general solutions for shallow, and deep trap distributions which in limiting cases become identical to the expressions obtained by others for a uniform spatial distribution of traps or for interface-charge-limited currents.

To conclude, it can be said that from the literature there does not seem to be any definite indication of SCLC in amorphous evaporated films of silicon oxide.

3.2.10 Impurity conduction

Mott and Twose [102] have considered impurity conduction due to the tunnelling of electrons from one impurity centre to the other, when these centres are close enough together for their wave functions to overlap. The total current in an impure insulator is due to the electrons in the conduction band as well as this inter centre tunnelling in the forbidden gap. At low temperatures impurity conduction dominates however. The presence of both the acceptors and donors is thought to be necessary for impurity conduction. Hill [65] has described impurity conduction due to electrons ionized from impurities which are so close to each other that their coulombic potentials overlap. Figure 3.12 shows the situation in an applied field, in which the ionized site may also act as a trap or scattering centre. He calculated

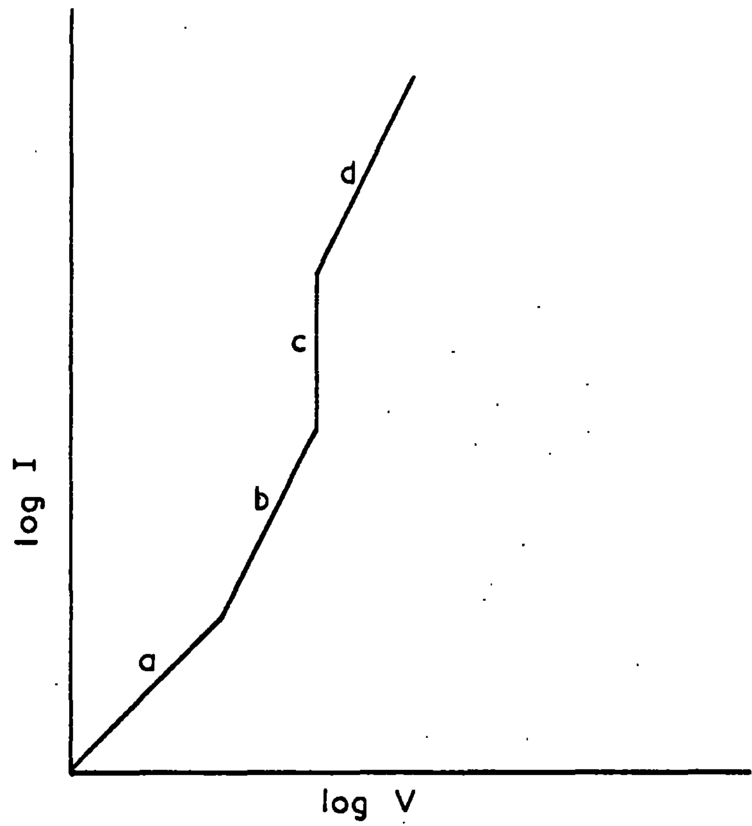

Fig. 3·11 I-V characteristic for SCLC

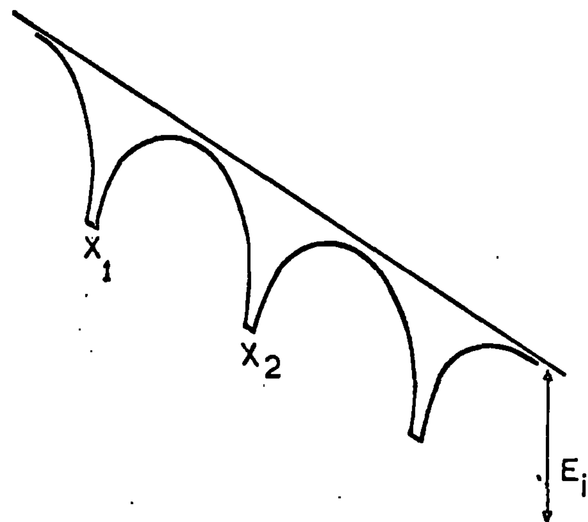

Fig. 3·12 Impurity conduction model after Hill (65)

the current density by assuming that the barrier is increased opposite to the field direction by an amount equal to the decrease in the forward direction and obtained

$$J = -2q\left(\frac{x q \mathcal{E}}{2m^*}\right)^{1/2} \exp\left[-\frac{E_i}{kT}\right] \sinh \frac{q^{3/2}\mathcal{E}^{1/2}\epsilon^{-\frac{1}{2}}}{kT} \qquad (29)$$

where x is the distance between an impurity centre and the position of the carrier when it is just entering the coulombic field of the next ion. E_i is the ionization energy under zero field condition.

Lamb [60] has considered conduction at low impurity levels due to the hopping or tunnelling of electrons from one site to the other. Jonscher [39] has summed up the salient features of hopping conductivity, three of which are:-

(a) linear dependence of current on voltage.

(b) an activation energy much lower than that of the relevant donor or acceptor

(c) monotonic increase of a.c. conductivity with frequency.

V. Ambegaokar et al [103] have reviewed the conductivity equation of Mott [104] for the thermally assisted hopping of electrons between randomly distributed traps. The equation is given by

$$\sigma \propto \exp\left[-(\lambda\alpha^3/\rho_0 kT)^{1/4}\right] \qquad (30)$$

where T is the temperature of the system, ρ_0 the density of states at the Fermi level, λ is a dimensionless constant, and α^{-1} is the distance for the exponential decay of the wave functions. This form of temperature dependence has been obtained in amorphous Ge, Si, C and VO, as referred to in the same paper. These authors have re-evaluated the constants of this equation and found its range of applicability.

3.2.11 Ionic conductivity

The movement of lattice defects or impurities due to the lowering of potential barriers by the applied field gives rise to ionic conductivity. Lamb [60] has calculated the current density due to the hopping of such ions by considering their motion, both in the direction of the field and opposite to it. Bean et al [105], studied the conductivity of tantalum oxide at very high fields and suggested modifications to the simple theory. According to this theory the field both creates the interstitial metallic ions and sets them in motion so that there is a critical field, below which both the number of ions and their mobility are field-dependent and above which only the ionic mobility increases. Harrop and Campbell [42] have divided the ionic conductivity into three field ranges.

(a) For fields less than 10^5 Vcm^{-1}, $\mathcal{E} q l \ll kT$ and the conduction is ohmic and given by

$$J = \frac{c}{kT} \exp - \frac{\phi}{kT} \qquad (31)$$

where l is distance between two sites, c is a constant and ϕ is the barrier height.

(b) For $\mathcal{E} q l \approx kT$, the current density is given by

$$J = J_o \exp \left[- \left(\frac{\phi}{kT} - \frac{\mathcal{E} q l}{2kT} \right) \right] \qquad (32)$$

(c) For $\mathcal{E} q l \gg kT$, no equation is given as the analysis is complex.

It has been pointed out that an activation energy of less than 0.1 eV and a high charge mobility usually indicate electronic conduction, whereas an activation energy greater than 0.6 eV and a low mobility are normally associated with ionic conduction although these are not hard and fast rules.

However, polarization effects in d.c. field (accompanied by an increase in resistivity with time at constant voltage), the transport of actual material and its build-up at the electrodes, and large transit times are all typical features of ionic conductivity.

3.3 Conduction in Films of Silicon Oxide

In this section, existing knowledge of conduction in silicon oxide is reviewed. This is relevant to two aspects of the present work in which:- (a) Measurements were made on the silicon oxide films from which the willemite was formed. These were originally intended as a quality control for the oxide, but the conditions turned out to be different from those of all published work. (b) It was suspected that the conduction in the willemite films could be largely controlled by an underlying residual layer of silicon oxide.

The Electronic conduction through evaporated films of silicon oxide (SiO_x) does not appear to have received attention before the early 1960's and the first detailed investigation seems to have been carried out by Hirose and Wada in 1964-65 [106,107]. Before this date the references on SiO_x are mainly concerned with the dielectric properties and the study of the quality of evaporated films. Here an attempt is made to show the present state of understanding of the subject with the references collected in historical order. A few papers have also been included which point out the difficulties in producing films with reproducible properties and the importance of various parameters which control the reproducibility. Table 3.1 has been prepared to show the evaporation and measurement conditions used in all the references.

Vacuum (Torr)	Partial pressure of O_2	Evaporation source	Rate of evaporation Å/sec	Substrate material and temperature	Electrodes	Subsequent heat treatment	Film thickness Å	Atmosphere for measurements	Reference No.
10^{-4}		W foil boat	0.55-29.5	soda glass and Pyrex (heated)	Al	annealed at 250°C and then cooled in vac. to 100°C before removal	1400-17000	air	108
Uninterrupted $<1x10^{-5}$		Ta, (D)	1-4 and 35	Pyrex, Vycor & microscope slides (heated)	Cu and Al		240-7000	air	120
Uninterrupted $5x10^{-7}$	$1x10^{-6}$ to 10^{-3}	W heated in Ta box	~10-200	sodalime and Vycor (diff. temperatures)	In, Pb, Sn, Al studied but Al preferred&used			air	121
Uninterrupted $<10^{-6}$	10^{-4}	Ta, (D)	10	glass & quartz slides first covered with 5000Å of SiO_x film	Al, Cr, Au studied, but Al used		1000-10,000	dry air	111
Uninterrupted $<10^{-6}$		Ta, (D)	50-60	glass microscope slides	Al		1000-10,000	air	112
Uninterrupted $<2x10^{-6}$	a range of values	Ta, (D)	A range of values	soda lime, microscope slides	Au		10,000, 12,000		122

Table 3.1

Continued

Continued

Vacuum (Torr)	Partial pressure of O_2	Evaporation source	Rate of evaporation Å/sec	Substrate material and temperature	Electrodes	Subsequent heat treatment	Film thickness Å	Atmosphere for measurements	Reference No.
$< 10^{-5}$	A range of values	Ta, (D)	A range of values	Corning 7059 glass substrate(200°C)	Al	annealed in air at 300 & 400°C for 2 hours	in the range of 5000, 6000		109
$<2x10^{-5}$		Mo boat	5,10-20 and 100	glass slides (150°C)	Al		few hundred to 10,000	in a dessicator	123
Uninterrupted $5x10^{-5}$ to $2x10^{-3}$		Ta chimney type source	20	mica glass, borosilicate glass and mono crystalline potassium bromide and sodium chloride	Al	up to ∿120°C studied	5000-20,000	air	110
Uninterrupted a range of values lowest $5x10^{-6}$		Ta boat arrangement	<10 a range of values	Corning 7059 glass	Al	200°C for 10 mins. in vacuum	3800-5500, four batches of different thicknesses	Cryostat wide temperature range	113
Uninterrupted 10^{-6}		silica crucible	20		Al		400-7000	Vacuum 5 m torr	73
Uninterrupted $5x10^{-6}$		Ta	10-30	Glass substrate 150°C	Al		a range of values	in vacuum and in atmosphere	114

Table 3.1

Continued

Continued

Vacuum (Torr)	Partial pressure of O_2	Evaporation source	Rate of evaporation Å/sec	Substrate material and temperature	Electrodes	Subsequent heat treatment	Film thickness Å	Atmosphere for measurements	Reference No.
Uninterrupted $5x10^{-6}$	$3x10^{-5}$	Ta(D)	10	glass ∿70°C due to radiation from the source	Al		4000-10,000	vacuum ∿10^{-6} torr	116
$3x10^{-5}$		Mo boat radiation heated by a tungsten filament	different rates studied	quartz and glass slides	Au,Al	heat treated at different temperatures	10,000-120,000		106,107
Uninterrupted $1-3x10^{-6}$		Ta boat	25	Corning 7059 at 150°C	Al		5000-30,000	Vacuum	117

Footnote: (D) - Dramheller source

Table 3.1 Comparison of experimental conditions from different references "for the production of evaporated films of silicon oxide."

Siddal [108] investigated the preparation and properties of evaporated films of SiO and found that pinholes could be reduced by burnishing an evaporated layer with a Selvyt polishing cloth before depositing a further layer of oxide. Further reduction in pinhole density took place by discharging a 4μF capacitor across the electrodes several times. The surface of the bottom electrode was found to be important in determining the quality of the oxide film and annealing in vacuum prevented or delayed the peeling of the films from the substrate. He studied the leakage current through capacitors of different film thicknesses made by depositing the films at different rates. At 20°C the current was interpreted as due to ionic conduction due to the slow polarization.

The dielectric strength and properties of deposited SiO films for use in capacitors have been studied by several authors. Their conclusions can be summed as follows:-

1. An evaporated oxide film on the substrate before the deposition of the lower metal electrode smooths out irregularities.
2. Aluminium is preferred as the electrode material because of its good surface finish.
3. Substrate surface, electrode surface finish and deposition rate of the oxide all influence the dielectric breakdown and its reproducibility.
4. For reproducible properties, the composition of the film must be accurately controlled; it depends on the deposition rate and the partial pressure of oxygen.
5. The evaporated films may contain Si, SiO and Si_2O_3 depending on the relative impingement rates of SiO and O_2 on the substrate.

6. Heating of the substrate during evaporation helps to overcome cracking and peeling off. Steensel [109] found that the films deposited at a substrate temperature of 200°C did not show cracking and peeling.

7. Nishimura et al [110], have pointed out that, depending on the temperature of evaporation, the films absorb H_2O, O_2 and CO_2 on exposure to the atmosphere.

Hirosė and Wada [107] studied the dielectric properties and d.c. conductivity of vacuum deposited SiO films in great detail. The films had pinholes which were thought to have been due to surface irregularities and dust particles on the substrate. Discharging a 3μF capacitor charged to 100 V was found useful in curing the pinholes. The films were found to be perfectly amorphous and the degree of oxidation was found to depend on the rate of deposition, the atmosphere and on the subsequent heat treatment. It was concluded that highly oxidized films tend to peel off from the substrate, probably due to high internal stresses. For films in the thickness range 1000 to 10,000Å they found three regions in the I-V characteristics, linear below 0.1 V, curving about 0.1 V, but with log I proportional to $\sqrt{V}$ above 10 volts. The ohmic conductivity was approximately $1.5\times10^{-11}\,\mho\,cm^{-1}$.

Hirose and Wada also studied the effects of temperature, different metals and film thickness. The current was found to be electrode independent and bulk-limited. Their voltage-thickness plots for constant currents were straight lines, which showed a uniform field distribution throughout the film. However, these straight lines did not pass through the origin which was interpreted as being due to the presence of aluminium oxide below the electrodes. The ohmic conductivity was thought

to be due to the hopping of electrons and silicon ions. The high-field conductivity was interpreted as due to field-enhanced thermal excitation of electrons into the conduction band - the Poole Frenkel mechanism. In interpreting their results they used a value of 12 for the dielectric constant, which has been subjected to criticism by later workers.

Johansen [111] investigated evaporated films of SiO, 98% SiO + 2% Al powder, 97% SiO + 3% Al powder, and 68% SiO_2 + 32% Si powder over a wide range of temperatures, with different metal electrodes. He found the conductivity to be electrode-independent at room temperature and for fields of 1-5x10^6 volts cm^{-1} it was of the form

$$\sigma = \sigma_0 \exp(\beta\sqrt{\mathcal{E}} - v)/kT$$

where σ_0 is independent of electric field $\mathcal{E}$. The value of β obtained experimentally is 0.21x10^{-4} eV $(m/v)^{1/2}$ compared with 0.18x10^{-4} eV $(m/v)^{1/2}$ for Schottky emission assuming a value of ϵ = 4.5 for the dielectric constant, though this was ruled out because of the electrode-independent behaviour. He therefore suggested that the conduction was due to Schottky emission from Si islands into the bulk SiO_2. The value of β was calculated as for emission from the electrodes, using the dielectric constant of ϵ = 3.8 for SiO_2 giving β = 0.2x10^{-4} eV $\left(\frac{m}{v}\right)^{1/2}$ in close agreement with experiment. For low voltages ionic conduction was proposed with positive oxygen vacancies as the charge carriers since space charge accumulation was proved to occur.

Hartman et al [112], studied films prepared under a variety of conditions using different electrodes and found the electrode independent current to be described by an equation of the form

$$J = \alpha S \exp(\beta\sqrt{V} - Y/kT)\left[1 - \exp(-\beta^2 V)\right] \qquad (33)$$

where α and γ are constants and S is the film thickness. V is the applied voltage, and

$$\beta = S^{-1/2}\left[\psi/kT + \phi\right] \qquad (34)$$

ψ and ϕ are constants. They found that the value of β and the activation energy were inconsistent with Schottky emission, and that the dielectric constant and the slope of the log I versus $\sqrt{V}$ plots were also inconsistent with the Poole-Frenkel effect. They did not reach any conclusion and referred to Frölich's model [62] of a dielectric which was used by O'Dwyer [61] to calculate the conductivity for films of a few hundred to a few thousand Å thickness. This model is shown in Fig.3.6, Section 3.2.6. They calculated a value of 5.8 ± 0.1 for the dielectric constant of their films.

Stuart [73] found evidence for bulk limited conduction in his films and ruled out Schottky emission. He fitted his results to the equation

$$I = I_o \exp\left(\tfrac{1}{2}\beta\sqrt{V}/kT\right) \qquad (35)$$

using Simmon's model of dielectric (Fig.3.8, Section 3.2.7), thereby showing the voltage dependence of the conductivity to be like the Schottky effect and the slopes of the graphs to match the Poole-Frenkel effect. The use of the high frequency value of the dielectric constant has been emphasised, because the emission of an electron is a fast process during which the associated ion remains stationary. Hirose and Wada, and Johansen were pointed out to have used very high and low values respectively for the dielectric constant. Good agreement was found between the experimental and theoretical values of β (Poole-Frenkel) for the films investigated as shown below.

Film thickness Å	expt/theor
425	1.06
1200	1.07
3200	1.09
6400	1.07

Stuart has also shown that this model explains the results of Hirose and Wada and Hartman et al.

Servini and Jonscher [113] have made an extensive investigation of d.c. conduction, photoconduction and thermally stimulated currents in SiO_x films of different thicknesses. These were evaporated using different vacuum and deposition rates. They found four different regions of conduction. At low fields and high temperatures (up to approximately 0.5 V and 297 to 413°K from their diagram) the conduction is ionic ohmic and hydrogen and sodium ions are thought to be the mobile species. Above this field a non-linear dependence of current on voltage is found. Above approximately 3 volts and 167 to 413°K log I versus $\sqrt{V}$ is a straight line which is temperature-dependent. In between these regions the I-V relationship is of the form $I \alpha V^n$ where n is approximately 1.5. The fourth region, at high fields and low temperatures, is independent of temperature. For the region where $\log I \propto \sqrt{V}$ the following equation is proposed

$$I = I_0 \exp\left[q\left(\beta\sqrt{\mathcal{E}} - V_g\right)/kT\right] \qquad (36)$$

where $\mathcal{E}$ is the average field, V_g is the barrier height for thermal excitation and $\beta = \left(\frac{q}{a\pi\epsilon_r\epsilon_0}\right)^{1/2}$

a would be 4 for Schottky emission and 1 for the Poole-Frenkel effect. β was found to be slightly dependent on conductivity and a value of $2.3 \pm 0.1 \times 10^{-5}$ eV $\left(m/V\right)^{1/2}$ was obtained from the slope of log I versus $\sqrt{V}$ plots which agrees

very well with the Schottky effect if the high frequency dielectric constant is 3. In spite of this, these authors believe that the conduction cannot be due to the Schottky effect as it does not explain such high conduction through insulating amorphous films of appreciable thickness, and they consider a modified Poole-Frenkel model as a possibility. A hopping process over field-lowered barriers, in which the carrier is recaptured after thermal excitation, has therefore been suggested.

Timson and Hogarth [114] found an irreversible decrease in the conductivity of approximately 40% on exposure of the film to air. The precise value depended on the evaporation rate on depositing the film. Absorption of moisture from the atmosphere, giving rise to free H^{+} and O^{2-} ions, is thought to be responsible. At low fields (below 10^{6}V/cm) an ohmic and at high fields a Poole-Frenkel type conduction mechanism was considered to be acting.

Adachi and Hariu [115] presented a model of the dielectric containing many Poole-Frenkel sites, which are positively charged when empty and neutral when occupied, to explain bulk-limited conduction over the whole range of the observed I-V characteristics. The results of Stuart [73] were successfully explained by this theory. A value of 5.1 for the dielectric constant was obtained from capacitance measurements.

Navik [116] investigated the ionic conductivity in SiO capacitors by subjecting them to step voltage signals of up to 1.5×10^{6} V cm^{-1} and analysing the slow charge and discharge current-time responses in terms of Debye type polarisation. A linear I-V relationship was proposed for the low voltage region which was space charge free. For

high voltages a conductivity relationship of the form proposed by Johansen was suggested. The capacitors were subjected to applied voltages of 100 volts for up to two years but no electrolytic effects were observed, which proves that the conduction was purely electronic.

Timson and Wickens [117] found that the conduction in their films was ohmic up to approximately 5×10^4 V cm^{-1} and then obeyed equation (36) where β had values between 1.95×10^{-5} and 2.1×10^{-5} eV $\left(\frac{m}{V}\right)^{\frac{1}{2}}$. They proposed a modified Poole-Frenkel model to explain the whole I-V characteristic, assuming a donor level twice the distance of the Fermi level below the conduction band edge. As shown in Fig.3.13 an electron can be directly excited from the donor into the conduction band (process 1) and it can have translational motion after thermal activation (process 2) giving the total current equation

$$I = I_{01} \exp\left(\frac{-V_g}{2kT}\right) + I_{02} \exp\left(2\beta\sqrt{\mathcal{E}} - V_g\right)\Big/2kT \quad \text{———} \quad (37)$$

where V_g is the depth of the donor which was found to be 0.97 eV. They suggested that a true Poole-Frenkel plot of log I versus $\sqrt{V}$ should have the extrapolated ohmic conduction subtracted from it at high fields.

Adachi et al [118] successfully explained their own results and those of Hirose and Wada, Stuart and Hartman et al by proposing a modified Poole-Frenkel model in which the electrons move by a constant release and trap process over many Poole-Frenkel sites. In this paper Adachi [118] has extended the theory briefly proposed previously. The I-V relationship was calculated by considering the motion of the electron both in the direction of the field and

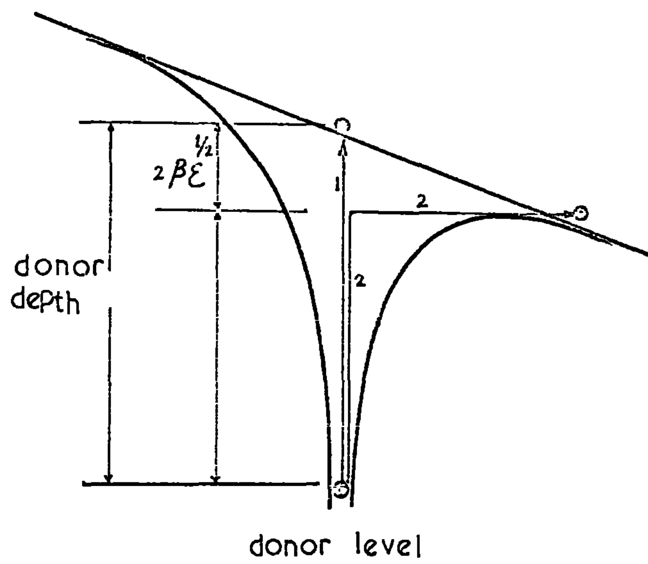

Fig. 3.13 Poole - Frenkel model
Timpson and Wickens (117)

against it, the result being:-

$$J = \frac{\nu\lambda}{2}\left(N N_c\right)^{1/2} \exp\left(-\frac{\phi_{1m}(V)}{2kT}\right)\left[1-\exp\left(\frac{qV\lambda}{2kTS}\right)\right] \quad \text{——} \quad (38)$$

ν is the attempt to escape frequency, λ is the distance an electron moves between release and re-trapping, N is the density of the Poole-Frenkel sites, and N_c is the density of states in the conduction band. Also

$$\phi_{1m}(V) = \phi_o - 2(1.25)^{1/2}\left(\frac{2.43\alpha}{\lambda^2} + \frac{qV}{S}\right)^{1/2} \text{ for } (\lambda > x > 0) \quad \text{——} \quad (39)$$

where ϕ_o is the depth of the Poole Frenkel sites from the bottom of the conduction band. ϵ_h is the high frequency dielectric constant, and $\alpha = q^2/4\pi\epsilon_h\epsilon_o$

The following values for the different constants were obtained:-

$$\nu = 10^8\, s^{-1}, \quad \lambda = 100\,\text{Å}, \quad N = 10^{18}\, cm^{-3}, \quad \phi_o = 1eV, \quad T = 295°K$$

It can be concluded from the above discussion that it requires strict control of the conditions of evaporation to produce SiO films with reproducible properties. The properties of the deposited films also change on exposure to the atmosphere, which is an additional factor affecting the results. The value of the slope of the log I versus $\sqrt{V}$ plots (β) is usually lower by a factor of 1.5 to 2 than the expected value. The low-field conduction in SiO films is ohmic but the high-field conduction is bulk-controlled and based on some form of Poole-Frenkel mechanism. An intermediate region between the two has not been well studied. Simmons [119] proposed a band model of the dielectric after examining six possible combinations of donor, acceptor and Fermi levels and he formulated a theory of the transition from electrode-

limited to bulk-limited conduction processes in metal-insulator-metal systems. He successfully applied his theory to the results of Hirose and Wada, Hartman et al and of Stuart. However, the transition voltage required for the above theory has not been found in any of the experimental work.

CHAPTER 4

SAMPLE PREPARATION TECHNIQUES

4.1 Introduction

In the course of this work thin film metal-oxide-metal (MOM) and metal-oxide-willemite-metal (MOWM) structures were fabricated on both silica and sapphire substrates. In all cases a base electrode film of platinum was first deposited on to the substrate by sputtering, followed by vacuum evaporated films of silicon monoxide and manganese activated zinc fluoride (ZnF_2:Mn) deposited through suitable masks. The films were then baked at a high temperature to convert the fluoride section into the phosphor willemite [3]. Top contacts of aluminium, gold or indium were added by evaporation of the particular metal or, alternatively platinum contacts were deposited by sputtering. However, most of the samples had only aluminium top contacts.

Since the fabrication process included the baking of the samples at high temperatures (described in detail in Section 4.4) the choice of the substrate material and the base electrode metal was very restricted. Due to the low cost and ease of availability of polished fused silica, the work was started and continued for more than a year with this substrate material. However the combination of the platinum base electrode and the silica substrate did not really prove to be successful because of the problem of cracks which were present on every sample. The consequent lack of reproducibility (Section 5.1) gave considerable problems even with the best processing treatment that could be developed. Hence after a few test samples made on sintered alumina substrates, the substrate material was changed to sapphire in all the

later work, and samples made with this were much more successfully used.

Full details of each stage of the fabrication procedure are given in the various sections of this chapter because of the ever-present possibility of the results being affected by impurities or structural defects in the films.

4.2 Sample Geometry

Figure 4.1 shows an exploded view of the standard type of test sample used in this work. Figure 4.2 shows the different stages used in their production and Figure 4.3, a cross section of one of the later samples.

In the earlier work, the 16x10 mm rectangular substrates were cut in the Department from optically polished circular discs of silica. The platinum film base electrode of 3000Å thickness (not accurately controlled) and 12x6 mm area was deposited after extensive cleaning of the substrate. The silicon oxide films were deposited over an area of 8x5 mm and a range of controlled thickness was used. Zinc fluoride films which were deposited on part of the oxide area also varied in thickness from sample to sample. The area of 4x3 mm on the earlier samples was changed to 5x4.5 mm on the later ones.

4.3 Vacuum System

All the films were deposited in a high quality conventional vacuum system which could be adapted to either evaporation or sputtering. The system was based on an earlier one which had been built in the Department and a great deal of time was spent in improving its performance in order to

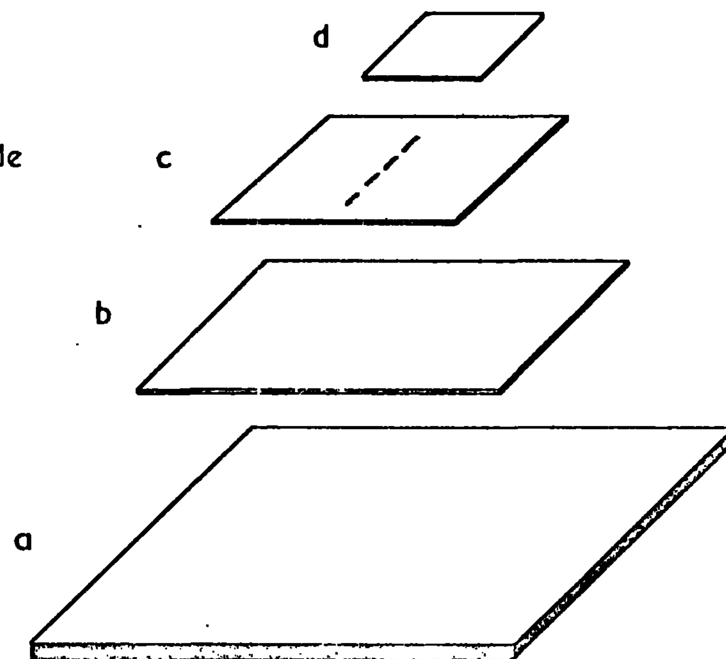

Fig. 4·1

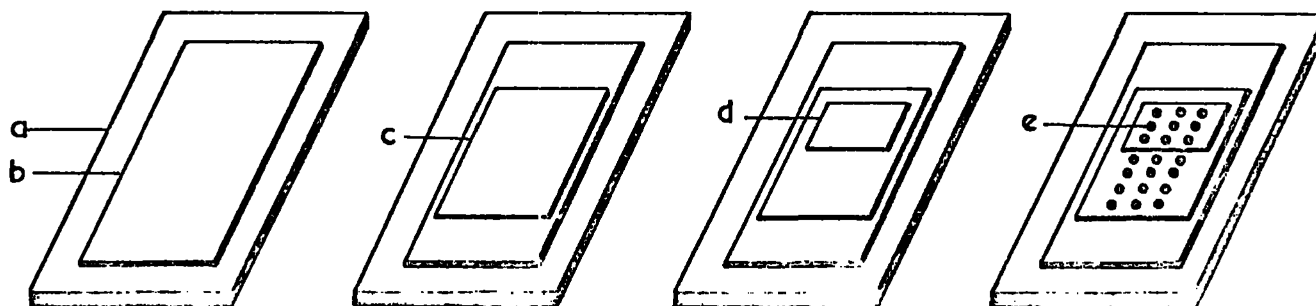

Fig. 4·2 Stages in sample preparation

a Top contacts
b Willemite
c Siliconoxide
d Platinum
e Substrate

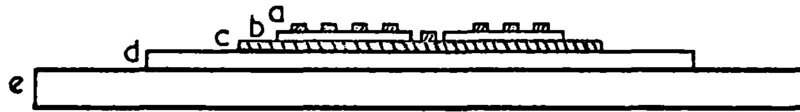

Fig. 4·3 Schematic cross-section of sample.

deposit the films in the best possible conditions. The final system was believed to be largely free of hydrocarbon vapours and it could achieve an ultimate of 3×10^{-7} torr with a degassing rate of better than 1×10^{-5} torr/s. Except for SiO, films of other materials could be evaporated in a genuine vacuum of 2×10^{-6} torr. These figures probably represent the ultimate which an oil diffusion pumped, Viton sealed system is capable of and they were not easily achieved.

4.3.1 Description

Figure 4.4 shows a block diagram of the vacuum system. The Pyrex bell jar (29 cm diameter, 35 cm height) was evacuated by an Edwards 4" oil vapour diffusion pump series EO4 Model B9O3, through a liquid nitrogen trap. The trap was connected to the bell jar base-plate via a quarter swing butterfly valve. The diffusion pump was backed by an Edwards rotary pump model ES2OO. To keep the system free from rotary pump oil vapours, a foreline trap with alumina balls was installed in the backing line. Silicone 7O4 oil was used as the diffusion pump fluid. The gases from the rotary pump outlet were passed through an oil mist filter before emission to ensure that the laboratory atmosphere around the bell jar was free from oil mist.

The pressure in the bell jar was measured with an Edwards IG2HB ionization gauge mounted in the base plate, and the backing pressure was measured by a Pirani gauge. A needle valve was used for the controlled admission of high purity argon for sputtering. All high vacuum parts of the system were eventually sealed with Viton 'O' rings. Internal parts were made of stainless steel and kept immaculately clean with trychloroethylene and acetone, and baking at 95°C

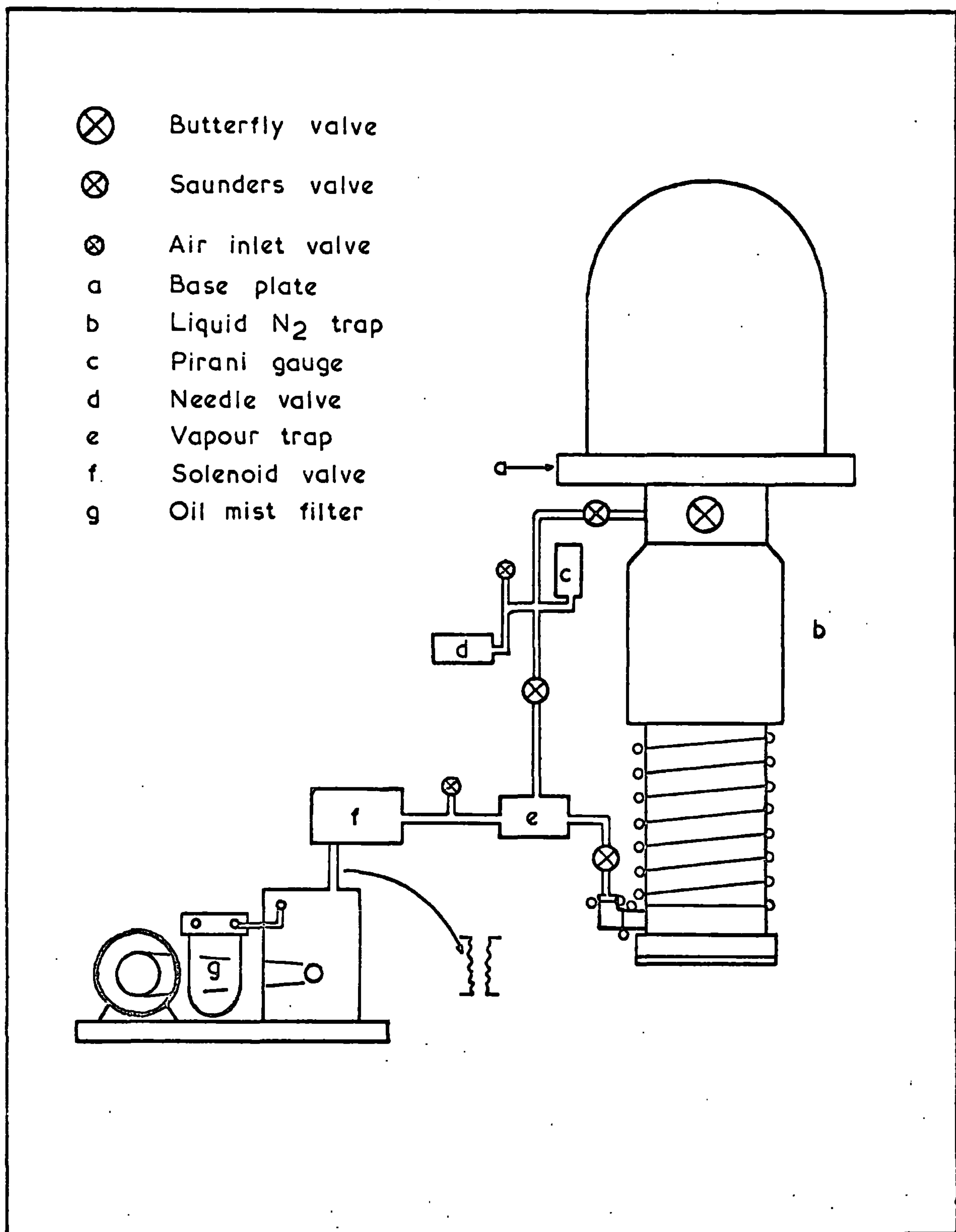

Fig. 4·4 Block diagram of the vacuum system.

before assembly. The bell jar was kept clean by regular washing with concentrated acid solution followed by degreasing with trychloroethylene and acetone and drying with a hot air blower. The Viton seals were wiped clean and moistened with high vacuum silicone grease before use. The system was always kept under vacuum and pumped regularly.

The facilities for evaporation and sputtering inside the bell jar are described in Section 4.4.3. They used power supplies built in the Department. A general view of the vacuum system and power supplies is shown in Plate 1.

4.3.2 Development of vacuum system

The vacuum system described in Section 4.3.1 was developed to this form over about a year. It initially used a 2" Edwards diffusion pump model EO2 backed by Edwards ES35 rotary pump with a 2" liquid nitrogen trap between the diffusion pump and the base plate. A water cooled baffle valve Edwards Model QSB4 was fitted to isolate the vacuum. Also the arrangement of the backing line from the rotary pump to the base plate was initially quite different. This pump system was used to evacuate the same bell jar but with a different arrangement of lead-throughs in the base plate and it gave an ultimate vacuum of about 3×10^{-6} torr after long pumping periods, measured with an Edwards ionization gauge Model 1G2MA (later replaced). Also the pressure rose rapidly when the bell jar was isolated from the pump by closing the baffle valve giving a gas evolution rate of 0.34 lusecs. This performance was thought to be very unsatisfactory for the fabrication of the intended test samples which, it was hoped, would have reproducible characteristics if produced in sufficiently good

Plate 1 General view of the vacuum system and power supplies.

conditions. Hence a systematic procedure was followed to eliminate leaks and degassing sources in the system [124]. Changes were measured from the time required for the pressure to rise from 2 to 10×10^{-5} torr after closing the baffle valve following a fixed pump down time. This procedure led to the replacement of a number of rubber 'O' rings by Viton 'O' rings, improved cleaning procedures for the baffle valve and base plate fixtures, replacement of the whole backing line by an improved design using a Saunder's valve at the entrance to the bell jar, and the replacement of the ionization gauge by an Edwards Model 1G2HB in an improved mounting. After these changes the system could quickly reach a steady ultimate of 1.5×10^{-6} torr with a reduced degassing rate of about 0.02 lusecs. Even this performance did not meet the cleanliness and vacuum conditions aimed at, so that the small pumps and trap were eventually replaced by the 4" system described in Section 4.3.1.

4.4 Sample Fabrication

4.4.1 Mask production

The areas of the various films deposited on the samples were defined by masks, which were produced from 0.005" thick copper sheet. Master drawings, seventeen times the size required for the top contacts and four times for other films, were made and photographically reduced to the right size. Copper masks were produced from these negatives using standard photolithographic techniques. The final masks were cleaned and degreased before being stored in separate paper envelopes ready for use. The handling was done with cleaned stainless steel tweezers.

4.4.2 Substrate cleaning

As described in Section 4.1 silica and sapphire substrates were used for sample fabrication. Since the silica substrates were obtained by cutting from discs on a diamond saw, they were probably contaminated by wax, proteins, diamond saw dust and oil apart from airborne dust and lint. The cleaning process used consisted of holding the rectangular substrate in a silica frame (specially made to prevent the substrate's surface from being scratched by rubbing against the walls of the beaker) and agitating ultrasonically in a range of liquids. Carbon tetrachloride was used first for dissolving remnants of black wax. After this the substrate was washed successively in Teepol, water, concentrated nitric acid, water, sodium hydroxide solution, deionized water and isoprophyl alcohol. Then after a final wash in Electronic Grade methanol, the substrates were stored in the same solvent until loaded into the substrate holder in the evaporator.

For sapphire substrates, which were already supplied as 1.3x1.9 cm rectangles by Adolf Meller Co. U.S.A., the following cleaning process was found to be satisfactory:-

The substrate was held in the silica holder and agitated in the ultrasonic bath successively in Teepol, deionized water, isopropyl alcohol, Electronic Grade methanol, Electronic Grade trichlorethane before final washing and storage in Electronic Grade methanol. This and the final loading into the substrate holder, was carried out in a laminar flow cabinet in filtered air. Hot air from a blower inside the cabinet was used to dry the substrates just before loading.

4.4.3 Deposition of films

(a) Sputtered base electrode

Sputtering in a glow discharge was used to deposit the platinum base electrode film [125,126]. Of the different electrode arrangements described in the literature a fairly simple one was used [127,128], in this work as shown in Fig. 4.5. The cathode (target) was a solid lump of Pt:40%Rh, about 1 cm diameter and 0.5 cm thick, suspended 2.1 cm above the earthed stainless steel substrate holder. The main problem with this arrangement was to confine the discharge to the cathode itself. Although insulating shields are not usually preferred for this purpose, a glass tube was successfully used here to carry the H.T. wire up to the target from the electrode post. The inside of this tube became coated with the wire material [129], and had to be replaced after a few runs to remain effective. The cathode lead through the base plate, electrode post, was shielded by a metallic earthed cylinder up to the point where the wire took over. This arrangement gave satisfactory performance for sputtering platinum although cooling the target would be necessary for lower melting point metals [130].

Films deposited by sputtering in argon were smooth and shiny and appeared to be free from defects. However, they cracked and partly peeled off the silica substrates during a high temperature bake. This indicated that the fabrication of a sample on a silica substrate with platinum and silicon oxide films might be quite a problem, due to differential thermal expansion. However, the lack of choice of alternative materials made it worthwhile trying to overcome the difficulties. Since metallic films which form

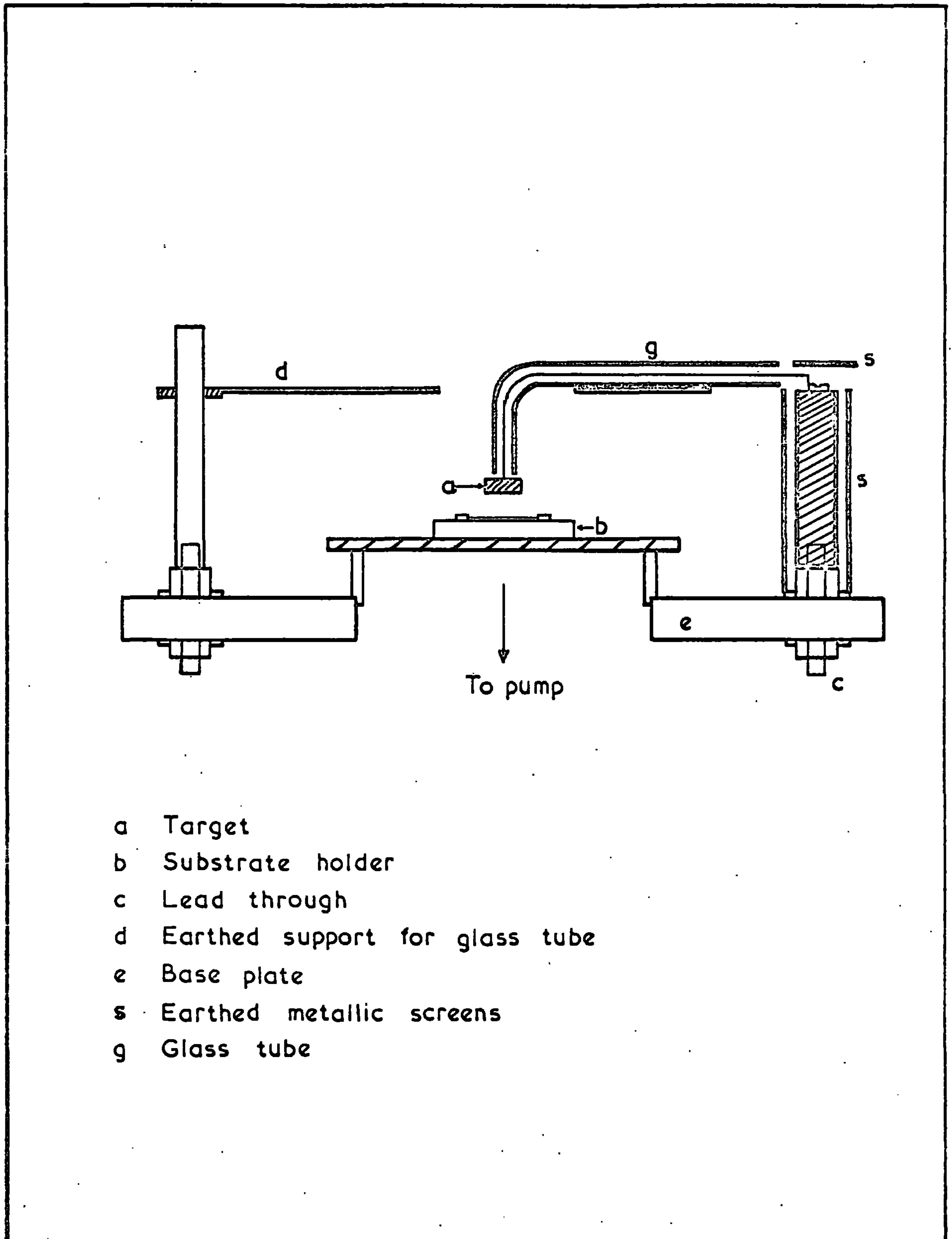

Fig. 4·5 Sputtering arrangement

either an oxide or some other form of chemical bond at the interface between the film and the substrate usually stick well to the surface [131-133], a better procedure was to sputter the platinum in air for the first seven minutes to get an oxide mixed deposit before sputtering it in argon [127]. The air pressure required was about 0.15 torr with 1.5 kV applied. This gave a light brownish deposit of a few hundred Å thickness after which the bell jar was re-evacuated to a steady pressure of about 5×10^{-7} torr. Argon from a cylinder of high purity grade (BOG) was allowed in to a pressure of approximately 0.05 torr through a nylon tube and the needle valve, and the main sputtering was carried out at approximately 2 kV, 5 mA d.c. At this voltage the target to substrate distance was about twice the width of the Crook's dark space as required to get a high deposition rate [130]. This gave a platinum film of about 3000Å thickness in 30 minutes. The platinum disc reached a dull red heat after this time and hence, to avoid excessive contamination of the film, fresh argon was bled in every 10 minutes, with the diffusion pump throttled to keep the pressure,and hence the current, constant.

(b) Evaporated films

Silicon monoxide (Vacuum Deposition Grade obtained from Semi Elements Inc. U.S.A.) was deposited by evaporation on to a selected area of the platinum film defined by a mask, followed by another deposition of 1% manganese-activated zinc fluoride (ZnF_2:Mn) on a smaller area as defined by a second mask.

The structural appearance and the stresses in the final willemite films were found to vary with the temperature and rate of evaporation of the oxide. As described in

Chapters 5 and 6, four series of samples were made on silica substrates and six individual samples on sapphire. The temperature and rate of evaporation of the oxide used in the fourth and subsequent series appeared to be the most successful and will therefore be described first.

The SiO was evaporated at an initial pressure of less than 1×10^{-6} torr which increased to about $2-3 \times 10^{-6}$ torr during evaporation. At $1200^{\circ}C$ the deposition rate was about $6Å$/sec for a source to substrate distance of 11 cm. The total thickness deposited varied from 1000 to $1400Å$. A tantalum box source obtained from R.D. Mathis Co. was modified for the above evaporation by adding baffles and a chimney, as shown in Fig.4.6. The source temperature was measured approximately using a platinum rhodium thermocouple, which was spot welded to the back of the box. The above mentioned conditions for the evaporation of SiO were reached after a series of experiments described below.

The evaporation of oxide on all the earlier samples was carried out at an indicated source temperature of $1130^{\circ}C$. In some initial trials the box source was fitted with half-height baffle strips only. Although the SiO powder was loaded in the two side sections of the partitioned box only, it was found that a few particles were ejected when the source was heated and these spoiled the deposited films. The height of the baffles was therefore increased which cured the problem and reduced the rate of evaporation. Other problems of the films peeling off were overcome with improved cleaning techniques but the cracks and the lack of reproducibility of electrical measurements on the oxide films were hardly affected.

It was thought that these problems were due to stresses in the oxide films in addition to the mismatch between the coefficients of expansion of the oxide and platinum [134], and that the former might be overcome by evaporating the oxide at a higher temperature. An indicated temperature of 1263°C was therefore used for the samples of this third series. This necessitated using a platinum rhodium thermocouple as the temperature was above the limit for chromel alumel. At this temperature the baffles tended to move inside the box so that they had to be spot welded in place. At the same time the chimney was added to the source to further reduce the rate of evaporation. As described in Chapter 5 the oxide films then appeared to be free from defects and better than the previous films. However, in the course of the high temperature willemizing bake, the films now cracked into small pieces. To try to overcome this a compromise evaporation temperature of 1200°C was tried because the literature recommends 1150-1250°C for the evaporation of defect free silicon oxide films. Although the oxide was successfully evaporated at this temperature, as described in the beginning of this Section, ~~but~~ it is still felt that for producing oxide films with more reproducible properties, better control over the temperature of the source and the evaporation rate is desirable.

The ZnF_2:Mn (zinc fluoride) was obtained from Levy West & Co., and was evaporated at a temperature of 855°C from a platinum pepper pot source at a pressure of less than 1×10^{-6} torr which increased to about 1.5×10^{-6} torr during evaporation. The deposition rate was 1 to 1.5 Å/sec. The temperature was indicated on a Honeywell temperature controller

using a chromel alumel thermocouple, spot welded to the back of the dimple in the evaporation source. The temperature and rate of evaporation were selected after some preliminary work on deposition on glass slides. The melting point of ZnF_2 is 872°C and it has a vapour pressure of 3.7×10^{-1} at about 868°C, while the melting point of MnF_2 is 930°C and its vapour pressure is 3.7×10^{-3} torr at 868°C. The cathodo-luminescence of the deposited films showed however that both constituents evaporated satisfactorily.

With the pepper pot source (shown in Fig.4.7) it was difficult to keep the rate of evaporation even within the limits of 1-1.5 Å/sec because of lack of precise temperature control and the fitting of the cover on the source. If slightly loose, the cover would be cooler than the dimple itself and the ZnF_2 would then tend to condense and block the holes in the cover reducing the rate of evaporation.

4.4.4 Willemite conversion reaction

After the deposition of the ZnF_2 films the samples were baked for fifteen minutes at about 955°C in a long silica tube furnace in a flow of 0.3 litres/min of dried and filtered oxygen. This made the fluoride and oxide react to produce the phosphor willemite. The temperature of the furnace was controlled by an Eurotherm controller. For the first series of samples a ten minute bake at 1100°C was used.

The thermal expansion problems which were shown up by cracks etc. were solved by changing this to fifteen minutes at 955°C, which did not appear to make any significant difference to the quality of the phosphor produced. Heating of the furnace to 955°C with the sample inside, where it

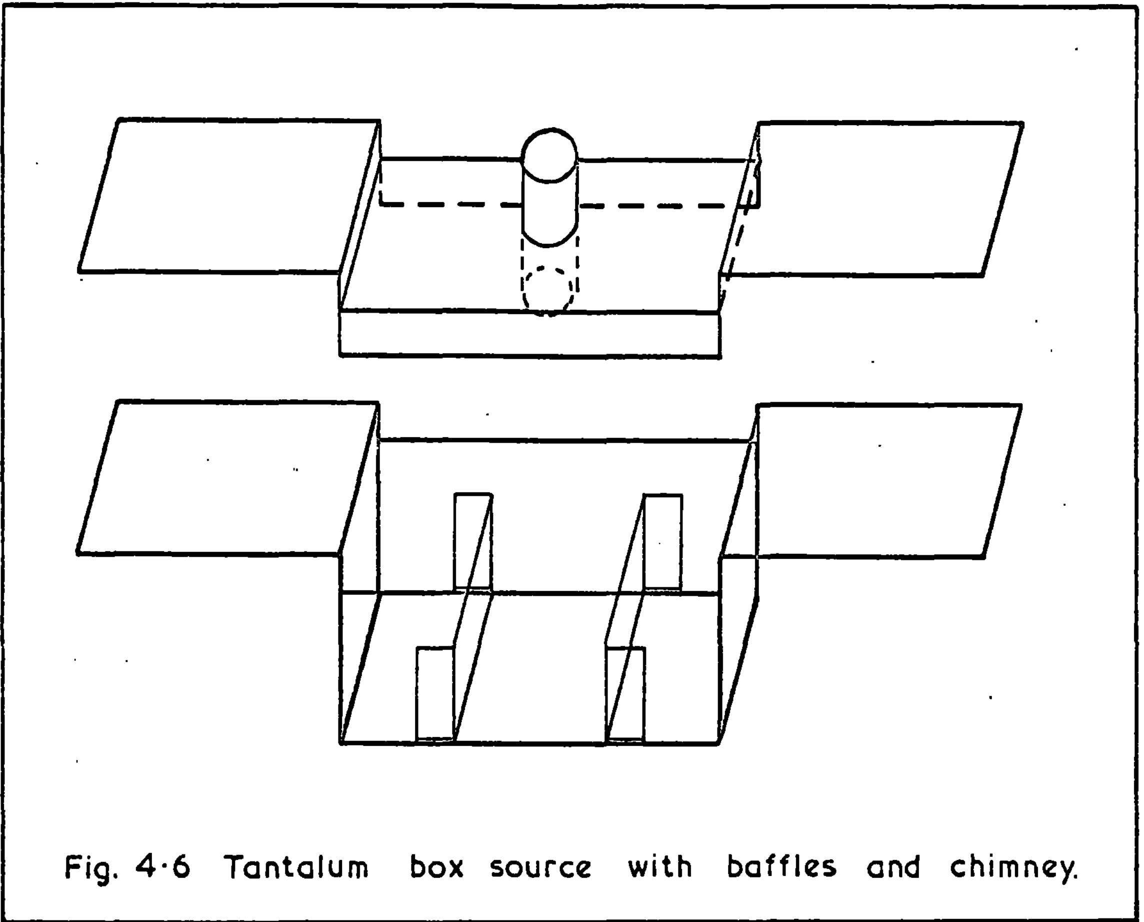

Fig. 4·6 Tantalum box source with baffles and chimney.

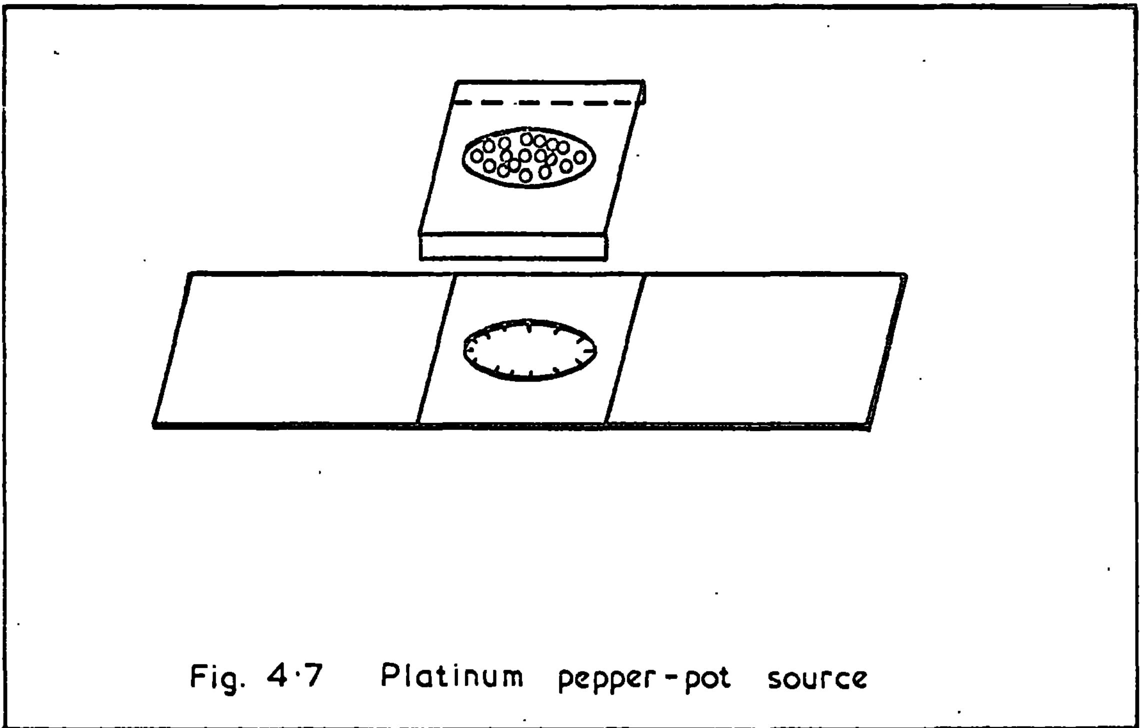

Fig. 4·7 Platinum pepper-pot source

was kept for fifteen minutes, and then leaving the sample to cool to about 100°C in the furnace, was found to be a good procedure which was followed as a standard after the first series of samples. The furnace took about 30 minutes to heat up and 1 hour to cool.

In the course of work it was noticed that neither the proportions of oxide to fluoride, nor the baking temperature were critical for producing the willemite phosphor. Examination of its cathodoluminescence with the naked eye did not show any significant difference in the brightness of the film produced in different conditions. This confirms other work done in the Department. The only case when a decrease in the brightness was noticed was for films less than 200 Å thick.

The mechanism for the formation of willemite may be as follows. It is thought that at the temperatures used for baking, the molten zinc fluoride reacts with the oxide surface to initially form small blobs of willemite. These probably coalesce to form an uneven surface and the reaction continues through this layer of willemite until it becomes sufficiently thick to stop the further diffusion of zinc. Alternatively the zinc fluoride may evaporate from the surface so terminating the reaction. Silicon oxide films of the type produced here are known to consist of a mixture of SiO, SiO_2 and Si [135,136]. The chemical reaction which is assumed to take place during the bake can therefore possibly be represented by equation of the form

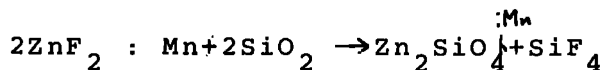

$$2ZnF_2 : Mn + 2SiO_2 \rightarrow Zn_2SiO_4{:}Mn + SiF_4$$

4.4.5 Top contacts

Aluminium top contact dots were used on all samples although some also had gold, indium and/or platinum top contacts. These contacts were deposited through a copper mask on both the oxide and willemite sections of the sample. Each of the early samples had 21 dots of 0.05 cm diameter. On the fourth and all later series of samples the area of the dots was reduced to decrease the number of defective ones. A new mask gave 32 dots each of 0.04 cm diameter. For the aluminium top contacts five nines purity starting material was deposited by evaporation in a vacuum of better than 1×10^{-6} torr from multistranded tungsten filaments. High purity gold was evaporated from tungsten baskets and high purity indium was evaporated from a molybdenum boat to form top contacts of these two metals. The method for the deposition of the platinum top contacts was the same as used for the base film, except that the first step of sputtering in air was excluded.

The reference system followed for numbering the dots on all samples consisted of naming the rows alphabetically and the columns numerically. The counting was always done by keeping the willemite on the left; hence the dot on the top left hand corner of every sample was 1 AW. With the first contact mask described above there were three rows and seven columns, and on the second, four rows and eight columns. Hence a dot on the oxide on the bottom right hand corner on one of the later devices is referred to as 8DO.

4.5 Sample Measurement Techniques

4.5.1 Visual observations

As described in Chapter 5 the films on earlier

samples did not stick well, and showed cracks and buckling when examined with the naked eye. However, as the mechanical properties of the films improved, it was necessary to examine them under the microscope and that was only done when the sample was ready for electrical tests. This was to prevent the samples from collecting dust during handling.

The phosphor quality of the willemite films was tested by bombarding them in a high-frequency glow discharge and observing the brightness of their cathodoluminescence.

Film thicknesses were measured using a Watson 16x interference objective which was capable of measuring thicknesses down to 300 Å with some judgment. The films were sufficiently reflecting and did not need metallizing to see the fringe shift at the edge.

4.5.2 Electrical measurement

The I-V characteristics of the films were measured using a Vibron electrometer Model 33C (Electronic Instruments Ltd.) and a Farnell stabilized power supply Model L-30BT. The measuring circuit is shown in Fig.4.8. For higher ranges of the measuring resistor, the voltage across the sample was corrected by deducting the voltage drop across the Vibron from the applied voltage. In making the measurements the voltage was increased in small steps allowing a predetermined time for the current to decay to a steady value each time. The time between steps depended on the measuring resistor in use, 5 minutes for $10^{11}\Omega$, 3 minutes for $10^{10}\Omega$, and 2 minutes for $10^{9}\Omega$. One minute was given for $10^{8}\Omega$ but for the lower values of resistors no time was given.

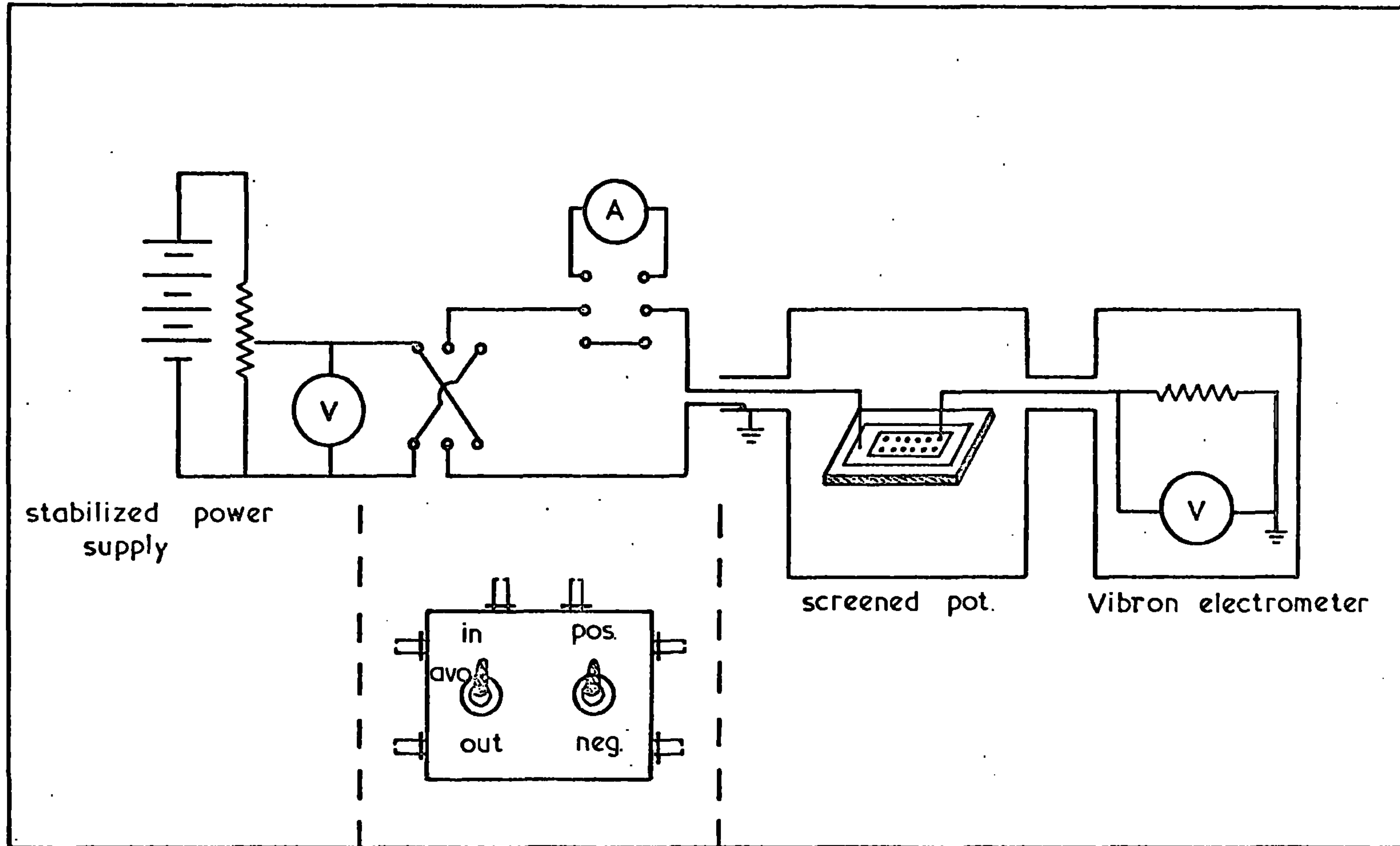

Fig. 4·8 Circuit for I–V measurements.

For probing the device a special apparatus was developed with a small x-y stage inside a circular enclosure, which could also be partially evacuated. This is shown in Fig. 4.9. The connection to the base electrode film of the sample was made with a brass clip, and that to the top contact dot was a micromanipulator probe with a gold wire and made by Research Instruments Ltd.

Fig.4.9 A view of the complete probing apparatus

CHAPTER 5

RESULTS FOR SAMPLES ON SILICA AND SINTERED ALUMINA SUBSTRATES

5.1 Description of Samples

The samples described in this Chapter were made on silica substrates, except for the last two which were on sintered alumina. These two samples were very useful in deciding on the choice of the very expensive sapphire substrates for later work, the results of which are presented in Chapter 6. The silica substrate samples have already been described in general terms in Chapter 4 in connection with the fabrication techniques.

Four series of samples were made on the silica substrates, and each series under a different name represents one major change in the fabrication methods, and one further attempt towards the production of better and reproducible samples. The first series of eleven samples, A_{7-1} to A_{7-11}, (so called because seven samples were made earlier on unpolished glazed silica substrates which are not included here) represents the early stages of the work in which some of the basic methods of device fabrication were established (Section 4.4). Based on these principles six samples, A_{18-1} to A_{18-6}, were made to study the effects due to the changes in cleaning, sputtering and baking procedures. In the third series only three samples HT_1 to HT_3 were made as the high temperature used for the evaporation of oxide on these samples did not prove successful. The fourth series with slightly different cleaning procedure and medium temperature oxide evaporation appeared to be much more successful than all the previous ones right from the start and hence eleven samples were made, which were called MT_1 to MT_{11}. The last three of the samples in this series were test samples, two of which were made on pressed sintered alumina

claimed to have a surface roughness of approximately 3 μ inches. Although the films on this sample did not crack or crinkle, they appeared to be dull and frosty to the naked eye and hence this sample was not completed. The next sample in this series was made on a polished sintered alumina substrate to which the films adhered well with a shiny surface so that it was completed and tested electrically.

In all the samples made, it was suspected that a thin layer of oxide remains under the willemite. In an attempt to eliminate this the last sample made on a silica substrate had the zinc fluoride deposited before the oxide. The standard bake was then given to see whether willemite films could be produced by this process. However this experiment was completely unsuccessful as the film erupted like a bubble during the bake probably due to the melting of the zinc fluoride below the oxide film.

The standard procedure used for sample fabrication in the fourth series was found to be very satisfactory and this procedure was therefore followed in the work on sapphire substrate samples described in Chapter 6.

5.2 Visual Examination of Samples

To assess their mechanical quality the films on all samples were examined under the microscope. The problems associated with the earlier samples were so grave that it was necessary to examine each film before proceeding for the next step, in spite of the ever present danger of the surface of the film collecting dust particles while under the microscope. On the first seven samples from the first series, flakes of the films peeling off the substrate were visible to the naked eye. However by the end of the first series this was overcome

by making changes in the cleaning, sputtering and baking procedures and the samples in the second series were free from defects, to the naked eye although cracking and crinckling of the film could be seen under the microscope. A high temperature was used to evaporate the oxide for the samples of the third series (Section 4.4.3) but it gave worse results and the oxide films were badly cracked after the willemizing bake. The evaporation temperature was again changed, and the samples in the fourth series had many fewer defects. The very fine network of cracks could be seen only under x200 magnification. Two samples were made on alumina in this series and their films appeared to be free from all the mechanical defects which were present on silica substrates. However the polishing lines on the polished alumina substrate were visible through the films and even through the top contacts. Willemite films of different thicknesses were produced in this range of silica substrate samples by evaporating different proportions of fluoride and oxide. The quality of the phosphor produced was judged by observing the relative brightness of the cathodoluminescence with the naked eye. The results are described in Section 5.6.

At the end of the electrical measurements almost every willemite dot was examined for electroluminescence by applying voltages up to the breakdown value. Table 5.1 has been produced to summarize the results of the above observations on all samples. Willemite was removed from one of the silica substrate samples in a controlled etch of dilute acetic acid in order to estimate the depth of reaction of the fluoride with the oxide. After confirming (by testing for cathodoluminescence) that the willemite had been removed the sample was examined under the microscope. This showed that there were no depressions or other marks on the surface of the oxide

	BEFORE BAKE			AFTER BAKE				
	Pt film	Oxide film	Fluoride film	Pt film	Oxide film	Fluoride film	Cathodo-luminescence (CL)	Electro-luminescence (EL)
First series earlier	lifting during film depositions but smooth and shiny before	shiny but with platinum lifting	same as oxide except for colour difference	buckling and lifting	breaking into chips	same as oxide	usually bright green	not tested
later	smooth and shiny, some lifting at the edges	smooth and shiny, some had pinholes	similar to oxide	frosty at the edges and some cracked all over	films mostly not lifting, but cracks on some could be seen with naked eye	some similar to oxide some flaking off	same as above	not tested
Second series	smooth and shiny	smooth and shiny as above	similar to oxide	better than the last ones	cracks still present but perhaps less dense	similar to oxide		one sample gave weak EL
Third series	smooth and shiny	smooth and shiny, appeared to be very reflecting		area under the oxide affected	badly cracked and peeled off	same as oxide	not examined	not tested
Fourth series	all smooth and shiny	smooth and shiny to the naked eye	same as oxide	smooth and shiny a few showed signs of peeling at the edges fine pattern of cracks visible on some samples	incidence of cracks very variable not noticeable to the naked eye	similar to oxide	higher brightness for thicker samples	three samples gave weak EL

Table 5.1 Results of visual observations on silica and alumina substrate samples.

from which the 600Å of willemite was removed so that there had been negligible attack by the reaction.

The following two reasons, together or separately, may be responsible for the above result.

(a) As described in Section 4.4. it is possible that during the conversion bake the fluoride reacts just with the surface of the oxide by melting and forming grains, which are too small to be seen through the optical microscope.

(b) The oxide outside the willemite area may evaporate by a small amount during the bake (e.g. measurements on the oxide of sample MT_1 show a decrease in this thickness after the bake) so that after the removal of the willemite, there is no step between the two areas.

5.3 Results for the Silicon Oxide Films

All of the samples prepared had a section of oxide which was not converted into willemite and this contained some top contact dots. Hence whenever possible, measurements were ~~were~~ made of the I-V characteristics of the oxide to compare different thicknesses, and films evaporated at different temperatures. This was done to check the quality of the oxide and to compare the results with the published work and with the willemite measurements on the same sample. Unfortunately because of the ever present problems of the film cracking, the quality of the films could not be accurately assessed. Furthermore the present oxide films had been subjected to a high temperature bake which accentuated the mismatch with the substrate. All the deposited oxide films described in the literature were either directly evaporated or have been annealed at comparatively low temperatures (about 300°C).

Also, none of these films appear to have been deposited on platinum probably because of the mismatch between the coefficients of expansion.

Since the emphasis of this work was on making good quality films of willemite, the characteristics of the accompanying oxide were only measured for those samples in which the willemite had reasonable physical and electrical properties. A selection of the better results is presented here and the more incomplete and scattered results have been excluded. The samples of the fourth series had 20 top contact dots and the rest of the samples had 12 dots on the oxide. The dots were always of aluminium except on some samples of the fourth series where they were as specified. Almost all of the results of the first series of samples were very disappointing; the variation of current with voltage was extremely unstable and irregular. Curves for two samples measured with a positive voltage applied to the base electrode are shown in Figure 5.1.

The results of the second series were better than for the first, corresponding to the improved appearance of the samples, and the current fluctuations were reduced by a fair amount. However, the oxide films appeared to be porous and they also gave long decay times for every step of increasing voltage. The films broke down at low voltages and gave irreproducible characteristics. From the six samples only five dots could be measured and these are shown in Figure 5.2.

The first sample of the third series was almost completely destroyed when the oxide, which initially looked much better than previously, flaked off during the bake. To overcome this problem the oxide was evaporated at a reduced rate for the remaining three samples of this series on which the films did not break as badly. Some I-V measurements are

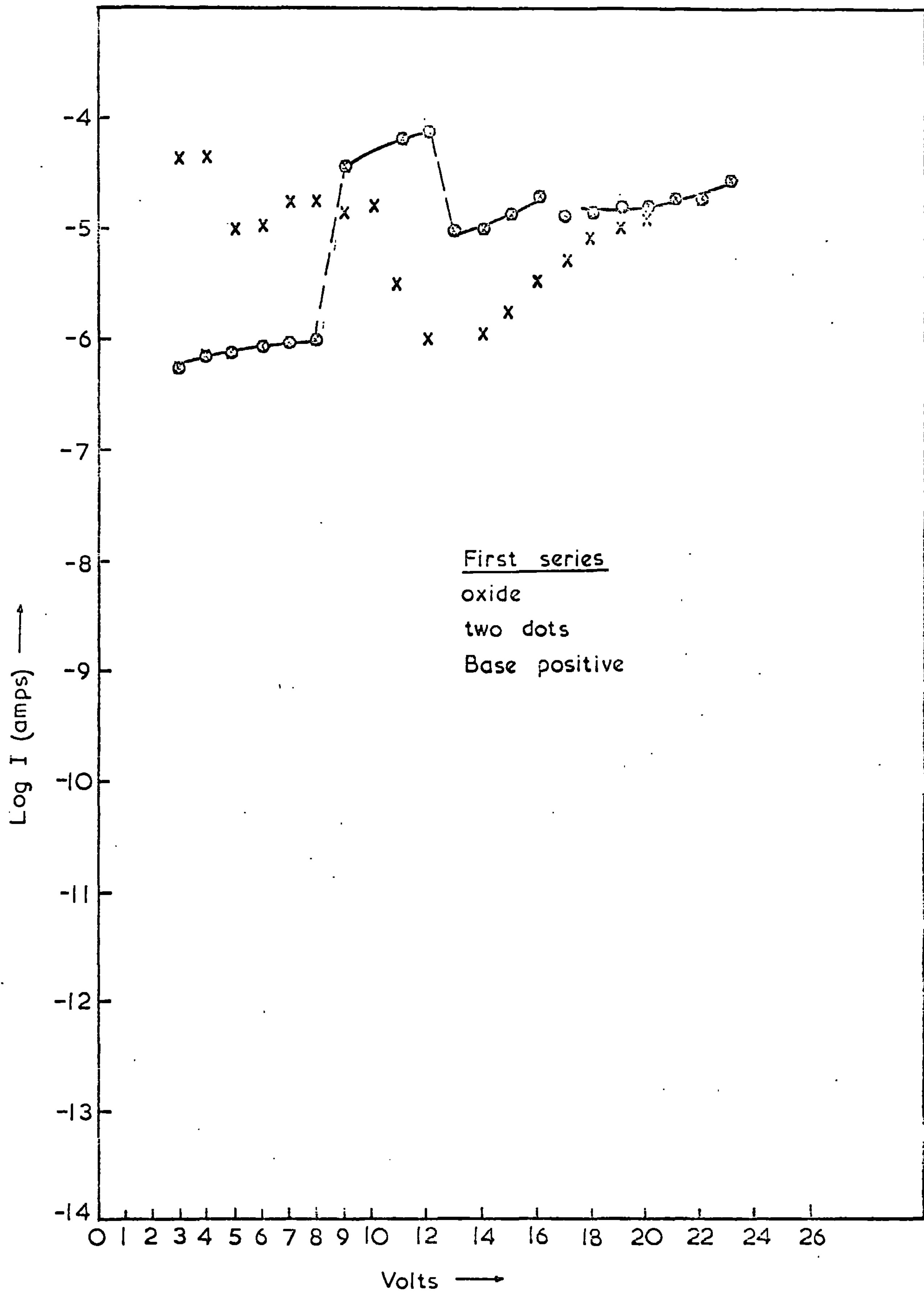

Fig. 5·1

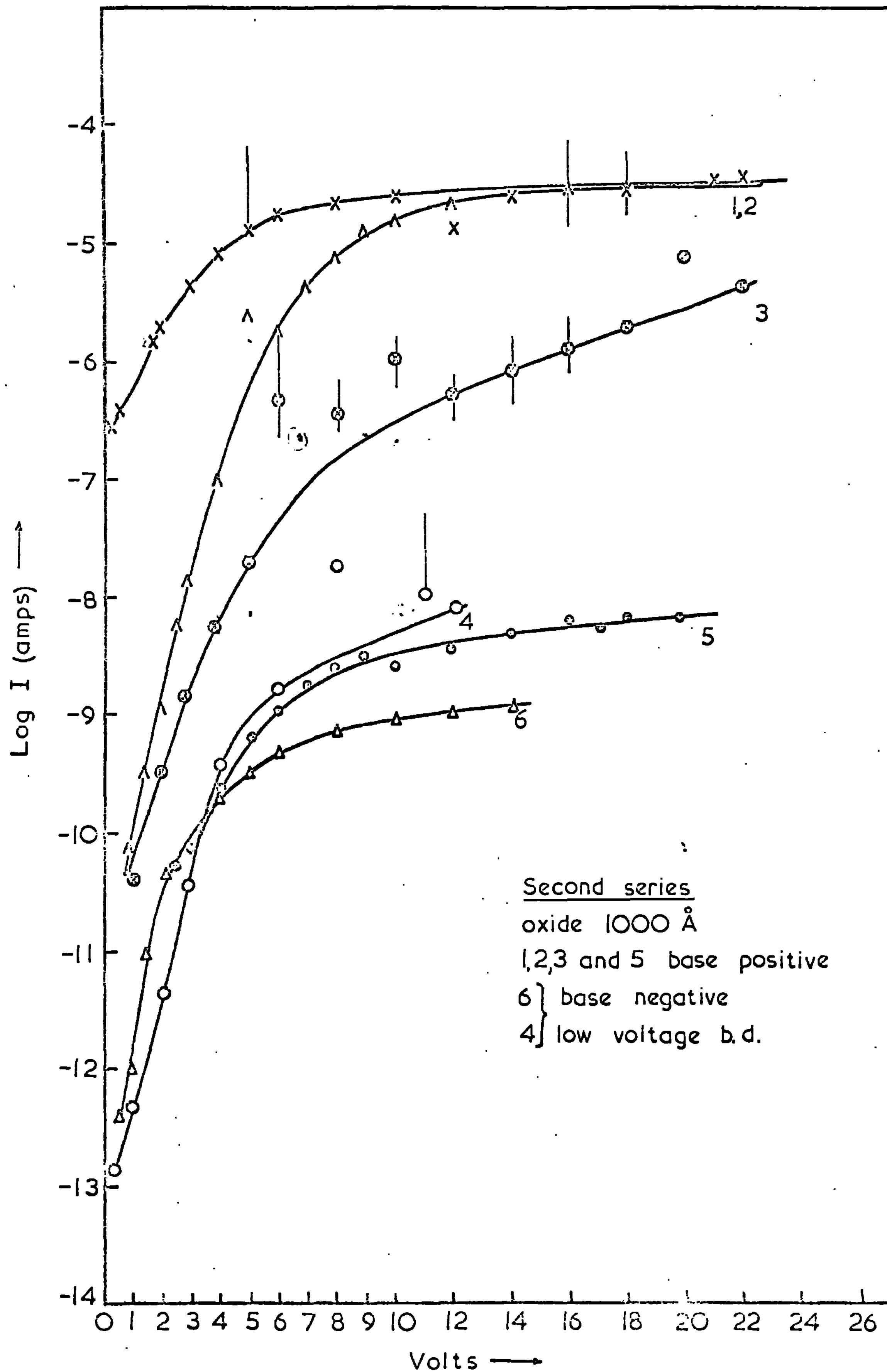

Fig. 5·2

shown in Figure 5.3. Although the currents were very unstable they showed some reproducibility from dot to dot.

The results of the fourth series of samples were better still. The improved appearance and electrical behaviour of the first sample prompted the study of different metals for the top contacts and indium, gold and platinum were used. Samples MT_1 to MT_4 had $\sim$1400Å of oxide. Only three dots could be measured on MT_1 as shown in Figure 5.4. These curves have been smoothed and the points removed for clarity. Seven dots could be measured on MT_3 which had all aluminium contacts and these are shown in Figure 5.5. These have also been smoothed out. Samples MT_2 and MT_4 failed in preparation and the resulting film had cracks up to the top contacts and a tendency to peel off. Samples MT_5 to MT_7 had aluminium, gold and indium top contacts on 1200Å of oxide. Much time was not spent on the measurements of oxide, since the main aim of preparing good willemite films was not met even on these samples. However all of the dots tried had low resistance and showed low voltage breakdowns. The indium dots passed typically 85mA at one volt increasing to about 800mA or higher at 15 volts, when the dot became red hot. This was not accompanied by any breakdowns. The characteristic of one gold dot from sample MT_7 is shown in Figure 5.6a.

MT_8 and MT_9 also had multiple top contacts. MT_8 had approximately 1000Å oxide and only one aluminium dot could be successfully measured as shown in Figure 5.6b for positive base polarity. MT_9 had approximately 800Å of oxide on which one gold dot could be partly measured as shown in Figure 5.7

It was always suspected, and later confirmed by the results of the etching experiment described in Section 5.2, that a film of oxide remains underneath the willemite on every

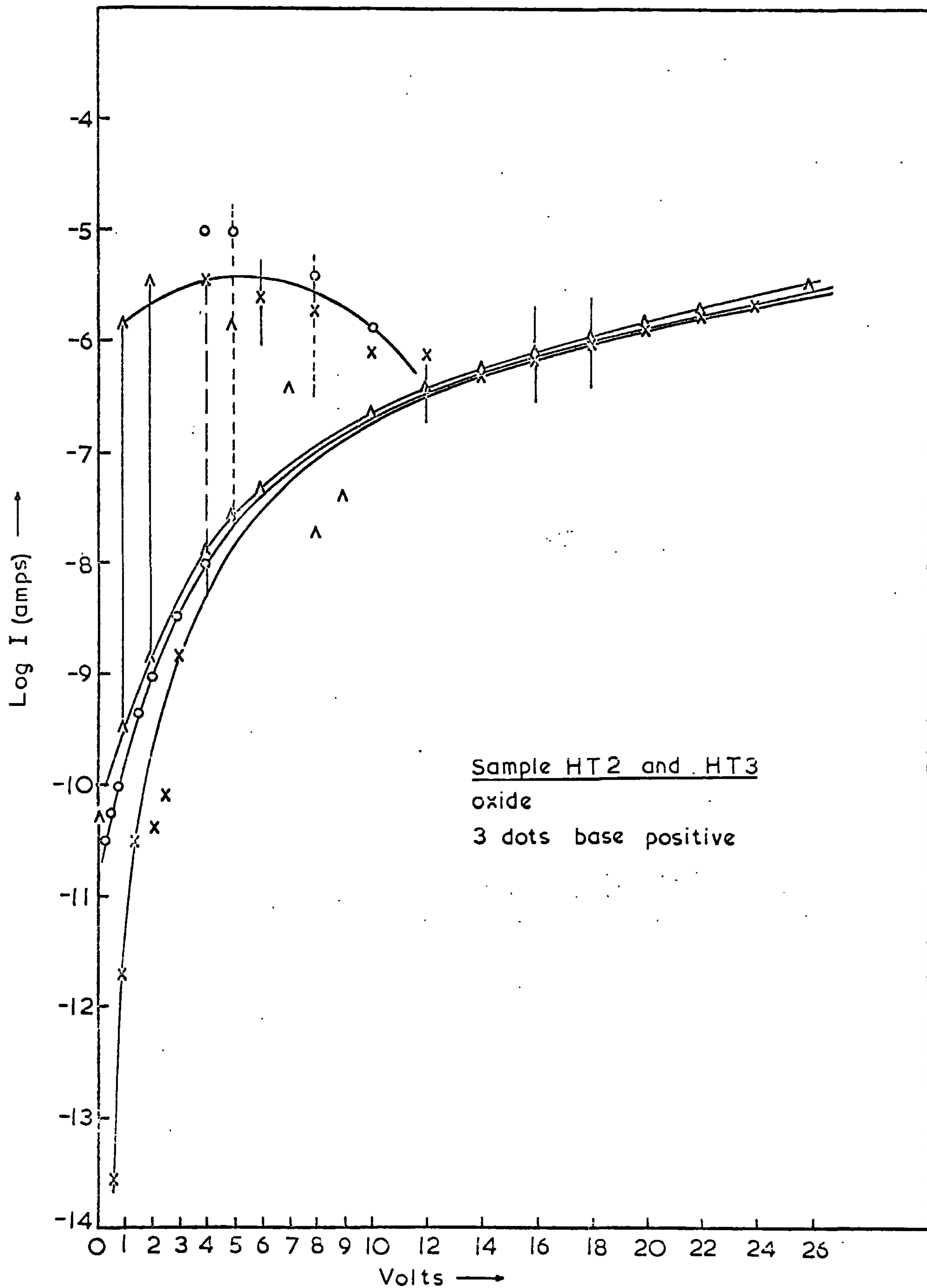

Fig. 5·3

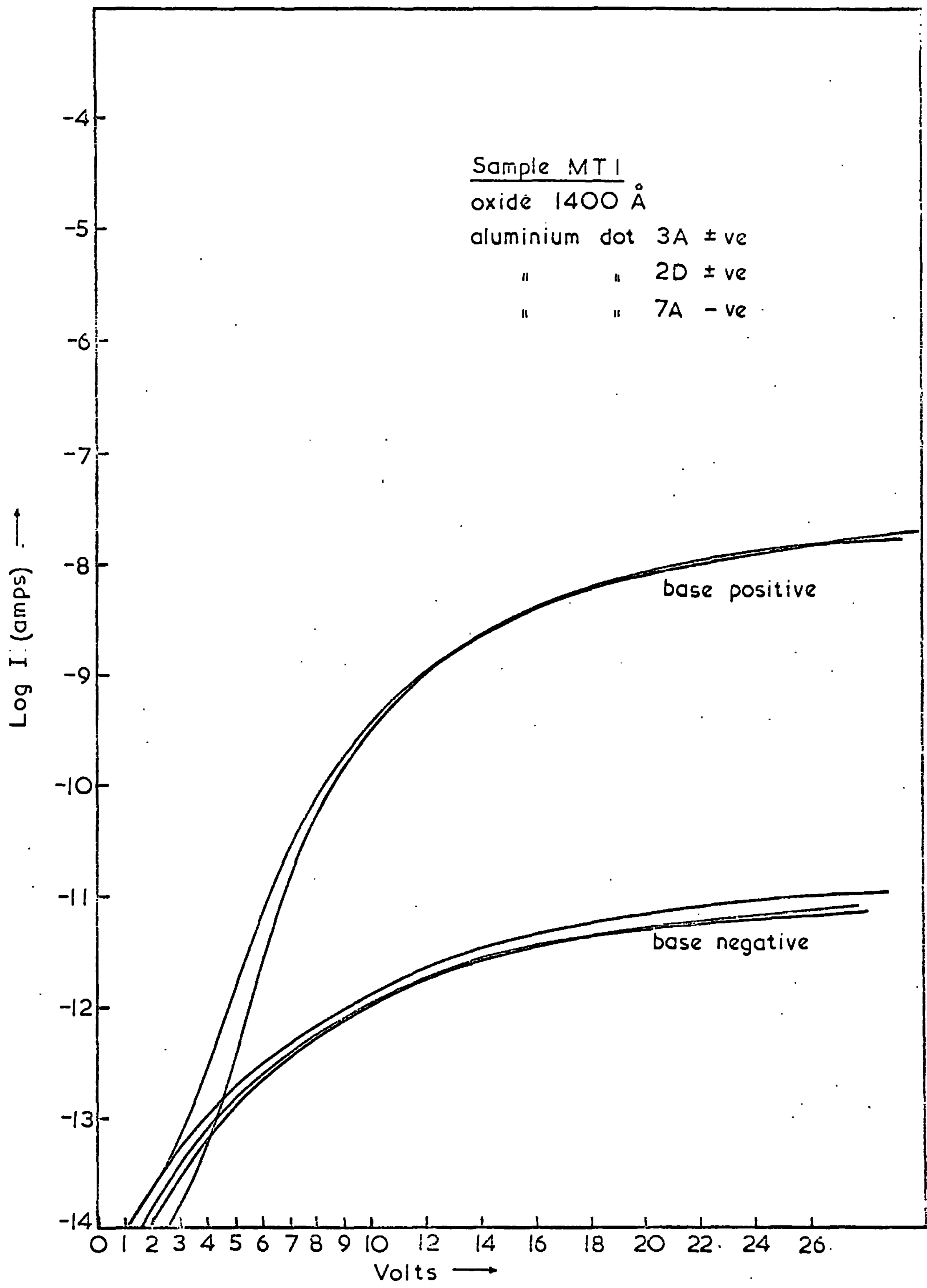

Fig. 5·4a

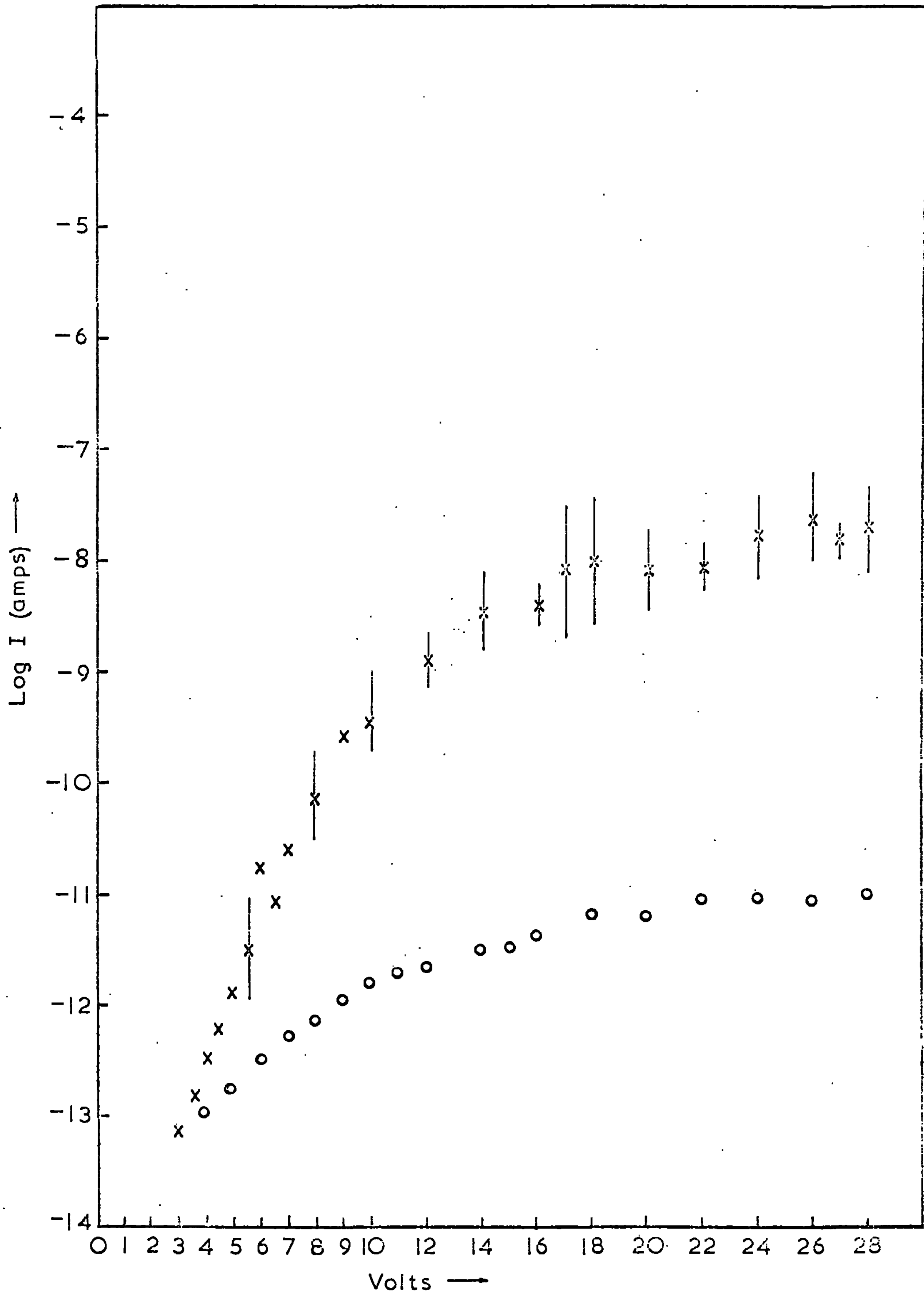

Fig. 5·4b

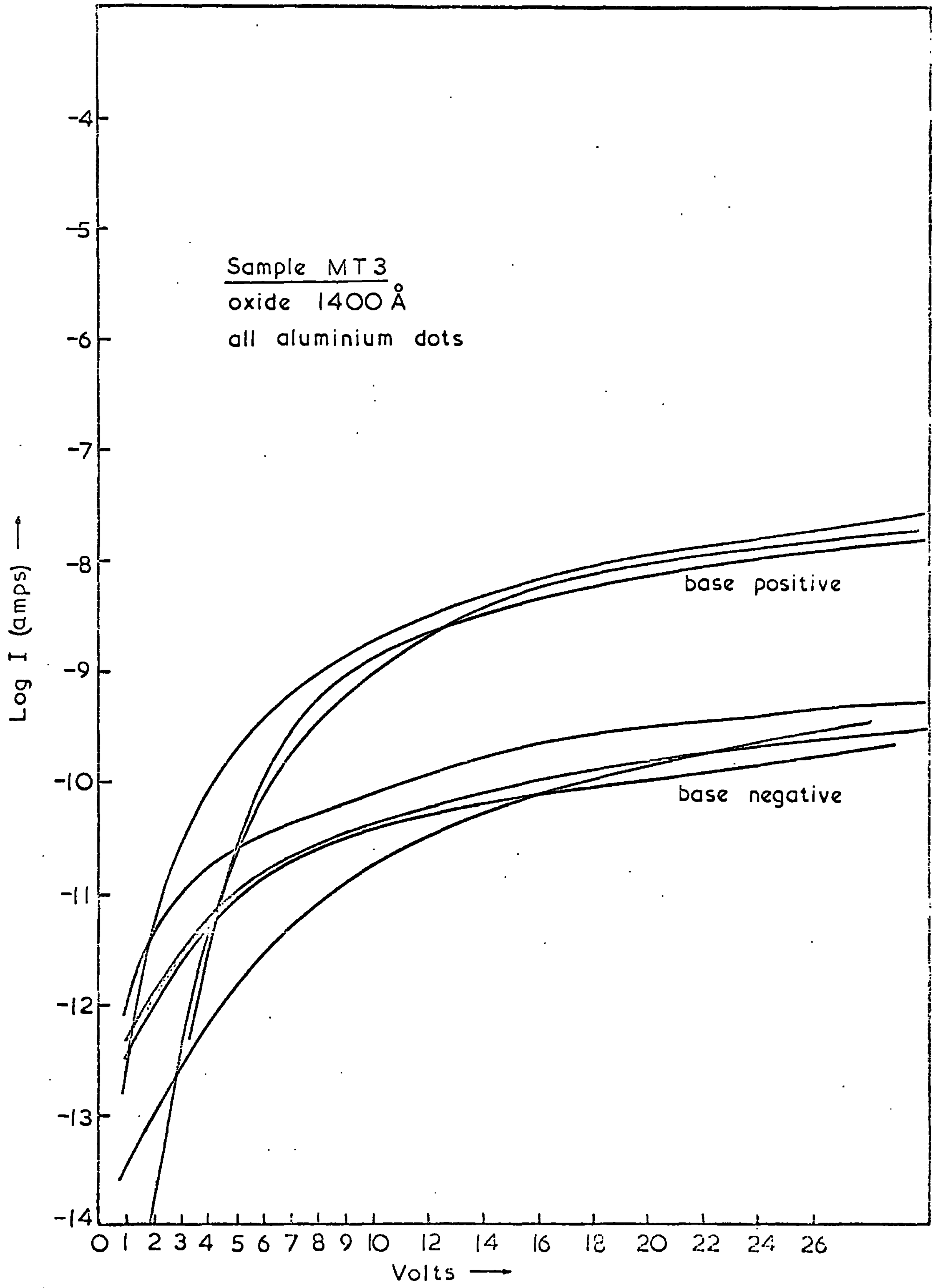

Fig. 5·5

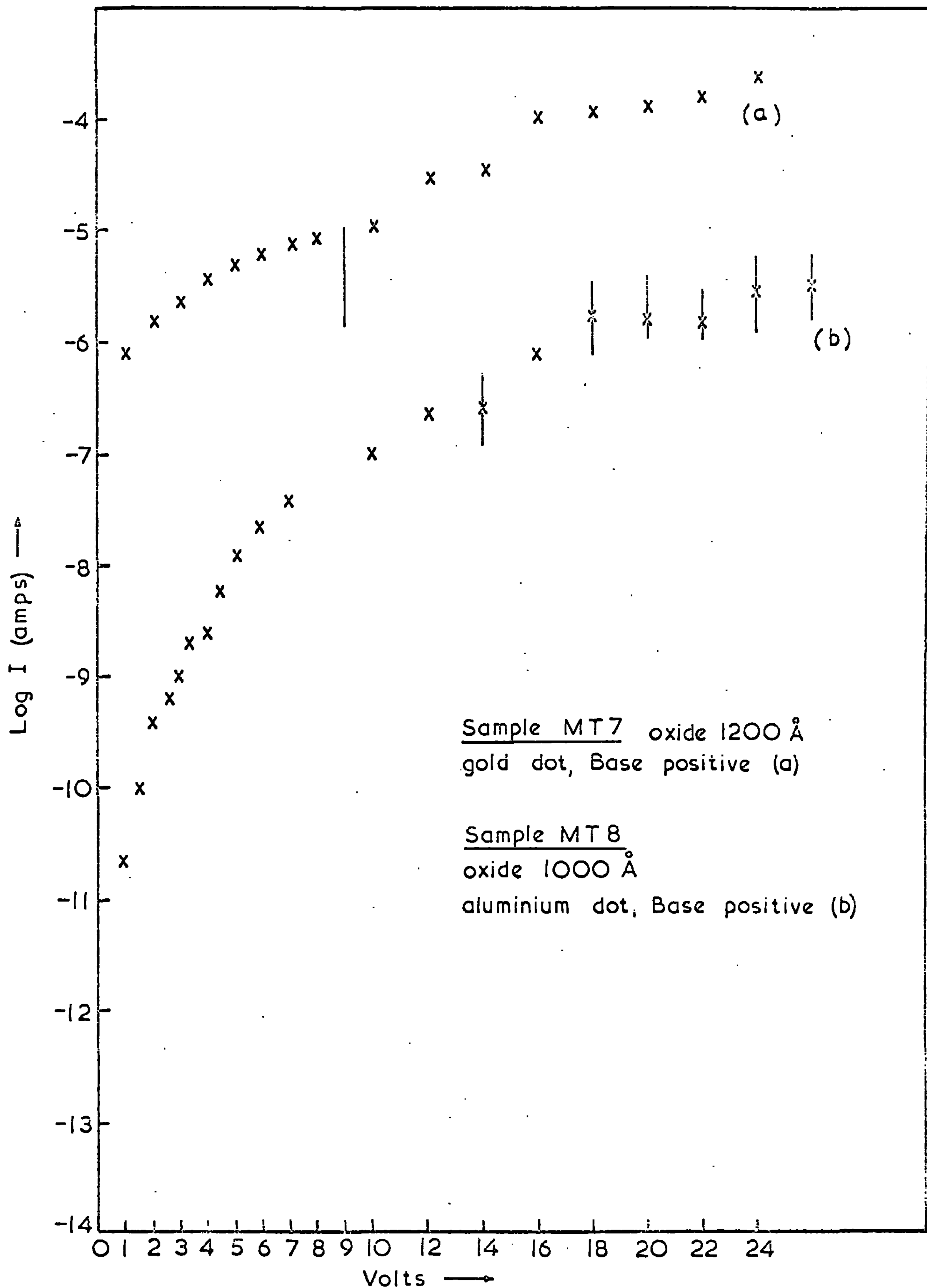

Figs. 5·6 (a) and (b)

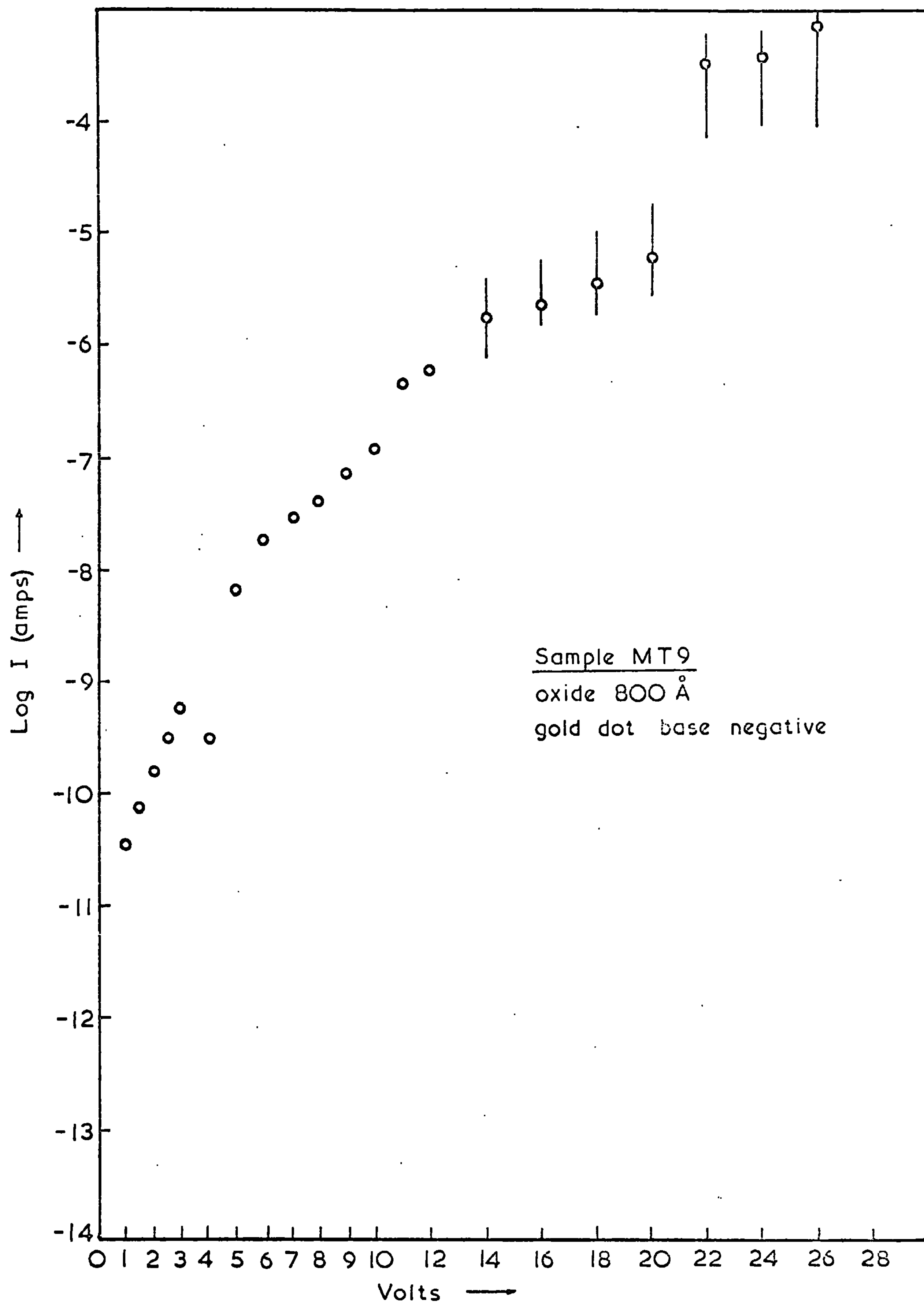

Fig. 5·7

sample. In an attempt to eliminate this film, some samples were made on silica substrates by depositing zinc fluoride directly on to the platinum film, before the oxide. This experiment was not successful because the films of fluoride and oxide disrupted and turned into flakes during the bake, and no electrical measurements could be made.

The last sample of this series on which some measurements were tried used the sintered alumina substrate. However, all the dots on this sample again showed very low resistance.

5.4 Results for the Willemite Films

Each of the samples had nine top contact dots on the willemite areas except for those in the fourth series which had twelve. Most of the top contacts were of aluminium although platinum, indium or gold was used on some samples.

The results for willemite films on the first series of samples were very similar to those for the oxide sections on the same samples (Section 5.3). Curves for two aluminium dots on willemite are shown in Figure 5.8 to illustrate the extreme fluctuations of current which were accompanied by self healing breakdowns on these samples.

The second series was slightly better and the characteristics of three dots from one sample for the positive base polarity are shown in Figure 5.9. These curves have been smoothed out and the points removed for clarity. Measurements for negative polarity could not be made in most cases because of breakdown at the higher positive voltages which were applied in the hope of observing electroluminescence. This sample had 1400Å of willemite on 1000Å of oxide. For the first time, electroluminescence was observed on this sample for the above three dots with light emission starting at a

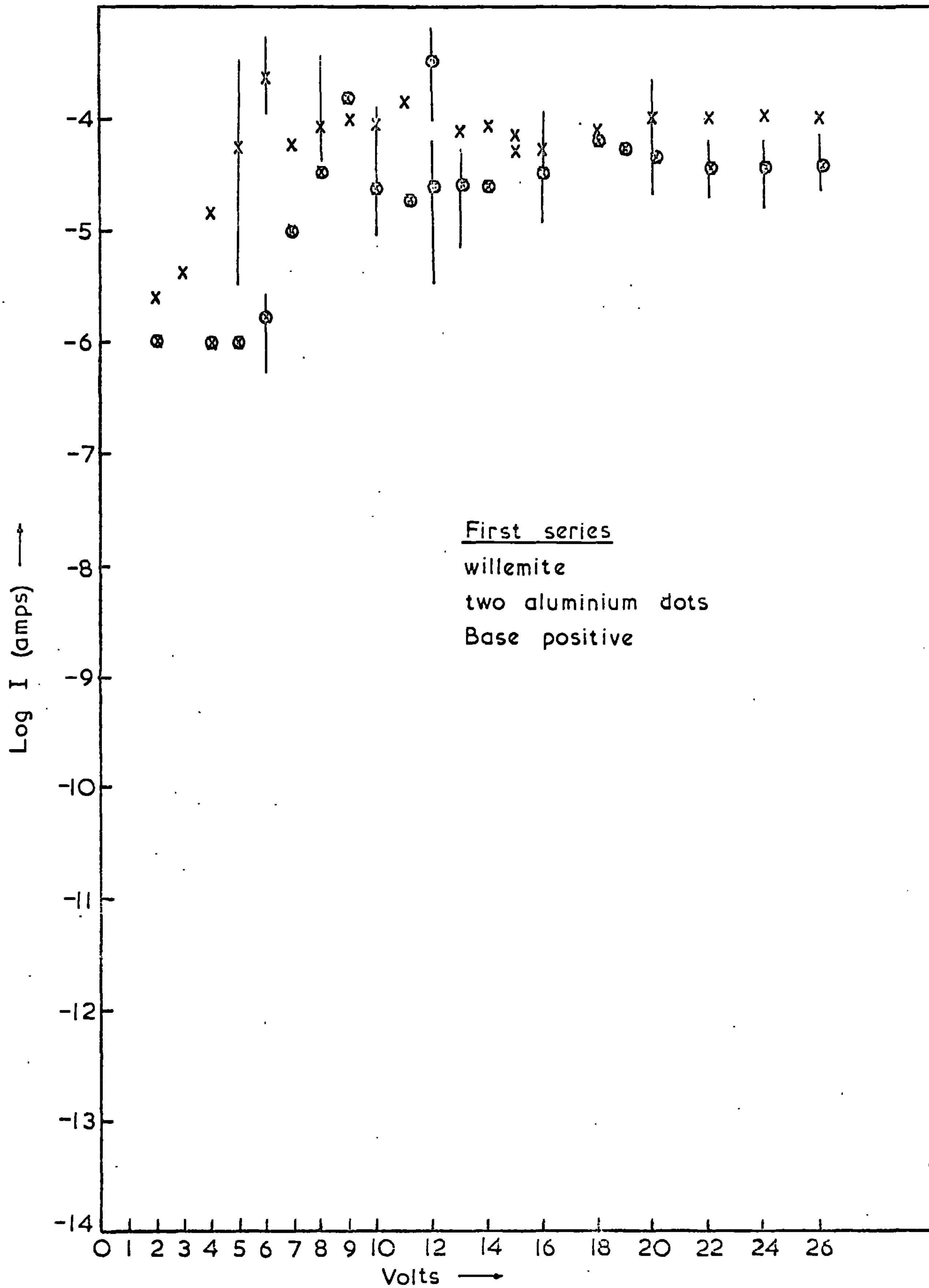

Fig. 5·8

voltage of around twenty volts. Under x100 magnification the dots appeared to be glowing uniformly light green. The light was not accompanied by any big changes of current, but these dots ultimately broke down at about 28 volts. The electroluminescence was reproducible below the breakdown voltage. None of the other dots on samples in this series could survive voltages greater than about 6 volts and some passed very fluctuating currents before breaking down.

The willemite films of the samples in the third series were badly cracked and broken, and no measurements were possible on any of them.

The willemite section of the fourth series of samples was also better, like the oxide, and some successful measurements for the positive base polarity were made on a few of the samples. Sample MT_1 had 2400Å of willemite on 1400Å of oxide. Out of the nine aluminium dots five could be measured for the positive base polarity only, giving the curves shown in Figure 5.10. Four of these dots gave electroluminescence similar to that of sample A18-3 of the second series which was described above. The onset of electroluminescence varied from about 24 volts to 26 volts from dot to dot, while the current through all of them was about 8-10μA at these voltages. The brightness of all the dots was about the same. In all of the characteristics a fair amount of scatter is noticeable up to about 15 volts. The other four dots on this sample showed low resistance and self healing breakdowns from the beginning but did not give electroluminescence.

Sample MT_2 had the same film thicknesses as MT_1 but produced very scattered results and most of the dots gave high currents. Two curves for the positive base polarity were a little better and they have been re-plotted in Figure 5.10.

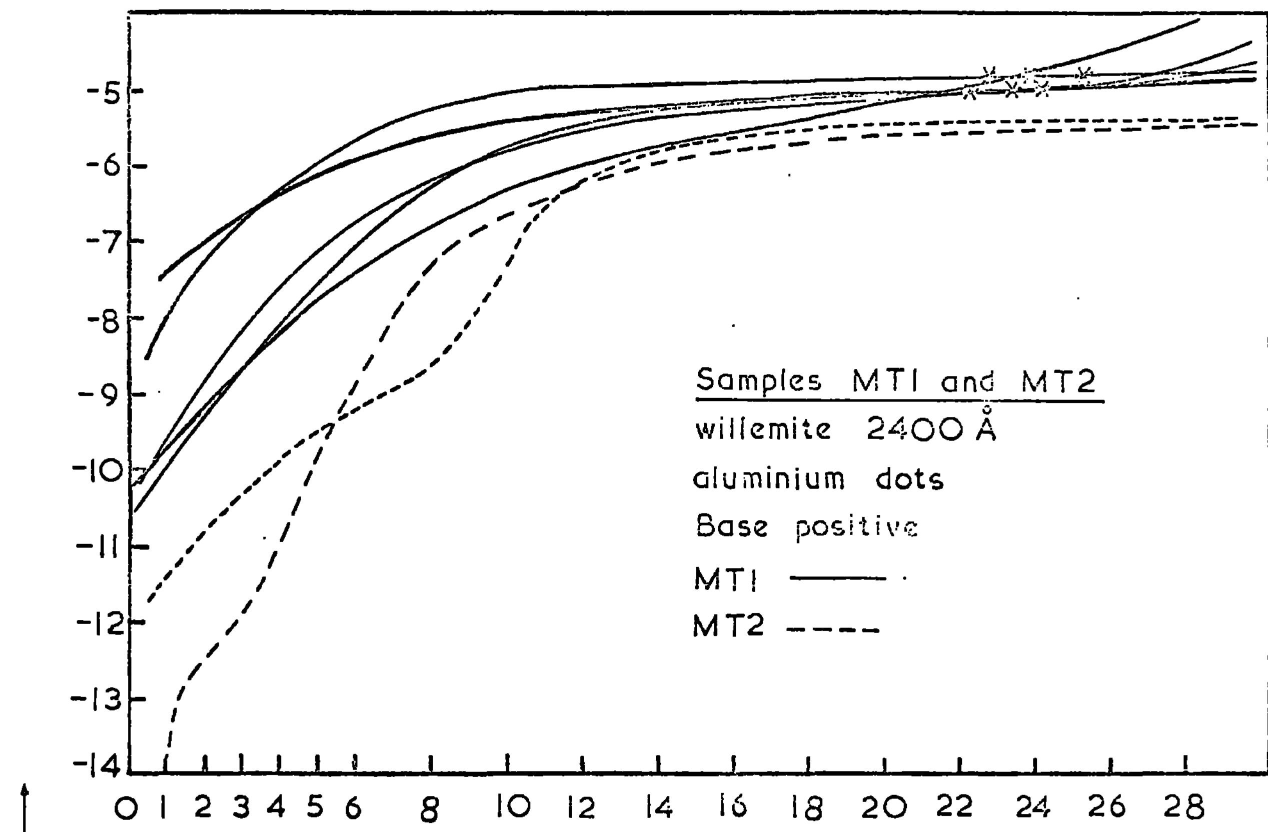

Fig. 5·10

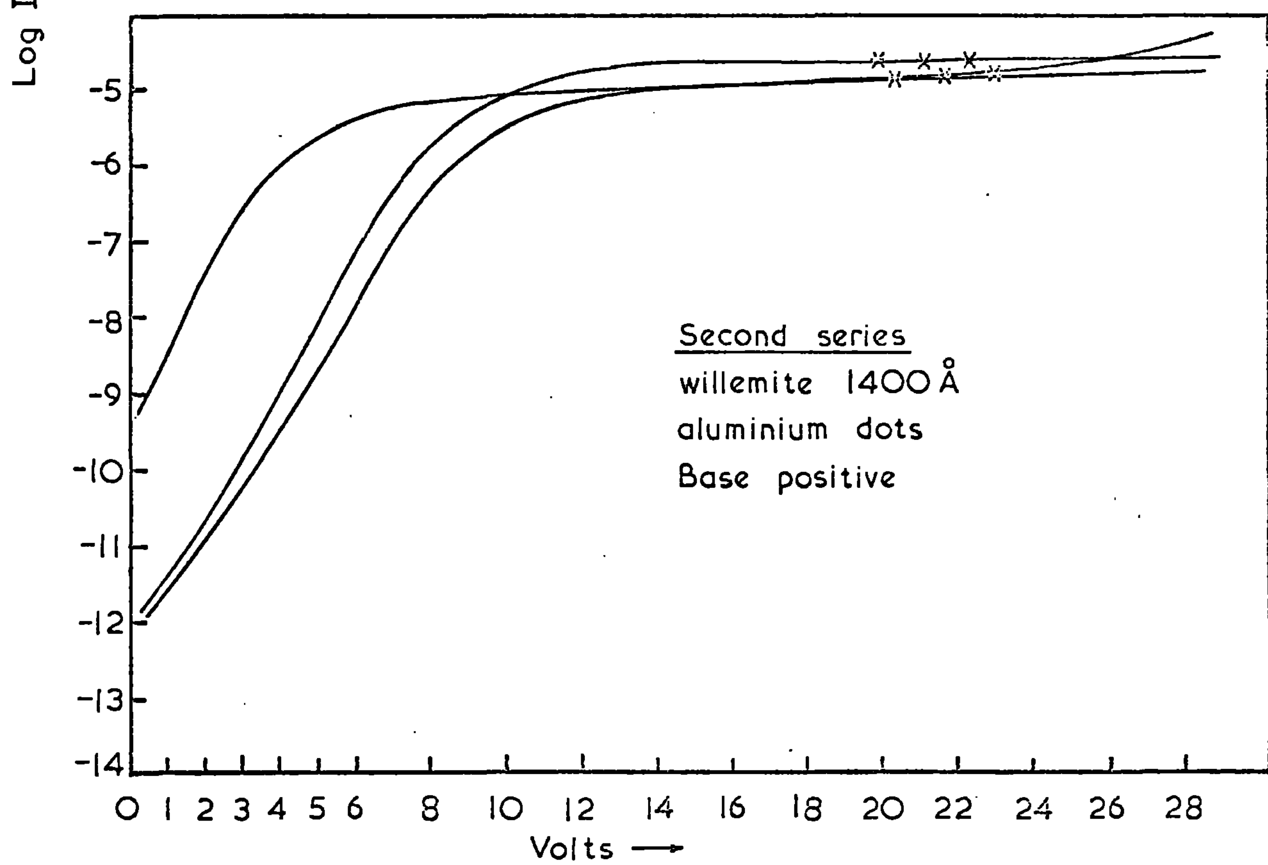

Fig. 5·9

These are very similar to the curves obtained from MT_1 but without electroluminescence in this case.

Sample MT_3 which had about 600Å of willemite on 1400Å of oxide also gave better and reproducible results. It had twelve aluminium dots on the willemite and five of these could be measured for positive polarity, two for negative and three for both polarities of the base electrode. The dots which passed higher currents for the positive base polarity did not necessarily do the same for the opposite polarity. The smoothed curves are shown in Figure 5.11 and the two marked with stars are for dots which gave electroluminescence starting at about 22 volts. The corresponding current of 5 and 15 microamperes for the two dots was fairly steady and the brightness was perhaps slightly greater than for the ones described previously.

Sample MT_4 had deep cracks and no successful measurements could be made. MT_5 had about 200Å of willemite on 1200Å of oxide and curves could be drawn for only two aluminium dots for positive base polarity as shown in Figure 5.12.

The remaining samples in this series, with the exception of the last two, had gold and indium top contacts in addition to aluminium. Figure 5.13 shows the only curve for sample MT_6 (200Å W, 800Å oxide) and Figure 5.14 shows the three curves for sample MT_7 (200Å W, 1200Å oxide) for two gold and one aluminium dot. All of the indium dots behaved exactly as those on oxide and passed high currents.

5.5 Stability of Currents

All the results were affected to some extent by variability of the current measurements which must be taken

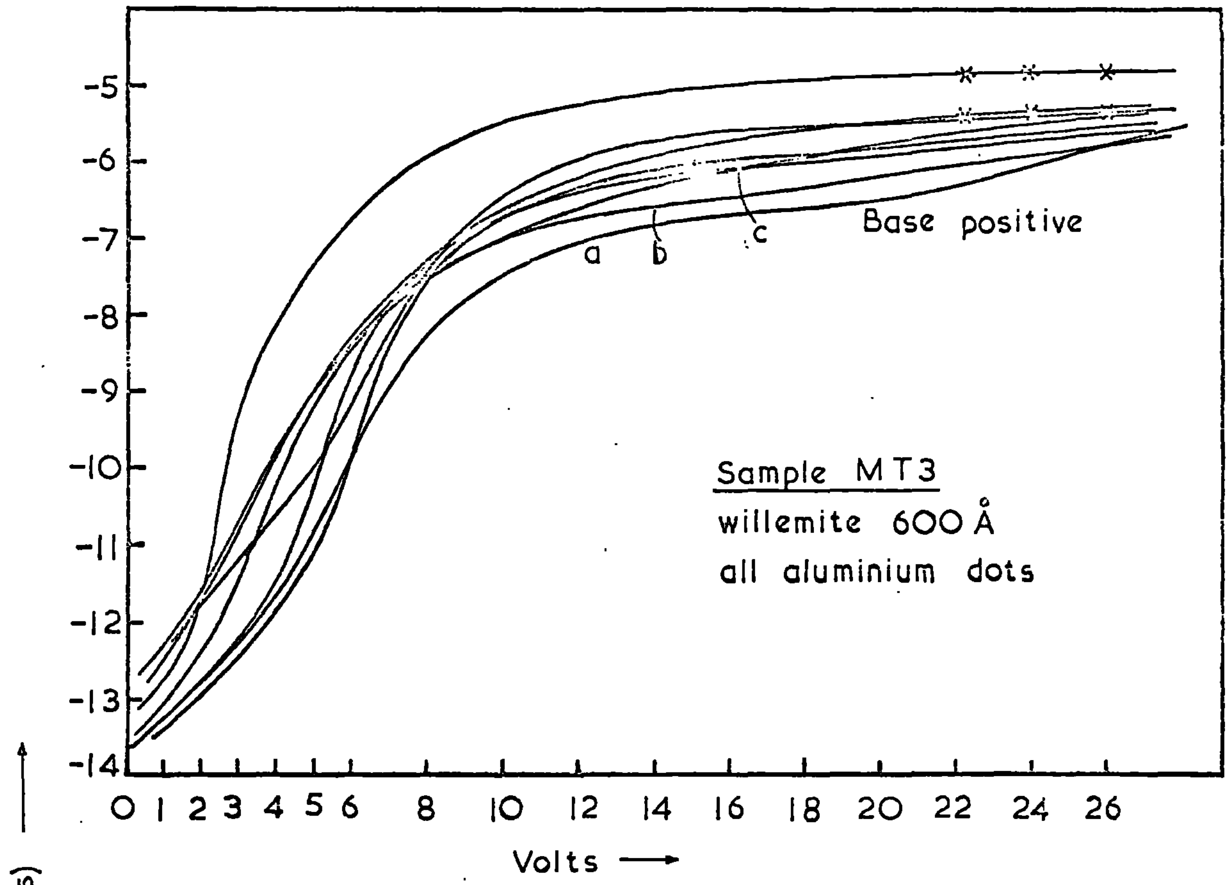

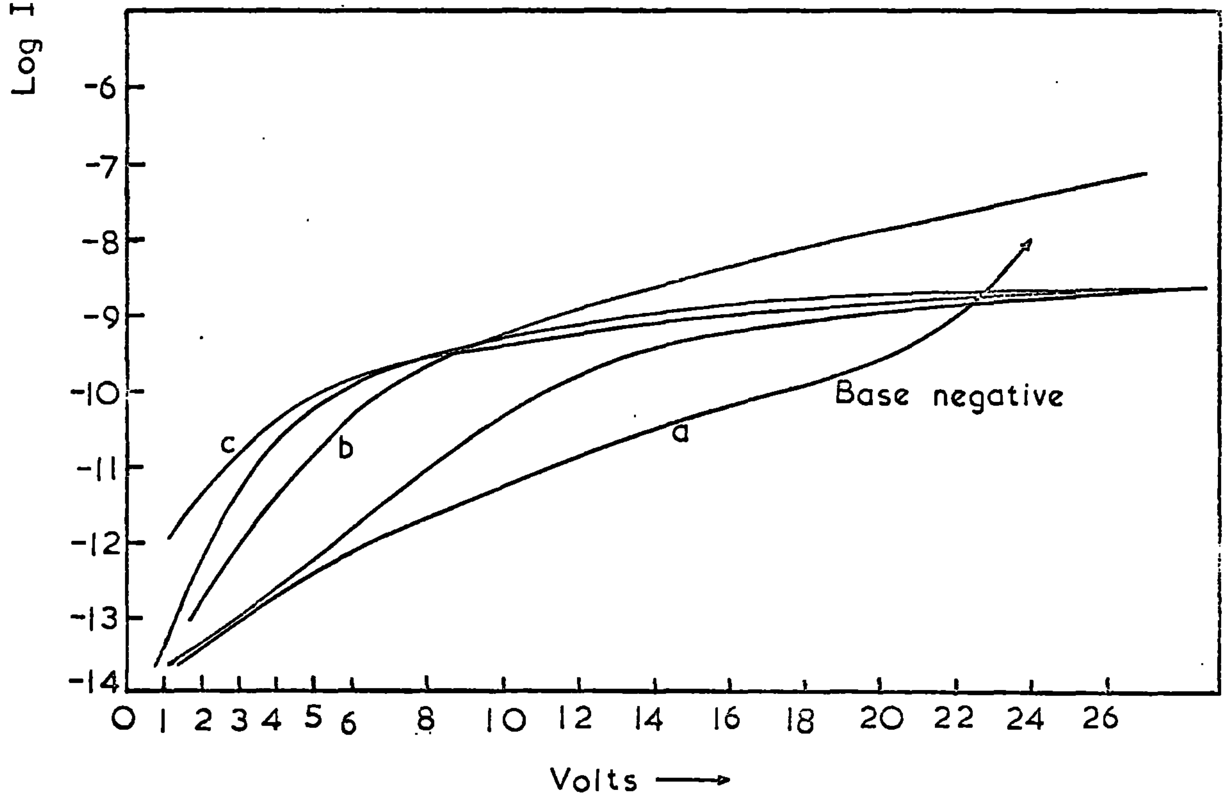

Fig. 5 11

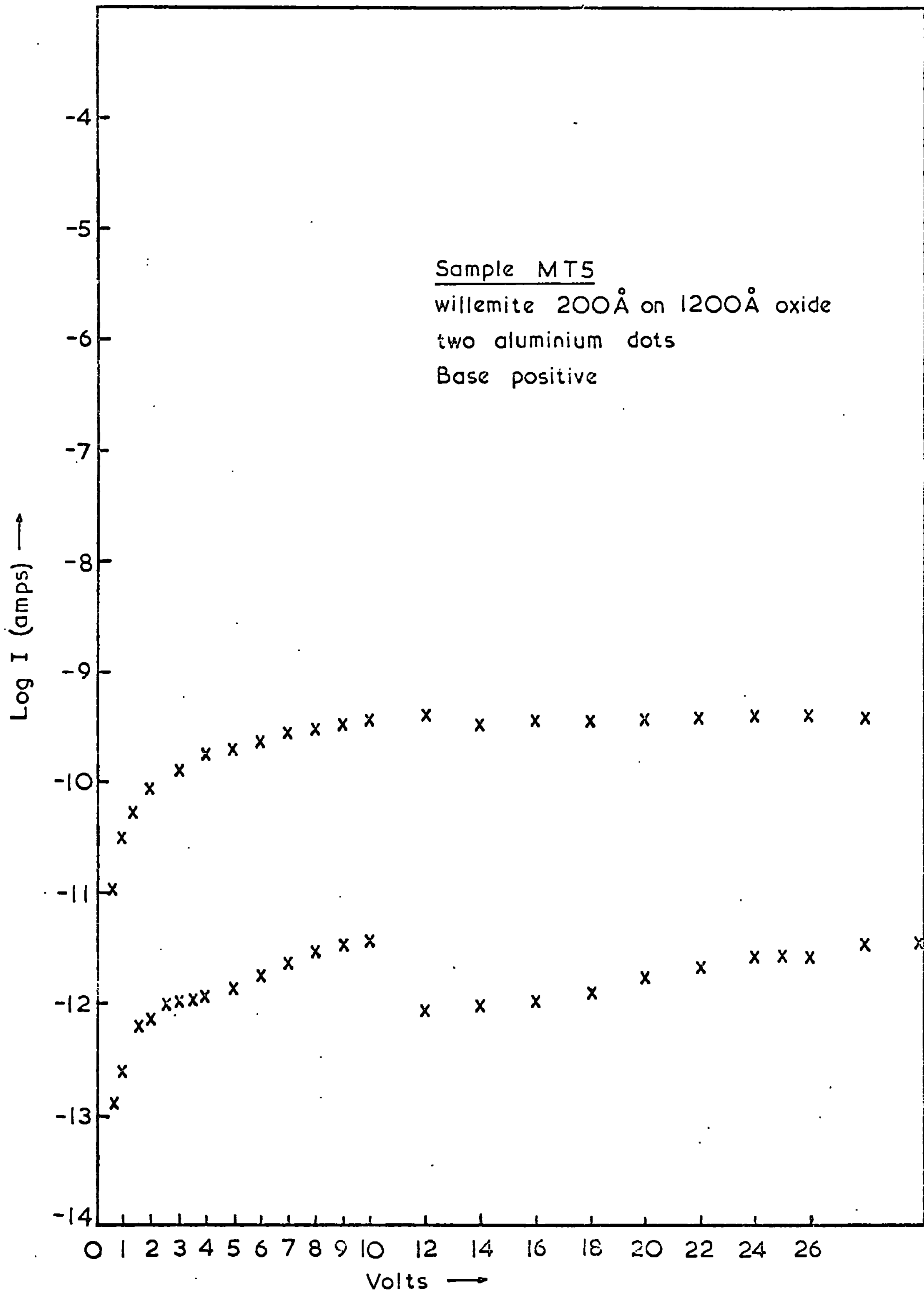

Fig. 5.12

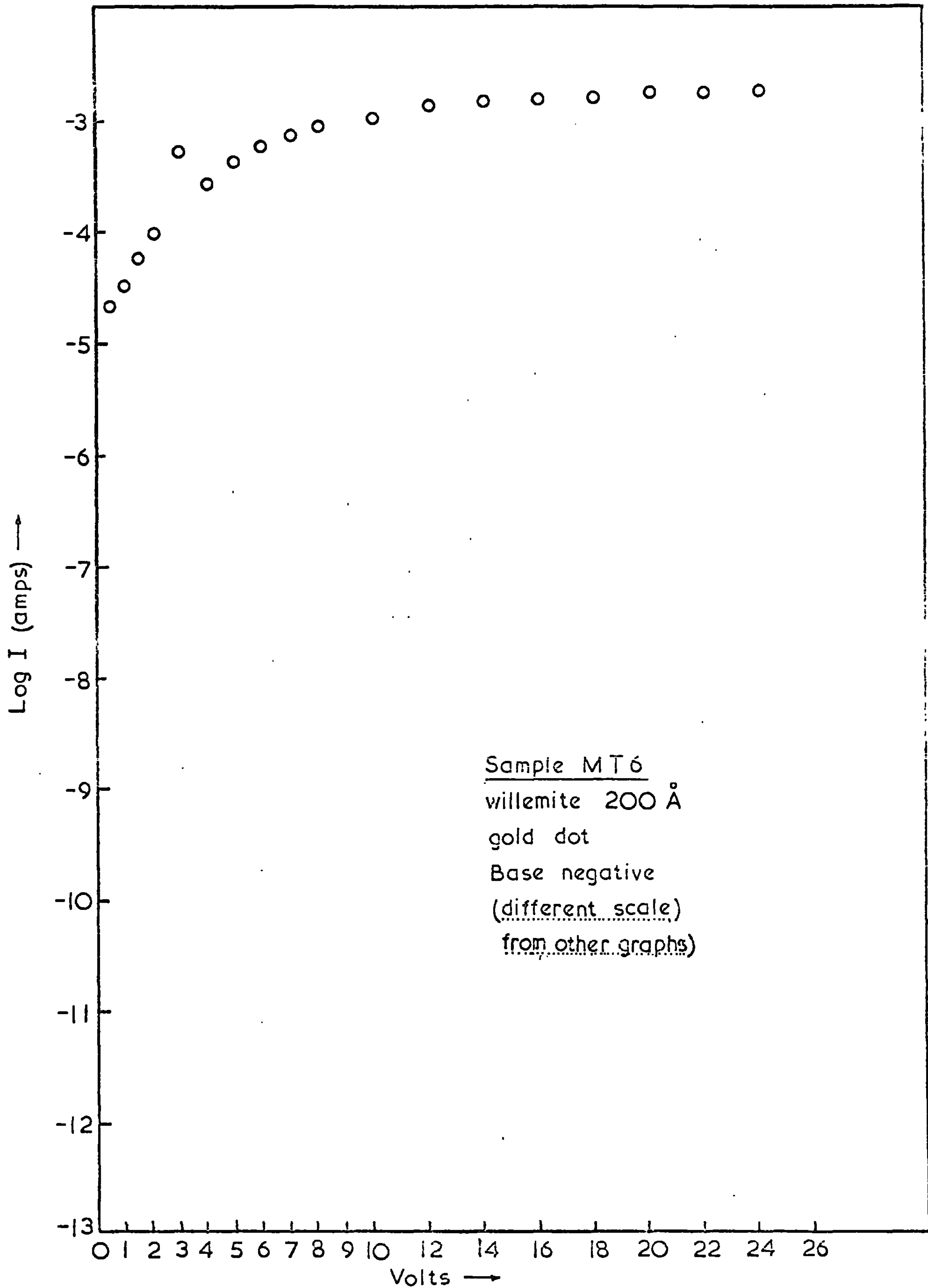

Fig. 5·13

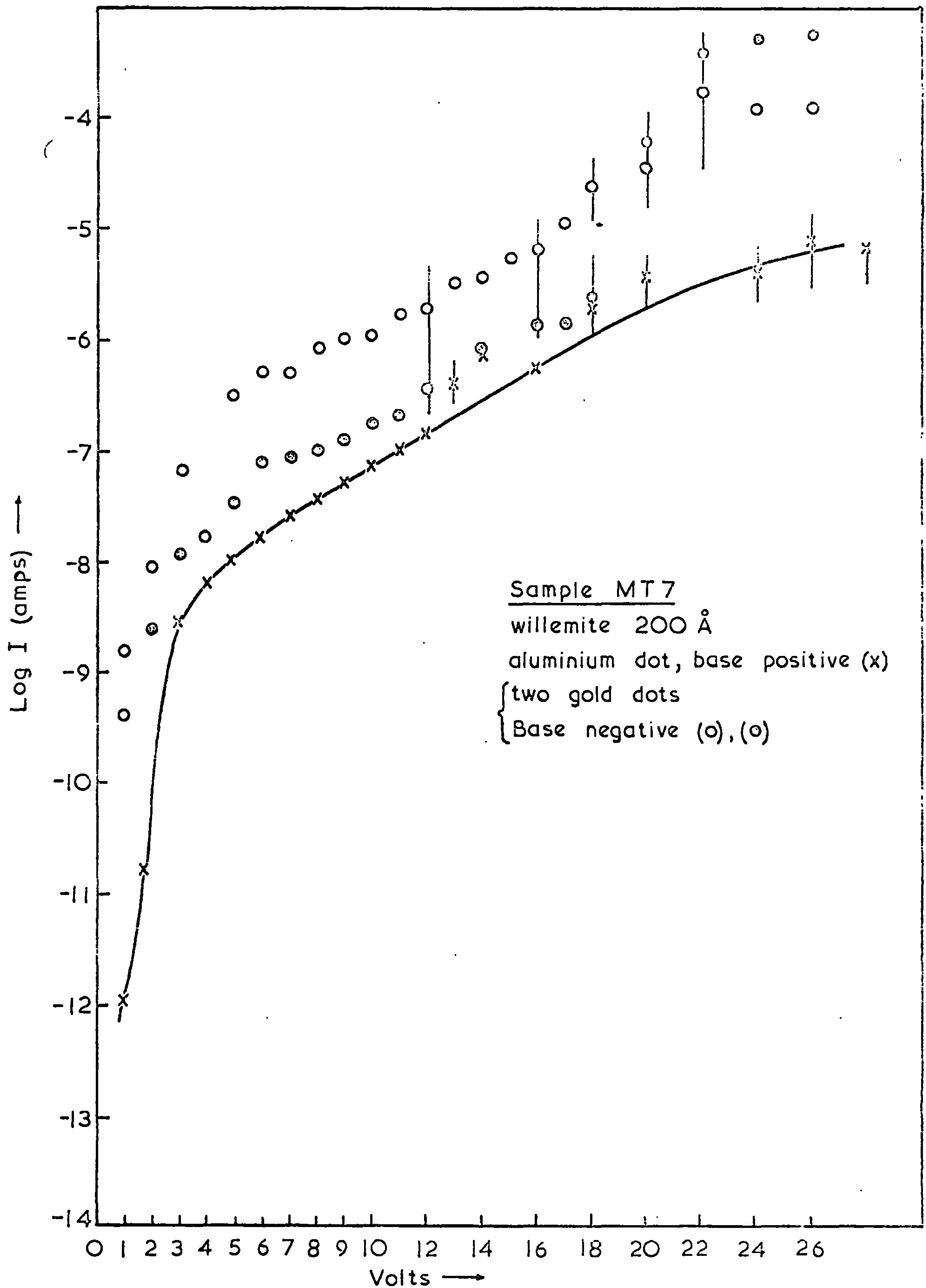

Fig. 5·14

into account in interpreting the curves presented in Sections 5.3 and 5.4. Variability was of the following types:-

a. 'Polarization', i.e. current decay following an increase in the voltage applied to the sample.

b. Random fluctuations in current as observed on the vibron.

c. Variability from point to point seen on plotting the measurements. This was probably due to uncertainty in the readings due to b.

d. Variability between the I-V curves of different top contacts on one sample and between measurements on nominally identical samples.

The earlier samples on silica substrates gave very unstable currents for both oxide and willemite as shown typically in Figures 5.1 and 5.8 respectively. Improved processing led to better samples which gave much smoother but scattered I-V curves although still irreproducible from dot to dot. (Figures 5.2 and 5.9). The current decay could generally be explained by the electrometer time constant which varied with the measuring resistor range. Longer times were obtained for the higher resistor values. (Section 4.5.)

All of the samples on silica showed fluctuating currents, although some had very small fluctuations and others considerable. There was no noticeable difference between oxide and willemite in this respect. The fluctuations eventually decreased as the quality of the films improved. Some measurements showed severe fluctuations over at least an order of magnitude in current. The maximum and minimum values were then noted towards the end of the few minutes measuring time, before increasing the voltage. Figure 5.4b

shows their values for a case where the current fluctuated predominantly for the positive polarity. In some samples the fluctuations were greater for one polarity, while in others they were similar for both polarities. The fluctuation range is shown by vertical bars on graphs having current points. Where there is no bar the fluctuation was negligible. The usual procedure was to draw a smooth curve approximately through the centre of the fluctuation range as shown in Figure 5.4b. Such smooth curves are the ones given for the majority of the results in this Chapter because inclusion of points for multiple curves is extremely confusing. Each curve had at least twenty points and fluctuations shown in Figure 5.4b are greater than obtained in many of the later samples. The accuracy of the smoothed shape of the curves is naturally determined almost entirely by the fluctuation level. The variation between nominally similar samples or between different dots on the same sample was, however, usually greater than the uncertainty due to fluctuations.

5.6 Cathodoluminescence of Samples

All the willemite films made showed green cathodoluminescence largely irrespective of the initial thickness of the fluoride used and of changes in baking procedures. As judged by the naked eye it can be said that films which were less than about 200Å in thickness glowed only pale green, while all the thicker films showed bright green cathodoluminescence. If there was any difference between the latter it was perhaps that the larger thicknesses of ZnF_2 gave brighter cathodoluminescence.

5.7 Conclusions

The experimental work described in this Chapter leads to the following conclusions, which will be discussed in detail in Chapter 7.

(a) Fused silica was not a suitable material for the sample substrate as shown by the severe adhesion and cracking problems experienced on earlier samples. These problems were only partly overcome by improvements in processing.

(b) Alumina is probably suitable as a substrate material if it is polished to a high degree of smoothness.

(c) Films on earlier samples, in which cracks could sometimes be seen with the naked eye, gave violently fluctuating high currents and low breakdowns in both oxide and willemite areas.

(d) Films on the later sample (some from the second and the fourth series) on which cracks could be seen only under the microscope, passed less fluctuating currents which were moderately reproducible from dot to dot and from sample to sample.

(e) Oxide films which were deposited at low temperatures had rough (sand-like) appearance in x200 magnification and gave low voltage breakdowns. Films deposited at high temperatures had smooth, shiny appearances, but they became badly cracked and lifted during the bake. Films deposited at medium temperature (fourth series samples) were of better appearance and they gave relatively smooth I-V curves (as in (d) above).

(f) For the electrode combination of platinum and aluminium, the currents were always higher for the positive polarity of the platinum. (Figures 5.4 and 5.5. for oxide and 5.11 for willemite). Indium contacts gave short circuits and gold, low voltage breakdowns.

(g) Study of different thicknesses of ZnF_2:Mn to produce willemite has not shown any critical dependence of the cathodoluminescent brightness on the relative proportions of oxide and fluoride.

(h) Weak green electroluminescence was sometimes observed at approximately 6 to 8 volts below breakdown on samples having 600Å, 1400Å and 2400Å thickness of willemite, but not in any film thinner than about 600Å and the brightness increased with voltage. The samples showing electroluminescence were not necessarily those with the highest currents.

(i) In spite of the variability, the current always appeared to be higher in willemite than in oxide of the same sample (See Figures 5.9 and 5.2, 5.10 and 5.4, and 5.11 and 5.5).

(j) The etching experiment proved the existence of a layer of oxide below the willemite.

(k) The current at a constant voltage increases with willemite thickness for the same thickness of oxide.

CHAPTER 6

RESULTS FOR SAMPLES ON SAPPHIRE SUBSTRATES

6.1 Description of Samples

To overcome the crinkling and cracking problems that have been present in all the samples on silica substrates, the later ones were fabricated on sapphire substrates, as soon as they became available, as described in Chapter 4. In all, six samples were fabricated and were called S_1 to S_6. Each was intended to investigate particular effects and most of them were of composite construction with regard to film thickness and top metal contact type.

Sample S_1 was intended largely as a mechanical sample rather than for electrical tests. It was thought that the thermal expansion problems would be greatest with SiO_2 films rather than silicon oxide (SiO_x) films as deposited (Section 4.4). Therefore after the deposition of platinum and silicon oxide the substrate was given a long bake ($\sim$2 hours) in a flow of 0.3 litres/minute of oxygen at 1000°C to convert the oxide film to this form. After the bake the films did not show any of the cracks which had been the familiar pattern on previous silica substrate samples (Section 5.3).

Examination of the sample under the microscope showed that the appearance of the oxide was fine and grainy. Seven very small circles with rough edges, perhaps pinholes, which did not appear to penetrate all the way through, were also noticed. Apart from this, there were fine scratches or lines all over the films which were probably nucleated on the polishing or rolling marks on the substrate. The thickness of the oxide was measured before as well as after the bake and about half of the silicon oxide appeared to have evaporated in

the bake (Table 6.1). Zinc flouride was deposited and baked for willemization to make sure that the films of the samples to come would not crack because of the difference in co-efficient of expansion of sapphire and oxide and zinc flouride films. Microscope examination showed that the willemite film was fine and grainy like the oxide film and proved that the thermal expansion problems had been overcome. This sample was therefore completed with aluminium top contacts and some electrical measurements were made, as described in Sections 6.3 and 6.4.

After successful completion of the first sample S_1, on a sapphire substrate, sample S_2 was fabricated using the standard techniques of film deposition as used for samples on silica substrates (Chapter 4). This sample was intended to compare the results with the earlier work on silica substrates. Unfortunately in the course of preparation, only ∿200Å of zinc flouride was deposited instead of 600Å aimed at. This sample, like the previous one, had only one area of willemite formed from this deposit. Top contacts of two different metals, aluminium and platinum were deposited to study the difference in characteristics due to these, if any, and the tests detailed in Sections 6.2-6.5 were carried out.

Sample S_3 was the result of another effort to make a sample, the results of which could be compared with some of the earlier work on silica substrates. This sample had the same thickness of silicon oxide film as the previous but had two areas of willemite, one of which was ∿200Å thick (to compare it with the last sample S_2) and the other was thicker (see Table 6.1). The top contacts on this sample were of aluminium and gold. Hence this sample was used not only to compare the results with the past samples but also to study

the effects due to the change in thickness of zinc flouride and to further investigate the effects of different top contacts.

Since zinc flouride reacts with silicon oxide even in the absence of extra oxygen to produce cathodoluminescent films of willemite, attempts were made to fabricate samples by baking in an inert atmosphere of argon. The idea was that this would probably ensure more complete reaction with the oxide film. Unfortunately the first attempt was unsuccessful as sample S_4 failed in the final stage of preparation due to drastic overheating of the aluminium baking furnace.

In the next sample, S_5, a change had to be made in the last step of the cleaning of the substrate. Electronic grade trichloroethylene was used instead of trichloroethane because the first solvent was not available at that time. For reasons which are not clear, this change caused the films on S_5 to crinckle and peel off from various points after the bake in argon. Though top contacts of aluminium were deposited on this sample, no successful measurements could be made.

The third argon baked sample, S_6, was completed satisfactorily after the last two failures. For this sample Electronic Grade isopropyl alcohol was used in the final stage of substrate cleaning instead of trichloroethylene, and this was found to be as satisfactory as the trichloroethane used for S_1 and S_2. Sample S_6 had the same thickness of silicon oxide as for the other samples on sapphire substrates. There were two willemite areas; one was about the same thickness as in part of the sample S_3, and the

other one was a little thicker (Table 6.1). The top contacts on this sample were platinum and aluminium.

Sample No.	BEFORE BAKE		AFTER BAKE		Contacts
	Initial Oxide Å	Initial zinc fluoride Å	Final Oxide Å	Final Willemite Å	
S_1	700	∿200	700	∿200	aluminium
S_2	1300-1400	200	1300-1400	∿200	platinum & aluminium
S_3	1400	200 & 800	1400	∿200,700	gold & aluminium
S_6	1400	700 & 1000	1400	700 & 1000	platinum & aluminium

Table 6.1 showing the thickness and contacts on sapphire substrate samples.

6.2 Visual Observations on Samples

Examination under the microscope was primarily necessary to make sure that the films were neither cracking nor peeling off from the substrate and also to closely examine the nature of the surface of the films. Sample S_1 was examined under the microscope after every stage in the fabrication, as this was a test sample (Section 6.1). The remaining samples were examined, only after they were completed with top contacts, and were ready for electrical measurements so as to avoid dust from settling on the films between the fabrication stages. Table 6.2 shows the results of observations. The surface of the top contact dots of all devices was again examined after completing the measurements and Table 6.3 (p.83) compares the results of the effect of argon and oxygen bake.

Sample No.	Surface of base	Surface of oxide	Surface of willemite	Cathodoluminescent brightness*
S_1	x450, smooth grainy look, lines of the substrate noticeable	x450, like platinum, lines of the substrate and pits or pinholes noticeable	like oxide	B
S_2	x450, smooth, not grainy, lines of substrate noticeable	x450, smooth, lines of the substrate and pits or pinholes noticeable	similar to oxide	between A and B
S_3	same as above	same as above	same as above	200Å portion more towards B 900Å portion between A and B
S_6	x450, smooth, but just lifting at edges of oxide at some points	x450, smooth, just about breaking and peeling off at the lines of the substrate. x100, lines still noticeable	similar to oxide, thinner willemite slightly better. x100 patchy colours	both willemite portions similar. C. glow was uniform. *A bright deep green B light green C weak green

Table 6.2 showing the results of the visual examination of films after completion

It will be seen that the difficulties associated with the silica substrates described in Sections 5.1 and 5.2 have been overcome by the use of the sapphire substrates.

Cathodoluminescent willemite films can be produced by using different proportions of zinc flouride and silicon oxide. In the present series of samples on sapphire substrates, the thickness of silicon oxide films was more or less kept constant and three different thicknesses of zinc flouride were used.

Cathodoluminescence examination of the samples was carried out to see that the willemite films produced were good phosphors and to find out any difference in brightness due to either the thickness of the zinc flouride or differences in the baking procedure. However this test was not expected to be very precise because it relied merely on the visual estimation of brightness and/or colour. The results are given qualitatively in Table 6.2.

Voltages of up to nearly the breakdown value were applied to many of the test dots on every sample at the end of the electrical measurements to look for electroluminescence (E.L.). In many cases this was done in almost complete darkness. Some dots glowed before breaking down only on sample S_3. This glow appeared to be the same as the E.L. observed on some previous occasions, but it was not reproducible (see Section 5.4).

In order to estimate the depth of the oxide which is used up during the bake for willemization, an etching experiment was performed on a sample after completing the measurements. Only willemite was removed from the top of the oxide in an acetic acid etch which does not attack

silicon oxide. The sample was then examined for cathodoluminescence to confirm that no traces of willemite were left. Examination under the microscope (x100) showed that the colour of the oxide was the same throughout, which meant that the surface was uniform on this scale. This was also confirmed by the measurements with the interference objective which did not show any change of thickness across the area. These results are the same as the ones obtained from this experiment on a silica substrate sample, as described in Section 5.2.

6.3 Electrical Measurements on Silicon Oxide Films

As described in Section 4.4 all the samples made included some top contacts on the free surface of the silicon oxide films so that electrical measurements could be made to check the quality of the oxide and for comparison with the published work on silicon oxide. Results for oxide on earlier substrates were given in Section 5.3 and this section gives the corresponding ones for samples on sapphire substrates.

As mentioned in Section 6.1, the thickness of the silicon oxide films was kept as constant as possible on every sample on sapphire. Table 6.1 shows that this was achieved fairly well, taking into account that the evaporation rate was not completely under control (Section 4.4).

Sample S_1 initially had the same thickness of oxide as the rest, but in the extra oxygen bake (see Section 6.1) the thickness decreased to 700Å as shown in Table 6.1, probably due to re-evaporation. This reduction in thickness was probably also accompanied by some changes in the composition and hence properties of the oxide. The I-V characteristics have been measured for ten out of twelve

dots on the oxide of this sample. Some dots were measured for positive polarity of the base electrode only and some for negative, and measurements were usually terminated by breakdowns. On two dots measurements could not be carried out as these passed high currents at very low voltages and were close to being short circuits. Smoothed curves of some results for silicon oxide on sample S_1 are given in Figure 6.1 which shows the typical variation from dot to dot with the points omitted for clarity. In some dots the current was also found to fluctuate by up to an order of magnitude. In spite of the variability however, Figure 6.1 shows that the currents are higher by about three orders of magnitude with the base positive than with it negative.

Samples S_2 and S_3 were fabricated in the same way but S_2 had four platinum and twelve aluminium top contacts on the oxide area, whereas S_3 had only four aluminium top contacts. Five of the aluminium top contacts on S_2 had cracks, which appeared to have developed from the scratches on the substrate and since one of these gave very badly fluctuating currents they were not thought to be reliable. The remaining aluminium dots gave smooth and reproducible curves from dot to dot, four of which are plotted for both polarities as shown in Figures 6.2 to 6.7. Curves for only two platinum dots could be plotted and these are shown in Figures 6.6 and 6.7. These measurements confirm the strong dependence on top contact metal found with the slightly different oxide of sample S_1.

Two of the four test areas on sample S_3 broke down at low voltage. The I-V characteristics for the remaining two dots are shown in Figures 6.8 and 6.9. The curves for base negative and the single curve for base positive are

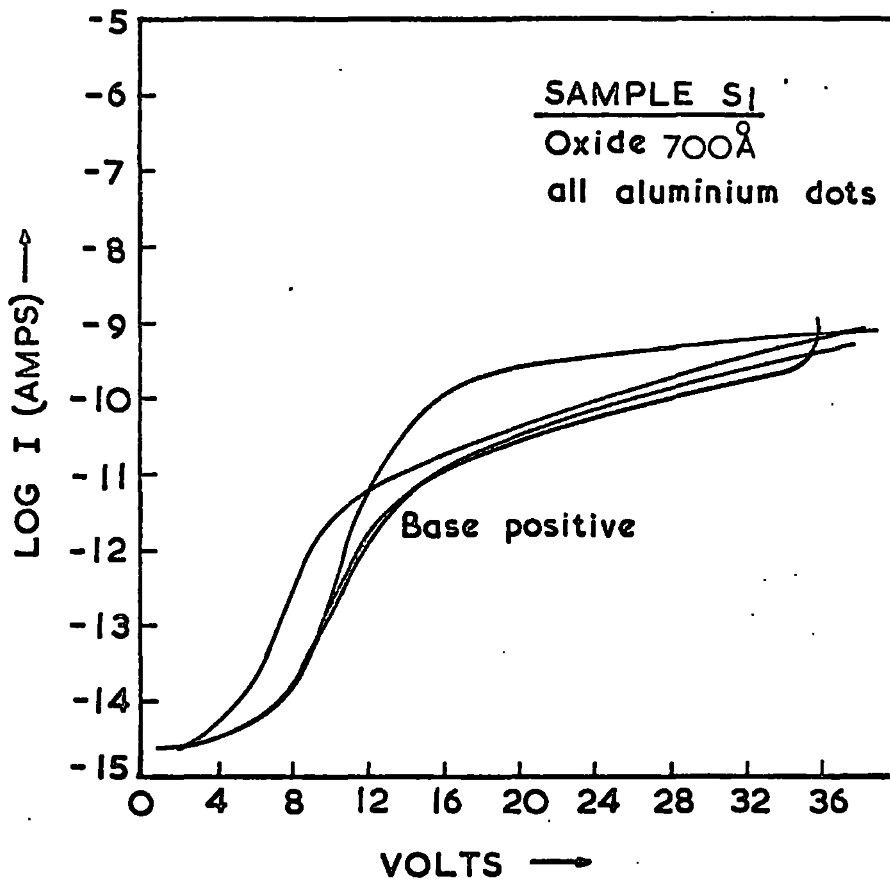

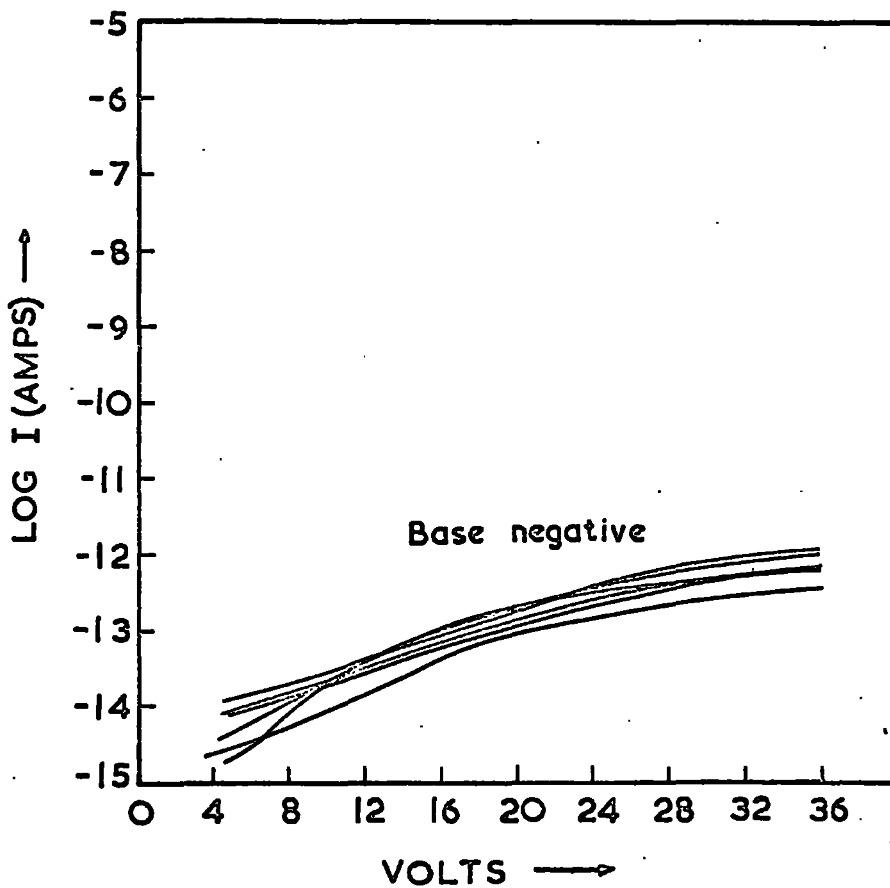

Fig. 6.1

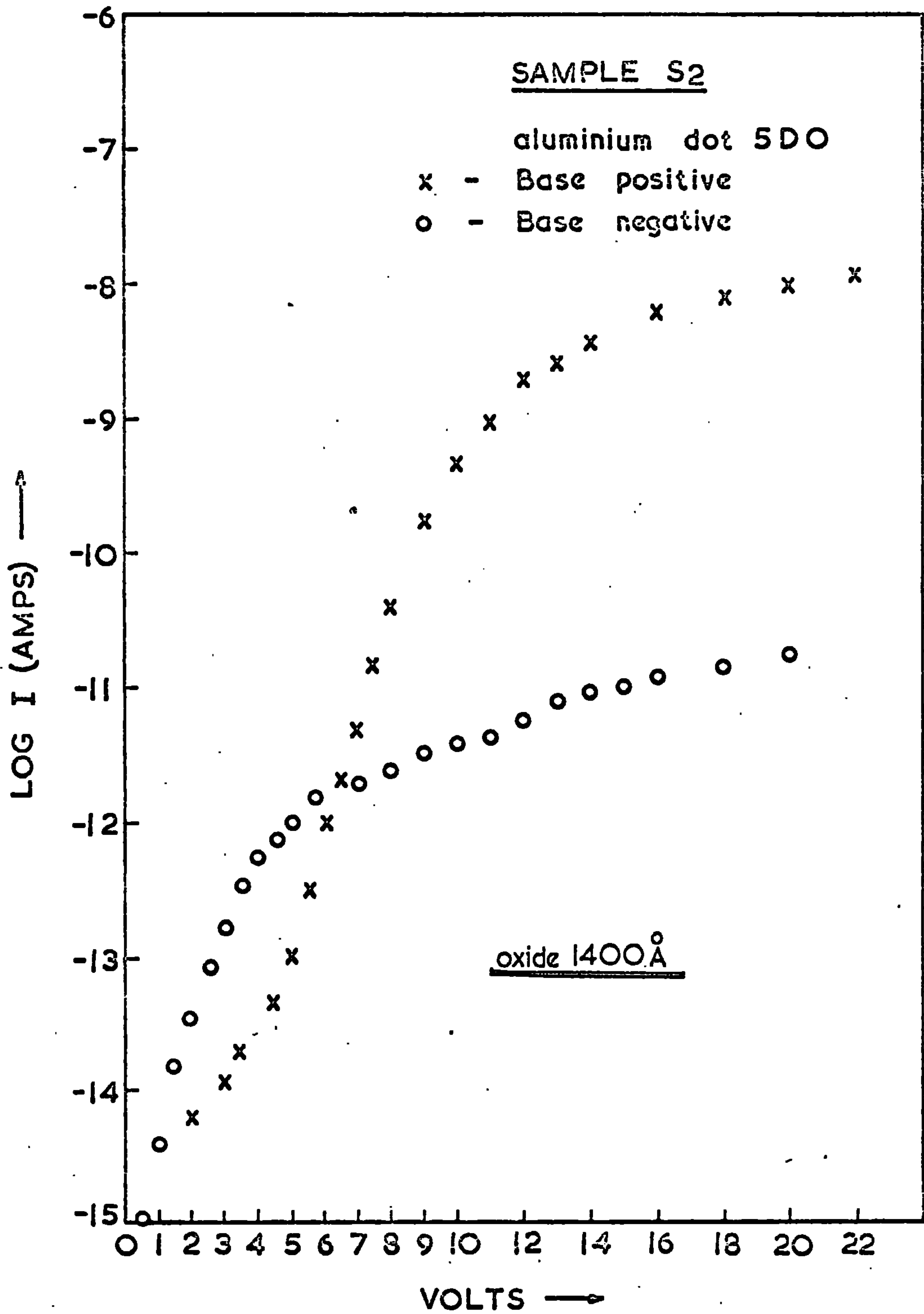

Fig. 6.2

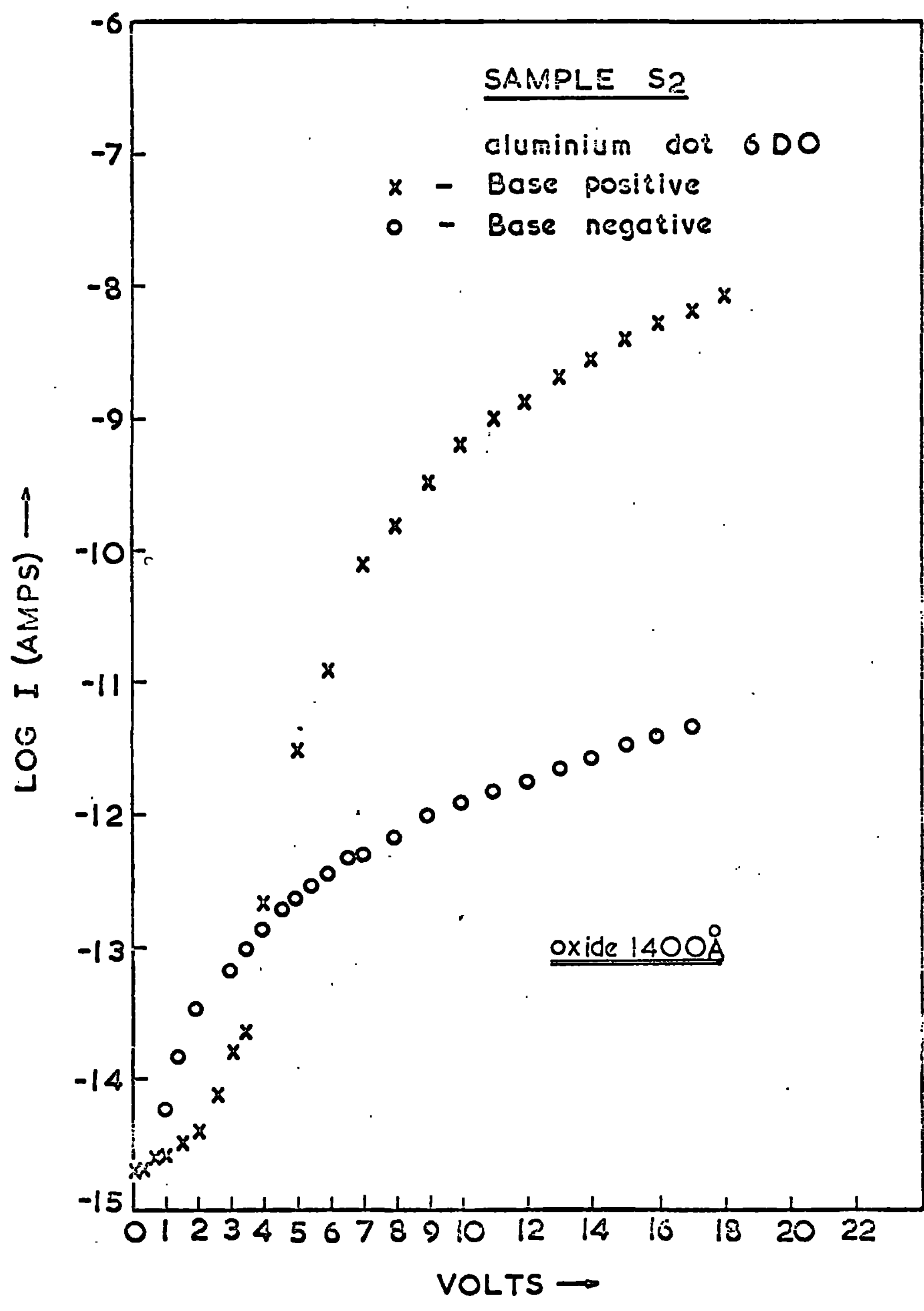

Fig. 6.3

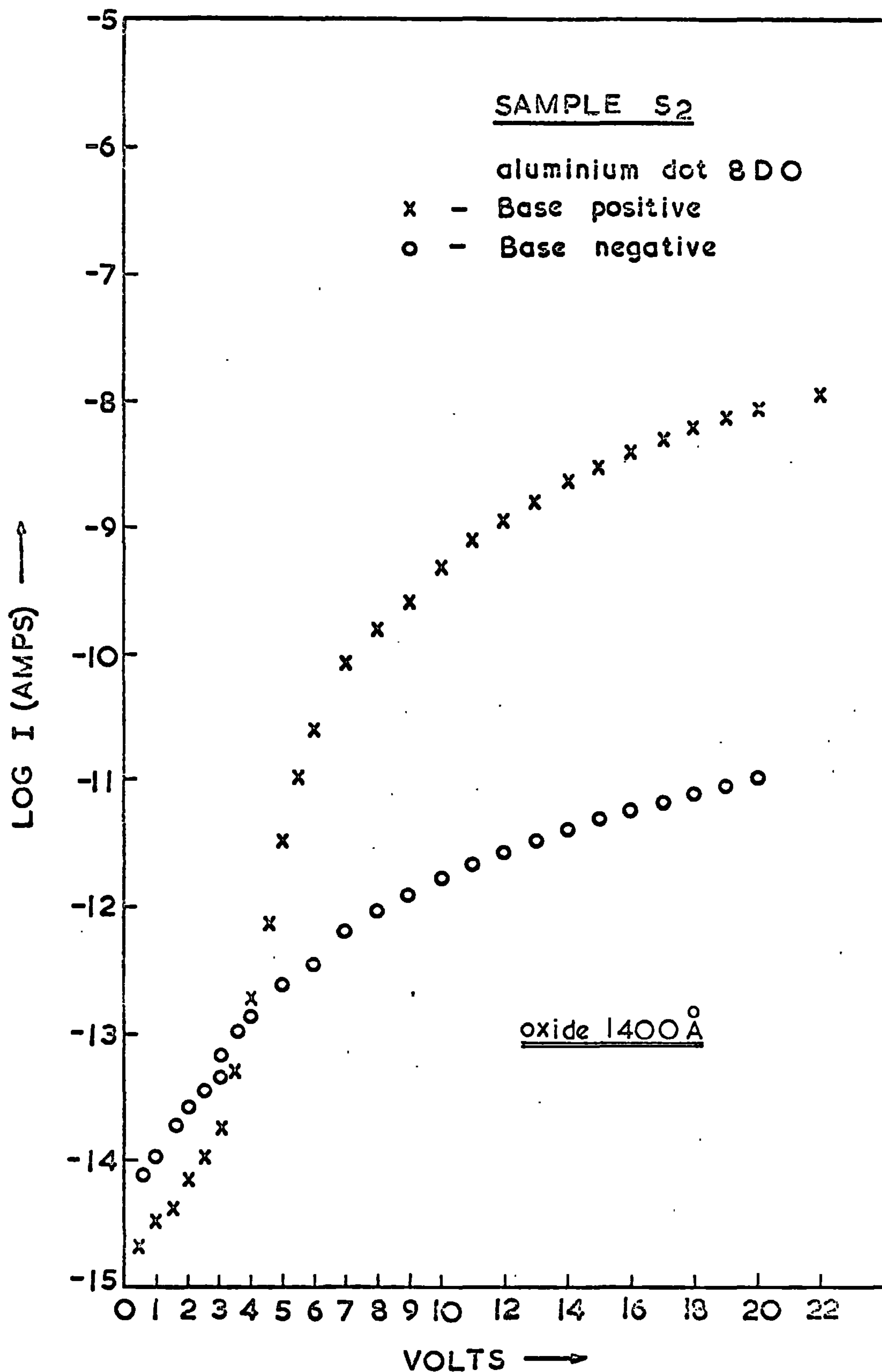

Fig. 6.4

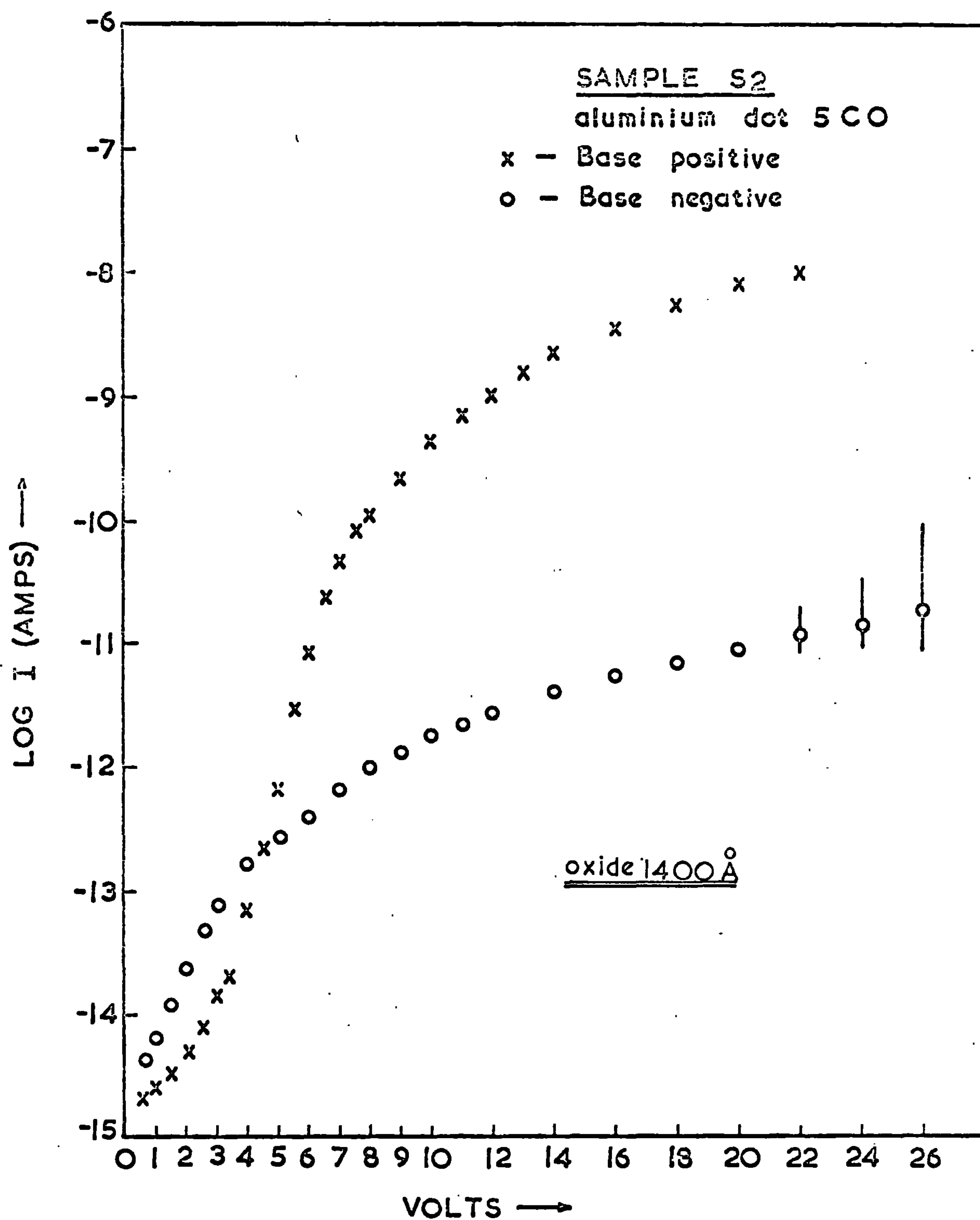

Fig. 6.5

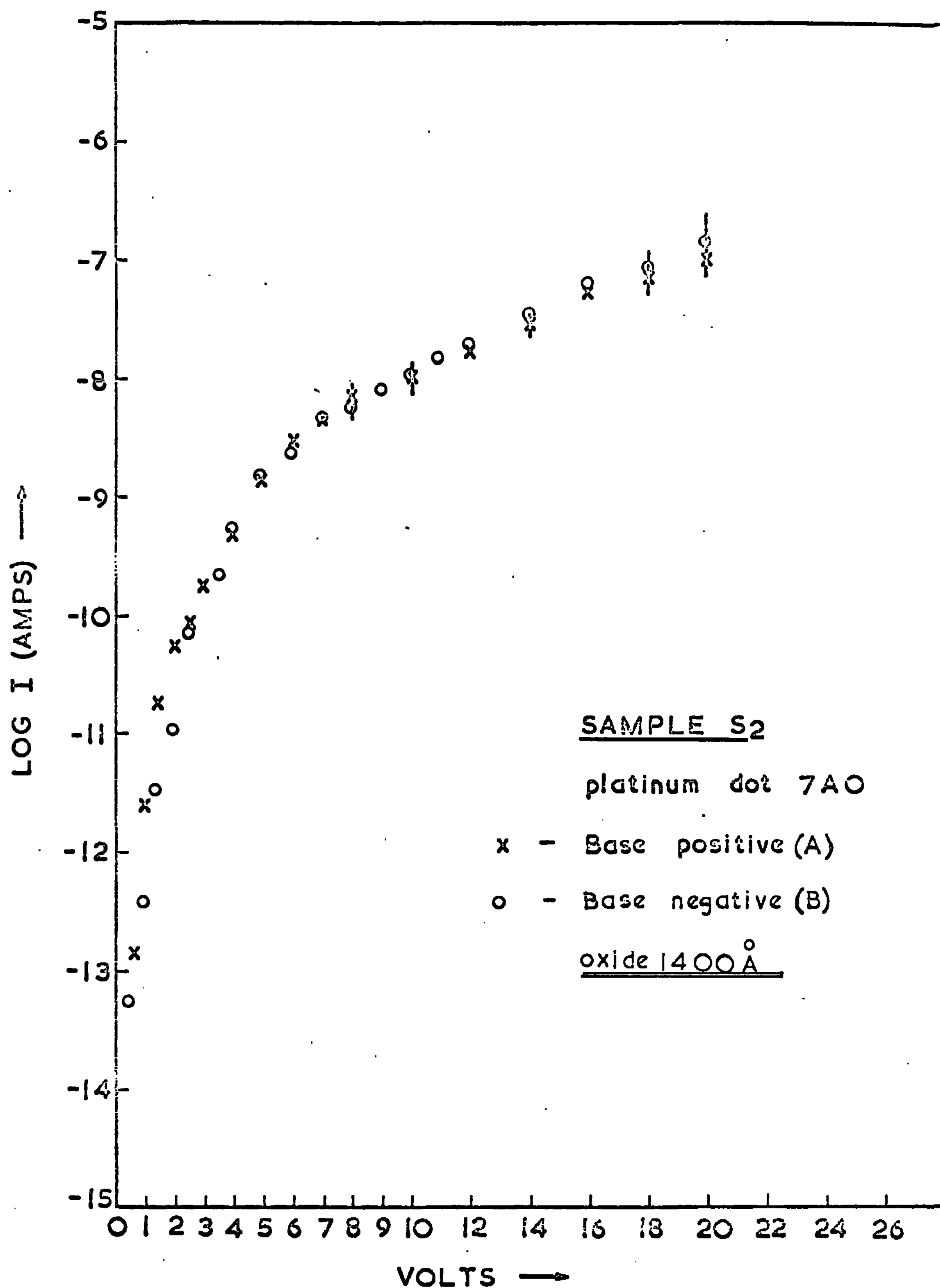

Fig. 6.6 A and B

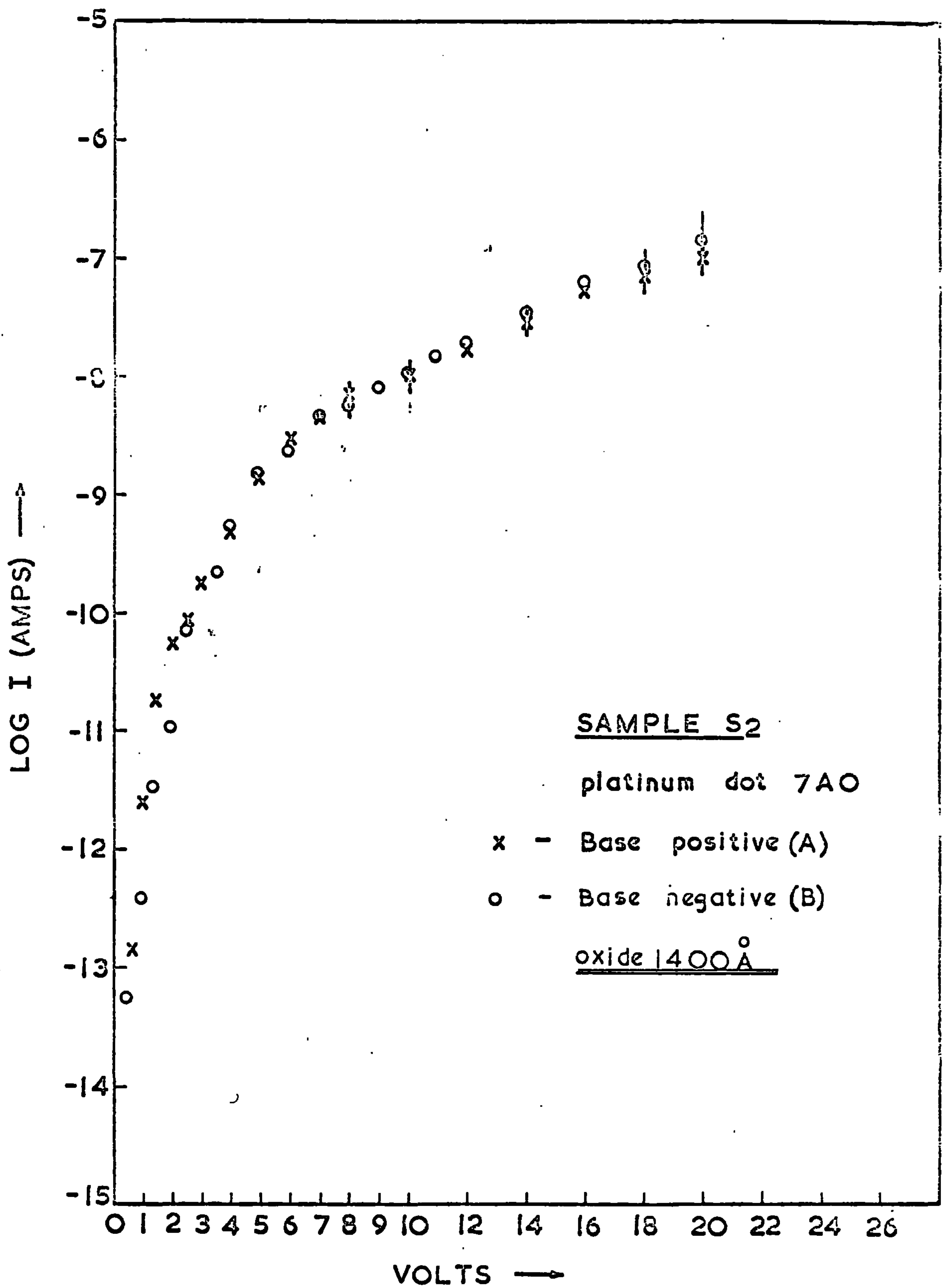

Fig. 6.6 A and B

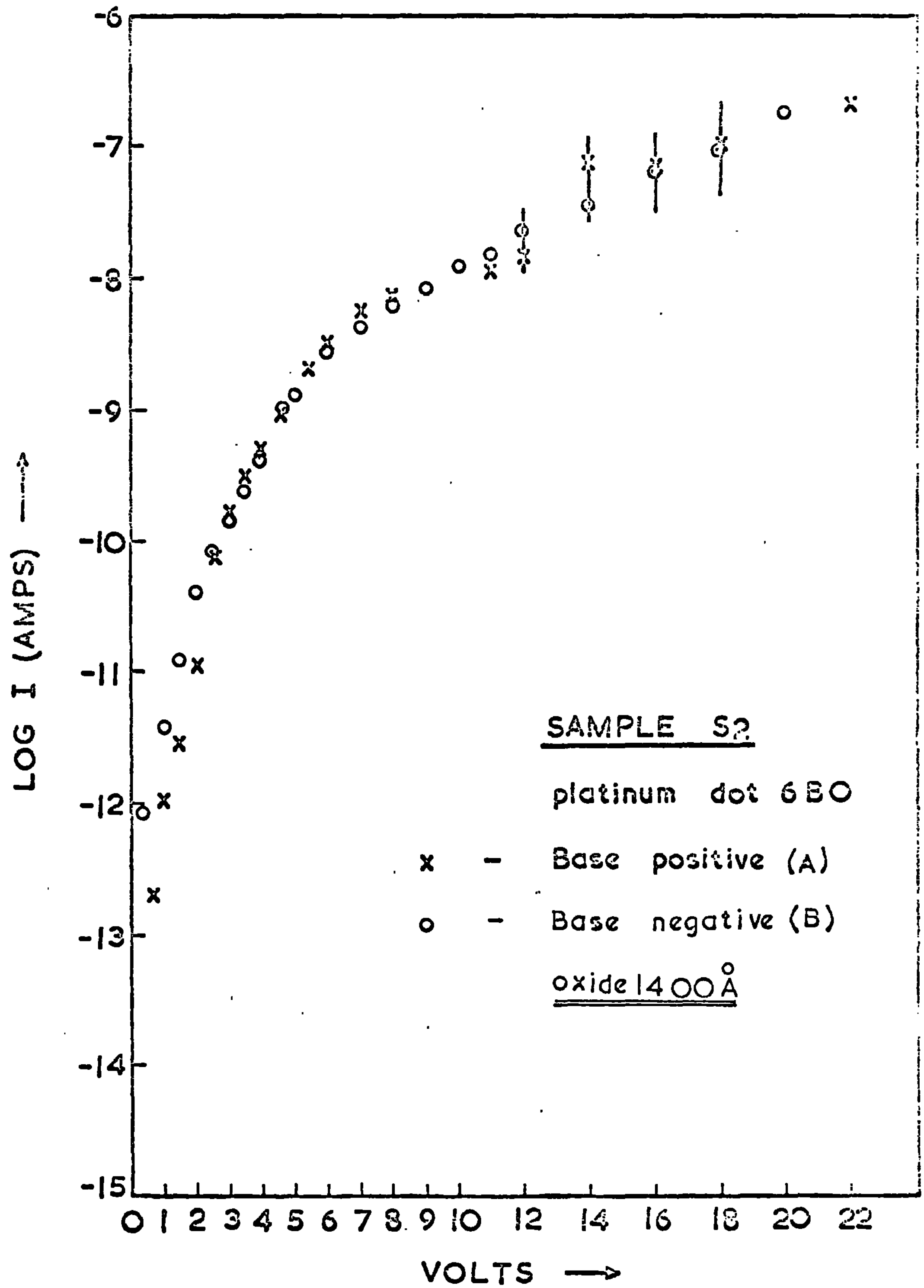

Fig. 6.7 A and B

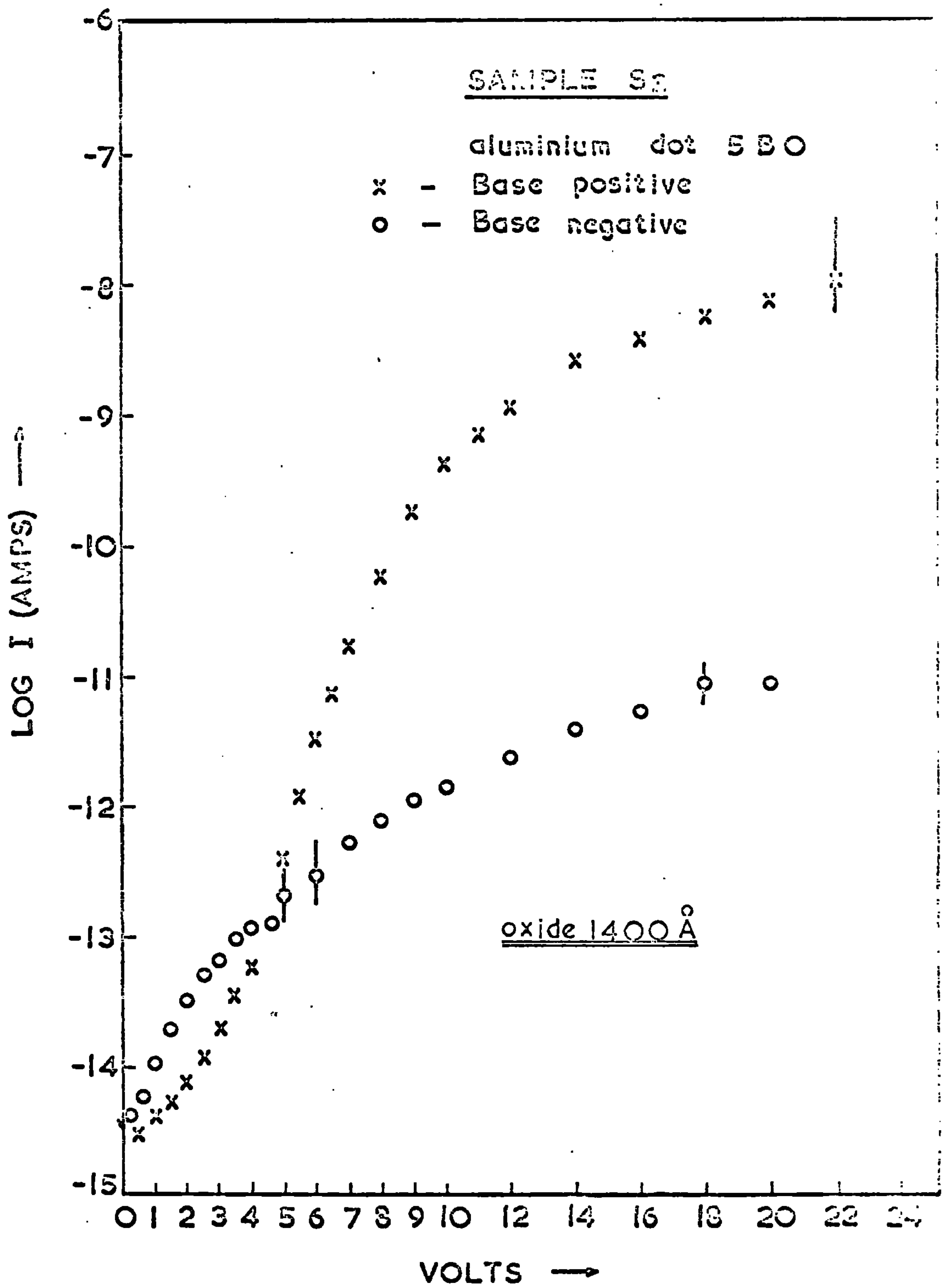

Fig. 6.8

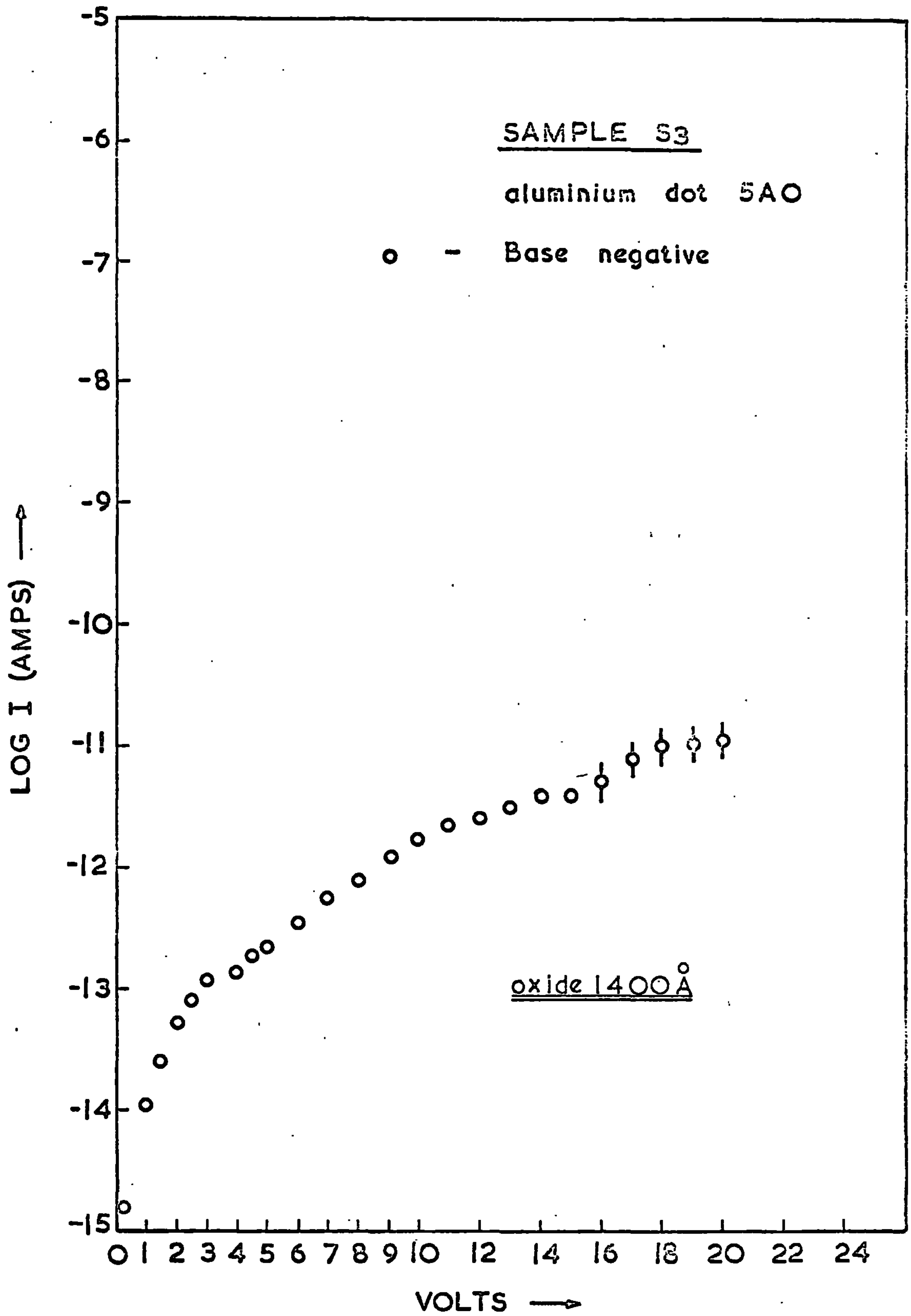

Fig. 6.9

almost indistinguishable from results obtained from the previous samples, showing that there is good reproducibility between samples made at different times.

Sample S_6 also had only four top contacts on the oxide area. Although the oxide did not seem to have been as adversely affected by argon bake as the willemite areas on this sample (see Table 6.2), the I-V curve could be plotted for only one dot for both polarities as shown in Figure 6.10. One of the other test dots was completely short circuited and two broke down after I-V characteristics had been plotted for one polarity. The resulting measurements made with the base negative are almost the same for all three dots (Figures 6.11 and 6.12). Another interesting feature of these curves is that their shape is very similar to that of the curves from samples S_2 and S_3 for the same polarity, although the current is about four orders of magnitude higher for sample S_6.

6.4 Results for Willemite on Sample S_1

Sample S_1 was different from the others in that the oxide film was baked in oxygen before willemization (see Section 6.1). Altogether there were 20 aluminium dots on the willemite and I-V measurements were carried out for all of them. The measurements were for one polarity only as they were terminated in electrical breakdowns. The current with the base electrode positive was always very unstable, and it fluctuated up to about an order of magnitude in some cases. However the current for the opposite polarity was much more stable and smooth I-V curves were obtained in most cases. Curves for both polarities are shown in Figure 6.13 in which those for the base positive have been

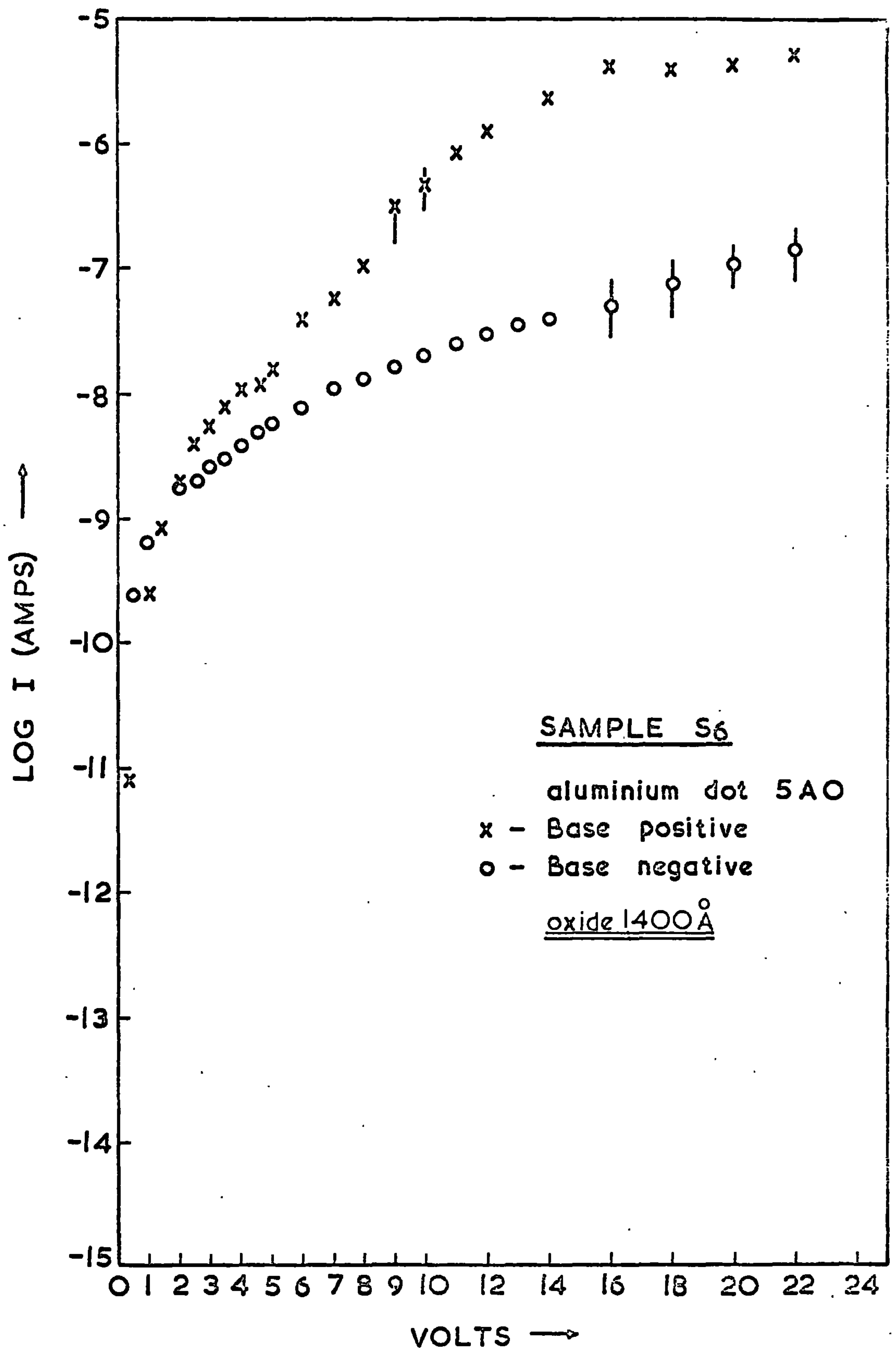

Fig. 6.10

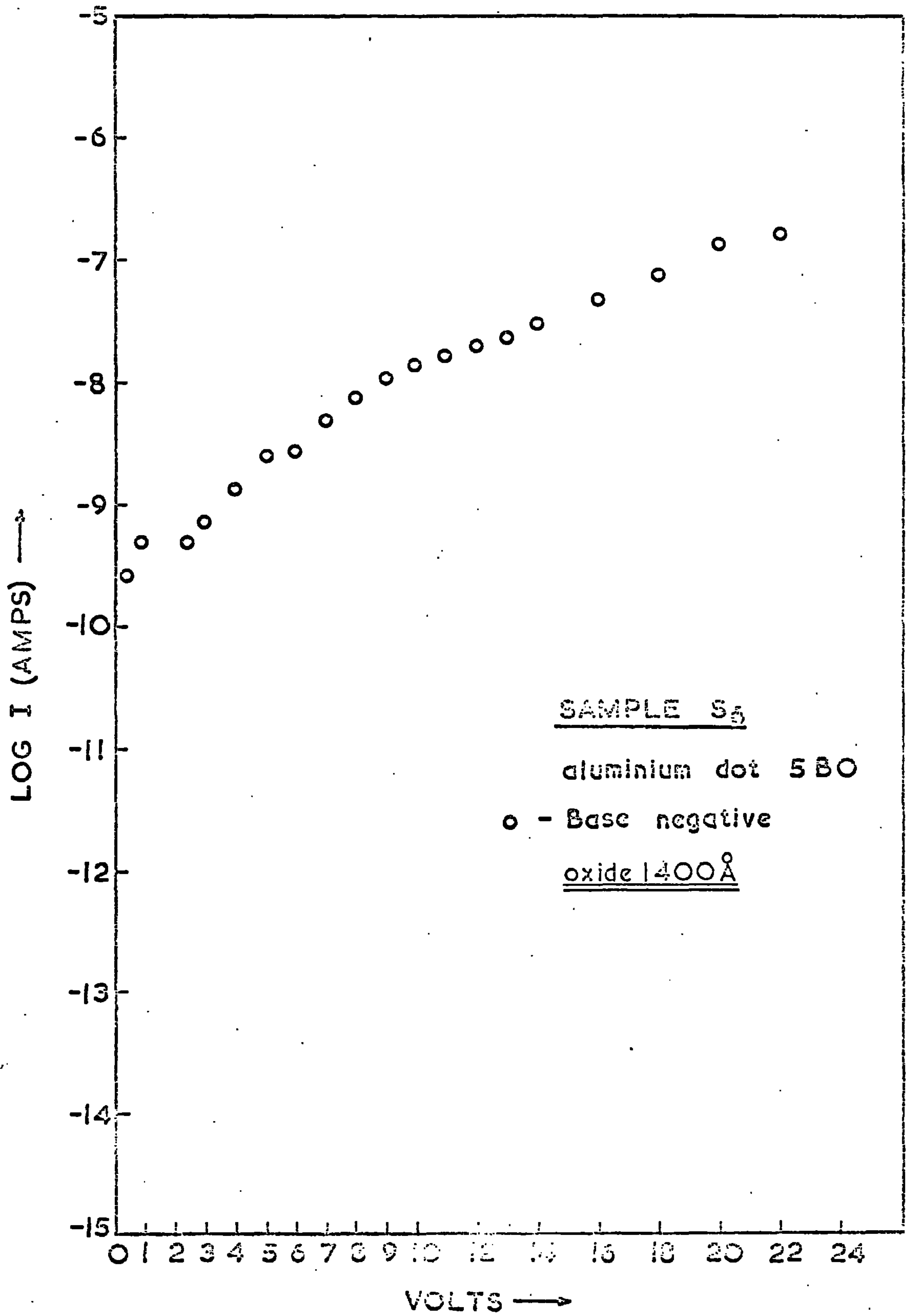

Fig. 6.11

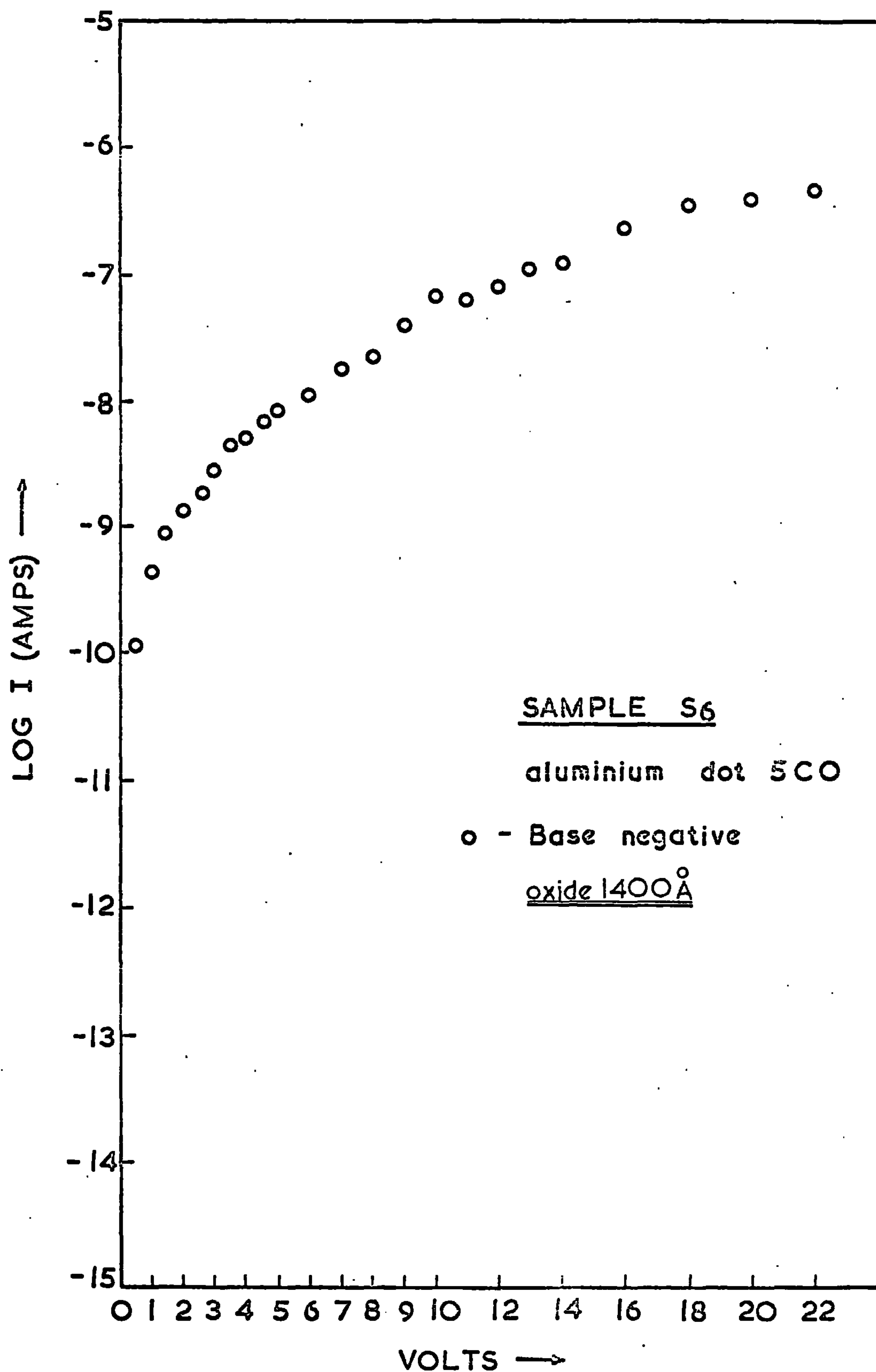

Fig. 6.12

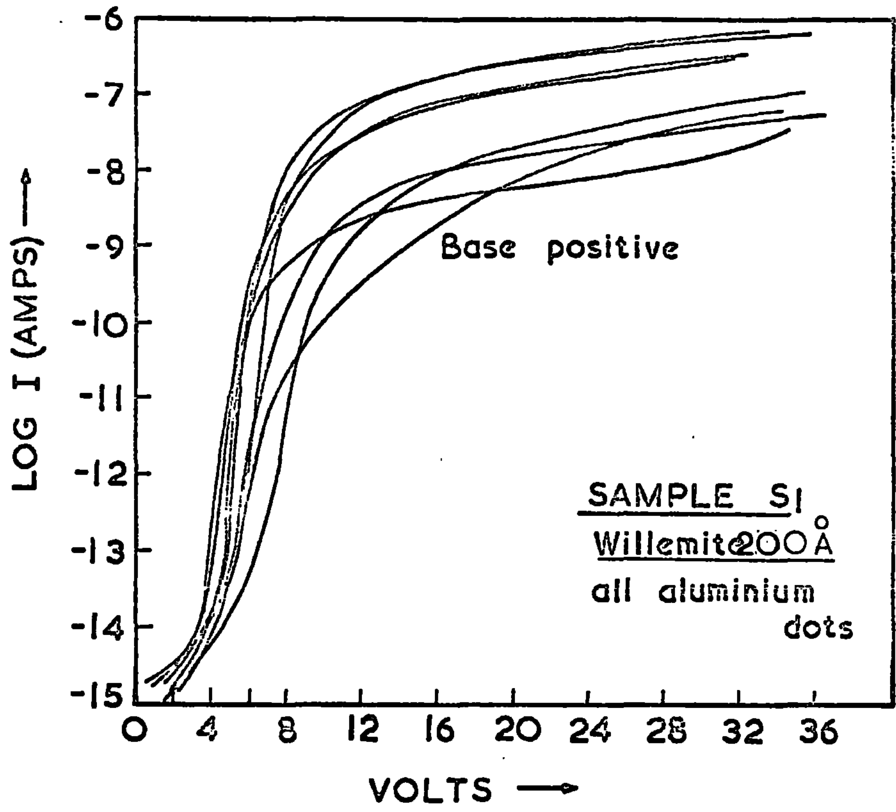

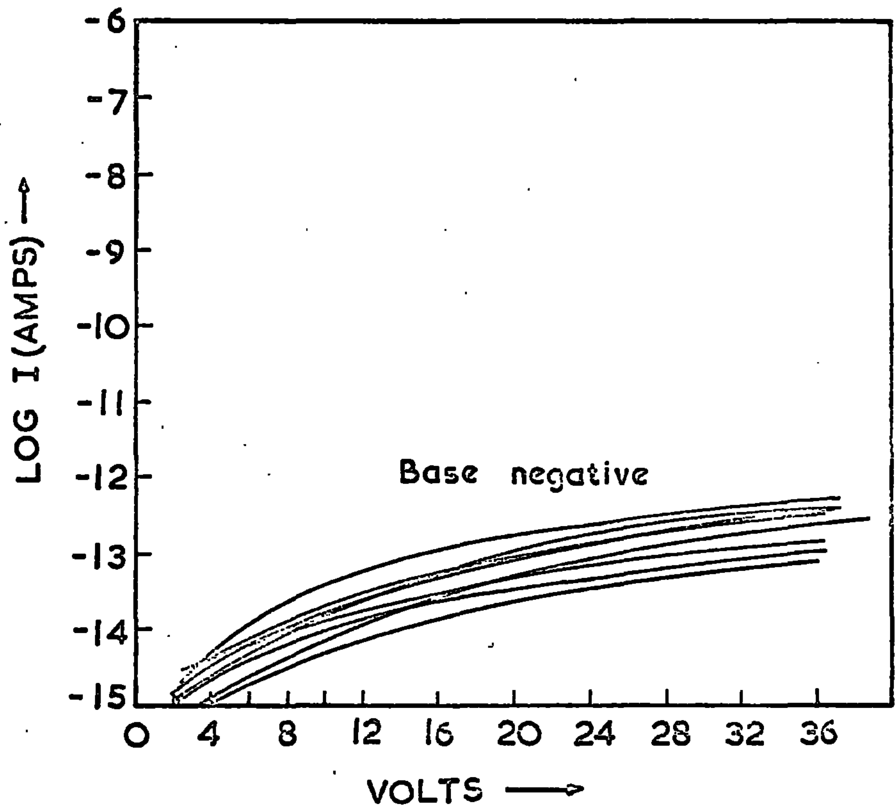

Fig. 6.13

smoothed out for clarity. Complete measurements could not be made on four of the dots because they broke down at low voltages and these are not included in Figure 6.13. Comparison with measurements on the oxide of the same sample, Figure 6.1, shows that the curves for the base positive have different shapes, but for the opposite polarity they are very similar for the two films. With the base positive, the current in the willemite is also about three orders of magnitude higher than in the oxide. The breakdown voltage for the willemite films appears to be about 40 V or higher.

6.5 Results for Willemite on Sample S_2

As described in Section 6.1, sample S_2 also had one area of willemite on which there were eight top contact dots of aluminium and eight of platinum. Only five of the aluminium dots were measured in detail as they gave smooth and reproducible characteristics as shown in Figures 6.14 to 6.18.

The curves for the base positive are of similar shape to those for the oxide on this sample (Section 6.3) but shifted towards the current axis for low voltages and overall, are about an order of magnitude higher in current. The curves for the base negative are not very smooth and the currents are much lower, showing strong polarity dependence again for this sample.

Only five platinum dots could be measured since the other three had cracks and gave high currents at low voltages. The ones measured are shown in Figures 6.19 to 6.21. The shape of these curves is very different and the current is very much higher even as compared with measurements on the oxide with the same contacts (Section 6.3). Also dots,

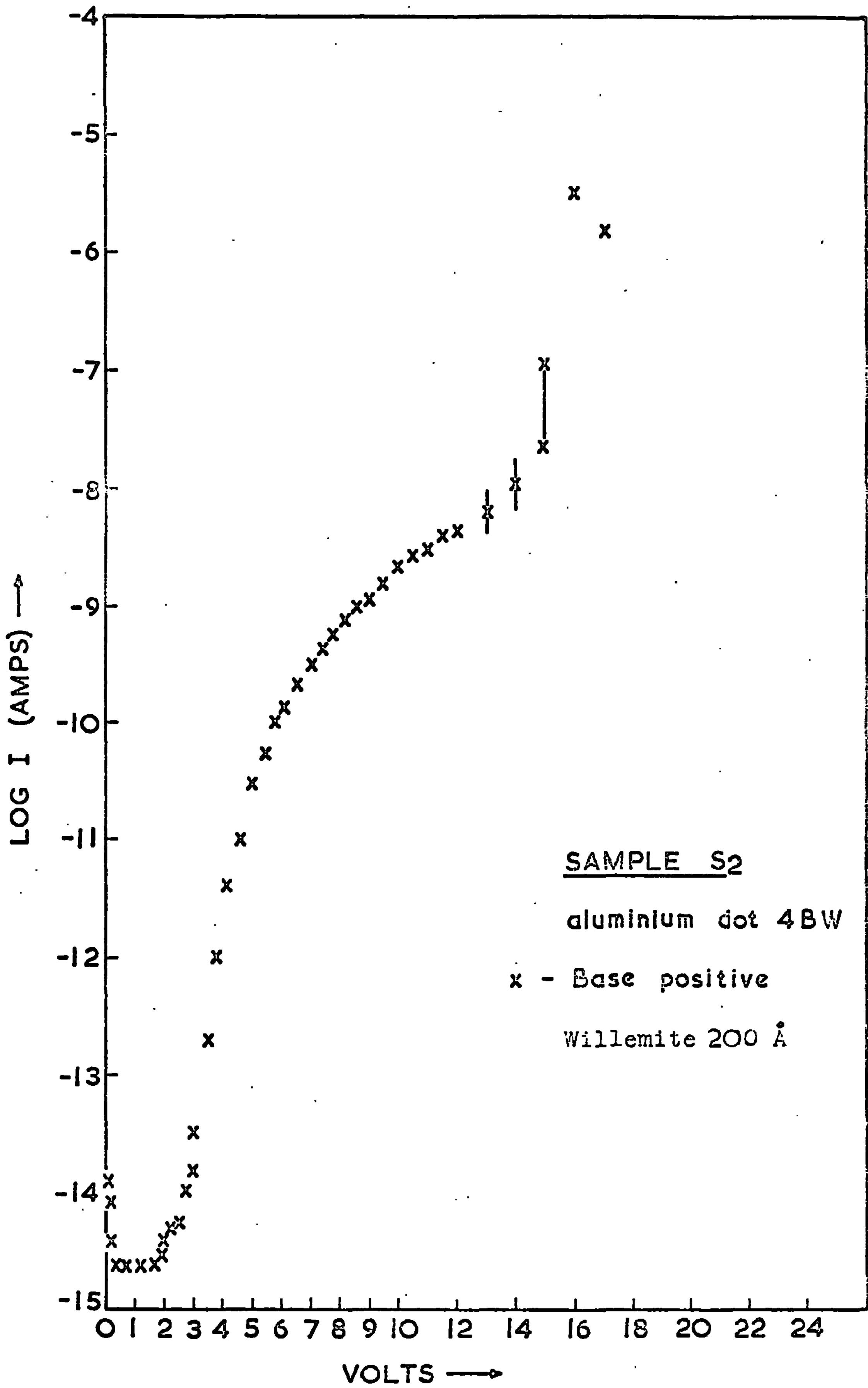

Fig. 6.14

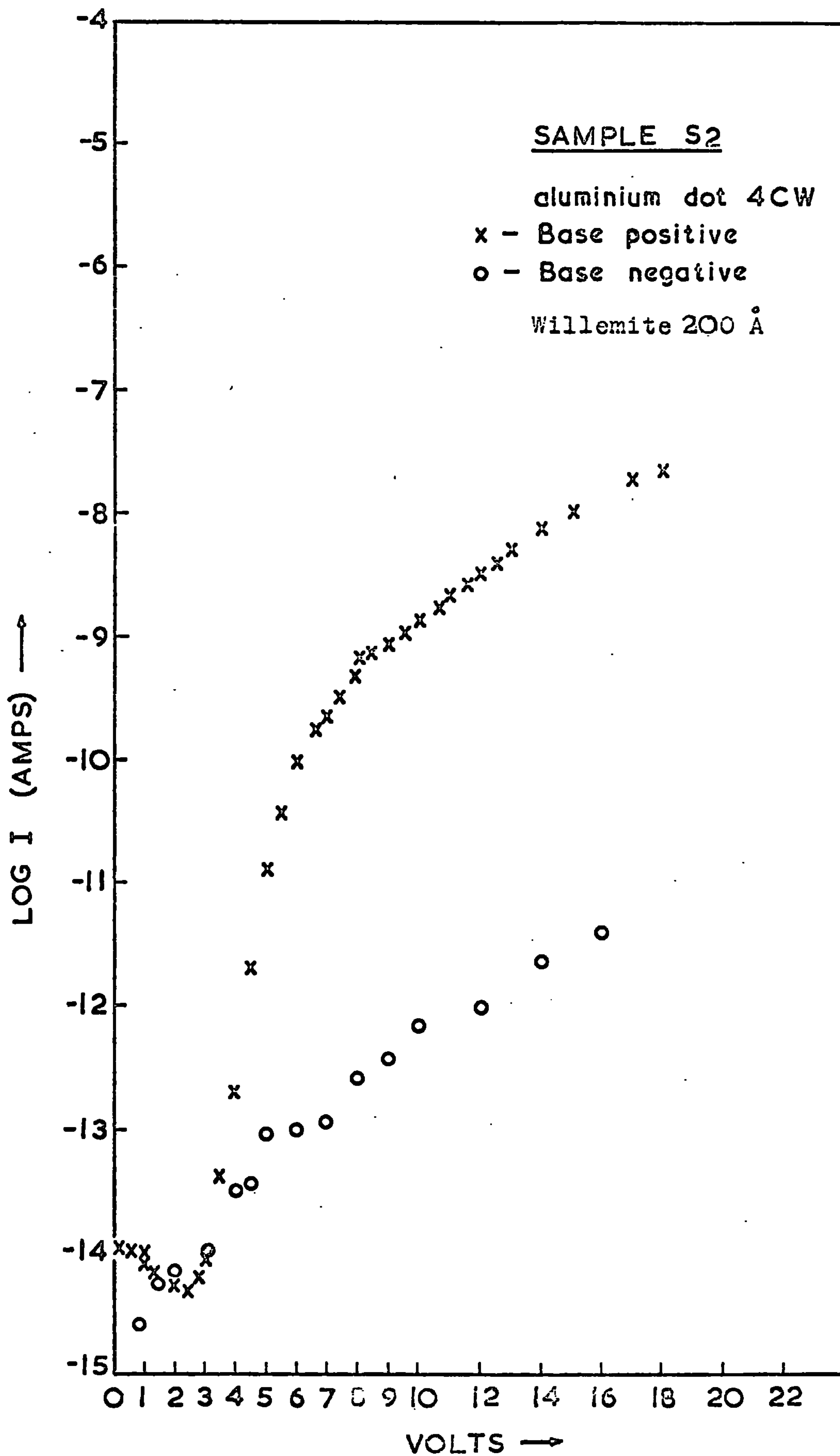

Fig. 6.15

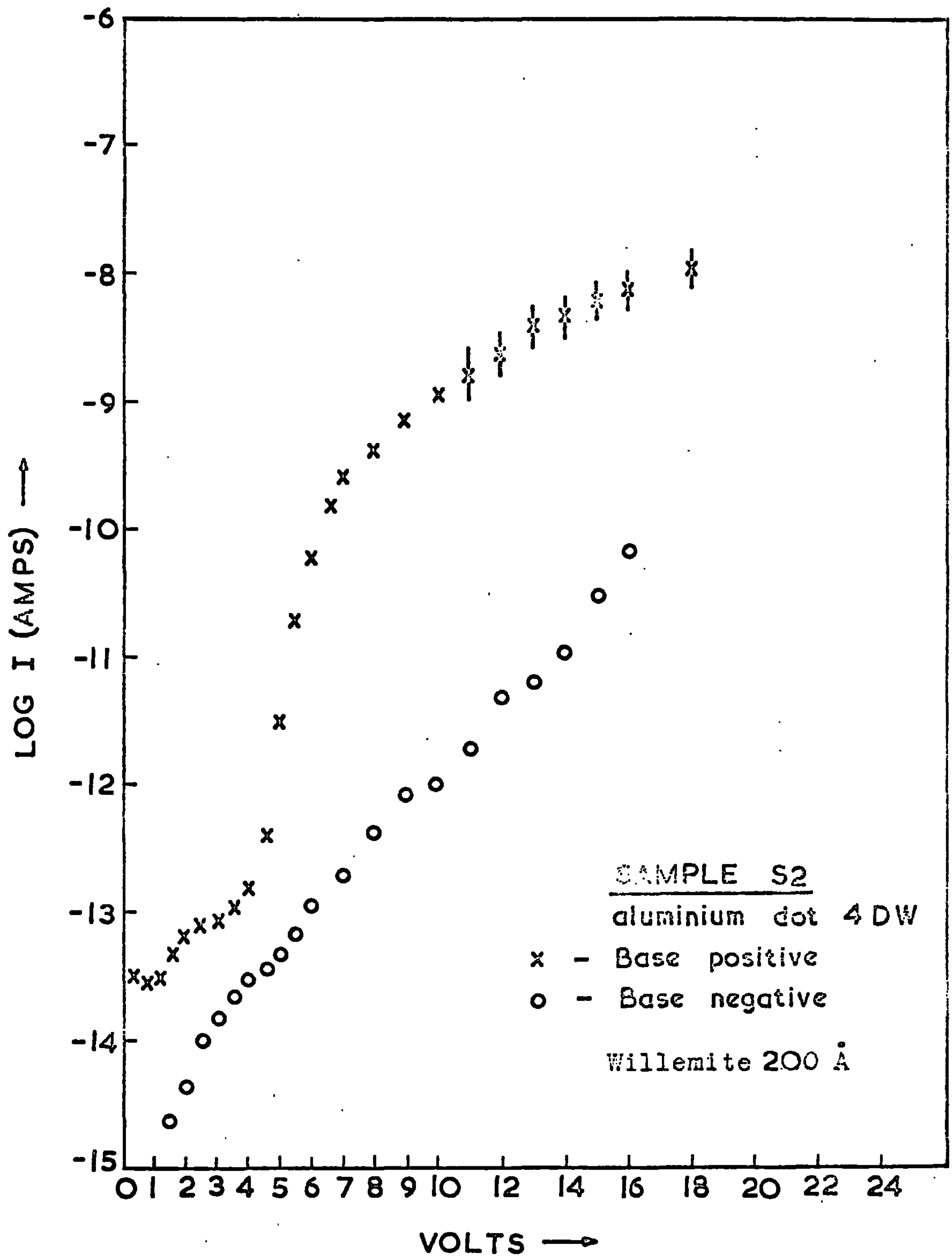

Fig. 6.16

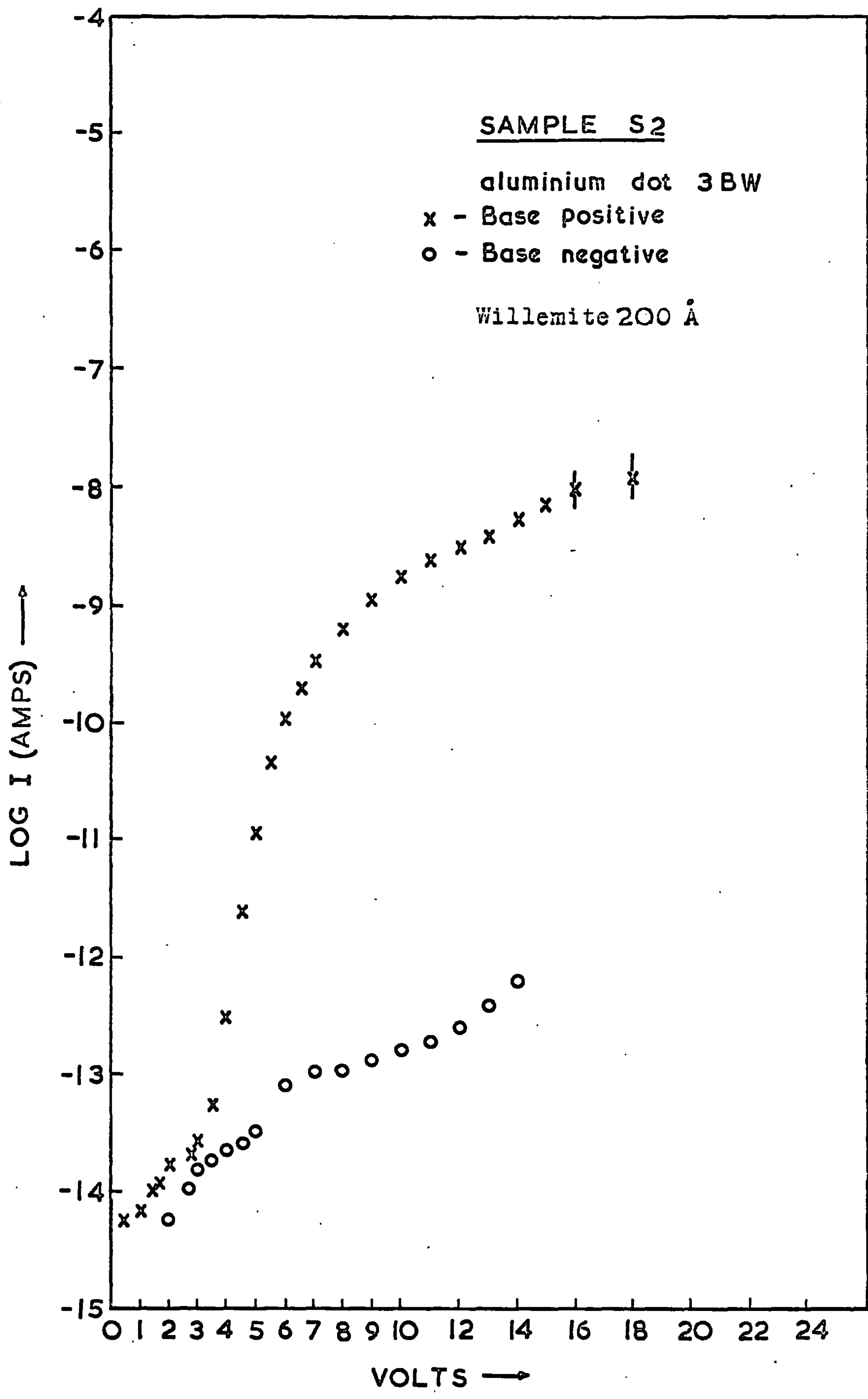

Fig. 6.17

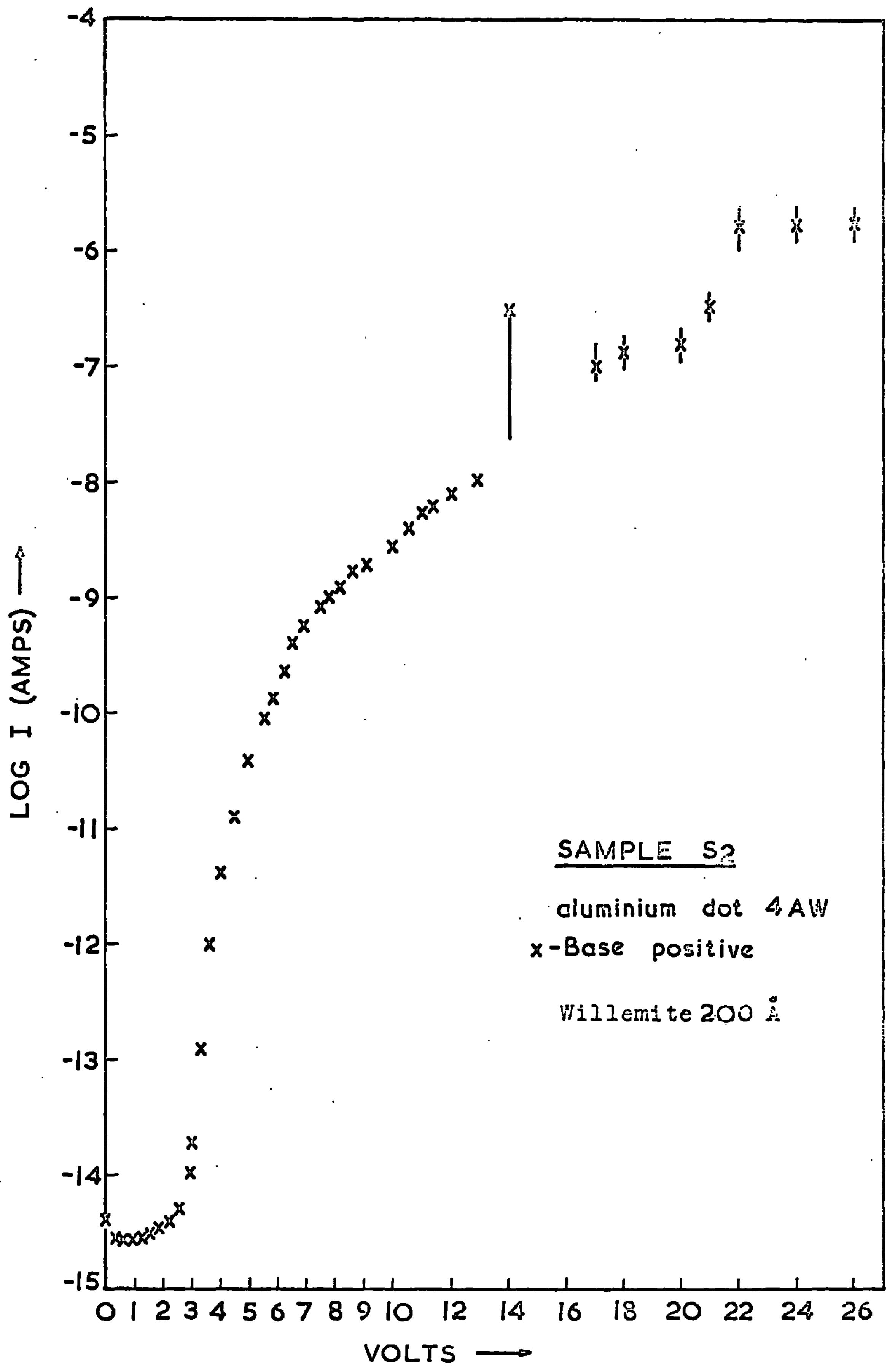

Fig. 6.18

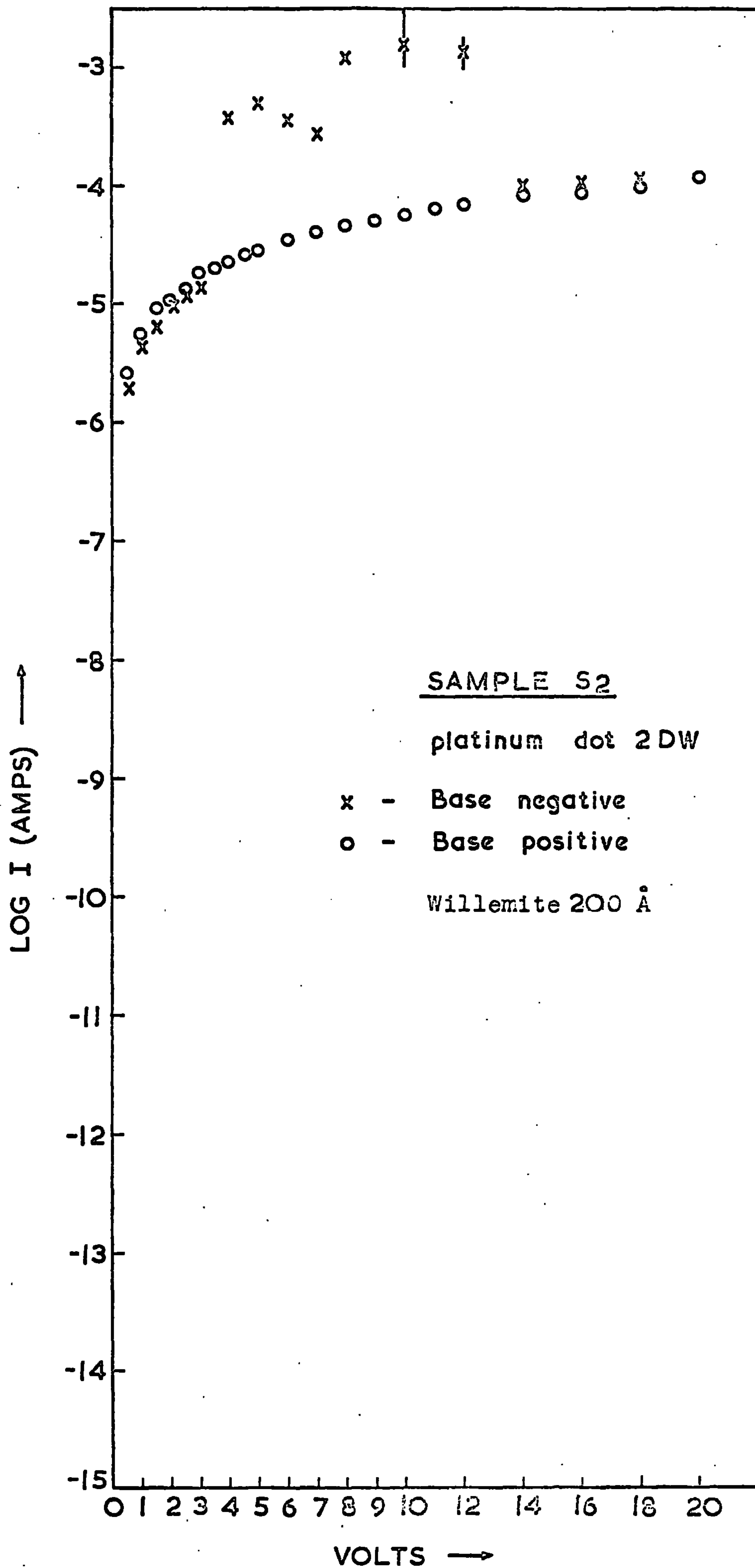

Fig. 6.19

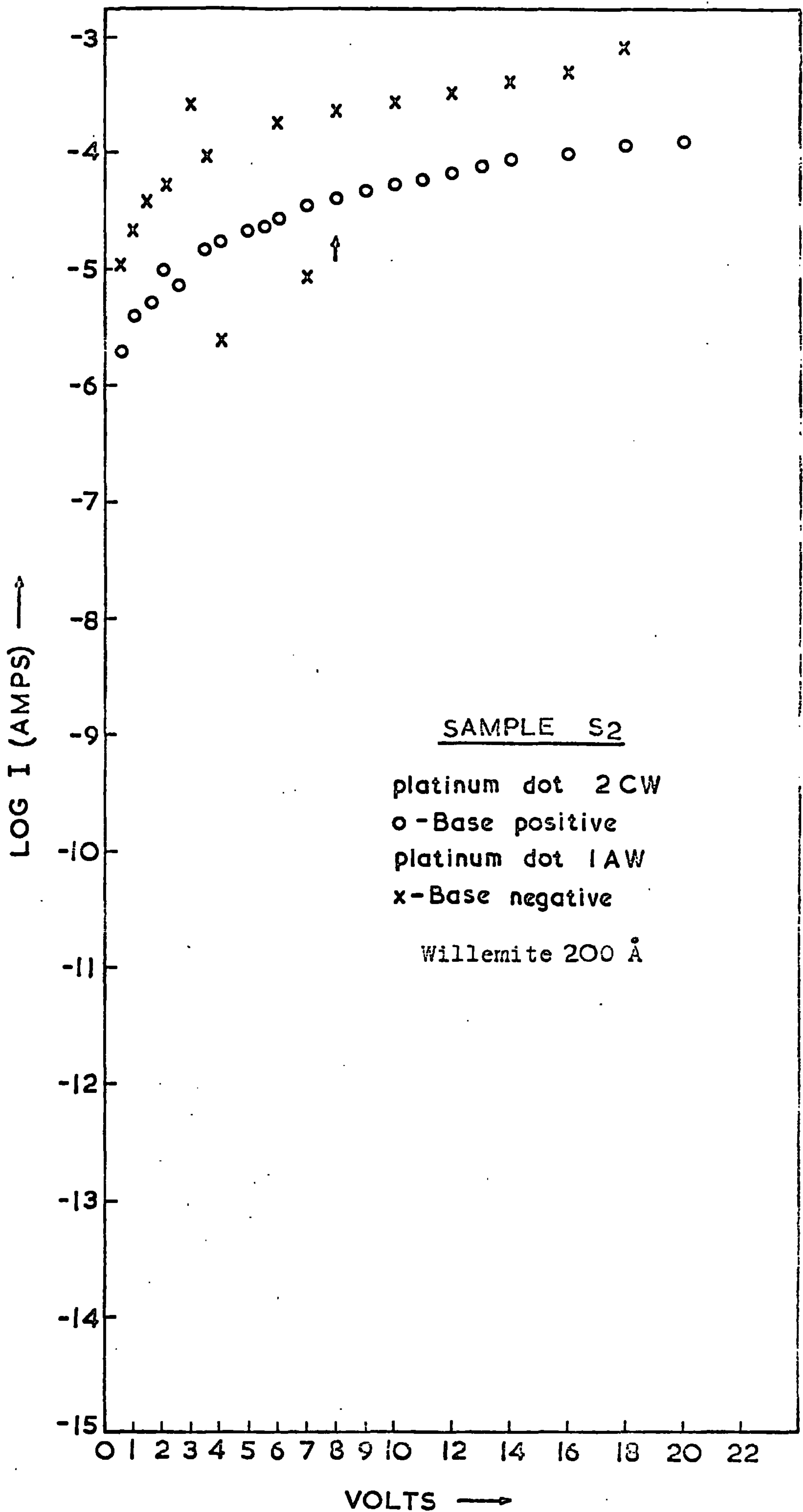

Fig. 6.20

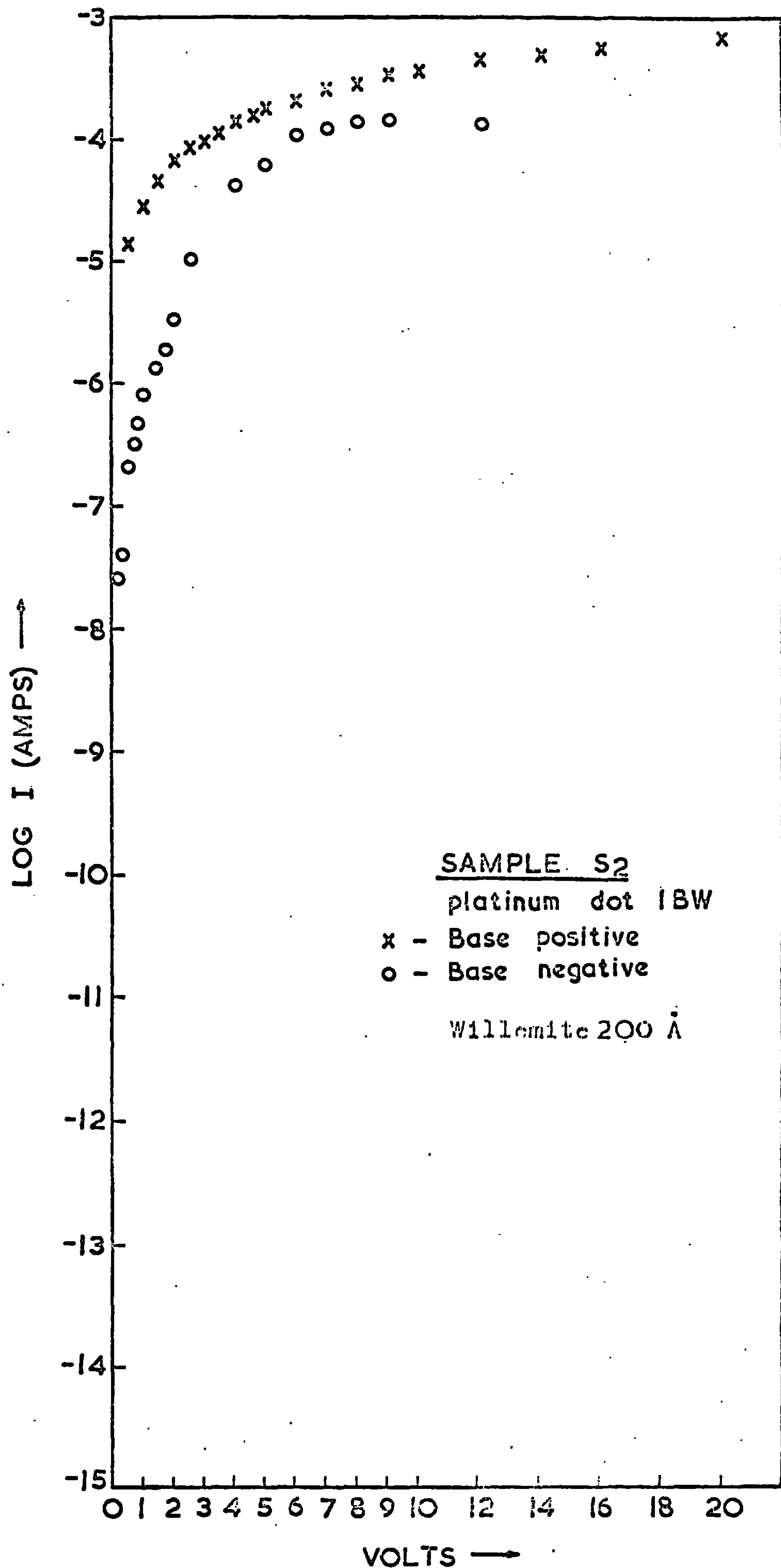

Fig. 6.21

1AW and 1BW, showed higher currents as compared to the rest. There does not seem to be any clear evidence of polarity dependence from these curves, although the current is possibly a little higher for low positive voltages applied to the base electrode.

Perhaps it is significant to note that on the oxide of this sample using the same platinum dots the range of current was roughly from 10^{-14}A to 10^{-7}A as against $>10^{-6}$A in the willemite. With aluminium top contacts on the other hand the oxide and willemite currents are not so much different.

6.6 Results For Willemite On Sample S_3

Sample S_3 had both 200 and 900Å thicknesses of willemite on the same oxide (Table 6.1). On the 200Å portion there were twelve aluminium and four gold top contact dots. Since the I-V measurements gave smooth and reproducible curves, only four of the aluminium dots were measured fully. These curves are shown in Figures 6.22 to 6.25 and are similar to those obtained for the aluminium contacts on sample S_2, showing some degree of reproducibility from sample to sample. The current is again higher for the base positive giving a strong polarity dependence. No completely successful measurement could be made on the gold dots because of the low voltage breakdowns. One I-V curve is shown in Figure 6.26 which was giving lower current as compared to the aluminium dots when it too broke down at 10 volts. On the 900Å portion of sample S_3 there were eight aluminium and four gold top contact dots. Again since the I-V characteristics were reproducible for the base positive, only five aluminium dots were measured. However, it was also possible to obtain smooth

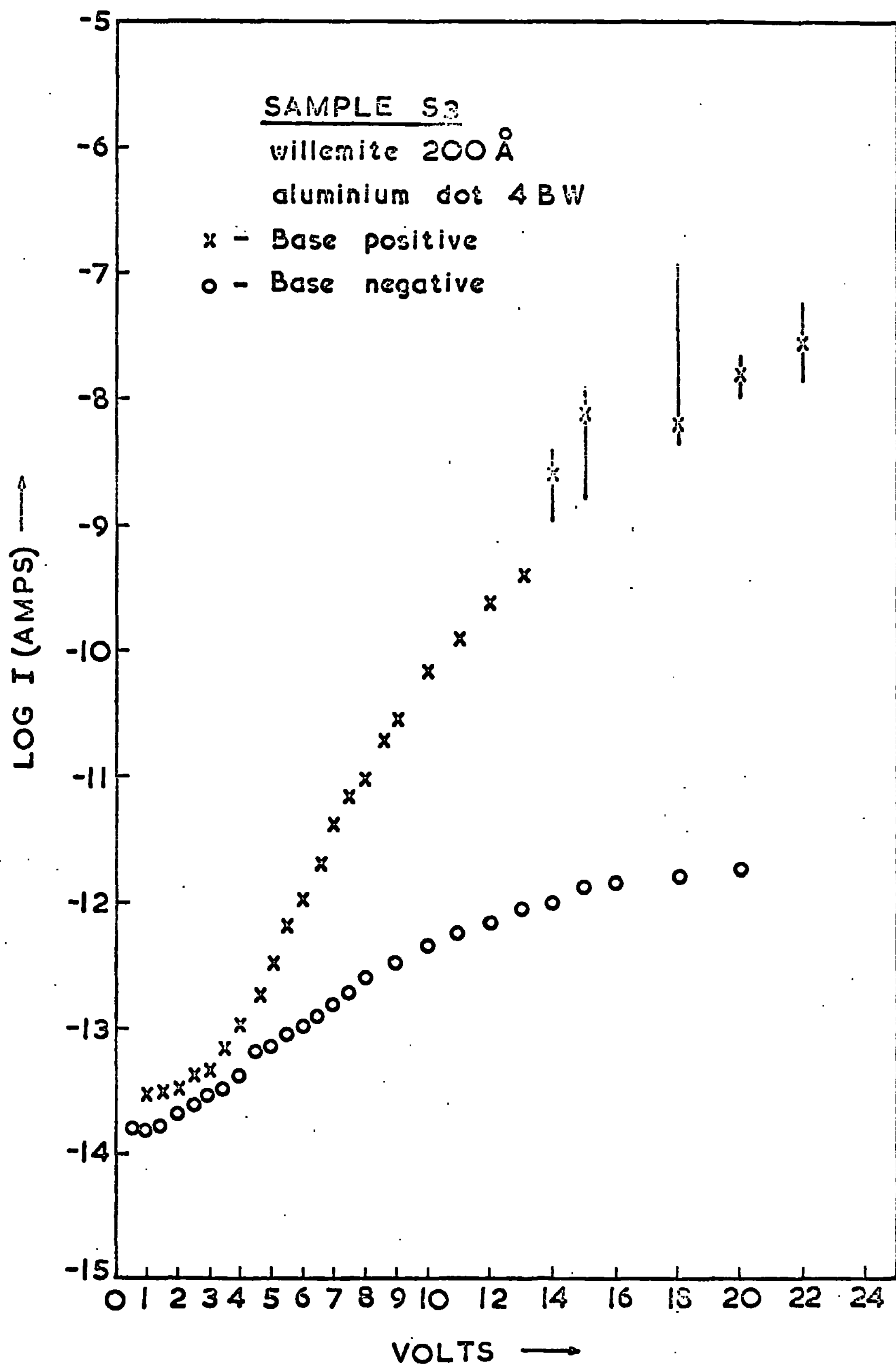

Fig. 6.22

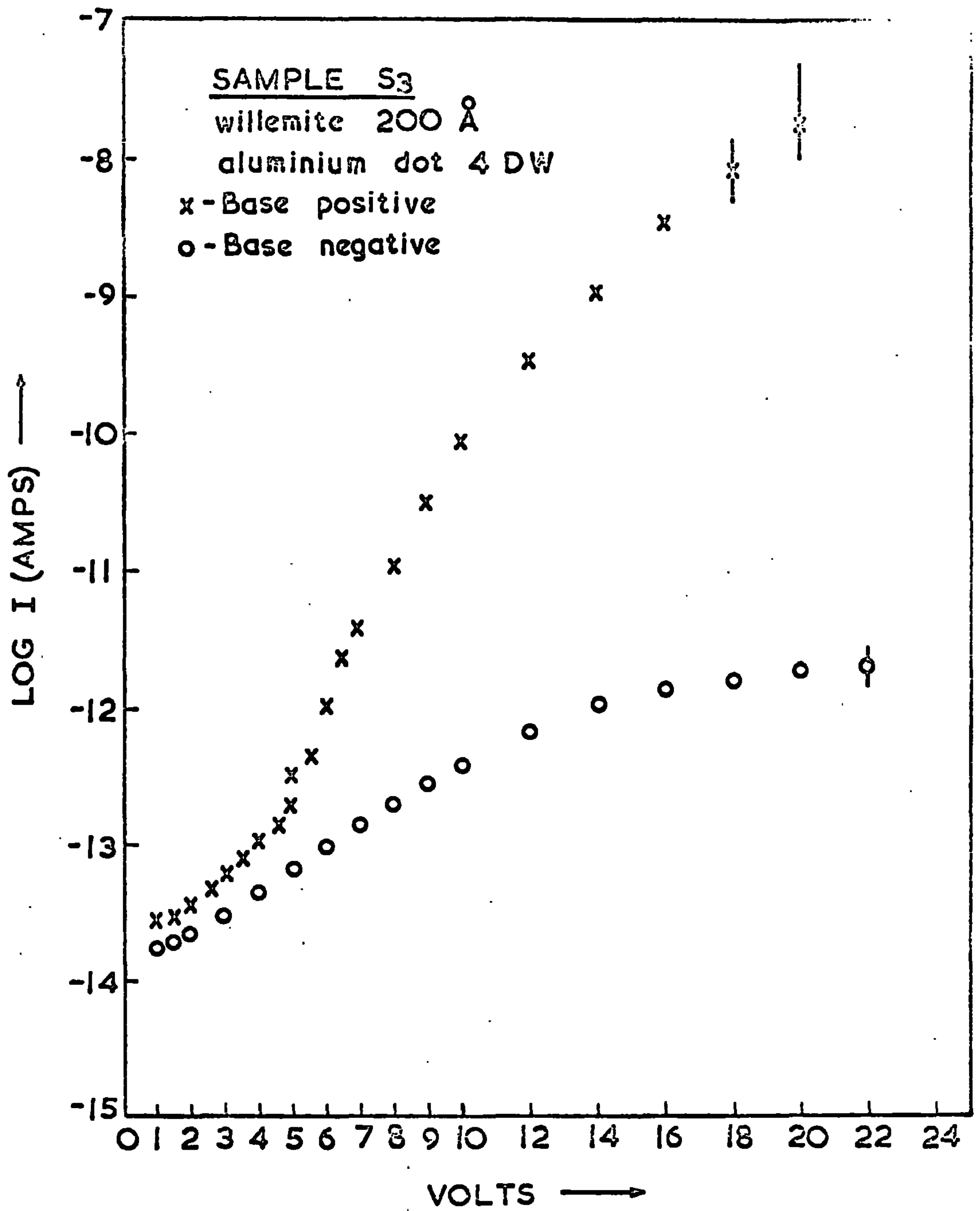

Fig. 6.23

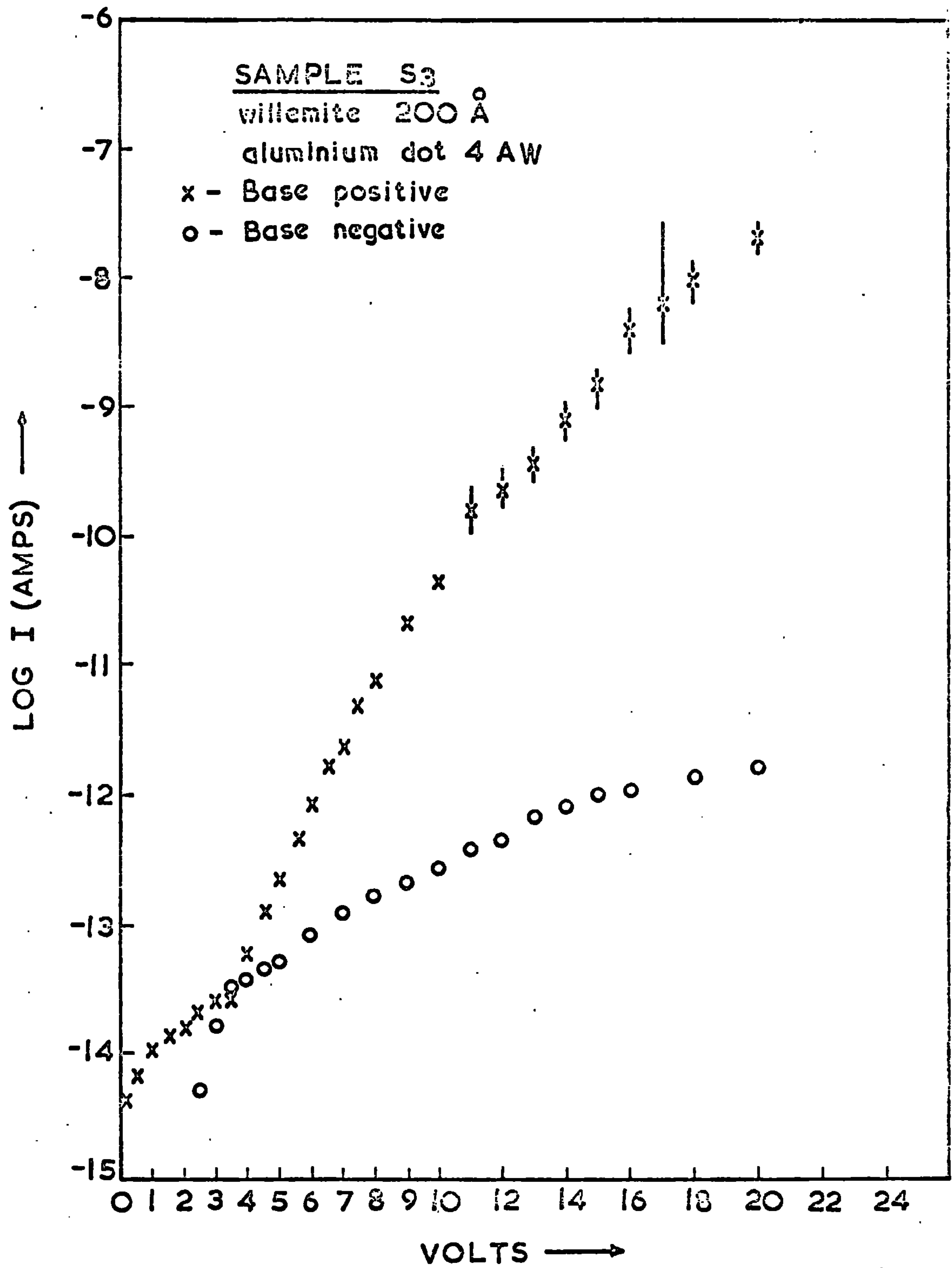

Fig. 6.24

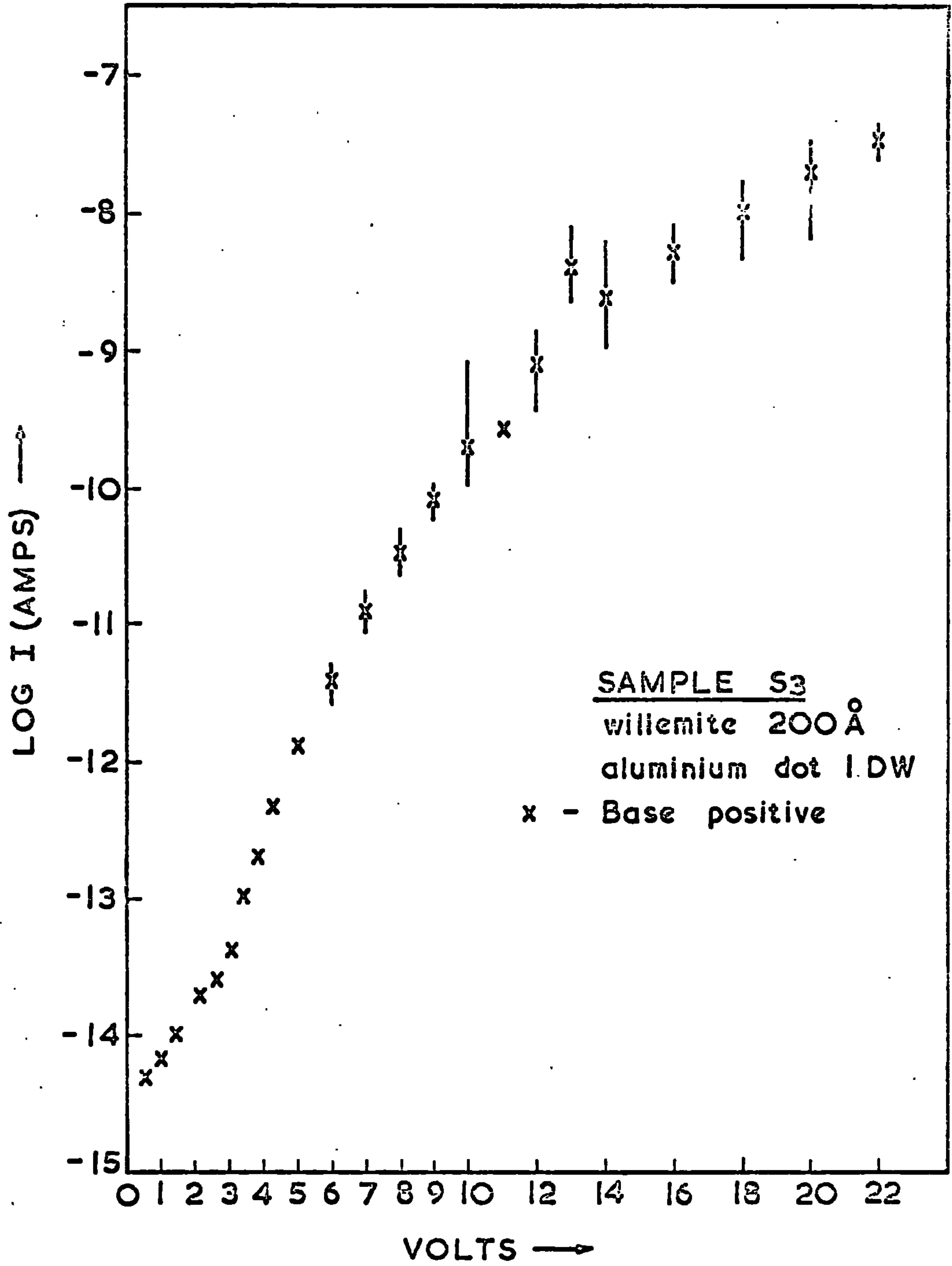

Fig. 6.25

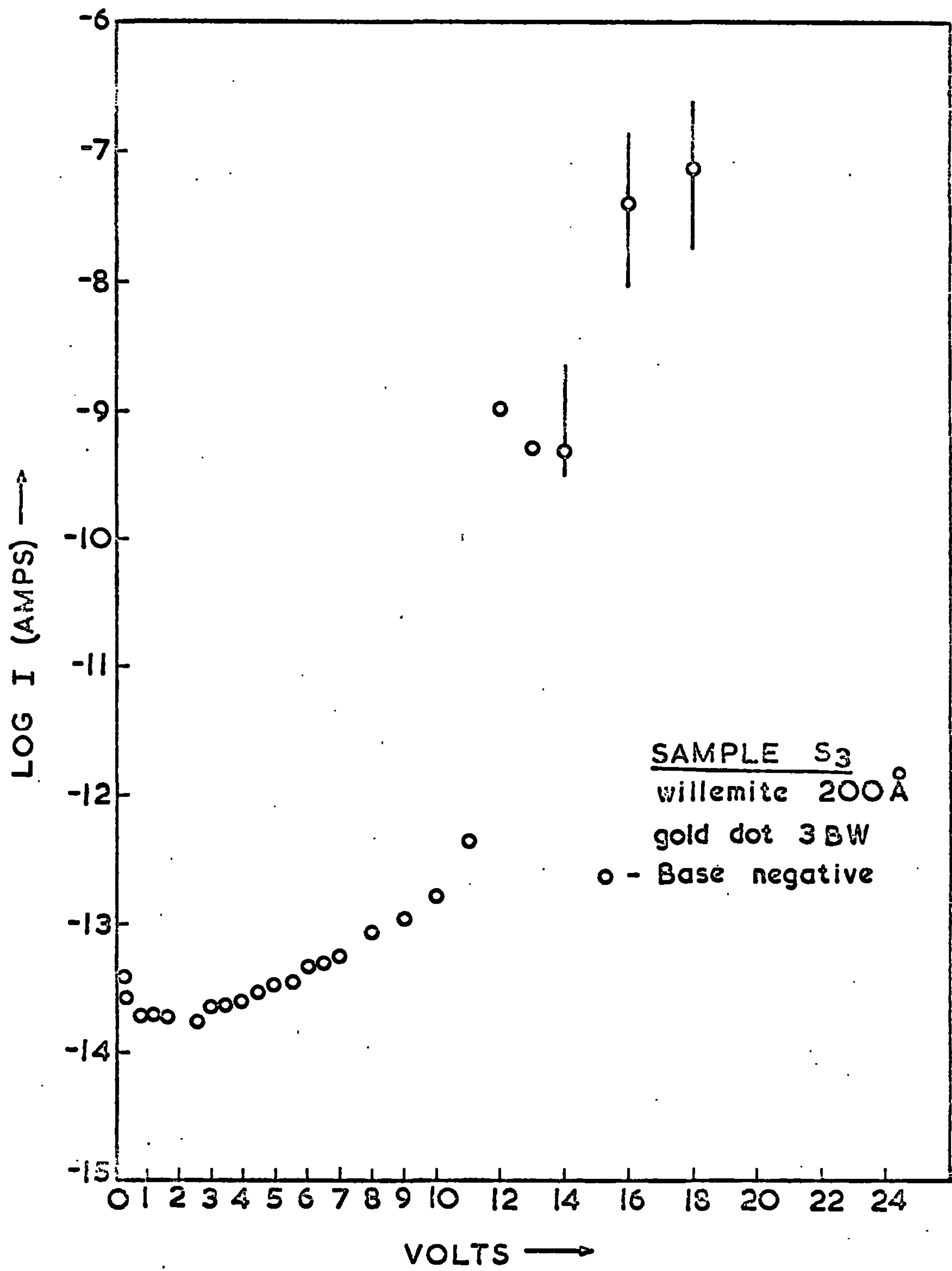

Fig. 6.26

curves for the three gold dots on this thickness of willemite. For the base negative, only one dot could be measured for each type of metal because of low voltage breakdowns. The curves are shown in Figure 6.27.

6.7 Results for Willemite on Sample S_6

As described in Section 6.1, sample S_6 was prepared to study the effect of the conversion bake in argon instead of oxygen, and to further investigate the effects of different thicknesses of willemite and different top contact metals. It had two regions of willemite which were ∿700 and 1000Å thick respectively. The results of the visual observations described in Table 6.1 were not very promising.

On the 1000Å portion there were eight aluminium and eight platinum top contact dots, while on the 700Å portion there were eight aluminium and four platinum dots. I-V characteristics were measured for all of them, but each one initially showed low resistance and partial breakdowns at low voltages (∿2V). Increasing the applied voltage appeared to remove the low resistance breakdown paths presumably by burning the defects and evaporating or spluttering the top contact metal around the probe. This led to the extensive damage of the surface ~~samples~~ of the top contact dots already noted in Section 6.6. In some cases the damage was not confined to the surface, but small holes all the way through to the substrate were observed under the low power of the microscope. After the measurements were completed the dots were classified according to the degree of damage and the ones least damaged were supposed to be the best as far as the reliability of the measurements was concerned. Starting from the least damaged ones, these were classified as having

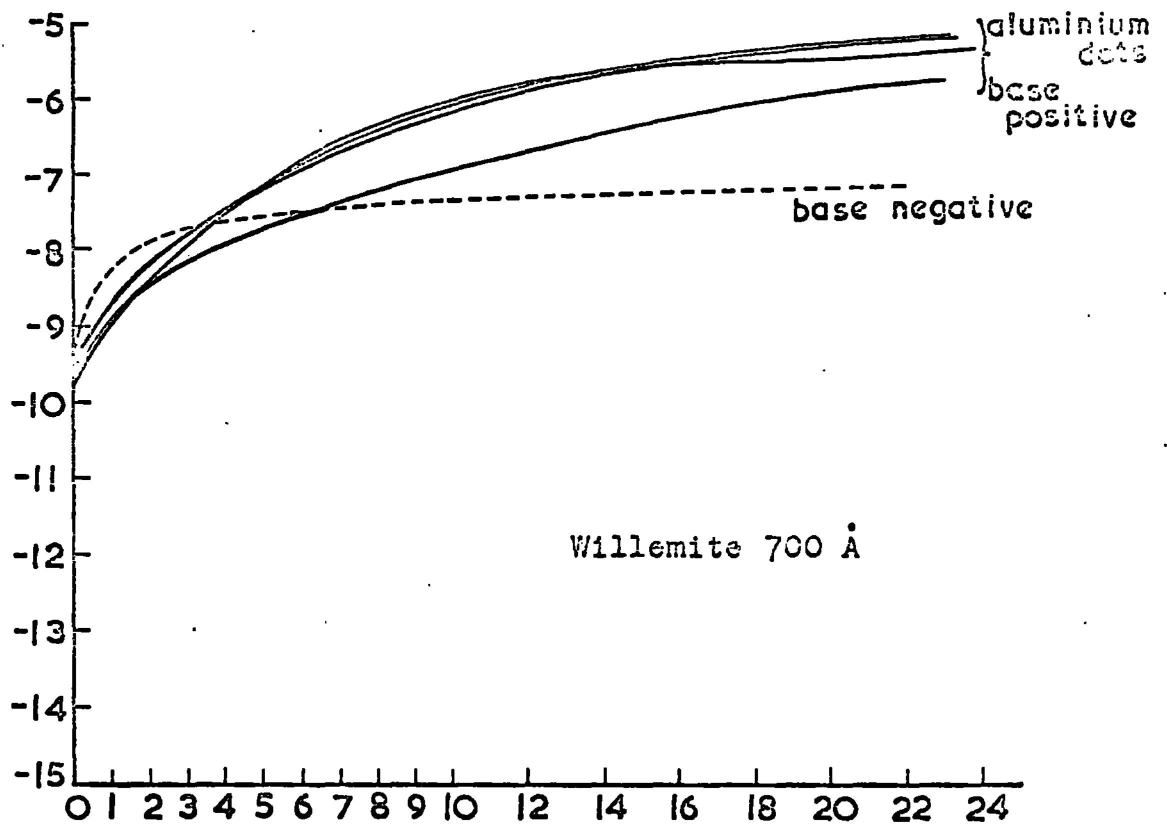

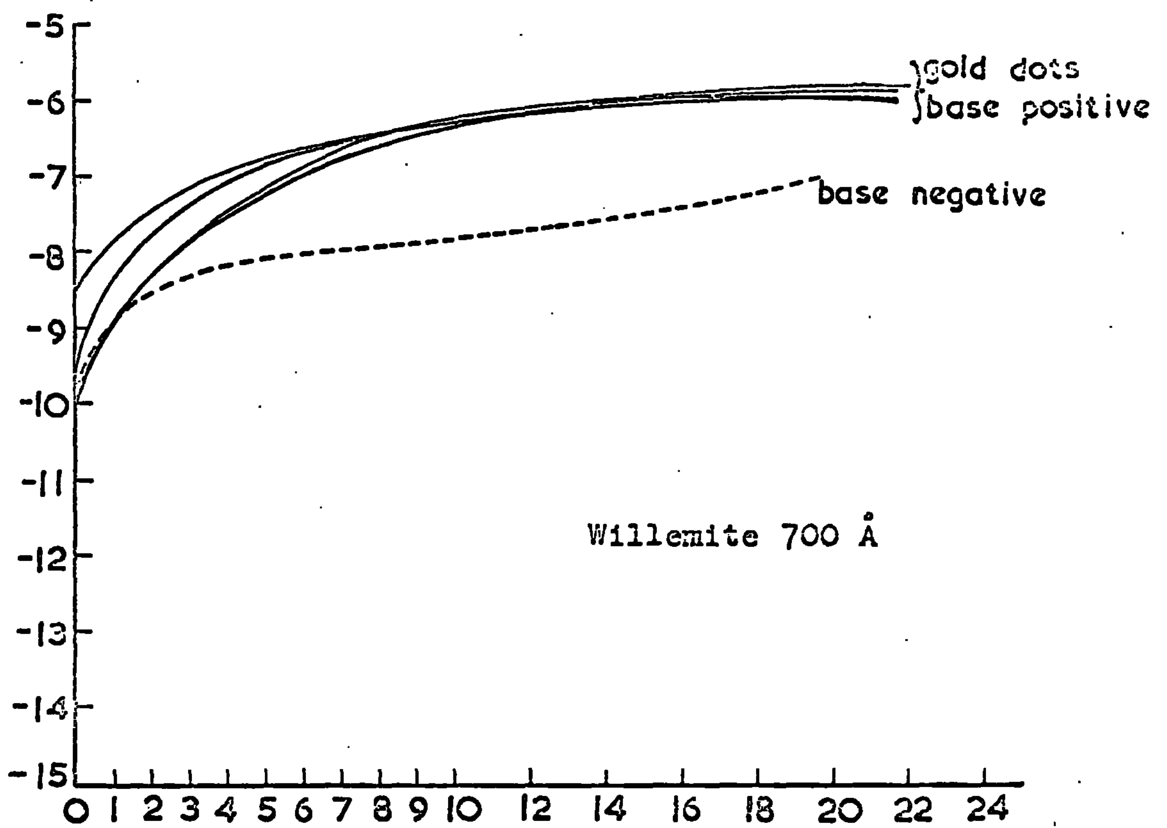

Smoothed I-V curves for sample S3

Fig. 6.27

slight damage, intermediate damage or heavy damage. No dot was completely undamaged. Similar damage was not nearly so extensive on previous samples.

On the 1000Å region one platinum and three aluminium dots were only slightly damaged and their I-V characteristics are shown in Figures 6.28 and 6.29. Figures 6.29 and 6.30,31 show the I-V curves for one slightly damaged and two intermediately damaged platinum dots for base negative. The former shows greatly reduced currents. Only one aluminium dot could be measured for both polarities but in general no polarity dependence is evident from the single polarity curves for individual dots. On the 700Å region one platinum and one aluminium dot was slightly damaged and could be measured for one polarity as shown in Figures 6.32 and 6.33. The one intermediately damaged aluminium dot could be measured for only one polarity as shown in Figure 6.34. Again there is about three orders of magnitude difference between the currents with the aluminium dots from the two categories. As a whole it appears that the bake in argon has adversely affected the electrical properties of the films on this sample. Table 6.3 has been produced to compare the occurrence of damage on this sample (S_6) with that on S_3, which also had two areas of willemite on the same oxide thickness, but was baked in oxygen. There can be little doubt about the significance of the differences.

	Number of dots on each sample			
Sample baked in	No damage	Slight damage	Int. damage	Heavy damage
argon	NIL	6	3	23
oxygen	28	very slight 4	NIL	NIL

Table 6.3 showing the "after measurement damage" to the dots of two differently baked samples.

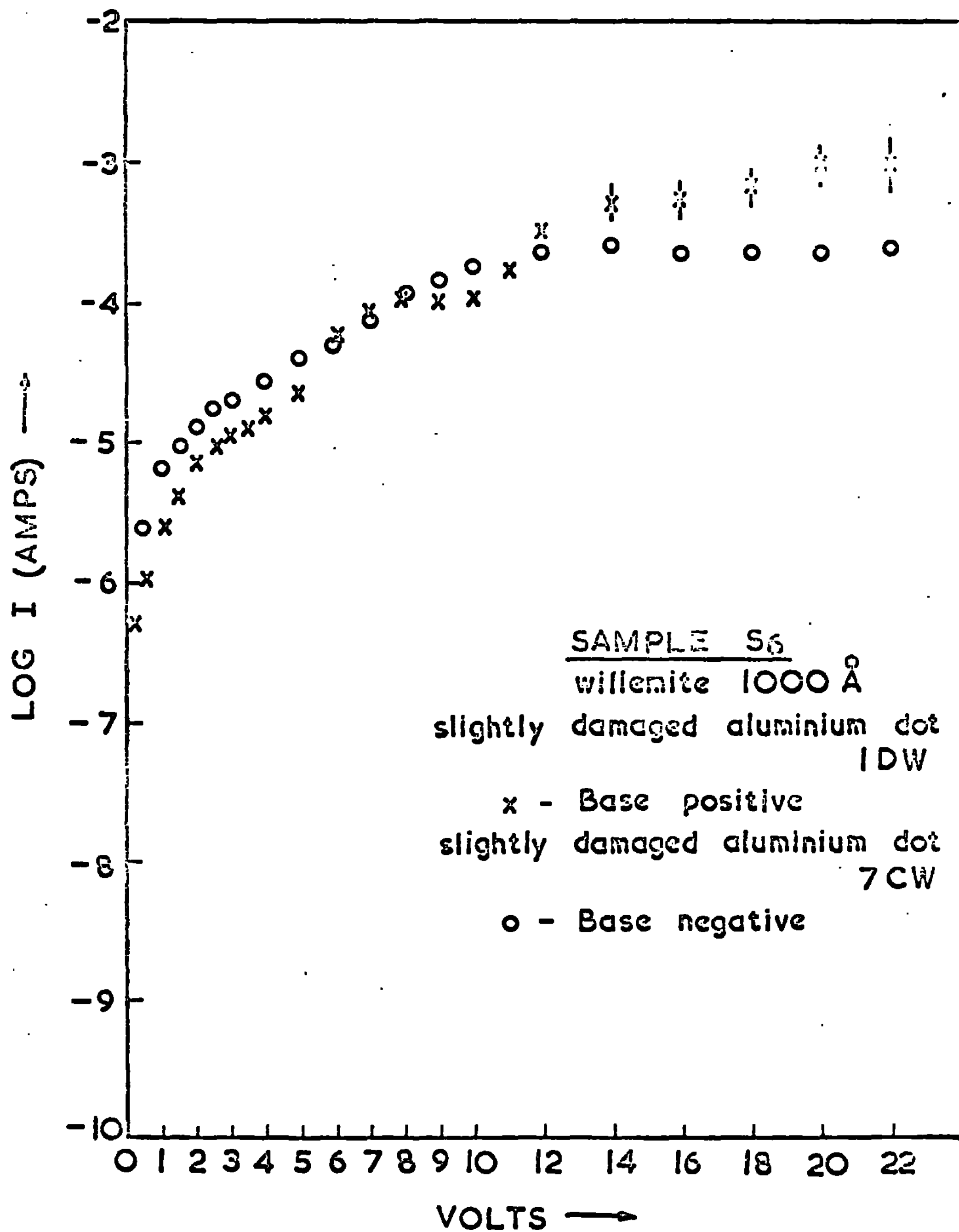

Fig. 6,28

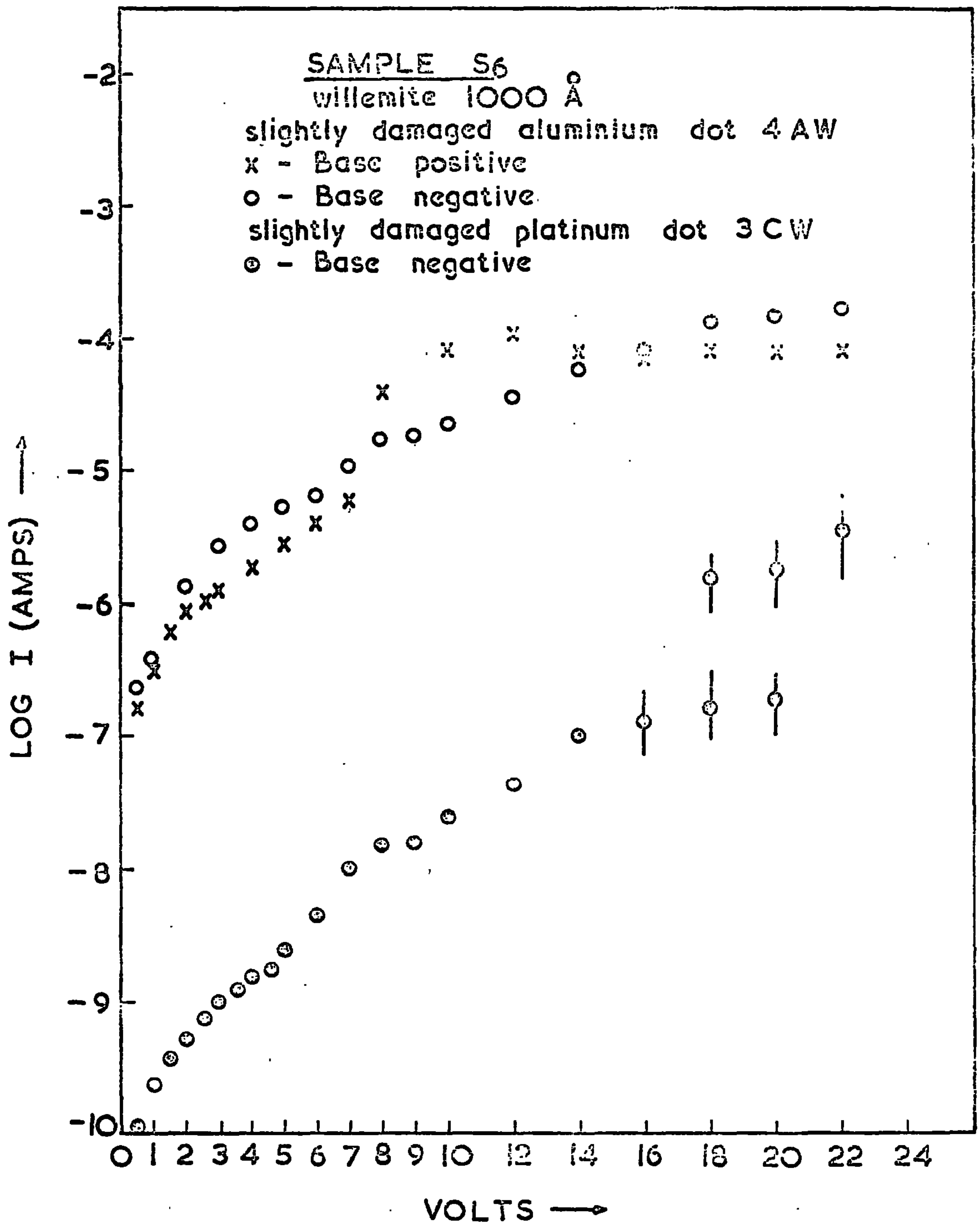

Fig. 6.29

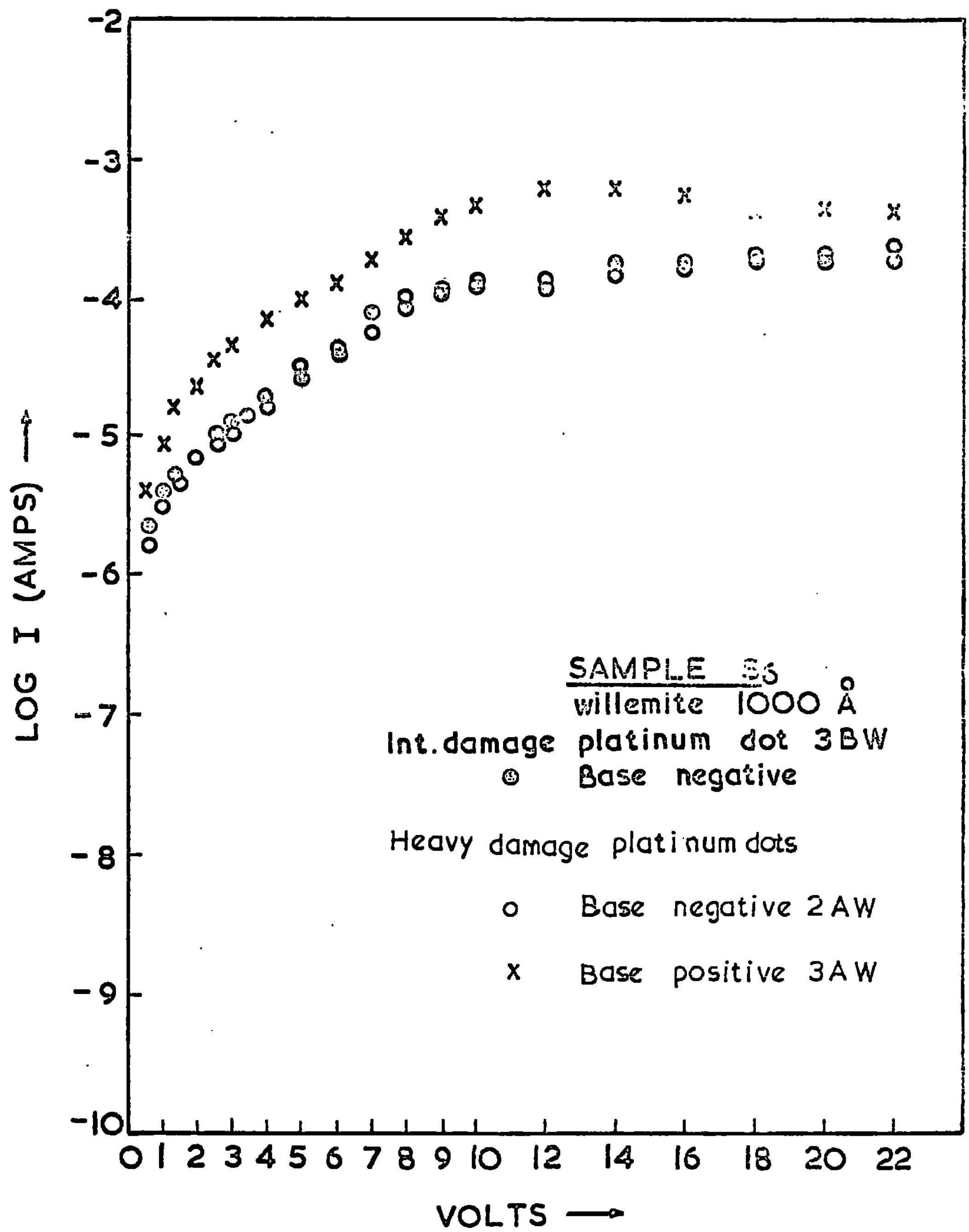

Fig. 6.30

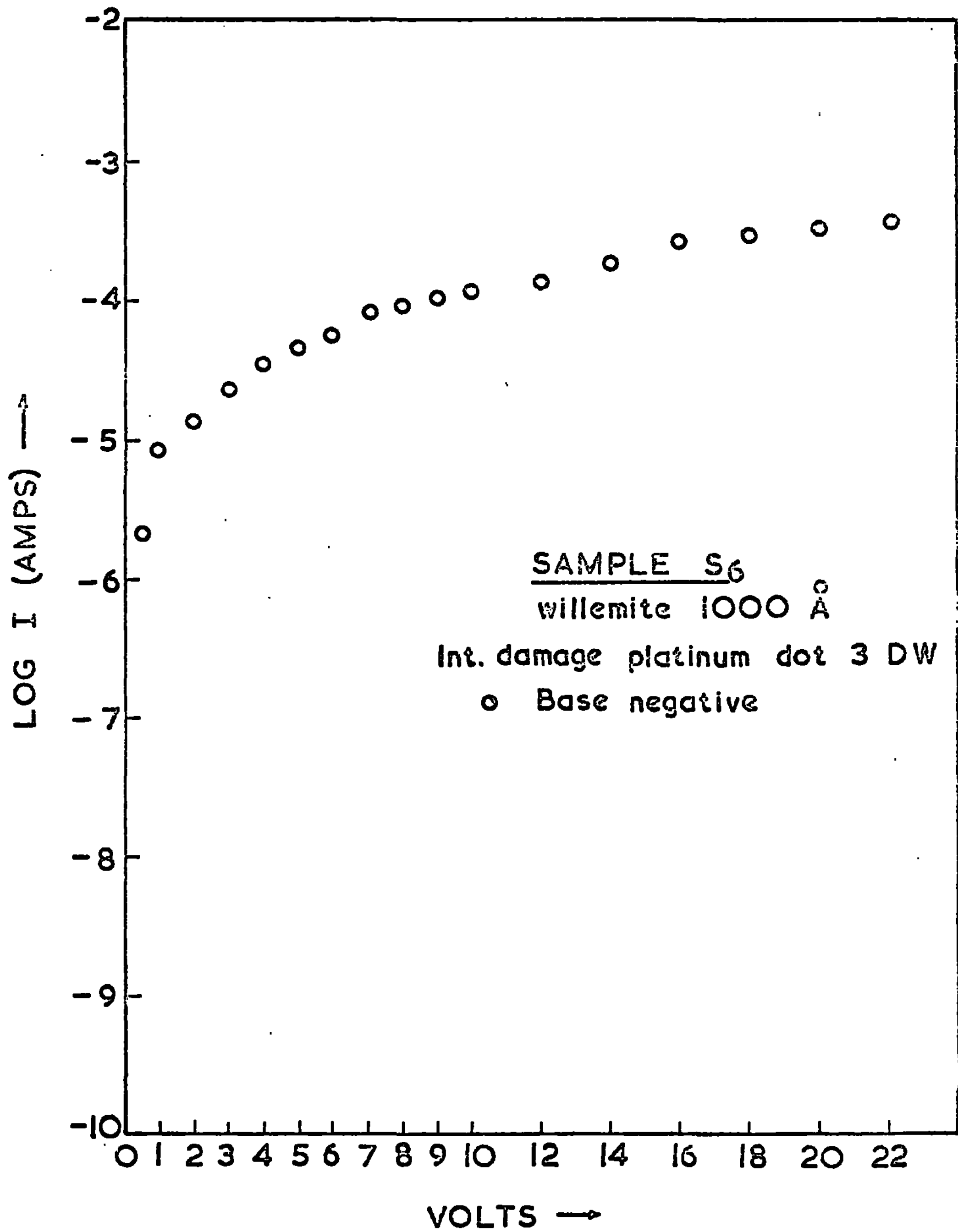

Fig. 6.31

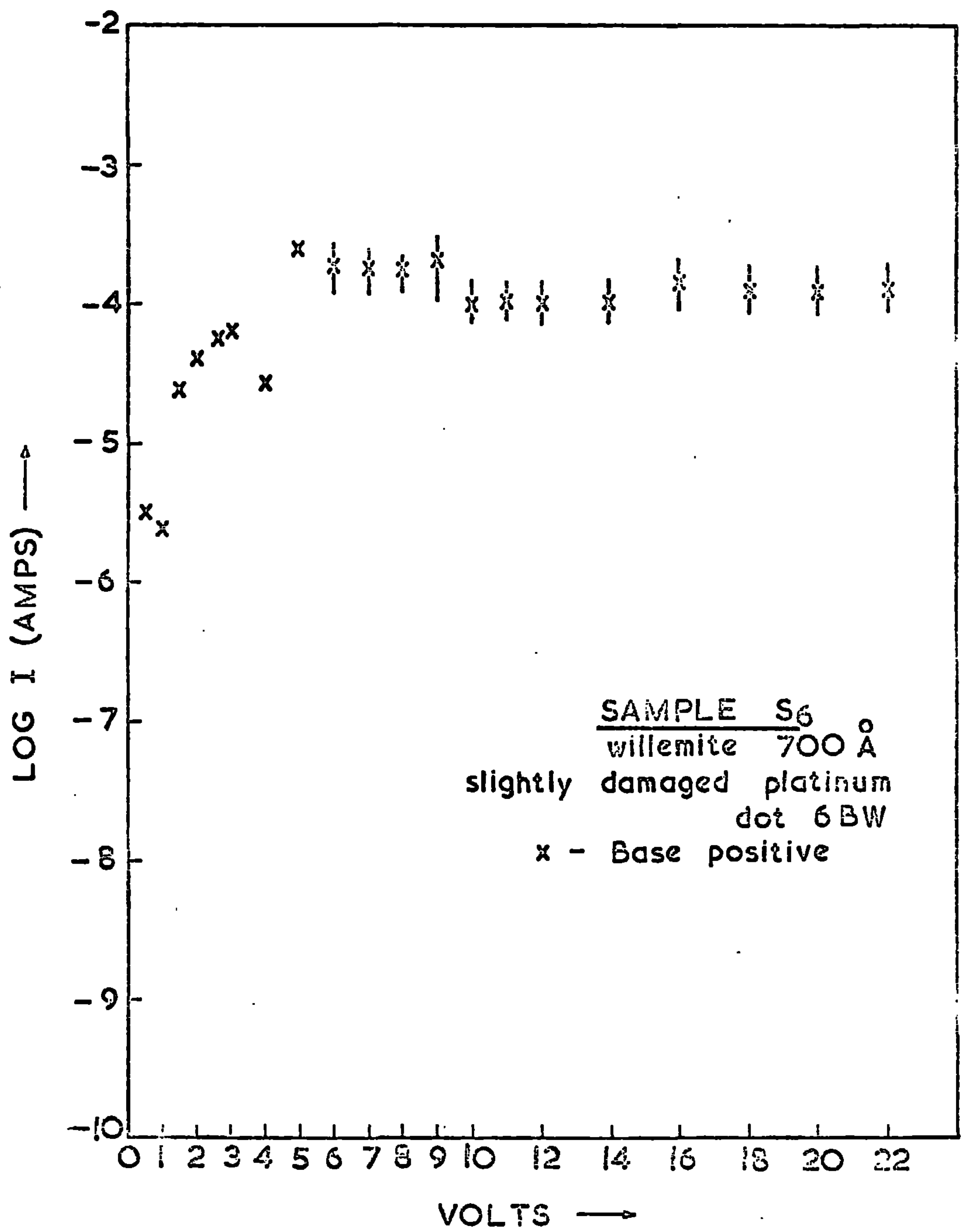

Fig. 6.32

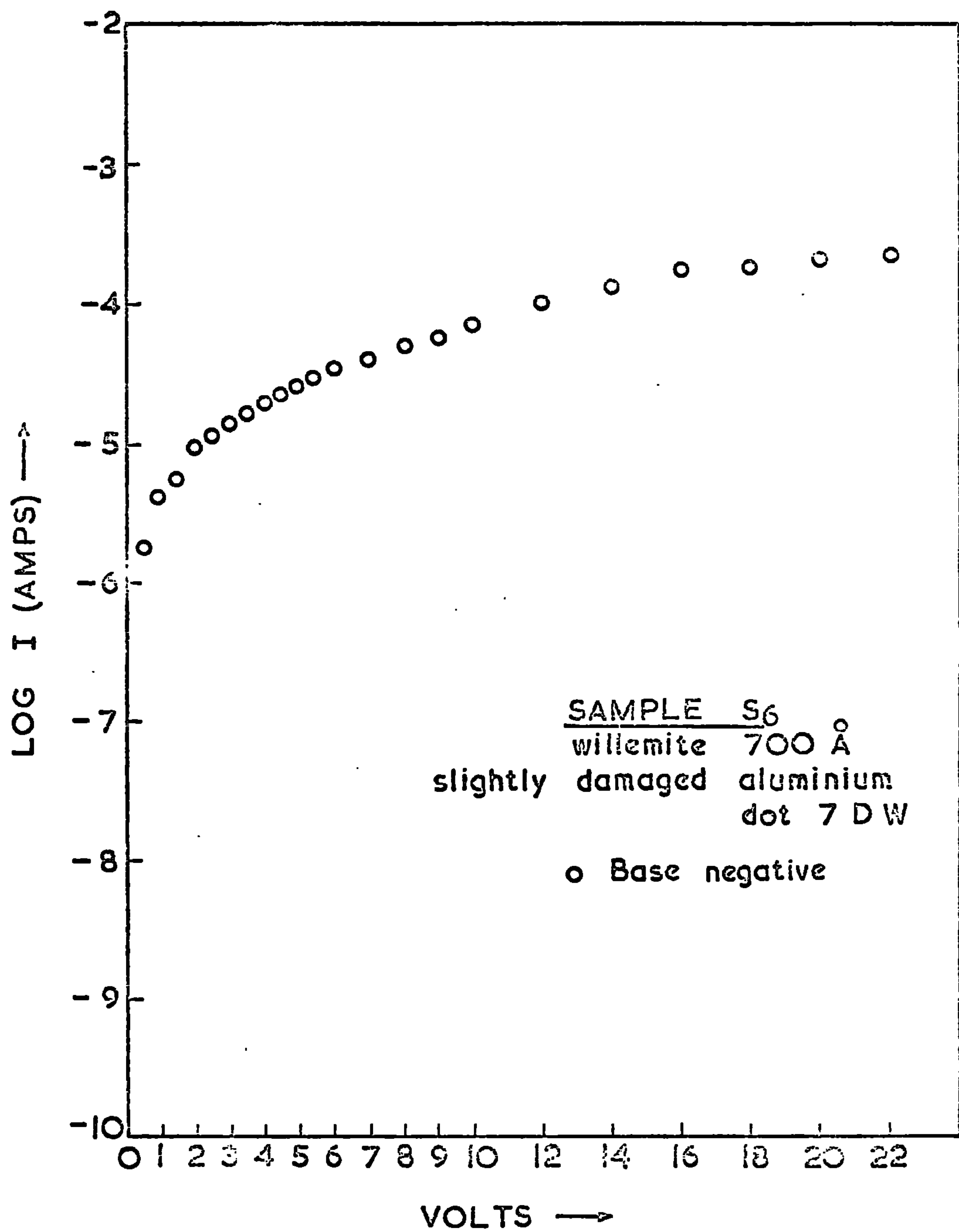

Fig. 6.33

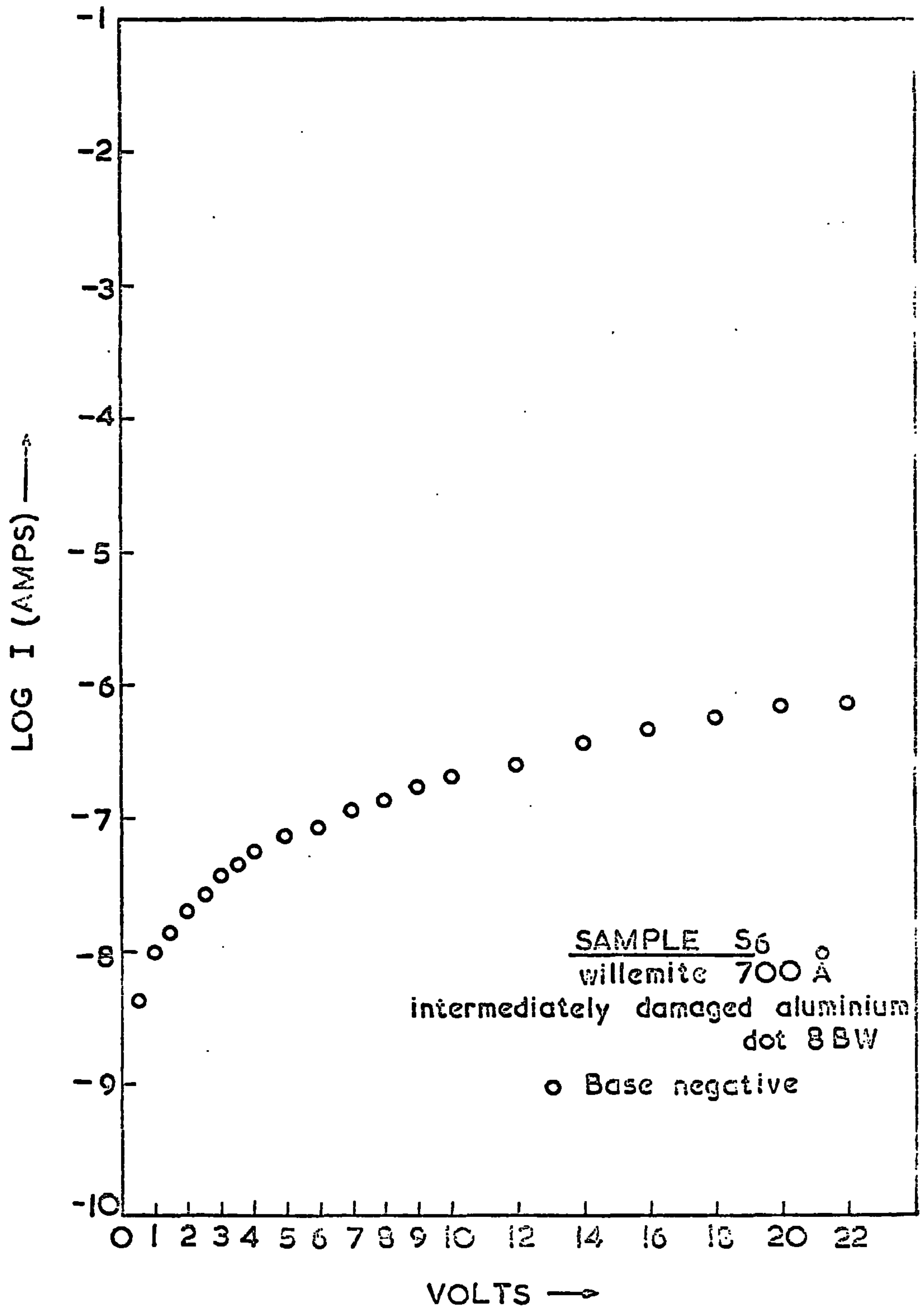

Fig. 6.34

6.8 Stability of Currents

Three different types of sample were made on the sapphire substrates. The first was an experimental sample for film adhesion studies which was followed by two standard test samples and finally by attempts at producing argon-baked samples as described in Section 6.1. The results of sample S_1 suffered from instabilities similar to the ones described in Section 5.5, but to a smaller extent. Samples S_2 and S_3 showed 'polarization' like any other sample (Sec. 5.5,a), but the random fluctuations of current, as observed on the Vibron (Sec. 5.5,b), and the variability from point to point were rare as compared to the results described in Chapter 5. The results for these samples are therefore much more meaningful than for the earlier ones. Sample S_3 showed the largest variability between the I-V curves from different dots, especially on willemite. Sample S_6 showed little 'polarization' as compared to the rest (probably due to the low value of the measuring resistance used for the comparatively high currents) and there was poor reproducibility from dot to dot. However, current fluctuations and scatter of the points for a particular dot were not very pronounced on this sample.

6.9 Luminescence of Samples

Green cathodoluminescence was observed on all the samples on sapphire substrates but the brightness varied between samples because of the processing differences. Table 6.2 shows the results of the comparative brightnesses. The results are in agreement with those of Chapter 5 (Sec.5.6).

Electroluminescence was not observed in any of the samples on sapphire substrates, except for some of the dots

of S_3 which showed pale green light immediately before breakdown.

6.10 Conclusions

The experimental work presented in this chapter leads to the following conclusions which are to be discussed in Chapter 7.

(a) Sapphire is proved to be a suitable material for this work, but it is felt that the surface smoothness (3 micro-inch claimed by the manufacturer) was not really fine enough.

(b) Except for the first sample, S_1, smooth I-V curves were obtained on the oxygen baked samples with good reproducibility from dot to dot and sample to sample, and with very few fluctuations.

(c) The results of S_1 were somewhat variable from dot to dot (Figures 6.1 and 6.13). The breakdown voltage was higher for both the oxide and willemite and the currents were lower as compared to all the later samples which were not similarly baked.

(d) On both oxide and willemite the currents were higher for the positive polarity of platinum with aluminium as the counter electrode.

(e) With platinum top contacts the I-V curves were very similar for both polarities (Figurs 6.6 and 6.7) and the currents were higher by at least an order of magnitude compared to the positive polarity of the Pt-Al combination.

(f) No critical dependence of the cathodoluminescence brightness on the relative proportions of oxide and fluoride was noticed even on these samples. (See Sec. 5.7(g)).

(g) Electroluminescence was not convincingly observed on any sample. Some dots on S_3 glowed weak green before breaking down, but this was not reproducible.

(h) The current in the willemite is generally higher compared to that in the oxide.

(i) As for the silica substrate samples (5.7(j)), an underlying layer of oxide was found on etching off the willemite.

(j) In the argon-baked sample (S_6) the electrical measurements themselves partly destroyed the top contact metallisation of many of the dots as shown in Table 6.3. The damage was negligible on the oxygen-baked samples.

CHAPTER 7

DISCUSSION OF RESULTS

7.1 Problems of Film Quality

As described in Chapter 5, all the work with silica substrates had problems due to the cracking and crinckling of the films. To start the work a substrate material and a base electrode metal were required which could withstand the high temperatures used during the fabrication. Since the film immediately in contact with the base electrode had to be evaporated silicon oxide it was decided to use fused silica substrates. However, for the electrode film a platinum-rhodium alloy (Sec. 4.4.3) was used because (a) it was easy to deposit this high melting point metal by sputtering, and (b) it should not oxidise appreciably. The coefficient of expansion (α) of silica is approximately 0.5×10^{6} deg^{-1} while those of platinum and rhodium are 11×10^{6} and 8.4×10^{6} deg^{-1} respectively. Apart from the heating due to platinum sputtering the sample had to withstand heating and cooling cycles during and after SiO evaporation, ZnF_2 evaporation and finally during the willemizing bake at approximately 955°C. The thermal mismatch led to the partial detaching of the base electrode film from the substrate on earlier samples, and to crinckling and cracking of the oxide willemite films on the later ones.

Figures 7.1 and 7.2 are photographs of one of the earlier samples on which the thickness of ZnF_2 was 2400Å. Figure 7.1 shows from left to right the platinum, SiO and willemite films having cracks which go through all three. The cracks became less frequent with improvement in the processing techniques on later samples. Figure 7.2 shows the additional 'crazy paving' pattern obtained on this thick

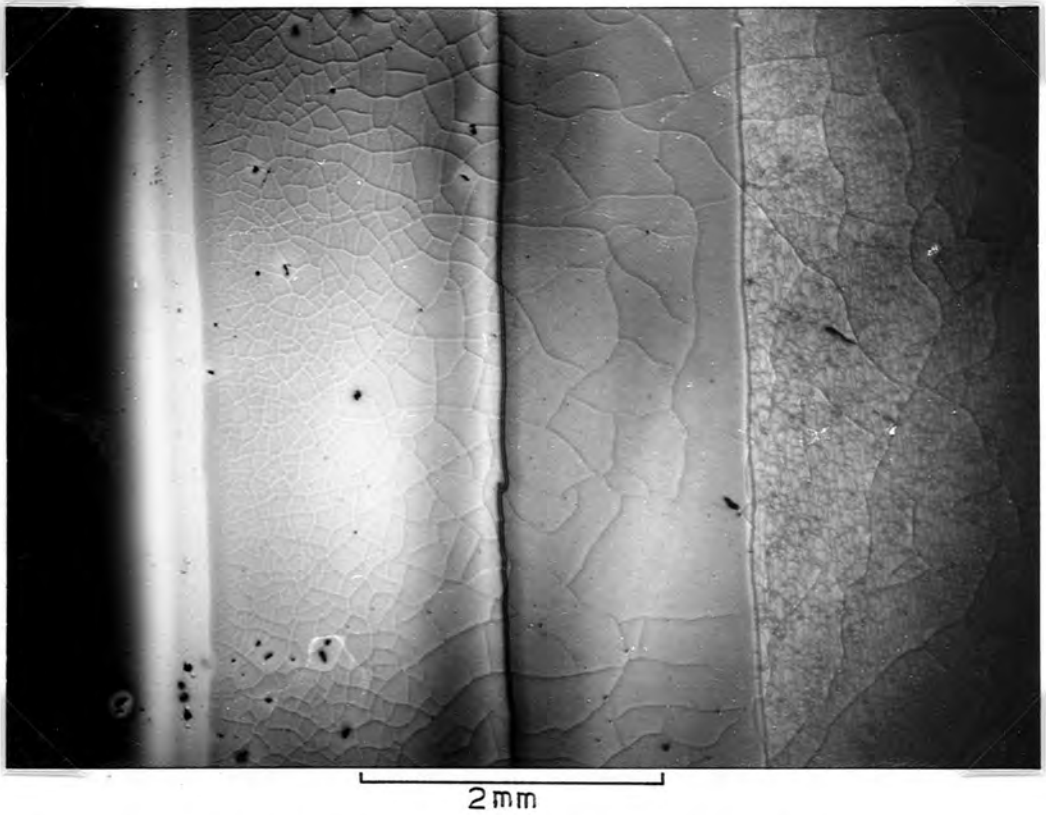

Fig.7.1 Cracks on Pt, SiO_x and willemite films on earlier samples.

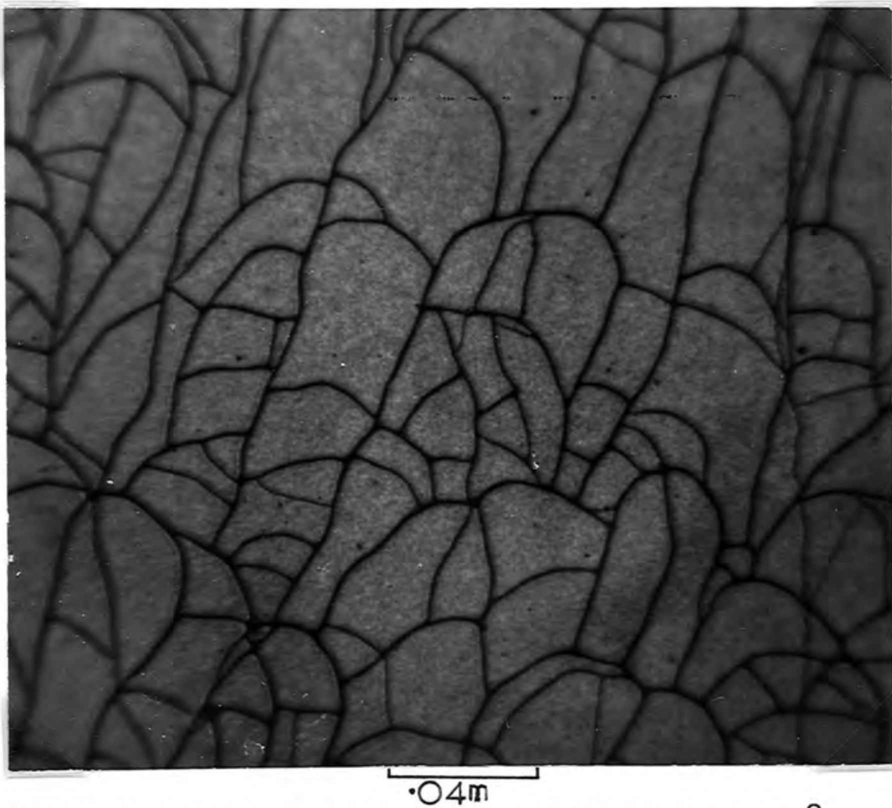

Fig. 7.2 'Crazy paving' pattern obtained on 2400 Å thick willemite.

willemite film. This pattern was definitely not due to cracks because under the interference objective and under the highest magnification available (approximately x400) no step or opening could be seen in the film. This pattern was not obtained on any of the later samples which were never as thick. It must be concluded that this pattern is due to some form of stress relief, grain boundaries and/or the precipitation of some constituent of the film.

The changes in processing techniques included different temperatures for oxide evaporation. It was found that the films on the first series of samples, which were evaporated at 1130°C, were dull and porous and they gave low voltage electrical breakdowns apart from cracking rather badly. This may have been due to absorption of water vapour from the atmosphere and further oxidation resulting in an increase of volume [139]. Some improvement was noticed by reducing the rate of evaporation.

Evaporation temperatures between 1250 and 1400°C are given in the literature for the production of SiO films with good mechanical properties. A temperature of 1263°C was therefore tried next and the resulting films were of much better appearance being smooth and shiny before the bake. However, since even these films cracked on baking, the evaporation temperature and rate was reduced to 1200°C and 6Å/sec to give a further considerable improvement. Table 3.1 in Chapter 3 has been prepared to compare the experimental conditions for evaporation used by different workers on silicon oxide films.

Even with the best oxide films the problem of cracking remained and this was mostly due to the difference of expansion between the metal and the substrate. To try to

overcome this, platinum ($\alpha=11\times10^{6}$ deg^{-1} vapour pressure 10^{-11} torr at $1335^{o}K$) might have been replaced by chromium ($\alpha=11\times10^{6}$ deg^{-1} vapour pressure 10^{-11} at $960^{o}K$ and 10^{-6} torr at $1330^{o}K$), which has been successfully used by other workers, or by nickel ($\alpha=12.8\times10^{6}$ deg^{-1} vapour press 10^{-11} at $1040^{o}K$). The better adhesion of these metals to the substrate might have prevented cracking although the wide difference in the coefficients of expansion of the fused silica and all of these metals would not have eliminated the source of the cracking. Oxidation of these metals may also have given problems. It was therefore considered better to change the substrate material to alumina which has a higher coefficient of expansion, $6\text{-}8\times10^{-6}$ deg^{-1}, than silica and a melting point of $2024^{o}C$, although this would be expected to accentuate the problem of thermal strain in the silicon oxide film itself.

Platinum films on ordinary sintered alumina did not show any of the familiar pattern of cracks, but because of the bad surface finish of this substrate material the films appeared to be frosty. Sintered alumina substrates with the best surface finish commercially available gave films which remained shiny and crack-free after the whole processing, but even with this substrate, the substrate polishing scratches were visible all the way through the films. The sapphire substrates which are produced for microwave integrated circuit applications were finally succesful and with these, no more mechanical problems were experienced. However, the claimed 3 micro inch (750Å) polish on these substrates was still not really smooth enough and the polishing lines could be seen on some of them under (x400) magnification.

Although the macroscopic problems of film quality were eventually overcome as described above, some of the best films probably still contained microscopic defects such as pin holes which may have affected the electrical measurements. These will be discussed further in Sections 7.4 and 7.5.

7.2 Willemite-Conversion Reaction

A brief account of the willemite-forming reaction was given in Section 4.4.4 and the following reaction equation was assumed.

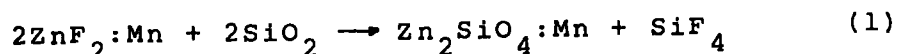

$$2ZnF_2{:}Mn + 2SiO_2 \longrightarrow Zn_2SiO_4{:}Mn + SiF_4 \qquad (1)$$

The mechanism of this section seems to be important in understanding the nature of the films produced and hence the results of the films made in different conditions are discussed in this section. The following facts emerge from the results of the studies of this material:-

(a) There was no appreciable difference in the quality of willemite, as judged by its cathodoluminescence, on films made by depositing different thicknesses of ZnF_2 (200 to 2400Å approximately). A decrease in the brightness was noticed for films thinner than approximately 200Å.

(b) Films which were prepared by baking in argon showed only weak cathodoluminescence.

(c) After removal of the willemite from the top surface, no reaction marks or steps were noticeable on the oxide under the highest magnification available (x400 approximately).

(d) The experiment in which ZnF_2 was deposited before the oxide was not successful.

To combine these facts, it is important to realize that evaporated films of silicon monoxide are known to contain a mixture of different silicon oxide species SiO_x, in which the ratio of silicon to oxygen varies [120,122,136]. The films also contain some free silicon. The films as deposited were incompletely oxidized because SiO powder was used and the average composition would not be greatly changed by the evaporation temperature due to the good vacuum used for the process (always better than $2x10^{-6}$ torr).

When a sample having a film of ZnF_2 on top of such oxide is heated in an oxygen atmosphere, the oxide oxidizes further and the reaction given by equation (1) probably occurs evolving SiF_4 gas. Since ZnF_2 melts at $872^{o}C$ it should wet the surface and the reaction continues until all the ZnF_2 has been used up or, if it is very much in excess, then a gradient can be expected with Zn_2SiO_4 at the surface of the oxide and a phase containing more ZnF_2 towards the free surface. The Zn_2SiO_4 may crystallise from solution, as its melting point is higher than the baking temperature used, which would explain the microcrystalline pattern observed in similar films in the electron microscope by Edwards and Rushby [14].

How the reaction continues after the solid phase of the silicate is formed at the surface of the oxide is open to further investigation, but one can expect some reaction to continue by the diffusion of zinc through the silicate until a certain thickness is reached. One can also devise some other chemical reactions, producing for example zinc oxide as an intermediate step which may also remain partly unreacted at the end of the reaction. A chemical analysis could be

made by collecting the SiF_4 liberated in the reaction. The 1% manganese fluoride used as an activator can also be imagined to react with oxygen and form manganese dioxide, which may remain on the surface. However, good willemite films cannot be produced in an atmosphere containing insufficient oxygen which is shown up by the near failure of the argon baked samples.

The failure to produce willemite films by depositing ZnF_2 under the oxide may have been due to the melting of ZnF_2 and then evolution of SiF_4 causing the film to erupt. It also follows from the above discussion that it is extremely difficult to produce willemite films by the present process which do not have an unreacted film of oxide underneath, in accordance with (c) above. The absence of any step on the surface of the residual oxide can probably be explained by the evaporation of silicon oxide outside the willemite area during the bake as already described in Section 4.4.4. The fact (a) described above cannot be related with the above discussion, and the explanation may lie in the limited energy of the bombarding ions and electrons used in the cathodoluminescence.

7.3 Discussion of Oxide Measurements

Chapter 3 presented a summary of published experimental work on silicon oxide and its preparation (Table 3.1). Electrical measurements on silicon oxide were made for comparison with the published work and with willemite. However the present films were necessarily baked in oxygen at a high temperature to form the willemite on neighbouring areas.

For this reason the results are not directly comparable with those on the evaporated silicon oxide films reported in the literature, and as a consequence the present oxide results have found importance in their own right.

All the oxide films made on silica substrates had relatively poor mechanical quality. The results of the first three series were very variable and fluctuating and are therefore not included in this discussion, but their physical properties (adhesion, mechanical strength and appearance) are important because these led to changes in evaporation rate and temperature which later gave better quality films. The properties of the evaporated films depend a great deal on the rate of deposition [109] because the ratio of the SiO molecules arriving at the substrate to the residual gas molecules (H_2O, O_2 etc.) affects the oxidation state of the film [121, 139], and thus the built-in stresses which are later released [108]. The quality of the films was improved even on the silica substrates by controlling the rate and temperature of evaporation and the results for the later samples (the fourth series) are worth comparing with the still better ones of Chapter 6.

The oxide films on sapphire substrates, for which the results are described in Chapter 6, did not pose any major problems due to fluctuations, variability or low-voltage breakdowns during measurement, and they were of good mechanical quality. Some problems were, however, anticipated because of the defect nature of the film and lack of strict control of the deposition conditions.

Samples S_2 and S_3 had 1400Å of oxide and were made in similar conditions at different times. The most extensive

set of results was obtained for the aluminium dots on these samples. Figure 6.2 to 6.5 show remarkable similarity and hence reproducibility from dot to dot. Figures 6.8 and 6.9 from sample S_3 are also almost identical and show that good reproducibility could be achieved from sample to sample. Figure 6.4 has been selected as a standard for later analysis because it has very smooth curves for both polarities. Of the other curves referred to above, Figure 6.2 has the most different shape, although it deviates only slightly from Figure 6.4. In all of these the current is lower for the platinum base positive polarity at low voltage after which it crosses the opposite polarity curve to give much higher currents for the medium and high voltage ranges.

Figures 6.6 and 6.7 for platinum dots on sample S_2 are the only observations for top contacts of this metal on the oxide. These results show that there is no polarity dependence and again the curves for both dots are very similar. They are also identical in shape to the curves for aluminium dots for the base-positive polarity although the current is roughly an order and a half higher all through.

The results of sample S_1 shown in Figure 6.1 were more variable from dot to dot. This may have been due to the further selective oxidation of the incompletely oxidized species of silicon oxide and, perhaps, some mechanical damage due to extended high temperature oxygen bake. Some oxide also evaporated during the bake as shown by the thickness reduction. That the film is more completely oxidized is evidenced by the shift in the position of the I-V curves to lower currents and higher breakdown strengths in spite of the decreased thickness. Measurements on this sample

were carried out up to 36 V as against 18 V for the normal films.

The curves for aluminium dots for both polarities of the argon baked sample S_6 show higher currents than for the normal samples, as shown in Figures 6.10, 11 and 12. The shapes of the curves for base negative are very similar to those of the standard. However, because of the variability of the results the polarity dependence is less evident for this sample.

Having determined the main features of the Chapter 6 results for oxide, they can now be compared with the more variable results from Chapter 5. Figures 5.4 and 5.5 for the silica substrate samples are directly comparable with the standard of Chapter 6 as they are for 1400Å of oxide. Within the limits of experimental error, which were rather large on these samples, the results are certainly consistent with those of the standard on sapphire. The curves have the same general features and are very similar. Figure 5.6 and 5.7 are isolated results for aluminium and gold dots for different thicknesses of oxide, but in view of the variability they are insufficient to provide any real evidence of the effects of these changes.

Although not as many gold as aluminium dots were studied, they nearly all broke down at low voltages or gave very low resistances. This behaviour is not clearly understood. Top contact metal thicknesses lower than 1000Å are known to favour self healing breakdowns, but in this work greater thicknesses were usually used and therefore such breakdowns would not be expected to be frequent. Further, self healing breakdowns are known to occur in

aluminium which evaporates at a relatively low temperature or immediately forms an insulating oxide. It is suspected that the gold permeated the pinholes and cracks in the present films and that the conducting channel did not heal even after the passage of a considerable current. The indium dots all gave short circuits which may have been due to its running right through the defects in the film to the base electrode because of its low melting point.

The significant oxide results, as deduced from the discussion above, are all summarised in Figure 7.3. Curves (a), (a) and (b) are for 1400Å oxide thickness but curve (c) is for 700Å because of the extra oxygen bake. The results presented in this figure will be explained and interpreted in the next chapter.

7.4 Discussion of Willemite Measurements

All the willemite films on silica substrates suffered from mechanical defects, and although the quality improved in the later samples, the results in Chapter 5 do not provide reliable evidence of the intrinsic properties of the films. They are however, important because they show the effects of the improvement in the physical properties of the films as has already been described in relation to the oxide parts of these samples.

The results from Chapter 6 are much more reliable. On Sample S_2 and one section of S_3, which had approximately the same thickness of willemite (about 200Å) the results were similar. As for the oxide most of the results were for aluminium dots. The curves for sample S_2 for the positive base polarity (Figs. 6.14 to 6.17) are very nearly identical in the intermediate and high voltage regions, but for low voltage

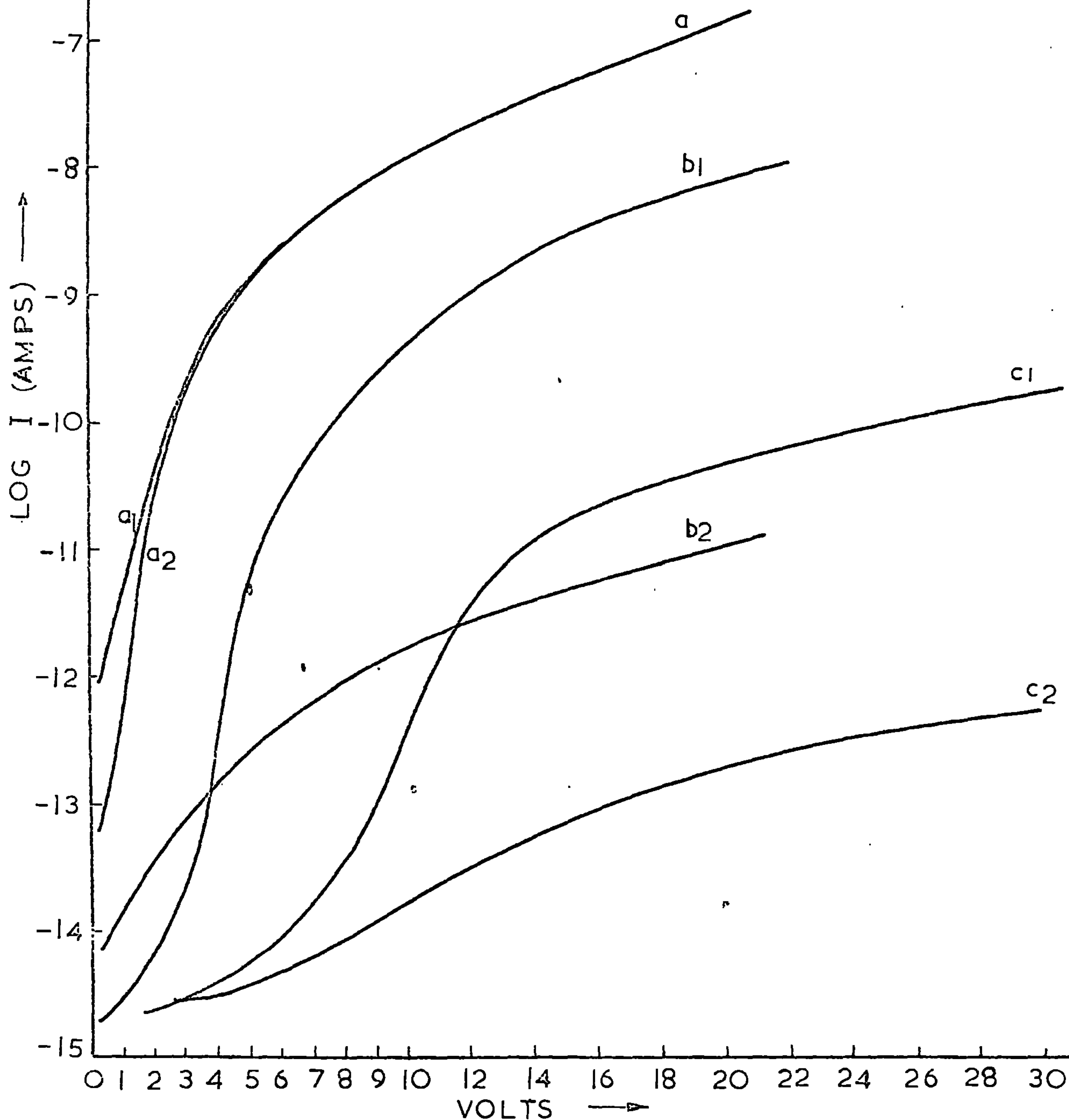

Fig. 7.3

there is variability. These curves also have some fluctuation and they are not as smooth as the curves on the oxide part of the sample. For base negative the curves are even more widely scattered (Figures 6.15-6.17) and are only similar at intermediate voltages. The current is however, definitely higher for base positive polarity for all samples, as found for the oxide. Because of the increased variability it is not so easy to select curves representing 'standard' behaviour. However, Figure 6.15 has been chosen for this purpose for Pt-Al electrodes.

The platinum dots on sample S_2 also give smoother curves for base positive and widely scattered ones for base negative. Because of the scatter the polarity dependence is not evident, but for both polarities the current is definitely higher than the highest current with the Pt-Al combination.

Assuming electronic conduction with cathode injection the negative polarity would be expected to give the more smooth and reproducible curves because of the fixed conditions at the base electrode which then forms the cathode. However, the results show that smooth curves are obtained when the base electrode is positive, which is when the conditions at the anode are more stable. The contacts are also different in two other respects:-

(a) The insulating film is deposited on the bottom electrode whereas, at the top, metal is deposited on the insulator and there can be no certainty that the two are the same.

(b) The base contact forms the metal-oxide and the top contact the metal-willemite interface.

The curves for sample S_3 for the same willemite thickness as S_2 do not agree closely with the standard as

they are flatter for the base positive polarity. The curves in Figures 6.22 and 6.23 are very similar, as are those of Figures 6.24 and 6.25, although the two pairs are rather different. Since the oxide results for the two samples agreed well, this indicates lack of control of the thickness of the willemite. For this sample it appears to be for the base negative, the curves are reproducible and smooth, as compared with the opposite polarity for S_2. For thicker willemite on S_3 (Figure 6.27), the current is higher for both polarities as compared to the standard. Because of the considerable amount of scatter for both the aluminium and gold dots, it is difficult to establish the effect of top contact metal. Unfortunately some of the results on willemite from Chapter 5 (Figures 5.12 to 5.14) are isolated and have no similar corresponding ones on sapphire. Also, as they are of doubtful reproducibility they have had to be excluded from further discussion. However, Figure 5.11 (600Å of willemite) can be compared with Figure 6.27. Both have the same general features except that the current in Figure 5.11 falls to lower values for low voltages than in the Figure 6.27, and the curves for base negative on silica have a lot of scatter. The willemite curves shown in Figures 5.9 and 5.10 are for samples in which the oxide was thinner than the willemite. These curves show fair reproducibility between several dots and are thus the only reliable ones from Chapter 5.

The results on willemite of Sample S_1 (heavily oxidized) were similar to those of the oxide on this sample as far as fluctuation and variability is concerned. The current was noticeably higher in willemite for the base positive polarity, while for the negative polarity the currents were rather

similar (Figs. 6.1 and 6.13). The willemite section of the film also had much higher breakdown strength like the oxide on this sample. The shape of the curves was similar to that of the standard especially for the base positive polarity.

From the two sections of willemite on Sample S_6 (argon baked), the scatter of the curves makes it very difficult to draw any conclusions. This is especially so because all of the top contacts were badly damaged to a degree that is significantly greater than for oxygen-baked samples (Table 6.3). However the current through the willemite was always higher than through the oxide on this sample.

In general, the results of Chapter 5 support the results of Chapter 6 wherever they can be compared. The current through the willemite was always higher for the positive base polarity for both the aluminium and gold dots.

Figures 7.4 and 7.5 have been prepared by redrawing the most significant curves for the willemite. These are to be used for the interpretation in the next chapter.

We can turn now to the detailed comparison of conduction in willemite and oxide of each sample. From all of the aluminium dots on Sample S_2, the current in the willemite is found to be slightly higher than in the oxide for the base positive polarity, and the shapes of the curves are very similar (Figures 6.15 and 6.4). There is more scatter in the willemite curves at higher fields. For the base negative the comparison is not possible because of the variability of the willemite curves. For the platinum dots the current is even higher in the willemite compared with oxide.

On the thinner section of willemite on Sample S_3 (Al dots only) for base positive polarity the current is

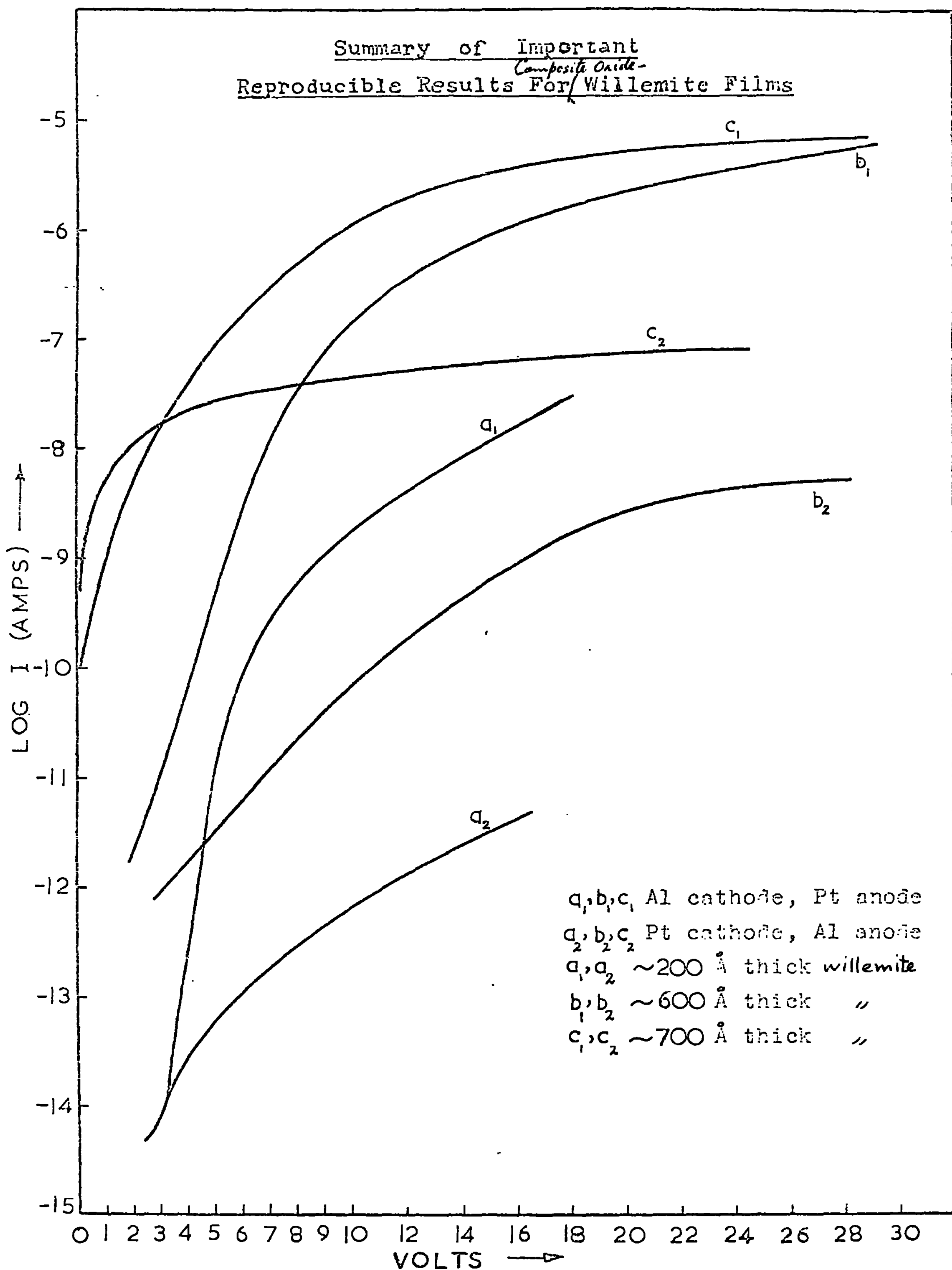

Fig. 7.4

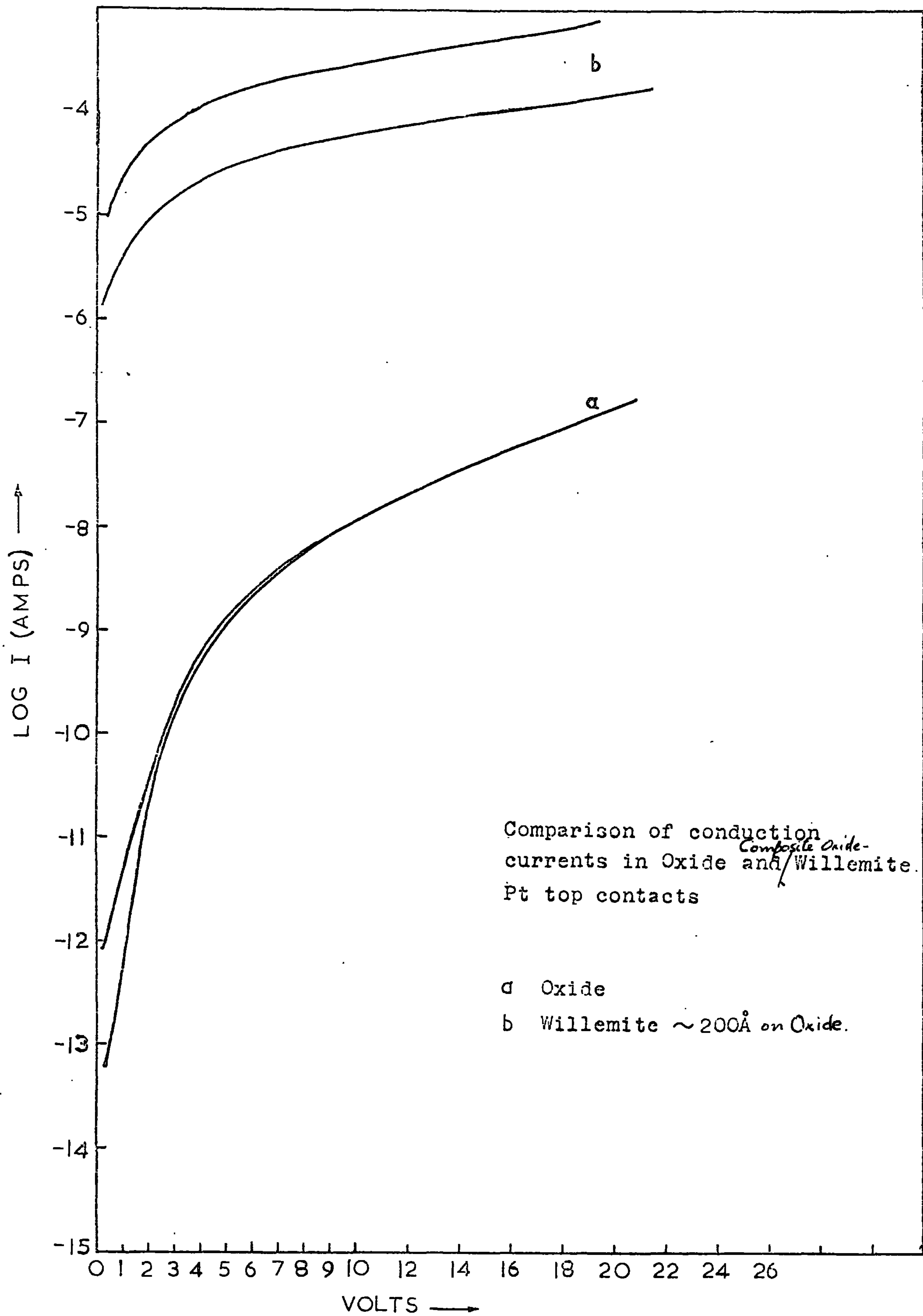

Fig. 7.5

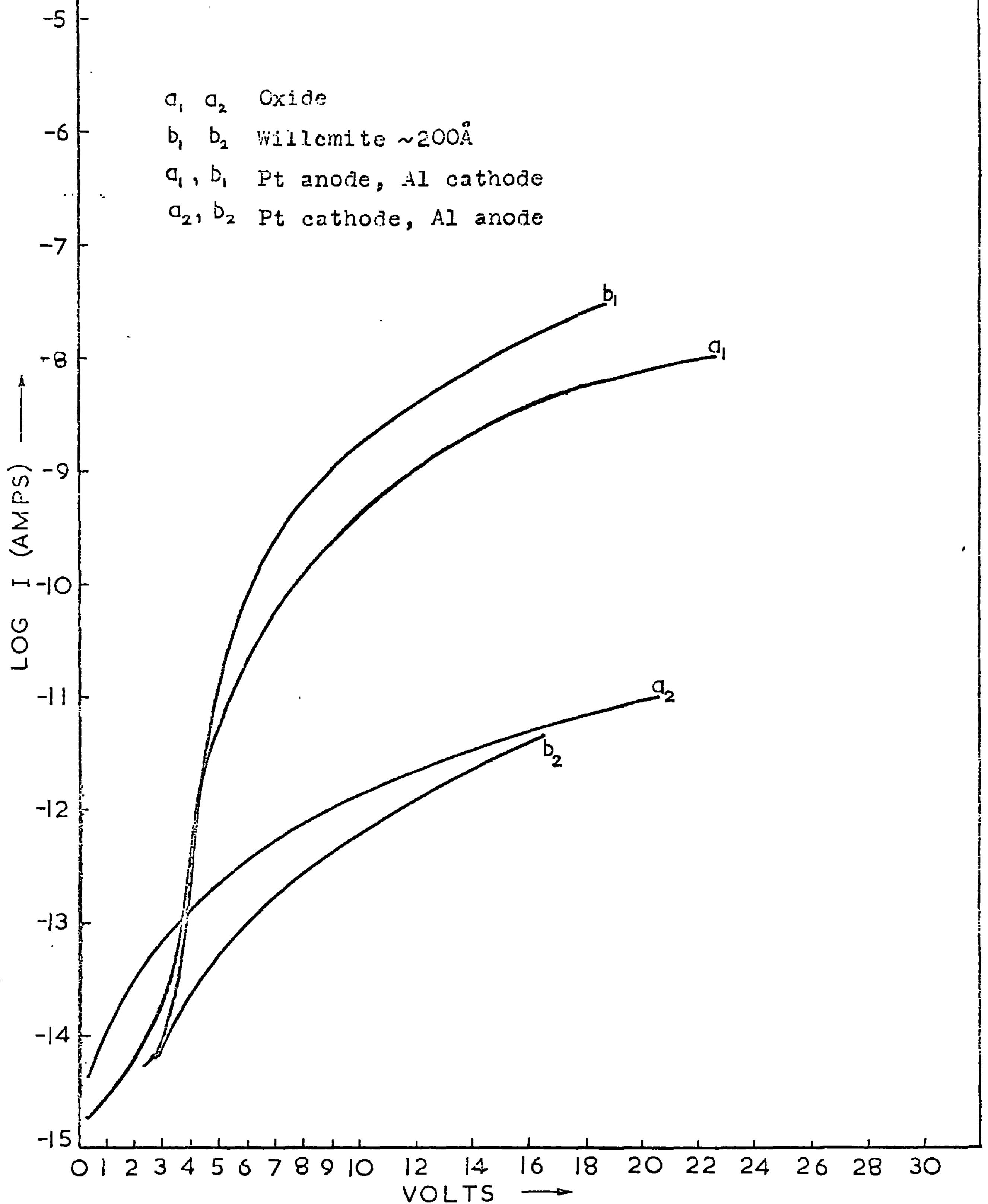

Fig. 7.6

only higher near the high voltage end of the curves because of their flatter shapes as compared to the oxide (Figs. 6.23 and 6.8). For the base negative polarity, the current appears to be consistently higher in the oxide. For the thicker willemite on this sample the current is higher for both polarities than in the oxide (Figs. 6.27 and 6.8)

The curves for the willemite on Samples MT_1 and MT_3 show currents which are about two to three orders of magnitude higher in willemite for the base positive polarity as compared to the oxide on these samples (Figs. 5.11 and 5.5). This can be noticed in spite of the spread of these curves. Unfortunately no curves were available for the base negative on willemite of MT_1, and the scatter of the MT_3 results for this polarity also made its comparison difficult. From the argon baked sample S_6 which also had two sections of willemite, higher current through the willemite is again evidenced in spite of the wide scatter.

CHAPTER 8

PHYSICAL INTERPRETATION OF RESULTS

Introduction

A review of the literature on conduction in thin evaporated films of SiO was presented in Chapter 3. It was shown there, that the high field conduction is normally explained in terms of a Poole-Frenkel process which assumes a uniform field in the bulk. For the present work it is required to explain the conduction results for rather different SiO_x films and for composite films having a thin layer of willemite above the oxide. The literature on phosphors shows that the characteristics of electroluminescence are often explained in terms of field intensification due to space charge barriers. These ideas are therefore examined in Sections 8.1 and 8.2 to find out whether they are important to the interpretation of the present results or whether it is reasonable to assume a uniform field as is normally done for such thin films.

8.1 Field Enhancement Phenomenon in Phosphors

The brightness B of the light emission from an electroluminescent material has often been found to vary with applied voltage, V, according to a law of the form

$$B = A \exp(-C/V^{\frac{1}{2}}) \qquad (1)$$

where A and C are constants for a particular cell. This is shown by the linearity of a graph of logB versus $1/V^{\frac{1}{2}}$ which is sometimes known as Alfrey-Taylor plot. Equation (1) has been shown to hold over 12 orders of magnitude of B for a.c. excitation of ZnS:Cu,Cl powder cells. [Fischer in Ref.15] and over 3 orders for ZnS:Cu,Cl single crystals [142].

DURHAM UNIVERSITY SCIENCE 4 JUL 1974 SECTION LIBRARY

It has been shown that several different physical processes could account for the brightness variation given by (1). These possibilities which have been well reviewed by Fischer [143,144] can be divided into two classes: (a) injection models and (b) impact ionization models.

Injection models for equation (1) postulate that the light emission is proportional to the number of carriers injected into the crystal from a metal or semiconductor contact. Such contacts generally have a space charge barrier and the injection law depends on the number of electrons that can go over or through the barrier. In the impact ionization models the extra carriers are produced by inelastic collisions of high energy electrons forming hole-electron pairs. The fraction of primary electrons accelerated to impact ionization energies in a field $\mathcal{E}$ increases as $\exp(-\text{const.}/\mathcal{E})$. To obtain appreciable ionization a very high field is required, normally greater than the average applied field. The ionization therefore occurs mostly in the enhanced field at a reverse biased contact barrier. The electrostatics of a simple Schottky barrier shows that the maximum field is proportional to $V^{\frac{1}{2}}$ so that impact ionization can explain the voltage dependence of electroluminescence given by equation (1). This was first proposed by Piper and Williams [145]. Alfrey and Taylor [146] improved the model to fit the observed variations of B with frequency and temperature.

For the present work it is necessary to know how the current associated with each of the above types of

model varies with applied voltage. Both models require field enhancement at a barrier and to a first approximation the current is proportional to the number of carriers and hence to the brightness. Experimentally Garlick and Tiagi [142] found that B = const I^y where I is the current and y was between 1 and 2. It therefore follows that for phosphors obeying equation (1), a linear graph of log I versus $V^{-\frac{1}{2}}$ might be expected.

8.2 Potential Barriers in Thin Insulating Films

Experiments on electroluminescence, leading to the interpretation outlined in Sec.8.1 are normally made on single crystals or on powder layers with a particle size above a few microns. It is now necessary to consider whether space charge barriers could have such a dominant effect in the much thinner films (approximately 1500 Å thick), which are the subject of this thesis.

Potential barriers are generally formed at contacts to crystals, at surfaces and at interfaces in composite films. The electrostatics calculations are the same for all cases but the boundary conditions vary. The most important cases are those of contact barriers and these will be considered in detail.

(a) Depletion layers

Depletion layers form when the work function ϕ_i of the insulator is lower than that of the metal ϕ_m. Fig. 8.1a shows the energy bands for a thick insulating film in equilibrium with two identical metal contacts. If the film has a donor density N_d cm^{-3}, the one dimensional Poisson's equation for the insulator can be written as

$$\frac{d^2V}{dx^2} = -\frac{qN_d}{\varepsilon_r\varepsilon_o} \tag{2}$$

where qV is the potential energy of the bottom of the conduction band.

For a thick film, the contacts can be considered independently and equation (2) gives the thickness ω_d of the depletion layer needed to accommodate the potential difference $\phi_m-\phi_{i/q}$ between the metal and the insulator (Fig. 8.1a).

$$\omega_d = \left[\frac{2(\phi_m-\phi_i)\varepsilon_r\varepsilon_o}{q^2N_d}\right]^{\frac{1}{2}} \tag{3}$$

The work functions of metal are normally in the range of 3-5.5 eV, and with electron affinities of insulators approximately 1-2 eV, it is reasonable to take $(\phi_m-\phi_i)$ equal to 2 eV to find the order of magnitude of the ω_d from (3). Using the value of 5 for the dielectric constant [147] of silicon oxide the depletion layer thicknesses are as given in Table 8.1.

N_d cm^{-3}	10^{13}	10^{14}	10^{15}	10^{16}	10^{17}	10^{18}
ω_d Å	1.07×10^5	3.3×10^4	1.07×10^4	3320	1074	332

Table 8.1:- Width of the depletion layer for different donor concentrations.

When the film thickness, s, is greater than 2 ω_d, the full depletion layers can form at each contact as shown in Fig. 8.1a. When the film thickness is less than 2 ω_d, equation (2) must be solved with boundary conditions representing both contacts simultaneously. The potential difference, ΔV, between the centre and the edge of the film

is less than $(\phi_m - \phi_i)/q$. In this case, Fig. (8.1b), the film is too thin to contain sufficient charge to form the full depletion layers, and

$$\Delta V = \frac{q N_d s^2}{8 \varepsilon_r \varepsilon_o} \qquad (4)$$

Equation (4) has been evaluated in Table 8.2 for a film thickness of 1500 Å and ε_r equal to 5, for values of N_d up to the maximum for which it applies, i.e. ΔV equal to 2 volts assuming this value of $\frac{\phi_m - \phi_i}{q}$ as for Table 8.1.

N_d cm^{-3}	10^{13}	10^{14}	10^{15}	10^{16}	10^{17}	$1.9\text{x}10^{17}$
ΔV volts	$1.017\text{x}10^{-4}$	$1.017\text{x}10^{-3}$	$1.017\text{x}10^{-2}$	$1.017\text{x}10^{-1}$	1.02	1.94

Table 8.2 Depression in the bands at the midplane for different donor concentrations.

These calculations show that for films of the order of thicknesses used in this work, the depletion layers at the two contacts do not form completely unless the donor concentration is greater than about 10^{17} cm^{-3}. Below this value of N_d, the depression in the bands becomes progressively less than $(\phi_m - \phi_i)$ and below 10^{15} cm^{-3} the potential drop due to the donor space charge (<10 mV) is quite negligible.

It will now be shown that the resistivity of the SiO_x films investigated was so high than N_d must be much less than even 10^{15} cm^{-3}. Ionized donors give an equal number n cm^{-3} of free electrons and hence a low field ohmic conductivity

$$\sigma = q n \mu \qquad (5)$$

where μ is the mobility. Table 8.3 shows the

conductivity values for $N_d = 10^{15}$ cm^{-3} for three different value of μ.

μ cm^3 V^{-1} sec^{-1}	10^{-3}	10^{-1}	10
σ $ohms^{-1}$ cm^{-1}	$1.6x10^7$	$1.6x10^{-5}$	$1.6x10^{-3}$

Table 8.3:-

The I-V characteristics of all the films (Fig.7.3) show highly non-phmic behaviour. However, assuming that an ohmic component of the current accounts for the conduction at very low field strengths, an upper limit of the conductivity of the films can be obtained. From Fig.7.3 it is seen that the highest current measured at one volt was about 2×10^{-12} amp. For a film thickness of 1400 Å and contact of 0.04 cm diameter this corresponds to a conductivity of 2.2×10^{-14} $ohms^{-1}$ cm^{-1} which is many orders less than the lowest value in Table 8.3. Putting it another way, the upper limit for N_d for this conductivity would be 1.4×10^8 cm^{-3} (for $\mu = 10^{-3}$ cm^2 V^{-1} sec^{-1}), as would be expected for a wide gap insulator such as silicon oxide.

From the above values it is concluded that depletion layer effects are negligible in these SiO_x films. However, it could be argued that the low conduction currents are due to the presence of full depletion layers. Table 8.2 shows that an ionized donor density of at least $10^{17}cm^{-3}$ would be required to obtain barrier effects and this would be most unlikely in a wide gap insulating film.

The possible effects of depletion barriers in the composite films containing willemite will be discussed in Sec. 8.6.

(b) Accumulation layers

If the work function of the metal is less than that of the insulator, accumulation layers are formed at the contacts as shown in Fig. (8.1 a) for a moderately thick film. In this case Poissons equation can be written as

$$\frac{d^2V}{dx^2} = - \frac{qN_c}{\varepsilon_r \varepsilon_o} \exp\left(- \frac{qV-\Phi}{kT}\right) \tag{6}$$

where Φ is the height of the barrier at the interface, and N_c is the effective density of states in the conduction band. $N_c = \left(\frac{2\pi m^* kT}{h^2}\right)^{3/2}$. From equation (6), the width of the accumulation layer, ω_a is given by

$$\omega_a = \frac{\pi}{2} \left[\frac{2kT\varepsilon_r\varepsilon_o}{q^2 N_c}\right]^{\frac{1}{2}} \exp \frac{\phi_i - \chi}{2kT} \tag{7}$$

The maximum rise in potential, which the film can accommodate due to accumulation regions at the contacts is $\frac{\phi_i - \phi_m}{q}$. In table 8.4, ω_a has been tabulated for three rather small values of $(\phi_i - \chi)$ for which the accumulation layers could fit within a thin film.

$\phi_i - \chi$ eV	0.1	0.2	0.3
ω_a Å	160	1200	7200

Table 8.4: Width of the accumulation region taking for N_c the room temperature value of 2.5×10^{19} cm^{-3} for $m^*=m$.

In practice $\phi_i - \chi$ may take values of up to 2 eV because $\phi_i > \phi_m$. The maximum rise in potential is then limited by the thickness of the film and at the midplane is given by

$$\Delta V = \frac{q\, s^2\, N_c}{2\, \varepsilon_r\, \varepsilon_o} \exp\left(- \frac{\phi_o}{kT}\right) \tag{8}$$

where ϕ_o is the value of qV for maximum rise in potential

at the midplane. Evaluation of Equation (8) for $S = 1500$ Å and ϕ_o equal to 0.2, 0.5, 0.8 and 1 eV gives respectively 3.3×10^{-1}, 2.03×10^{-6}, 1.12×10^{-11} and 4×10^{-15} volts for ΔV. It can be seen that for any value of ϕ_o greater than 0.2 eV, the value of ΔV is negligible so that the applied voltage would be dropped uniformly across the film. If ϕ_o is less than about 0.1 eV accumulation layers are localized at the contacts ensuring a plentiful supply of carriers for bulk limited conduction which again would be ohmic at low field strengths. For ϕ_o between 0.1 and 0.2 eV the situation would be similar but with a higher apparent film resistivity. It is concluded that accumulation layers could not lead to the very field dependent conduction observed.

In the above discussions of the surface barrier layers the effects of surface states and image forces have been neglected. As on a semiconductor surface, extra states would be expected to exist on the free surface of an insulator. Their action can be included by specifying a 'surface Fermi level' up to which the surface states are filled in equilibrium. To align the surface Fermi level with that of the bulk charge must be transferred to or from them, resulting in the formation of a depletion or accumulation layer under the surface. When a contact is formed to a surface with such states, the actual barrier height is modified by the surface potential. However, the calculation of the widths of depletion or accumulation layers is unaffected apart from a change of boundary conditions, i.e. barrier height. As the barrier heights are not known in any case, their modification by surface states is immaterial.

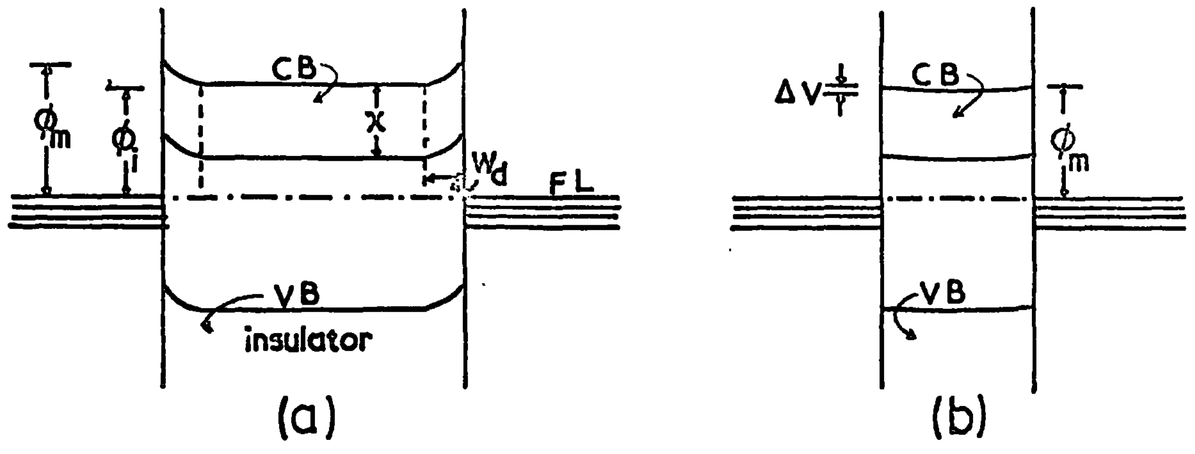

Contacts with depletion layers on, (a) thick film, (b) thin film.

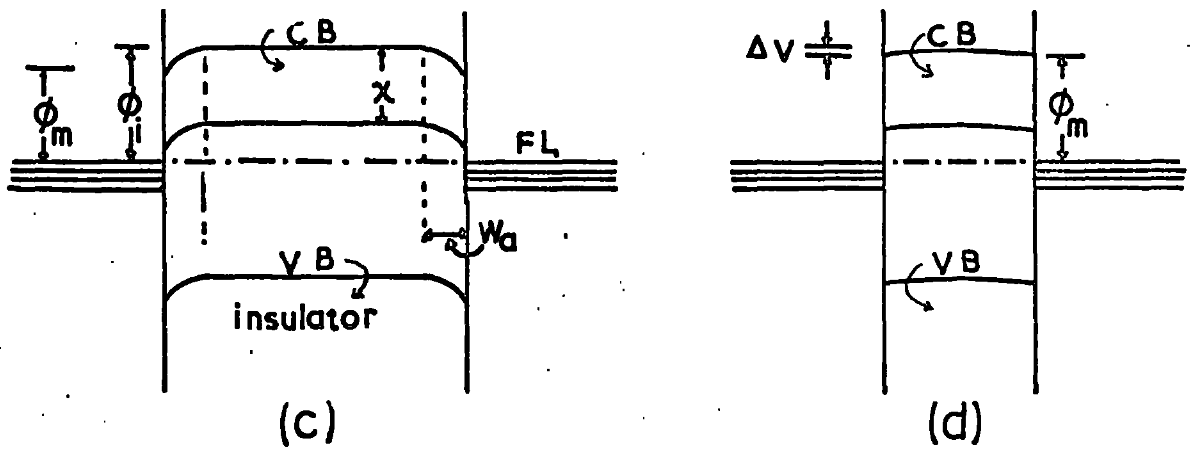

Contacts with accumulation layers on, (c) thick film, (d) thin film.

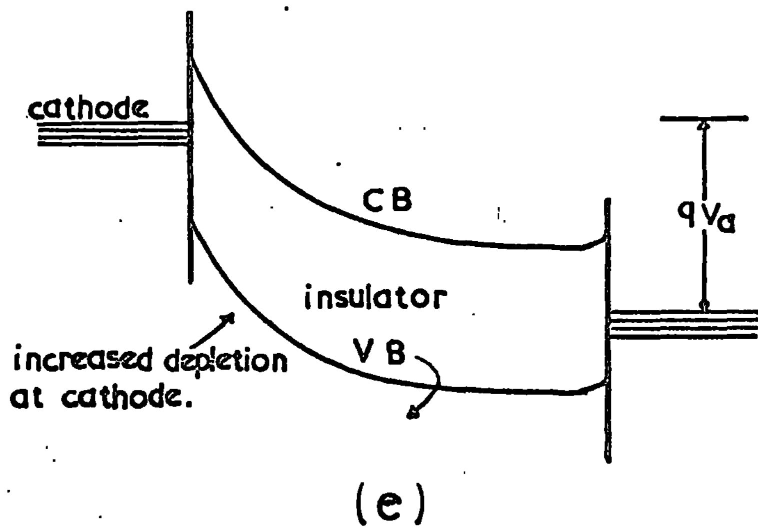

Fig. 8.1

Image forces round off the discontinuity in any type of barrier at the metal-insulator interface and are very important in determining the potential distribution in very thin (<200 Å) insulating films between metal electrodes. In thicker films, however, such as the ones under discussion here, their effect can be neglected over the bulk of the film.

8.3 Conduction Processes in Uniform Thin Films

It has been shown in the last section that space charge regions at the contacts to uniform thin insulating films of about 1500 Å thickness do not normally give appreciable potential variations in the bulk because of the limited distance available. There are two exceptions to this general conclusion. One is the depletion barrier formed when $N_d > 10^{18} cm^{-3}$ and the other is the accumulation layer for the condition $\phi_i - \chi \leqslant 0.1$ eV. In both these cases the space charge will be localized at the contacts and well within the film thickness. The accumulation layer will not affect the I-V characteristic because it simply represents a low resistance ohmic contact to the film. The depletion or Schottky type barrier will, however, have a high resistance so that its effect will later have to be considered in more detail.

Before doing this, the possible conduction mechanisms for the more likely uniform field conditions must be discussed. At sufficiently low field strengths, the conduction will always be ohmic and limited by the electron concentration, in the bulk. As the field strength increases the current rises well above the ohmic value and it may then become limited by the supply of electrons from the cathode. At sufficiently high fields the contact barrier at the metal-

insulator interface will be lowered to give a Schottky type characteristic (Equation 4, Chapter 3). Alternatively, if the current remains bulk limited the effective number of carriers will increase with field strength due to the field ionization of deep donors as in the Poole-Frenkel effect (Equation 11, Chapter 3). At very high field strengths the current will increase more rapidly still either due to tunnelling, for which $I \alpha \exp(-\frac{1}{\mathcal{E}})$, or carrier multiplication by impact ionization which will follow a similar law. Both of these processes give a rapid increase of current with applied voltage just before dielectric breakdown. Since no such increase was observed in the experimental work it may be concluded that if the field was uniform then the very high field process did not occur in our films. As all the measurements are clearly above the ohmic range they will therefore have to be explained by either Poole-Frenkel or the Schottky effect in this case.

The criteria for choosing between Poole-Frenkel conduction and Schottky emission have been the subject of a great deal of discussion in the literature on insulating films. The choice has invariably been for the former because of (a) lack of dependence of the current on electrode metal, and (b) the value of the slope of the logI versus $\sqrt{V}$ plot at high field strengths. The present work on SiO films is unusual in showing a strong electrode metal dependence from the comparison of aluminium and platinum for both anode and cathode. However, the results summarised in Fig. 7.3 show immediately that it is not pure cathode dependence. If the current were limited by cathode emission, an aluminium cathode would be expected to give a larger current than platinum

($\phi_{Al} \simeq 3.4$ eV, $_{Pt} \simeq 4.52$ eV) whereas the reverse of this is found. Also the use of aluminium as compared with platinum for the anode gave even greater reduction than for the reverse polarity. The electrode dependence is therefore not in agreement with a Schottky-emission type of conduction limitation. It will be explained in detail in Section 8.4, where it will be shown to be an electrode effect on bulk limited conduction and peculiar to the use of aluminium.

The second method of choosing between Poole-Frenkel and Schottky emission is from the plot of logI versus $\sqrt{V}$. The best results for SiO_x films with platinum electrodes (Fig. 7.3, curves a) have been replotted in this way in Fig. 8.2a. It can be seen that the graph is a straight line at high field strengths as expected for both conduction mechanisms. The slope of the straight line portion is 0.195×10^{-4} $eVm^{\frac{1}{2}}V^{-\frac{1}{2}}$. This may be compared with theoretical value of 0.19×10^{-4} and 0.095×10^{-4} obtained from Equation 3.8 and 3.3 for the Poole-Frenkel and Schottky processes respectively taking the value of 4.0 for the high frequency dielectric constant of vacuum deposited SiO_x [108]. It can be seen that the agreement with the Poole-Frenkel value is extremely good, particularly in view of the likely error in the measurement of film thickness (±10%). The value is also in good agreement with experimental values obtained by other workers. It is concluded that the results provide strong evidence for Poole-Frenkel conduction in the uniform SiO_x films with platinum electrodes. A more detailed comparison with the theory of this process will be given in the next section.

The above discussion is based on the assumption of a uniform field through the film thickness. The alternative to this assumption has been shown to be a depletion layer field intensification which will only be important in such thin films if the donor concentration is 10^{18} cm^{-3} or above. Although this appears to be most unlikely for SiO_x films of high purity, the likely consequences of depletion-barrier limited conduction should be considered here. Figure 8.1,c shows the band diagram for a thin film containing depletion (Schottky) barriers at both contacts. It is assumed that most of the applied voltage, V_a, is dropped across the reverse biased (i.e. cathode) barrier which is of much higher resistance than the bulk. The width of the cathode barrier is increased from the equilibrium value (Equation 3) because of the applied voltage and the maximum field strength, $\mathcal{E}_c$, which occurs at the cathode-insulator interface is given by

$$\mathcal{E}_c = \left[\frac{2N_d(\phi_m - \phi_i + qV_a)}{\varepsilon_r \varepsilon_0}\right]^{\frac{1}{2}} \qquad (9)$$

For a reverse biased Schottky barrier the current is limited by the number of electrons emitted from the metal [148]. For values of $\mathcal{E}_c$ up to 10^6-10^7 volts cm^{-1} the current is then given by the equation for Schottky emission

$$J = AT^2 \exp\left[\frac{(q^3\mathcal{E}_c/4\pi\varepsilon_o\varepsilon_r)^{\frac{1}{2}} - \phi_o}{kT}\right] \qquad (10)$$

Substituting from (9) shows that in this case

$$J \alpha \exp(\mathcal{E}_c)^{\frac{1}{2}} \ \alpha \ \exp(V_a)^{\frac{1}{4}} \qquad (11)$$

In very thin films with narrow depletion layers the value of $\mathcal{E}_c$ is likely to become high enough for electrons to tunnel through the barrier at comparatively low applied voltages.

Table 8.5 shows the values of $\mathcal{E}_c$ for $N_d \doteq 10^{18}$ cm^{-3}; larger values of N_d give still higher fields.

V_a (volts)	0	2	4	6	8
ω_d (Å)	332	469.5	575.06	664	742.4
$\mathcal{E}_c$ MVcm^{-1}	3.83	5.41	6.6	7.65	8.6

Table 8.5 Evaluation of cathode field in SiO_x for $N_d=10^{18}$ cm^{-3}, $\phi_m-\phi_i=2$ eV.

When tunnel emission predominates the current is given approximately by the Fowler-Nordheim equation:

$$J \propto \frac{1}{\mathcal{E}_c^2} \exp\left(-\frac{\text{const.}}{\mathcal{E}_c}\right) \tag{12}$$

Substituting from (9) shows that in this case

$$J \propto \frac{1}{V_a} \exp\left(-\frac{\text{const.}}{\sqrt{V_a}}\right) \tag{13}$$

In the present films a current variation of the form of (10) would therefore be expected to change to (12) for an applied voltage of a few volts or even less.

A further possibility is that impact ionization will occur at such high field strengths. The probability of ionization is proportional to $\exp\left(-\frac{\text{const}}{\mathcal{E}_c}\right)$. If the injected carriers cause ionization the current (Equation 11 or 13) is increased by this factor. Substituting for $\mathcal{E}_c$ the current would then be

$$J \propto \frac{1}{V_a} \left[\exp\left(-\frac{\text{const}}{\sqrt{V_a}}\right)\right]^2 \tag{14}$$

for the case of tunnel emission. Another possibility is that thermally generated carriers lead to impact ionization in the

depletion layer in which case

$$J \propto \exp\left(-\frac{\text{const}}{\sqrt{V_a}}\right) \qquad (15)$$

It can be seen that field intensification in a depletion layer can lead to a number of different I-V relationships. Since the experimental results show no rapid increase towards the higher applied voltages, the most likely process in the present films is the tunnel emission limited current, (13). The $\frac{1}{V_a}$ term in this expression would not affect it greatly compared with the exponential in which case it is of the Alfrey-Taylor form. Note that equation (15) is of the same form. The present results for the uniform SiO_x film with platinum electrodes are replotted as an Alfrey-Taylor plot in Fig. 8.2c, which shows that this form of variation is not obeyed. The same results are replotted in Fig. 8.2d for comparison with Equation (11). It can be seen that the graph is not linear except for a small section at the high field end. It is unlikely that a distinction between logI versus $V^{\frac{1}{2}}$ and logI versus $V^{\frac{1}{4}}$ could be observed at high field strengths.

For depletion layer controlled conduction it is therefore concluded that the Schottky emission at the cathode interface would be consistent with the experimental results and that there is no evidence for other mechanisms. The Schottky emission would only occur with $N_d \sim 10^{18}$ cm^{-3} as lower values than this would give insufficient space charge for a full depletion layer and higher values would increase the cathode field to a value where tunnelling would occur. There is no evidence for such a critical dependence of current on impurity concentration, either in the present work or in the literature. It therefore seems that depletion layer

effects are most unlikely in these films and that the uniform-field conduction model is much more appropriate.

Before reaching this conclusion it is necessary to discuss the possibility of space charge limited currents (SCLC). In Chapter 3, Sec. 3.2.9, it was shown that the SCLC's have been observed mostly in single crystal materials and thick insulators. Further the magnitude of SCLC expected from the film thickness of 1400Å and top contact area of 1.257×10^{-3} cm^2 is in the range of 1.5 amperes, even with the minimum values for the parameters μ and θ. Therefore this process is also not possible, as this value is several orders of magnitude higher than the observed currents. It can then be concluded that the most likely conduction process is the Poole-Frenkel mechanism.

8.4 Detailed Comparison of Uniform Film Measurements with the Poole-Frenkel theory

The discussion in Sec. 8.3 has shown that the Poole-Frenkel interpretation of the conduction in SiO_x films with Pt electrodes is the most probable. A more detailed comparison of the experimental results will now be made with the Poole-Frenkel model given by Adachi et al [118], which for SiO_x films, explains the complete shape of the I-V curves including the low field region. The current density J is given by:

$$J \doteq 5.57 \times 10^{-8} \frac{T^{\frac{3}{4}} \nu}{\lambda^{\frac{1}{2}}} \exp\left(-\frac{\phi_{1m}(V)}{2kT}\right) \left\{1 - \exp\left(-\frac{eV\lambda}{2kTs}\right)\right\} \ (\text{A.cm}^{-2}) \qquad (16)$$

where the symbols have been explained in Chapter 3, Sec.3.3 and will be discussed later in this section.

The present results are compared with some of the published work in Fig. 8.2(a and b) on logJ versus $V^{\frac{1}{2}}$ scale. The results are for various film thicknesses which affects the slope of the high field region and makes the precise comparison more difficult. It can be seen that the present films are more resistive than those prepared elsewhere and this must be due to the post-deposition bake in oxygen which the present films received (Sec. 4.4.4). This would be expected to increase their state of oxidation converting them towards the more insulating SiO_2. This interpretation is confirmed by comparing the standard curve (a in Fig.8.2) with curves d_1-d_4 (Fig. 7.2) for the argon baked and hence less oxidized films, and with those for the heavily oxidized films (c_1 and c_2, Fig. 7.3). It also agrees with the findings of Johansen [111].

Although the present films were more resistive than those reported elsewhere, the general shape of the logJ versus $V^{\frac{1}{2}}$ curve is closely similar. It has been shown in Sec. 8.3 that the slope of the high field region agrees well with the Poole-Frenkel theory. From Equation (16) (obtained by Adachi et al. [118]), the value of J_o which is the intercept of the high field line extrapolated back to the current axis at V = O, is given by

$$J_o = 5.57\times10^{-8} \frac{T^{\frac{3}{4}}\nu}{\lambda^{\frac{1}{2}}} \exp\left(- \frac{\phi_o - 3.49\alpha/\lambda}{2kT}\right) \quad (\mathrm{Acm}^{-2}) \qquad (17)$$

where ν is the attempt to escape frequency of the electron, λ is the average distance an electron travels between sites before being retrapped and ϕ_o is the depth of the Poole-Frenkel site from the bottom of the conduction band. Adachi et al were able to calculate these parameters from the

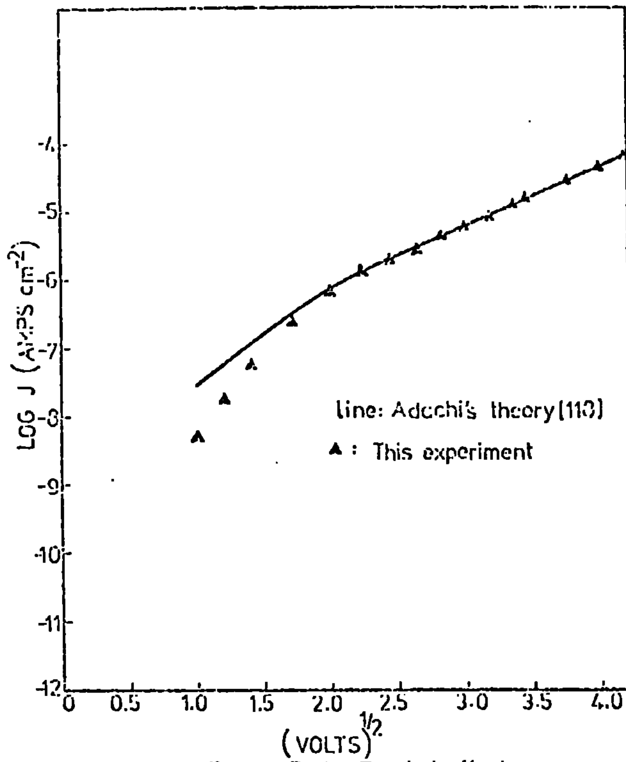

a. Plot of Poole-Frenkel effect

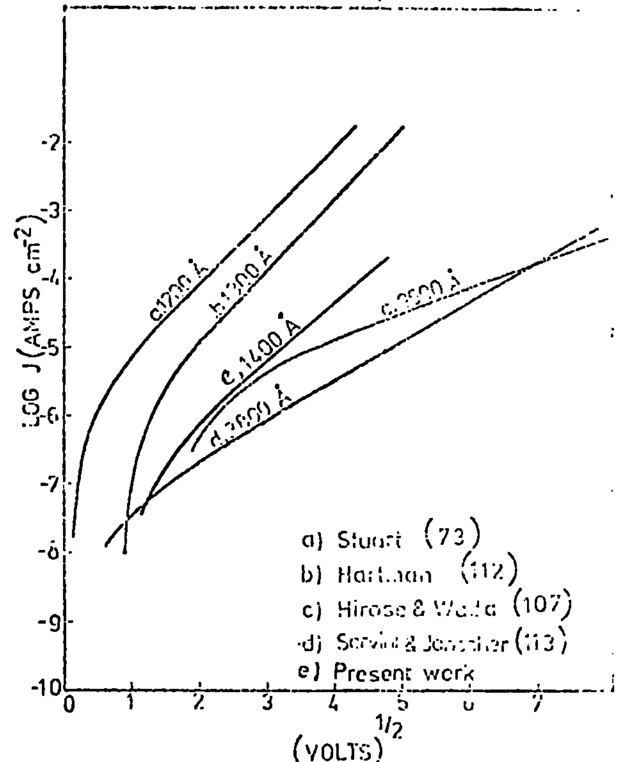

b. Plot of four of published SiO_x results

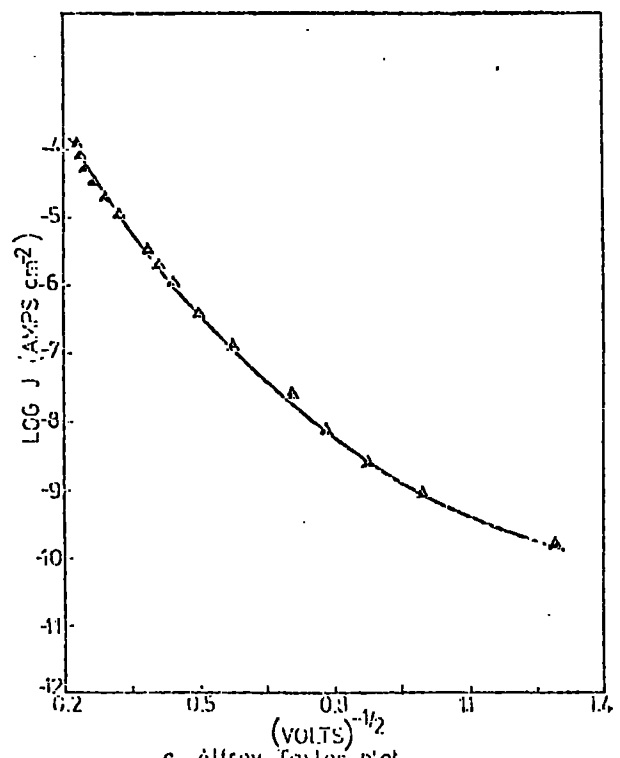

c. Allrey Taylor plot

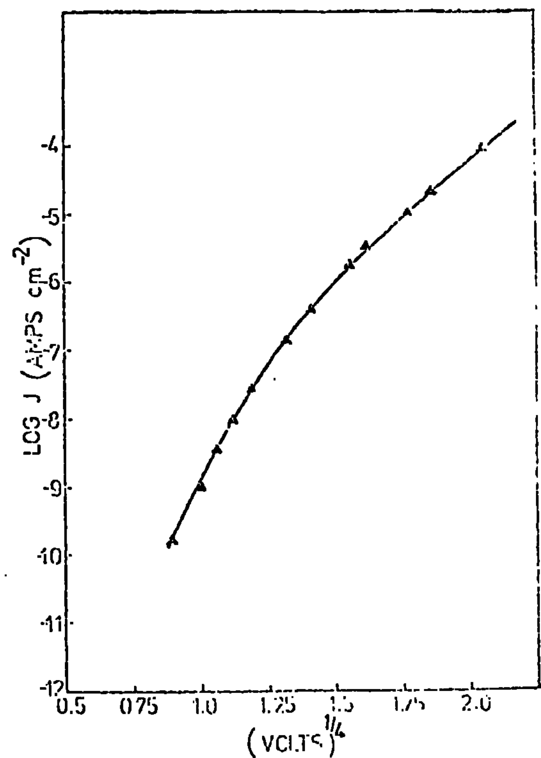

d. Plot of Schottky barrier

Fig. 8.2 Comparison of experimental results for SiO_x with different theories.

experimental data and hence the complete shape of the I-V curve. They used $\phi_o=1$ eV, $\nu=10^8$ sec^{-1} and $\lambda=100$ Å for films as deposited. The value of J_o obtained from the present work is 100 times less than the normal experimental value, due to the extra oxidation of the films. Oxidation would decrease the disorder in the film by filling the unsatisfied silicon bonds [140] and thus decrease the number of available Poole-Frenkel sites. This should have the effect of increasing the value of λ. Higher values of λ substituted in (17) shift the J-V curve downwards in accordance with the present experimental results. The value of ν on the other hand should decrease to account for the decrease in current (Equation (17)), because the net density of electrons contributing to the current is independent of this factor [118]. Taking the values $\nu = 10^7$ sec^{-1}, $\lambda = 237$ Å and keeping ϕ_o unchanged, the complete shape of the J-$V^{\frac{1}{2}}$ characteristic has been obtained from (16) and this is shown as a continuous line in Fig. 8.2a. It can be seen that the agreement is quite good in the high field range, but the experimental points deviate from this line as the field approaches zero. A more detailed comparison would require data for the thickness and temperature dependence of current for these films. These were not investigated in the present work. However, the agreement in the high field range supports the conclusion that the most likely conduction process is the Poole-Frenkel mechanism.

8.5 Conduction Process in Oxide Films with Pt-Al Electrodes

The last two sections presented a discussion on conduction in the present SiO_x films with platinum (Pt) electrodes. Currents with one aluminium (Al) electrode are lower than those with Pt as shown by the curves b_1 and b_2 in Fig. 7.3. Curve b_1 shows that for an Al cathode the current is less than that with the Pt, (curve a), but curve b_2 shows surprisingly that an Al anode has even larger influence on the current. These curves were also briefly discussed in Sec. 8.2. This anode dependence has never been reported in the literature, but a lot of experimental evidence for this behaviour was obtained in the present work as shown by the reproducible results in Chapter 6. This electrode dependence will be explained in terms of an Al_2O_3 layer under the Al top contacts, which is believed to be connected with the particular method of processing used.

All of the present films were baked for fifteen minutes in an atmosphere of oxygen before putting down the top contacts, and then for about five minutes at the end of the process (although in an atmosphere of nitrogen to aid adhesion of the aluminium). It is likely that the oxygen trapped in the oxide film in these conditions would have reacted with the Al layer in contact with it and formed a thin underlying film of Al_2O_3. This thin film of Al_2O_3 (which may be approximately 100 Å or less in thickness) between the Al top contact and the silicon oxide would be sufficient to form a barrier for electron transmission [138]. It is known that the bandgap of Al_2O_3 is greater than that of silicon oxide (10.0 and 8.5 eV respectively) and that it is more

insulating [68]. On this basis the model shown in Fig. 8.3 has been constructed. Assuming the conduction through silicon oxide to be still by the thermal ionization of electrons over the field lowered Poole-Frenkel sites, the decrease of current in the Al top contact samples is explained as follows with the help of the Al_2O_3 barrier.

When the platinum electrode is positively biased with respect to the aluminium (Fig. 8.3,a), part of the applied voltage is dropped across the Al_2O_3. Due to the lower conductivity the field in Al_2O_3 is higher than in silicon oxide. Hence electrons reaching the silicon oxide interface would have travelled through a less conducting material, so that the current would be less than the magnitude it will have in the absence of Al_2O_3. A cathode like platinum, which will not have such an oxide, would therefore give more current as observed. The exact nature of conduction through Al_2O_3, and of the voltage balance that would be achieved between the two films to give the same conduction is not known.

When the aluminium side of the device is biased positively (Fig. 8.3,b), more voltage will be dropped across the Al_2O_3 and less across the silicon oxide than in the opposite case discussed above. Electrons then travel through the conduction band of the silicon oxide up to the barrier with the wider band gap Al_2O_3 and pile up at the interface, resulting in a further increase of the field across the latter. The limit to the flow of electrons in our model is set up by an insulator-insulator barrier, which is different from the limitations due to contacts and to the bulk. With the increased field, some electrons are transmitted by the Al_2O_3, possibly by tunnelling into the conduction band.

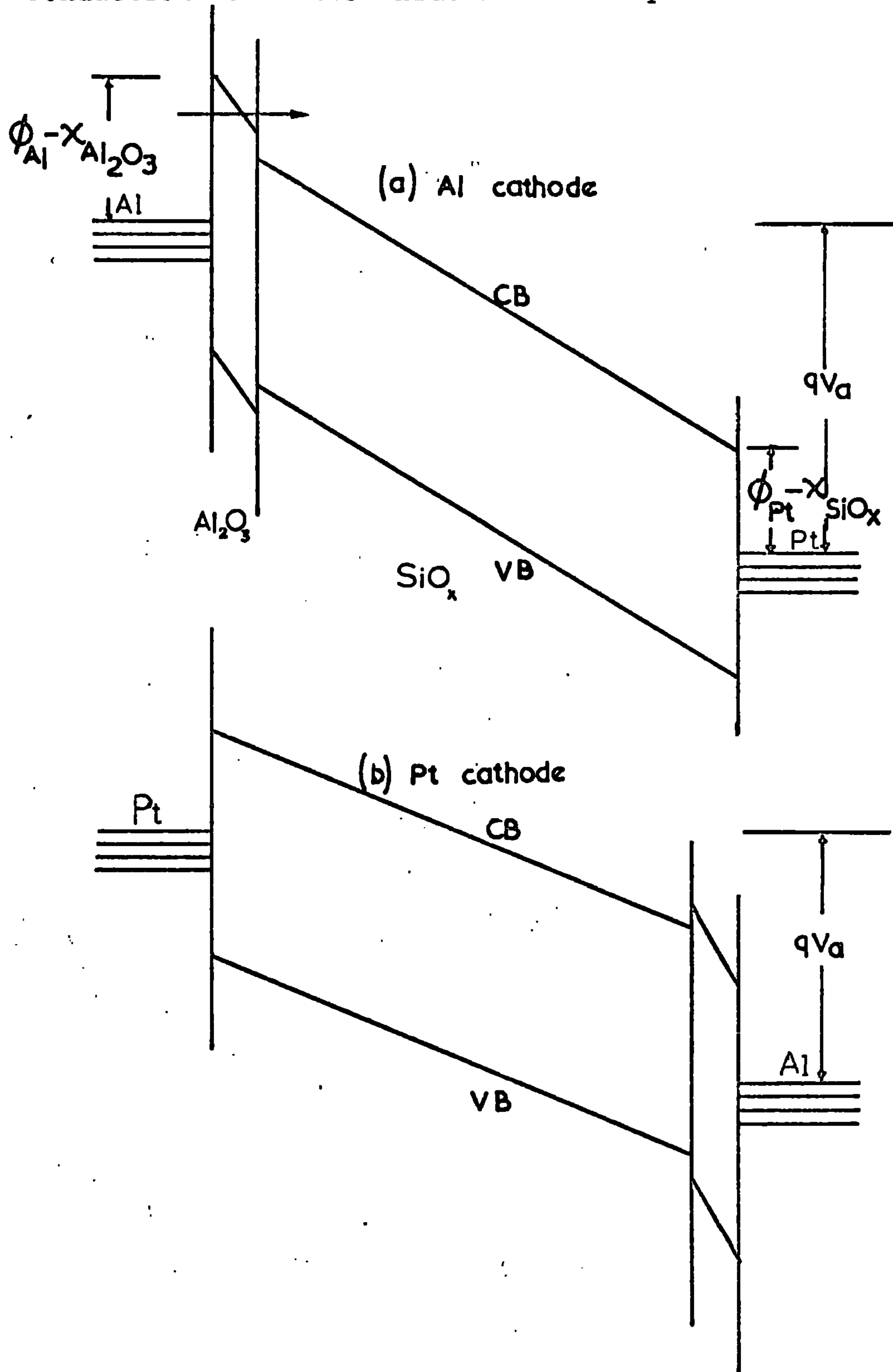

Fig. 8.3

Under equilibrium conditions the field across the silicon oxide for a given applied voltage would therefore be less than that for the opposite polarity, which explains the low level of current in curve b_2 in Fig. 7.3. An interesting feature of the conduction for this polarity is shown by the logI versus $\sqrt{V}$ plot which gives a good straight line but of a slope much greater than what could be interpreted as the Poole-Frenkel effect.

Fig. 7.3 also includes two curves of a more oxidized film. Curves c_1 and c_2 are for heavily oxidized film and show the same kind of polarity dependence as b_1 and b_2. These are also for Al cathode and anode respectively. The electrode dependence could be explained in the same way as for the normal films, but the lower level of current is due to the fact that the silicon oxide is more insulating.

8.6 Conduction Process in Composite Oxide-Willemite Films

A summary of the results for composite oxide-willemite films has been presented in Figs. 7.4 and 7.5 for Pt-Al and Pt-Pt electrodes respectively. Figures 7.5 and 7.6 include comparisons with the oxide results. In general, conduction through the composite films has similar characteristics to that in the silicon oxide alone, including the same electrode dependence with Al contacts, but the currents are considerably higher in some cases.

a. The construction of the composite-willemite films.

Before attempting to explain the results, it is necessary to describe the nature of the composite willemite films. In all the samples studied the willemite areas are thicker than the surrounding unreacted 1400 Å of SiO_x. In Chapter 5, Sec. 5.2, an experiment was described for estimating

the thickness of the oxide consumed in the willemite formation. On etching away the thin willemite film (200 Å) from one of the samples no marks of any sort were seen on the remaining oxide film with x100 optical microscope, although it must have been attacked to provide silicon for the formation of the zinc silicate phosphor. Later a film of 700 Å of willemite was etched off and this time, the oxide underneath was found to be a slightly different colour compared with the surroundings. Using the tables for SiO_2 interference colours, a depth of reaction of 100 Å or less was estimated. Even this degree of attack, however, provides sufficient silicon to form willemite on the thickness given. (Reaction equation Chapter 7, Sec. 7.2). These experiments show the main problem in the interpretation of the results, which is that the oxide thickness has hardly changed in the reactions and therefore willemite forms as a very thin film on top of it. This makes it extremely difficult to explain the generally greater currents in composite willemite films.

b. Possible barrier effects in composite willemite films.

The possible effects of potential barriers inside thin uniform films have already been examined in Sections 8.2 and 8.3, where because of the small thickness involved the potential distribution was shown to be very nearly uniform. In willemite films there is an additional possibility that a space charge barrier will form at the heterojunction at the oxide willemite interface and give rise to a non-uniform potential distribution. In the absence of information about this interface, the exact nature of these junctions cannot be discussed. However, on the basis of the discussion

presented in Sec. 8.2, it can be said that because the willemite films are so much thinner than the oxides, the potential change will be even less apparent.

Explanations will now be offered for the increased current with willemite and Pt top contacts (even though the complete thickness of the composite film has increased), the increase in current in willemite with thickness using Al top contacts and the strong polarity dependence observed with this metal which is the same as for the oxide. Explanations of these observations have been attempted based on the following two possibilities:-

(a) that zinc fluoride dissolves silicon oxide quite irregularly during the reaction (see Chapter 4, Sec. 4.4.4),

(b) that, during the reaction, physical changes take place in the silicon oxide to increase its conductivity. This probably occurs by the diffusion of certain types of impurities from willemite.

For both possibilities it is likely that the willemite is more conducting than the oxide as would be expected from its band gap at 5.4 eV compared with approximately 8.5 eV for SiO_x. Also, with impurities, it is probably an n-type semiconductor.

Possibility (a) is that the interface between willemite and oxide is not uniform and that the willemite penetrates deep into the oxide at some places. If this happens, then it will require only one channel of increased conductivity to account for the increase in current. This may explain the rise of current due to the formation of willemite, but difficulties arise when the explanation is sought for the increase of current with the thickness of willemite. One

more puzzling question is the limitation of current with the aluminium counter electrode (to approximately the oxide value). It is believed that the explanation of this may lie in the presence of Al_2O_3 under the aluminium similarly to the oxide case. G. Davies [26] found some evidence of the absorption and movement of oxygen through willemite films on silicon. It is suggested that the trapped oxygen in the film may account for the oxidation of the aluminium electrode in a manner similar to that described for the oxide films. However, a detailed consideration of this model shows that it does not seem to provide a sufficient explanation for the experimental results.

Possibility (b) is that when the zinc fluoride and silicon oxide react to form willemite, the oxide immediately in contact with it increases in conductivity. This may be due to the introduction of zinc as an impurity and/or due to the reduction in the number of traps. The depth of the region of increased conductivity would depend on the thickness of the starting material, i.e. the willemite film on top of the oxide.

In what follows, the willemite results have been interpreted by developing the above argument. We consider first the results for platinum top contacts, which are relatively simple as compared to those for aluminium. In Fig. 8.4 hypothetical band diagrams have been drawn for both positive and negative applied voltages. For a negative voltage on the top contact, the electrons pass first through the willemite. They then enter the more conducting region of the oxide which presumably gradually phases out into the evaporated form of silicon oxide. There would then be a larger voltage drop across this more insulating region and

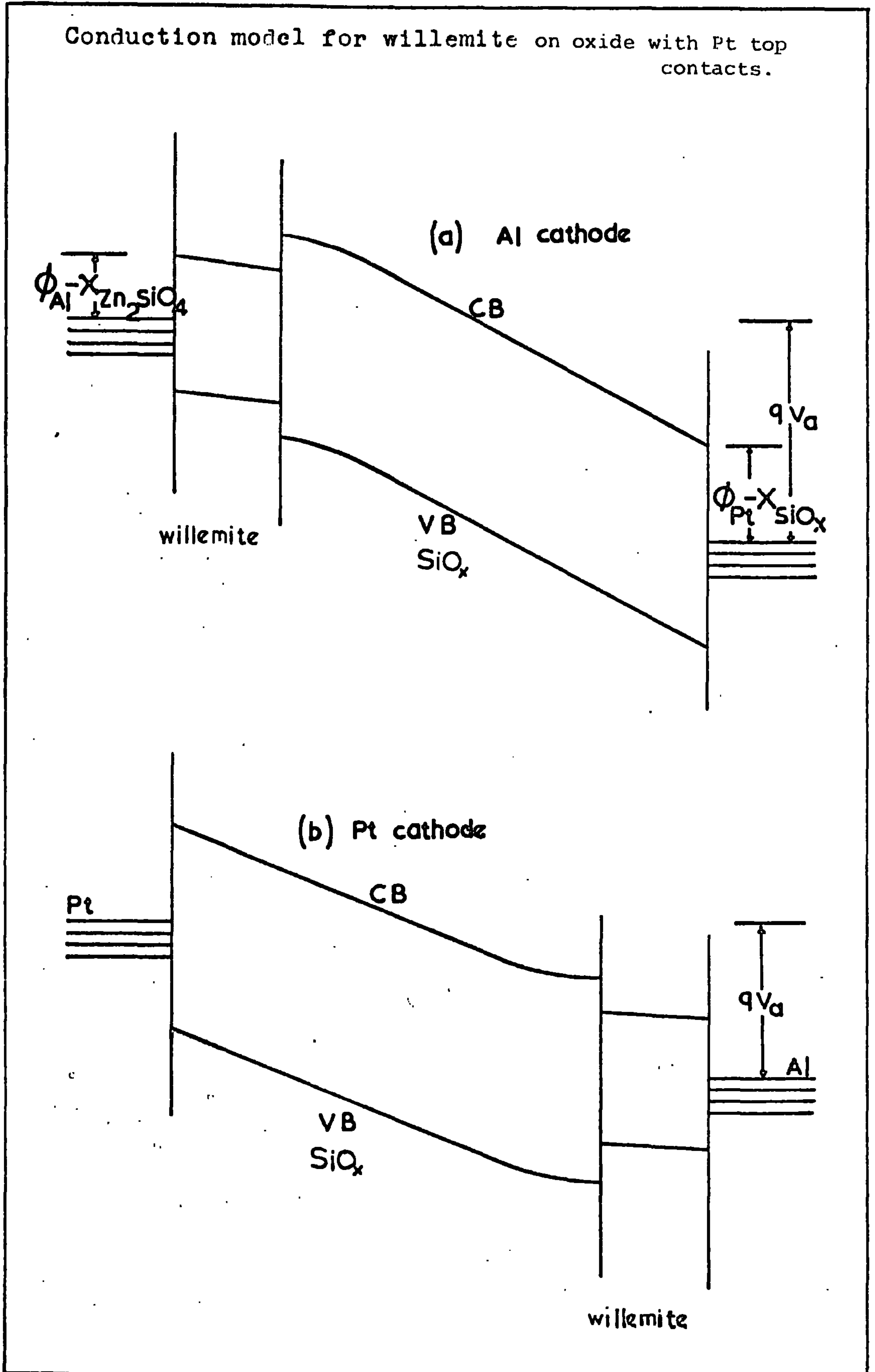

Fig.8.4

hence a higher field across it so that in equilibrium the current is constant. When the top contact is positive the bands are bent the other way and the electrons first travel through the more insulating oxide, then through the higher conductivity part and through the willemite to the top electrode. On this model, polarity dependence might be expected because the cathode contact is Pt-willemite for negative and Pt-SiO_x for positive polarity, although nothing is known for certain about these interfaces.

The available experimental results do not show whether there is any polarity dependence in willemite because of the scatter. Comparing the willemite conduction with that for the pure oxide for the same contacts and for an equal voltage (Fig. 7.5), it appears that the increased conduction in willemite must be entirely due to the higher conduction in part of the oxide underneath. It is also apparent that in the interpretation the presence of the willemite makes no difference because it is assumed to be more conducting than even the enhanced conduction of the oxide. This could be confirmed experimentally by measuring the conduction in the residual oxide after the removal of the willemite. There was no time for this experiment in the present work.

After discussing the increase of conduction through willemite films with platinum top contacts it is necessary to introduce Al_2O_3 again to explain measurements with aluminium top contacts. This interpretation would also be consistent with the one used for oxide. Fig. 8.5 shows hypothetical band diagrams for the two polarities of the willemite films with aluminium top contacts. For the negative voltage applied to the top contact the conduction process would be similar to

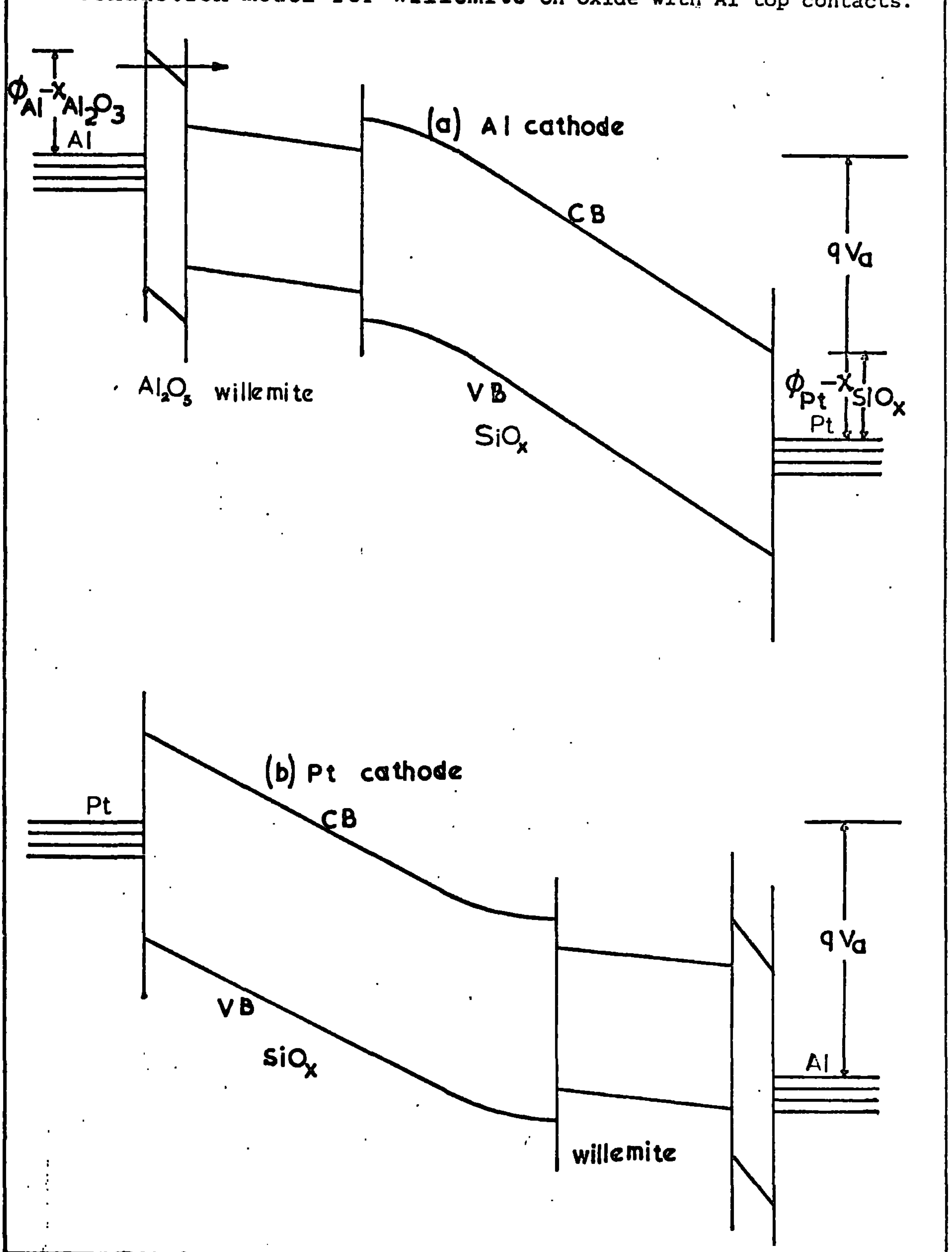

Fig. 8.5

the one described for platinum top contacts except that the current would now be limited due to the Al_2O_3 cathode barrier. The electrons would have to penetrate this barrier in order to get into the willemite and in this respect its behaviour is similar to that explained in connection with the silicon oxide results described in Sec. 8.5. For the case when a positive voltage is applied to the aluminium, the electrons travel first through the silicon oxide film and the willemite, and they then reach the barrier formed by the Al_2O_3. They would be expected to accumulate at the step in the conduction band edge between willemite and Al_2O_3. Due to the increased field across the Al_2O_3, which is less conducting, some electrons will penetrate it (possibly by tunnelling) although the current will be less than for the opposite polarity as is found. The step in the conduction band between willemite and Al_2O_3 would be expected to be greater than the corresponding one with SiO_x, so that the positive current in willemite would be even lower as is found (Fig. 7.6). The Al_2O_3 barrier turns out to be more important when the increase of current for the thicker willemite films has to be explained. It is thought that the region of the oxide of enhanced conductivity expands in proportion to the thickness of willemite. If this happens then, at a constant applied voltage, less voltage would be dropped across the silicon oxide and the difference in voltages would appear across the Al_2O_3 layer. The conduction through Al_2O_3 is probably largely due to tunnelling of electrons as has already been suggested. The tunnel currents are very sensitive to voltage variations hence even a small increase of voltage on the Al_2O_3 barrier would decrease the tunnelling thickness, thereby increasing the current

considerably. Thus, in equilibrium, when the same voltage is applied to willemite films of two different thicknesses, the thicker films would pass a much higher current. This model is therefore in accordance with all the experimental results for willemite in that it can qualitatively explain the electrode dependence and the increase in current with willemite thickness, but a lot more work on fundamental conduction processes would be required to evaluate it qualitatively.

8.7 Luminescence of Willemite Films

Some luminescent properties of willemite were described in Chapter 2, where the previous work on this phosphor was also briefly reviewed. The possibilities of its use in the fabrication of electroluminescent devices compatible with silicon technology were discussed in Chapter 1.

a. Cathodoluminescence.

The willemite films investigated here were brightly cathodoluminescent down to the minimum thickness of 200 Å studied. It appears that luminescence has never before been reported in this material in films thinner than one micron. The brightness of cathodoluminescence was fairly constant for the thicker films but the thinner willemite was not as bright. To check that these observations were not influenced by ionoluminescence or photoluminescence from the gas discharge used to excite the films they have also been tested under electron bombardment in vacuum. The resulting emission spectrum, as shown in Fig. 8.6, agrees well with that published for willemite. Also the brightness and colour agreed well with that excited by the gas discharge.

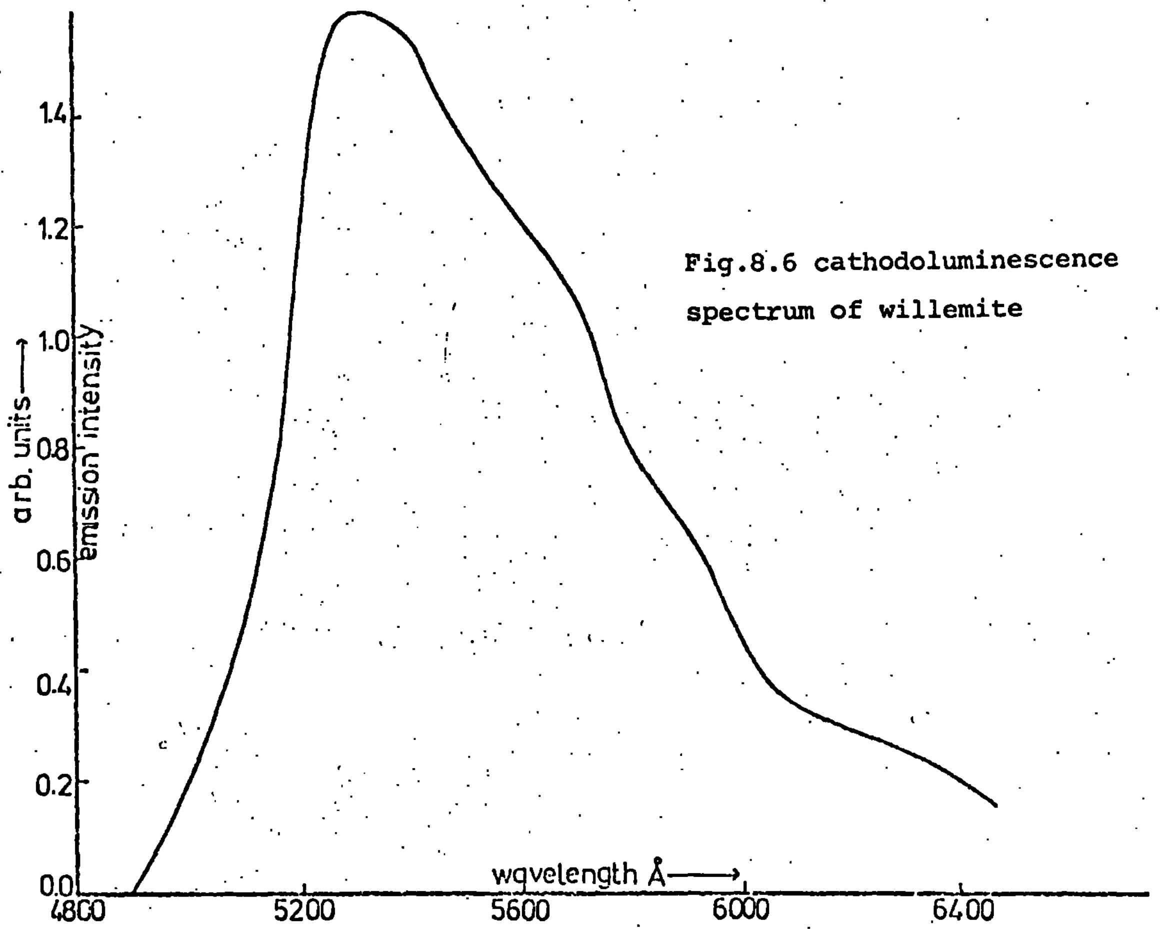

Fig.8.6 cathodoluminescence spectrum of willemite

In the light of the extensive discussion on cathodo-luminescence by Garlick and Sayer [149-151], the almost constant brightness observed for different thicknesses may be attributed to the limited energy of the bombarding particles. The decrease in brightness in the very thinnest films may have been due either to losses caused by the production of secondary electrons which were too close to the surface to remain inside, or due to recombination in the surface states of the phosphor.

b. Electroluminescence

The characteristic green emission from willemite corresponds to the transition of the 3d electrons of the Mn^{2+} ion between the 4_G excited state and the 6_G ground state which probably fall within the forbidden gap in zinc silicate. This transition can be achieved by the direct inelastic collision of an electron with the ion. Electrons with a minimum energy of approximately 2.65 eV are required to directly excite the 3d electrons. This transition can also occur by the resonance transfer of energy if an electron and hole recombine within approximately 100 Å of the Mn^{2+} ion. Electron energies 2 to 4 times the band gap are probably required to produce electron-hole pairs in zinc silicate, and these are only likely to be obtained at the breakdown field strength or immediately preceding it. Hence pair production is not an attractive process for obtaining electroluminescence.

In the present work electroluminescence was observed only in some 600 Å and thicker willemite films and only with Al top contacts. The light seen came only from the edges of the circular top contact and could not have been visible due to internal reflections because the thickness of the film

was less than half the wavelength of the light. It therefore must have been produced in the bulk of the film excited by the fringing field of the contact. Electroluminescence was observed well below the breakdown voltage and was not accompanied by flashes or sudden changes of current. Also the light emission was reproducible on a particular dot as long as the voltage did not exceed the breakdown value. Hence it cannot be related to either self-healing breakdown or spurious discharges in the film or its surroundings. The colour of the emitted light was also reproducible from one dot to another and from sample to sample in which electroluminescence was observed, showing again that it was a genuine effect in the willemite.

By making willemite sandwiched between metal electrodes, it had been hoped to find out whether the weak electroluminescence observed in devices made on silicon substrates was due to an insufficient number of electrons, or to electrons having insufficient energies. It is thought that the answer to this question lies in the observation that electroluminescence was observed only in samples with Al top contacts and also only with negative applied voltages. In Sec. 8.6 it was explained that, for this polarity, electrons tunnel through the Al_2O_3 barrier and then lose their excess energy by scattering in the willemite before reaching the SiO_x (Fig. 8.5). This excess energy is probably due to the difference of the band gaps of Al_2O_3 and willemite. It appears that those electrons which have sufficient energies excite the Mn^{2+} which subsequently emits light. On the basis of the difference between the band gaps of

Al_2O_3 (10 eV) and willemite (5.4 eV) the electrons tunnelling into the willemite might have initial energies of approximately 2.3 eV which could be increased sufficiently to excite the Mn^{2+} ion at the relatively high applied field strengths. It appears that the absence of tunnelling is the reason for never observing electroluminescence with positive voltages applied to the aluminium or with Pt top contacts.

It is concluded that electroluminescence of willemite films can be achieved by the injection of high energy electrons and that a large current alone is not sufficient.

CHAPTER 9

CONCLUSIONS AND SUGGESTIONS FOR FURTHER WORK

9.1 Main Conclusions

The work presented in this thesis has furnished useful information about thin willemite films and their possible use in the fabrication of an electroluminescent device based on silicon as described in Chapter 1.

In this work thin willemite films have been made for the first time by a process developed from that of Edwards [3]. To make the films on a metal rather than silicon substrate necessitated the evaporation of an initial film of SiO. The techniques developed were successful in that bright cathodoluminescent and occasionally electroluminescent films were produced. Few samples for electrical measurements could be produced on silica, but good samples with reproducible electrical properties were later produced on sapphire. It is inferred that in the fabrication process used, the films can easily have microscopic defects, if the coefficient of expansion of the substrate differs greatly from that of the base electrode metal (Pt) and if the substrate surface is not highly polished and great care is not exercised about the cleanliness.

Originally it was intended that a section of the oxide film would be converted entirely to willemite by the process described in Chapter 4. It was, however, proved that the willemite films produced by this process always have relatively thick underlying oxide. The initial oxide was not very much reduced in thickness because the reaction between ZnF_2 and SiO_x probably stops when a fairly thin willemite layer is formed. This was also suspected to occur

on silicon based devices, but there it has not been so easy to prove because oxide also continues to grow on the silicon during the willemite forming reaction.

The electrical properties of the composite willemite films have been compared with those of the unreacted oxide. A literature search has shown little study of deposited SiO_x films which have been baked in oxygen at such high temperatures after deposition, so that the present work is unique, so far as is known. It has been shown that, once the mechanical problems due to thermal mismatch between the substrate and base electrode have been overcome, oxide films prepared by this process have fewer defects, and that no treatment is needed to cure small self-healing-breakdown type of faults before the measurements give reproducible results. Small faults of this nature are common in evaporated films of SiO. It has been found here that the surface finishes of the substrate and the base electrode are extremely important for getting films with reproducible properties. The oxide produced by this process is much more resistive and had a higher breakdown field strength than the normal evaporated films. However, a bake in argon instead of oxygen tends to produce films with many defects and poor electrical characteristics. This may be due to the decomposition of SiO into Si and SiO_2. On the other hand a prolonged bake in oxygen gives films of higher resistivity and breakdown strengths.

With Pt-Pt electrodes, the conduction data in SiO_x have been interpreted in terms of the bulk-limited Poole-Frenkel effect and has been found to be in good agreement. This

effect is also commonly used for interpreting the conduction in 'as evaporated' films. However, with an aluminium contact the results show strong electrode dependence which has not been reported before and this has been interpreted as due to a layer of Al_2O_3 below the metal.

Conduction in the willemite films showed many of the same features as in the oxide. With microscopic defects, which were due to the thermal mismatch between the Pt base electrode and the silica substrate, the results were very variable but reproducible results were eventually obtained with the sapphire substrate samples. In general the conduction currents through willemite composite films were greater than in oxide of the same thickness and they showed the same polarity dependence with aluminium top contacts. Furthermore the thicker willemite films conducted more than thin ones.

These characteristics have been explained in terms of an increase in the conductivity of the silicon oxide near the willemite interface. With an aluminium electrode, an underlying layer of Al_2O_3 can explain the polarity dependence as for SiO.

The willemite films produced by this unique process are cathodoluminescent down to approximately 200 Å thickness. Except for the similar work with silicon substrates being carried out in the Department, no luminescence has previously been reported in willemite films thinner than about one micron. This must show good control of the phosphor film surface in the methods used here. Electroluminescence was occasionally observed on some samples with approximately 600 Å and thicker willemite films. It was reproducible when

seen and was always observed well below breakdown voltage. It was not achieved simply by passing relatively large currents: in some samples currents reaching a milliampere were passed with no light emission. However, when electroluminescence was observed it occurred below 10^{-5} amperes. This shows that electroluminescence can possibly be successfully obtained by injecting electrons with larger energies, but not necessarily in larger numbers.

This work has shown that there are prospects for a good electroluminescent device using willemite if techniques could be developed to get energetic electrons into the phosphor. Suggestions for further work with this objective are made in the following section.

9.2 Suggestions for Further Work

At the beginning of this work investigation of metal-willemite-metal structures looked straight-forward but the progress already made has raised many interesting and important questions that could not be followed up in the time available. As compared to other materials being investigated elsewhere for electroluminescent devices, willemite is an extremely good phosphor in thin film form. This work has shown that the techniques and structures used for the fabrication of the samples are basically suitable for a luminescent device. However, because a film of oxide, almost as thick as the initial oxide, was always found underneath the willemite, the properties of this material by itself could not be studied. Further investigations must therefore include a process for the elimination of this oxide layer.

Fabrication of samples without an oxide underneath the willemite can be approached in two independent ways. Co-evaporation of the oxide and zinc fluoride in the correct ratios followed by the standard fabrication procedure would be one. Evaporating a very thin film of oxide at the start (100-300 Å on different samples) and then thick zinc fluoride film would be the other method. Different zinc fluoride thicknesses would be required to furnish sufficient information about the effect of any residual oxide. A thin film of SiO of tunnelling thickness could also be evaporated on part of the willemite so produced and the I-V curves studied with aluminium or non-oxidizing metallic contacts on both parts. This would show whether electroluminescence due to electrons with tunnelling energies can be obtained reproducibly and would give insight into the conduction mechanism in willemite. Subjecting the willemite films to a step voltage for long periods of time and examination for electrolytic effects would prove whether the conduction is entirely non-ionic.

Some further samples (similar to the ones studied in this work) with a fixed thickness of oxide and different thicknesses of willemite would be required to study the I-V characteristics of the underlying oxide after the willemite is etched away. This would reveal whether the changes in conductivity of the oxide, proposed to explain the I-V characteristics of the composite film, are correct. With the development of ellipsometric techniques for thin film thickness measurements in the Department it should also be easy to estimate the amount of oxide used in the conversion reaction. This would be vital for the fabrication of improved samples by these methods.

Measurements on the oxide showed that with the fabrication techniques used, the oxide films had higher breakdown strengths, lower conduction current (with some electrode dependence) and probably better mechanical qualities as compared to the 'as evaporated' films. Further work would therefore be expected to yield more novel information about electronic conduction in these oxides. To get more reproducible electrical results, better control of the physical properties of the oxide would be desirable. Conduction studies of films obtained by evaporating SiO at different temperatures and then baked under the willemite forming conditions without zinc fluoride might result in the discovery of the best oxide to be used for devices in terms of dielectric breakdown and conduction current.

It was concluded in Sec.8.3 that the Poole-Frenkel conduction model agrees well with the present SiO_x results. This model could be further tested by investigating the electrode thickness and temperature dependence of the current in similar samples. If the bulk dependent Poole-Frenkel process is operative, the conduction should be completely independent of the electrode material and its polarity for non oxidizing metal contacts. This would eliminate the Schottky emission process which otherwise is difficult to distinguish from Poole-Frenkel conduction with certainty. Use of electrode metals which readily form an oxide, such as the aluminium used here,would prove whether the current is limited by the presence of an additional oxide film as proposed in Sec.8.5. This would open up an extensive area for future work which has been largely neglected in the literature on conduction in SiO_x films.

Investigations of the I-V characteristics for different film thicknesses would give information on the internal field distribution. For both the Poole-Frenkel and Schottky conduction processes the current for a constant field would remain independent of film thickness because the internal field is assumed to be uniform in these models. Thus a plot of voltage for a given current against film thickness would be a straight line for these processes. On the other hand, if contact barriers control the conduction, a large part of the applied voltage would be dropped in a small distance and the current at a constant voltage would not depend greatly on thickness. The same finding should apply to the SiO_x films with an aluminium electrode if the model proposed in Sec.8.5 is correct, since again the voltage is dropped predominantly across a thin layer, in this case Al_2O_3. In the unlikely event of space-charge limited conduction the current would vary as $\frac{V^2}{d^3}$.

The temperature dependence of conduction in solids nearly always provides the most certain method for distinguishing between different conduction processes. It is additionally important in thin film work because a range of measurements can be obtained on a single sample, so eliminating the problems of reproducibility in making thin film samples with different electrodes or thicknesses. However, in the present work the main interest was to make samples that might show bright electroluminescence and primary interest was therefore not concentrated on a study of the conduction mechanisms. In an effort to obtain electroluminescence, conduction measurements were made up to the highest possible field strengths and were always terminated by dielectric breakdowns of the film. It

was thought to be more important to obtain high field data at room temperature than low field measurements over a range of temperatures. This would not be true for a more thorough investigation of conduction.

To enable the effect of temperature variation to be measured, the apparatus used for probing the device would have to be modified to incorporate arrangements for controlled heating and cooling, and the measurement of the sample temperature. If the conduction is limited by the Schottky effect a plot of log $\frac{I}{T^2}$ against $\frac{1}{T}$ should give a straight line. For the Poole-Frenkel process a plot of log I against $\frac{1}{T}$ would be linear but it is unlikely that plots over a small range of temperature would enable one to distinguish between the two. For processes controlled by field intensification in space charge barriers, the current will not be sensitive to temperature, if tunnelling and impact ionization are operative. If electron emission over a contact barrier predominates the temperature variation would be the same as for the Schottky effect.

In SiO_x films with one aluminium electrode, the current through the oxide part alone would increase with temperature, but complications might arise due to the presence of Al_2O_3 under aluminium contact. When the anode is the platinum electrode more voltage will be dropped across the Al_2O_3 film since the conductivity of the SiO_x goes up and the current through the Al_2O_3 may or may not increase with temperature, depending on whether the electron transfer there is controlled by the Schottky emission or tunnelling. For the opposite polarity the current will go up only slightly due to the increased conduction in the SiO_x if the proposed process of tunnelling through the Al_2O_3 is correct. With both electrode

combinations, measurements over a range of temperatures would therefore be of great assistance for confirming the proposed conduction mechanism.

It is extremely difficult to predict the effects of electrode thickness and temperature changes on the hypothetical conduction models proposed in Chapter 8 for the composite oxide-willemite films because of the complex nature of electron transfer through two or three layers. With both contacts of non oxidizing metal, comparison of the temperature variation of the current in the oxide and in the composite oxide-willemite films might show whether the conductivity of willemite itself increases with temperature as would be expected for an n-type semiconductor. This could be done by etching away the willemite from a part of the composite oxide-willemite sample and putting fresh contacts on the residual oxide.

Some further information about the nature of conduction through willemite could be obtained by studying the variation of current with temperature using the method of thermally stimulated currents, particularly if the residual oxide could be eliminated.

Some electron microscope studies of willemite were carried out by Edwards and Rushby [14]. If continued, these could give information about the crystallite structure of the willemite formed by different methods. A scanning electron microscope would also greatly help the examination of the willemite-oxide interface after chemical removal of the willemite. Mass spectrometric analysis of the gases given off during the willemite forming reaction would prove useful to finding out if the reaction indeed takes place as expected.

With continued work on these lines there is a strong possibility of eventually being able to excite electroluminescence in thin willemite films. If the methods developed could be applied to films on silicon there would be a good chance of using willemite for solid state display devices.

REFERENCES

1. I.E.E.E. Trans. Electron Devices ED-18, pp.614-803 (1971)
2. Anon. Electronics May 24, 1971
3. G.S. Edwards, Ph.D. Thesis, University of Durham (1970)
4. J.L. Plumb, Jap, JAP 10, 326, (1971).
5. Toyo-o Miyata et al, Jap. JAP, 9, 615 (1970)
6. A. Vecht and N.J. Werring, J. Phys. D, 3, 105, (1970)
7. P. Lilley, P.L. Jones and C.N.W. Litting, J. Mat. Sci. 5, 891, (1970)
8. T.G.R. Rawlins and R.J. Woodward, J. Mat. Sci. 7, 257, (1972)
9. J.H. Schulman, JAP, 17, 902 (1946)
10. H.W. Leverentz, 'An introduction to Luminescence of Solids' (1950), J. Wiley, New York.
11. C.C. Klick and J.H. Schulmann, J. Opt. Soc. Amer. 42, 910 (1952)
12. C. Feldman and M. O'Hara, J. Opt. Soc. Amer. 48, 816 (1958)
13. George M. di Giacomo, J. Electrochem. Soc. 116, 313 (1969)
14. G.S. Edwards and A.N. Rushby, J. Mat. Sci. 6, 225, (1971)
15. P. Goldberg, 'Luminescence of Inorganic Solids,' (1966) Academic Press, New York
16. G.F.J. Garlick, 'Luminescent Materials' (1949) Oxford University Press
17. G. Destriau, Phil. Mag. 7, 38, 700, 744, 800, 855 (1947)
18. A. Bramley and J.E. Rosenthal, Phys. Rev. 87, 1125 (1952)
19. F.H. Nicoll and B. Kazan, Proc. IRE, 43, 1012 (1955)
20. R.C. Herman and R.H. Hofstadter, Phys. Rev. 57, 936 (1940)
21. G.F.J. Garlick and A.F. Gibson, Proc. Phys. Soc. 60, 574 (1948)
22. R.C. Herman and R.H. Hofstadter, Phys. Rev. 59, 78 (1941)
23. R.C. Herman and R.H. Hofstadter, Phys. Rev. 56, 212 (1939)

24. A.G. Hill and L.R. Aronin, Phys. Rev. 57, 1090 (1940)

25. M.J. Morant and G.S. Edwards, S. S. Electronics, 16, 173 (1973)

26. G.D. Davies, Personal Communications

27. M.J. Morant, Departmental report on the 'Luminescent Properties of Willemite' (1972)

28. A.I. Gubanov, Quantum Electron theory of Amorphous Semiconductors (1965) Consultant Bureau, New York

29. R. Grigorovici, J. Non. Cryst. Solids, 1, 303 (1969

30. P.W. Anderson, Phys. Rev. 109, 1492 (1958)

31. R. Grigorovici, Thin Solid Films, 9, 1 (1971)

32. M.H. Cohen, Physics Today, pg. 26, May (1971)

33. M.H. Cohen, J. Non.Cryst. Solids, 2, 432 (1970)

34. A.K. Jonscher, J. Electrochem. Soc. 116, 217C (1969)

35. N. Mott, Advanc. Phys. 16, 49 (1967)

36. N.F. Mott, Endeavour, 26, 155 (1967)

37. N.F. Mott, (ed.) Amorphous and Liquid Semiconductors (1970) North Holland Amsterdam

38. A. Miller and E. Abrahams, Phys. Rev. 120, 745 (1960)

39. A.K. Jonscher, Thin Solid Films, 1, 213 (1967)

40. S.R. Pollack and C.E. Morris, JAP, 35, 1503 (1964)

41. S.R. Pollack and C.E. Morris, Trans. AIME, 233, 497 (1965)

42. J.G. Simmons in 'Handbook of Thin Film Technology' (1970) Eds. L.I. Maissel and R. Glang, McGraw Hill

43. A.K. Jonscher, J. Vac. Sci. and Technol. 8, 135 (1971)

44. J.G. Simmons, Phys. Rev. Letters, 15, 967 (1965)

45. J.G. Simmons, J. Phys. D. 4, 613 (1971)

46. J.G. Simmons, J. Phys. Chem. Solids, 32, 1987 (1971)

47. J.G. Simmons, J. Phys. Chem. Solids, 32, 2581 (1971)

48. E.H. Rhoderick, Third Solid State Device Conference, Exeter (1969)

49. A. Miller and E. Abrahams, Phys. Rev. 120, 745 (1960)

50. A.K. Jonscher and P.A. Walley, J. Vac. Sci. and Technol. 6, 662 (1969)

51. D.V. Geppert, JAP, 34, 490 (1963)

52. J.G. Simmons, JAP, 35, 2472 (1964)

53. E. Burstein and S. Lundqvist, Tunnelling phenomenon in solids (1969), Plenum Press, New York

54. R.H. Fowler and L. Nordheim, Proc. Roy. Soc. (London) A119, 173 (1928)

55. W. Tantraporn, S.S. Electronics, 7, 81 (1964)

56. P.R. Emptage and W. Tantraporn, 8, 267 (1962)

57. M. Lenzlinger and E.H. Snow, JAP, 40, 278 (1969)

58. W. Schottky, Z. Physik, 15, 872 (1914)

59. C.R. Crowell, S.S. Electronics, 8, 395 (1965)

60. D.R. Lamb, Electrical Conduction Mechanisms in Thin Insulating films (1967) Methuen

61. J.J. O'Dwyer, JAP, 37, 599 (1966)

62. H. Frölich, Proc. Roy. Soc. (London), A188, 521 (1947)

63. Z. Frenkel, Phys. Rev. 54, 647 (1938)

64. C.A. Mead in 'Basic problems in thin film Physics' (1966) Eds. R. Niedermayer and H. Mayer. Vandenhoeck and Ruprecht, Goettingen.

65. R.M. Hill, Thin Solid Films, 1, 39 (1967)

66. R.M. Hill, Phil. Mag. 23, 59 (1971)

67. A.K. Jonscher, J. Phys. C. 4, 1331 (1971)

68. J. Antula, JAP, 43, 4663 (1972)

69. C.A. Mead, Phys. Rev. 128, 2088 (1962)

70. J.G. Simmons, Phys. Rev. 155, 657 (1967)

71. H.L. Taylor and J.R. Yeargan, JAP, 39, 5600 (1968)

72. C.A. Mead, JAP, 32, 646 (1961)

73. M. Stuart, B. Jap. 18, 1637 (1967)

74. A.K. Jonscher, J. Vac. Sci. and Technol. 8, 135 (1971)

75. A.K. Jonscher and C.K. Loh, J. Phys. C. 4, 1341 (1971)

76. Masayuki Ieda et al, Jap. 42, 3737 (1971)

77. J.L. Hartke, JAP, 39, 4871 (1968)

78. R.M. Hill, Thin Solid Films, 8, R21 (1971)

79. G.A.N. Connel et al, Phil. Mag. 26, 541 (1972)

80. E.L. Murphy and R.H. Good, Phys. Rev. 102, 1464 (1956)

81. W. Tantraporn, S.S. Electronics, 7, 81 (1964)

82. T. Mann in Reference 64

83. S.G. Christov, Phys. Stat. Sol. 17, 11 (1966)

84. S.G. Christov, Phys. Stat. Sol. 32, 509 (1969)

85. S.G. Christov, Contemp. Phys. 13, 199 (1972)

86. J. Dressner and F. Shallcross, S.S. Electron 5, 205 (1962)

87. N. Mott and R.W. Gurney 'Electronic Processes in ionic crystals' (1948) Oxford Press

88. M.A. Lampert, Phys. Rev. 103, 6 (1956)

89. M.A. Lampert, JAP, 29, 7 (1958)

90. M.A. Lampert, Phys. Rev. 125, 1 (1962)

91. M.A. Lampert and P. Mark, 'Current injection in solids,' (1970) Academic Press

92. A. Rose, Phys. Rev. 97, 1538 (1955)

93. J. Sworakowski, JAP, 41, 292 (1970)

94. P.A. Raykerus, Radio Engg. and Electron Physics 16, 675 (1971)

95. P.N. Murgatroyd, J. Phys. D. 3, 151 (1970)

96. J.L. Hartke, JAP, 39, 4971 (1968)

97. D. Dascălŭ et al, Rev. Roum. Phys. 10, 1201 (1970)

98. M.R. Boon, Thin Solid Films 10, 333 (1972)

99. D.L. Pulfrey et al, JAP 41, 2838 (1970)

100. A.H.M. Shousha and L. Young, Thin Solid Films 8, 383 (1971)

101. R.W. Brander, D.R. Lamb and P.C. Rundle, BJAP 18, 23 (1967)

102. N.F. Mott and W.D. Twose, Adv. Phys. 10, 107 (1961)

103. Vinay Ambegaokar et al, Phys. Rev. B. 4, 2612 (1971)

104. N.F. Mott, Phil. Mag. 19, 835 (1969)

105. C.P. Bean et al, Phys. Rev. 101, 551 (1956)

106. H. Hirose and Y. Wada, Jap. JAP 3, 179 (1964)

107. H. Hirose and Y. Wada, Jap. JAP 4, 639 (1965)

108. G. Siddal, Vacuum 9, 274 (1960)

109. K. Van Steensel, Microelectronics and Reliability 6, 261 (1967)

110. Yasuro Nishimura et al, Electronics and Commucations in Japan 52-C, 116 (1969)

111. I.T. Johansen, JAP. 37, 499 (1966)

112. T.E. Hartman, J.C. Blair and R. Bauer, JAP. 37, 2468 (1966)

113. A. Servini and A.K. Jonscher, Thin Solid Films 3, 341 (1969)

114. P.A. Timson and C.A. Hogarth, B. JAP. 3, L75 (1970)

115. H. Adachi, T. Hariu and Y. Shibata , Jap. JAP 10, 812 (1971)

116. G. Navik, Thin Solid Films 6, 145 (1969)

117. P.A. Timson and P. Wickens, Thin Solid Films 5, R55 (1970)

118. H. Adachi, Y. Shibata and S. Ono, J. Phys. D. 4, 988 (1971)

119. J.G. Simmons, Phys. Rev. 166, 912 (1968)

120. S.W. Chaikin and G.A. St.John, Electrochem. Tech. 1, 291 (1963)

121. D.B. York, J. Electrochem. Soc. 110, 271 (1963)

122. T.A. Anastasio, JAP. 38, 2606 (1967)

123. Y. Inagaki et al, Electrical Engg. in Japan, 89, 107 (1969)

124. Handbook of Vacuum Physics Vol. 1 (Gases and Vacua) 1964. Ed. A.H. Beck, Pergamon

125. O.S. Heavens, Thin Film Physics (1970) Methuen

126. Thin Film Microelectrons (1965), Ed. L. Holland, Chapman and Hall

127. L. Holland, Vacuum deposition of thin films (1963), Chapman and Hall.

128. J.S. Colligon, Vacuum 11, 272 (1961)

129. L.I. Maissel and J.H. Vaughn, Vacuum 13, 421 (1963)

130. L.I. Maissel in Physics of Thin Films (1966) Eds. G. Hass and R.E. Thun, Academic Press

131. R.W. Berry, P.M. Hall and M.T. Harris, Thin Film Technology (1968), Van Nostrand

132. R.C. Williams and R.L. Backus, JAP. 20, 98 (1949)

133. D.S. Campbell in Reference 42

134. J. Priest, H.L. Caswell and Y. Budo, Vacuum 12, 301 (1962)

135. G.W. Brady, J. Phys. Chem. 63, 1119 (1959)

136. A.P. Bradford and G. Hass, J. Opt. Soc. Amer. 53, 1096 (1963)

137. J. Priest, H.L. Caswell and Y. Budo, JAP 34, 347 (1963)

138. M. Stuart, Phys. Stat. Sol. 23, 595, (1967)

139. C.E. Drumheller, Kemet Co. Research Report "Properties and applications of SiO" Feb.(1960)

140. G. Siddal and G.S. Giddens, Proc. IERE/IEE Conf. Applications of thin films in Electronic Engineering London, July 1966

141. J.W. Strange and S.T. Henderson, Proc. Phys. Soc. 58, 368 (1946)

142. R.C. Tyagi and G.F.J. Garlick, B. JAP, 17, 747, (1966)

143. A.G. Fischer, Proc. of International Conf. on Lum., 1765-1781, (1966)

144. Photoluminescent Materials and Devic-es (1965) Ed. S. Larach Van Nostrand.

145. W.W. Piper and F.E. Williams, Phys. Rev. 87, 151, (1952) and B. JAP Suppl. 4, 39, (1954)

146. G.F. Alfrey and J.B. Taylor, Proc. Phys. Soc. 68, 775, (1955)

147. A.E. Hill and G.R. Hoffman, B. JAP, 18, 13, (1967)

148. S.M. Sze, Physics of Semiconductor Devices (1969), J. Wiley

149. G.F.J. Garlick and M. Sayer, J. Electrochem. Soc. 109, 678, (1962).

150. M. Sayer, Proc. Phys. Soc. G.B. 78, 1017, (1961)

151. G.F.J. Garlick, B. JAP, 13, 540, (1962)

DURHAM UNIVERSITY SCIENCE
4 JUL 1974
SECTION LIBRARY